

Evaluation of the Performance of Gas Tankless Water Heaters

by

Peter William Grant

B.S., Michigan Technological University, 2007

A thesis submitted to the

Faculty of the Graduate School of the

University of Colorado in partial fulfillment

of the requirement for the degree of

Master of Science

Department of Civil, Environmental and Architectural Engineering

2010

This thesis entitled:

Evaluation of the Performance of Gas Tankless Water Heaters

Written by Peter William Grant

Has been approved for the Department of Civil, Environmental and Architectural Engineering

Moncef Krarti, PhD, PE, LEED-AP

Michael Brandemuehl, PhD, PE

Jay Burch, PhD

Date_____

The final copy of this thesis has been examined by the signatories, and we
Find that both the content and the form meet acceptable presentation standards
Of scholarly work in the above mentioned discipline.

Grant, Peter William (MS, Civil, Environmental and Architectural Engineering)

Evaluation of the Performance of Gas Tankless Water Heaters

Thesis directed by the National Renewable Energy Laboratory Senior Scientist, Dr. Jay Burch and the University of Colorado Professor, Dr. Moncef Krarti

Tankless water heaters (TWHs) are generally thought of as an efficient method of producing hot water, and receive incentives in various federal, state, and utility programs. However, it has up to now been impossible to know the actual efficiency for any specific draw pattern. In addition, TWHs have been used in conjunction with solar systems, and it is uncertain what the impact of pre-heated water will be on THW operation. To address these questions experiments have been performed to fully understand and characterize behavior of TWHs, and a new TRNSYS component has been developed embodying that understanding. The model is multi-node in the heat exchanger, with ad-hoc control features mimicking observed behaviors. The TRNSYS model was calibrated to several hours of data, yielding burn efficiency of 80.2%, capacitance of 8.36 ± 0.6 kJ/C, and total loss coefficient of 12.99 ± 4 kJ/hr-K. The model was validated against several draw profiles, and used to carry out analyses of performance with different draw profiles used in the Building America Program. Efficiency depends on the draw, varying from 77% for low use to 65% for high use.

Acknowledgements

I'd like to thank Jay Burch for the effort he put in to ensure that this project happened. From acquiring funding to teaching me about the many steps and intricacies of experimental research, Jay had a huge impact on this research from start to finish.

I'd also like to thank Moncef Krarti for his assistance developing this thesis. During our meetings over the years Moncef helped me clarify any number of misunderstandings and was always patient when helping me understand new concepts. In addition, he had the perseverance to keep saying "Presentation is important" until I actually realized that presentation is indeed important.

Matt Duffy also deserves my thanks for taking the time to answer numerous questions about both the FORTRAN language and how to work with TRNSYS.

Ed Hancock helped me with instrumentation, both choosing sensors and installation issues, several times. But he always said it was nothing, so thanks for nothing Ed.

Contents

Chapter 1: Introduction and Literature Review	1
1.1 Introduction	1
1.2 Market Analysis.....	2
1.3 Tankless Disadvantages.....	3
1.4 Tankless Advantages	6
1.5 Potential Solutions.....	9
1.6 Rinnai Water Heater Operation	10
1.7 Recommended Research Needs	12
1.8 Thesis Sections.....	13
Chapter 2: Multiple-Node Model for Tankless Water Heaters	15
2.1 Previous Water Heater Modeling	15
2.1.1 TRNSYS Water Heater Models	15
2.1.1.1 Type 940: Single Node Tankless Water Heater.....	15
2.1.1.2 Type 4: Multiple Node Storage Tank Water Heater	25
2.1.2 First Principles Models	27
2.2 Modifying TRNSYS Type 940.....	28
2.3 Model Verification Analysis.....	36
2.3.1 Steady State Efficiency and UA Values	37
2.3.2 Flow Rate Below Minimum Simulations	40
2.3.3 Capacitance Tests.....	42
2.3.4 Subjected to a Flow Pattern	44
2.3.5 Nodes Required for Convergence.....	50
2.3.5.1 Flow Rate Greater than Minimum Flow Rate.....	52
2.3.5.2 Flow Rate below Minimum Flow Rate.....	55
Chapter 3: Test Facility Description and Modes of Operation	57
3.1 Overall System Design.....	57
3.2 Images of the Experimental Apparatus	59
3.3 Heat Exchanger Thermocouple Placement	64
3.4 Water Temperature Measurement Calibration.....	66
3.5 Water Flow Rate.....	73
3.6 Natural Gas Flow Rate	76

Chapter 4: Experimental Design	79
4.1 Tankless Heater Performance Testing	79
4.1.1 Steady State Efficiency	79
4.1.2 Response to Rapid Changes in Flow Rate System Design	83
4.1.3 Response to Gradually Decreasing Inlet Water Temperature System Design	84
4.1.4 Minimum Flow Rate System Design	87
4.1.5 Parameter Derivation and Validation	88
4.2 Addition of a Small Tank Testing Design	91
4.2.1 Cold Water Slug Testing Design	94
4.2.2 Small Tank Stratification Testing Design	95
4.2.3 Tepid Outlet Testing Design	96
4.2.4 Small Tank Bypass Valve Design	96
Chapter 5: Experimental Results	98
5.1 Performance and Behavior of Tankless Heater Results	98
5.1.1 Steady State Efficiency Results	98
5.1.2 Response to Rapid Changes in Flow Rate	101
5.1.3 Response to Gradually Decreasing Inlet Water Temperature	104
5.1.4 Minimum Flow Rate Results	110
5.1.5 Parameter Characterization and Validation Results	112
5.2 Addition of a Small Tank Results	116
5.2.1 Cold Water Slug Results	116
5.2.2 Small Tank Stratification Results	121
5.2.3 Tepid Outlet Results	125
5.2.4 Small Tank Bypass Valve Results	126
Chapter 6: Model Validation Analysis	132
6.1 GenOpt Results	132
6.2 Validation via Characterization Test	135
6.3 Validation via Changing Flow Pattern	137
Chapter 7: Efficiency Simulations	144
7.1 Efficiency Sensitivity Analysis	144
7.2 Building America Standard Benchmark Draw Profiles	151
7.2.1 Two Bedroom House	152
7.2.2 Four Bedroom House	154
7.2.3 101 Liter/Day Household	157

Chapter 8: Conclusions and Recommended Continued Research	161
8.1 The Model	161
8.2 Steady State Efficiency.....	162
8.3 Use in Conjunction with Solar Hot Water.....	162
8.4 Efficiency Sensitivity and Draw Profile Efficiency	163
Works Cited.....	165
Appendix A: Derivation of Multiple Node ‘a’ and ‘b’ Terms	167
Appendix B: Solution of Differential Equation for Final Temperature	169
Appendix C: Derivation of Δt From the Solution for $T_{\text{Node,Final}}$	170
Appendix D: Building America Draw Profiles	171
Appendix E: Campbell Scientific Datalogger Program.....	175
Appendix F: TRNSYS Component Code	195

List of Figures

Figure 1: Schematic of Parts in Rinnai Water Heaters [13].....	2
Figure 2: Flowchart of Initial Control Logic in Type 940 [10].....	19
Figure 3: Flowchart of Control Logic when Heater is on in Type 940 [10]	20
Figure 4: Flowchart of Control Logic when Heater is Off in Type 940 [10].....	21
Figure 5: Flow in TRNSYS Type 4 Stratified Storage Tank [11]	26
Figure 6: Temperatures and Heat Transfer Rates during the Flow Pattern.....	47
Figure 7: Water Flow Rates during the Flow Pattern.....	47
Figure 8: Percentage Differences between TRNSYS Simulation and Hand Calculations under Steady State Burning Conditions	52
Figure 9: Error in Environmental Losses During Steady State Flow	54
Figure 10: Percentage Difference between TRNSYS Simulation and Hand Calculations Under No Burn Conditions	56
Figure 11: Schematic of Full Test System	57
Figure 12: Wide-Scale View of the Entire Test System.....	59
Figure 13: View of the Storage Water Heaters.....	60
Figure 14: Close-Up View of the Controls and Thermocouples in the 23.3 L Tank.....	61
Figure 15: Close-Up View of the Rinnai R75Lsi Heater	63
Figure 16: View Depicting the Flow Rate Control Manifold	64
Figure 17: Location of Thermocouples on the Heat Exchanger	66
Figure 18: Ice Used to Determine Location of Thermocouple 20	72
Figure 19: Comparing the Measured Water Flow Rate to the Generated Signal.....	75
Figure 20: Comparison of Two Natural Gas Flow Meters.....	78
Figure 21: Steady State Efficiency Test Schematic	80
Figure 22: Response to Gradually Decreasing Inlet Temperature System Schematic.....	85
Figure 23: Small Tank System Test Schematic.....	94
Figure 24: Steady State Efficiency as a Function of Set Temperature.....	99
Figure 25: Steady State Efficiency as a Function of Gas Draw Rate.....	100
Figure 26: Temperature Fluctuations in Response to Changing Flow Rate (565 kg/hr Standard Flow).....	102
Figure 27: Temperature Fluctuations in Response to Changing Flow Rate (338 kg/hr Standard Flow).....	103
Figure 28: Temperatures and Flow Rates in a Test during Which the Outlet Temperature did not Exceed the Set Temperature.....	105
Figure 29: Calculated Heat Rates in a Test during Which the Outlet Temperature did not Exceed the Set Temperature	106
Figure 30: Temperatures and Flow Rates in a Test during Which the Outlet Temperature Exceeded the Set Temperature.....	106
Figure 31: Calculated Heat Rates in a Test during Which the Outlet Temperature Exceeded the Set Temperature	107
Figure 32: Sensitivity of Heater Turn-On Algorithm to Water Flow Rate.....	108
Figure 33: Sensitivity of Heater Turn-On Algorithm to Set Temperature	109
Figure 34: Compiled Minimum Flow Rate Results.....	111
Figure 35: Temperatures during Parameter Characterization Data.....	113
Figure 36: Water and Gas Flow Rates during Parameter Characterization Data.....	113

Figure 37: Temperatures during Model Validation Test.....	114
Figure 38: Flow Rates during Model Validation Test.....	115
Figure 39: Temperatures Recorded During a Cold Slug Test with no Cold Water Slug.....	117
Figure 40: Temperatures Recorded During a Cold Slug Test with a Cold Slug.....	118
Figure 41: Summary of Cold Water Slug Results with 1 °C Deadband.....	119
Figure 42: Summary of Cold Water Slug Results with 5 °C Deadband.....	120
Figure 43: Temperatures Recorded in the Small Tank during a Cold Water Slug Test.....	122
Figure 44: Water Flow Rates Recorded During the same Cold Water Slug Test.....	123
Figure 45: Temperatures in Small Tank When Maintaining Set Point.....	124
Figure 46: Steady State Outlet Temperature from the Small Tank under Varying Set and Flow Conditions.....	125
Figure 47: Temperatures Recorded During a Cold Water Slug Test with the Bypass Valve.....	127
Figure 48: Temperatures Recoded During a Similar Cold Water Slug Test without the Bypass Valve.....	128
Figure 49: Temperatures Recorded During a Tepid Outlet Test with Bypass Valve.....	129
Figure 50: Temperatures Recoded During a Tepid Outlet Test without the Bypass Valve.....	130
Figure 51: Normalized χ^2 Values with Changing UA and Capacitance.....	134
Figure 52: Error in Cumulative Natural Gas Consumption during Characterization Test.....	135
Figure 53: Natural Gas Flow Rates during Characterization Test.....	136
Figure 54: Outlet Temperatures during the Changing Flow Pattern Test.....	138
Figure 55: Natural Gas Flow Rates during the Changing Flow Pattern Test.....	138
Figure 56: Water Flow Rates during Changing Flow Pattern Test.....	139
Figure 57: Error in Cumulative Natural Gas Consumption during the Changing Flow Pattern Test	142
Figure 58: Sample Results from a Simulation.....	146
Figure 59: Effect of Draw Duration and Delay Length on Cumulative Efficiency.....	146
Figure 60: Impact of Draw Heat Demand and Delay Duration on Cumulative Efficiency.....	148
Figure 61: Impact of Draw Duration and Ambient Temperature on Cumulative Efficiency with 30s Delays.....	150
Figure 62: Impact of Draw Duration and Ambient Temperature on Cumulative Efficiency with 2.13 hr Delays.....	150
Figure 63: The Two Bedroom House Draw Profile.....	152
Figure 64: Flow Rates and Temperatures during the Two Bedroom House Draw Profile.....	153
Figure 65: Draw Pattern for the Four Bedroom House.....	155
Figure 66: Flow Rates and Temperatures during the Four Bedroom House Draw Profile.....	156
Figure 67: Low Use Household Draw Profile.....	158
Figure 68: Simulated Results to the Low Use Draw Profile.....	159

List of Tables

Table 1: Advantages and Disadvantages of Tankless Water Heaters [14].....	2
Table 2: Inputs and Average Heat Exchanger Temperature for Each Test.....	38
Table 3: Heat Transfers from TRNSYS and Theoretical Calculations for Each Test.....	38
Table 4: Percent Error Associated with Table 2.....	38
Table 5: Conversion Efficiencies at Steady State Conditions.....	38

Table 6: Variables and Temperatures in Below Minimum Flow Rate Tests	41
Table 7: Comparing TRNSYS Component to Theoretical Calculations when Below Minimum Flow	41
Table 8: Errors Associated with Table 4	41
Table 9: Theoretical Capacitance Check with Varying Flow Rate	43
Table 10: Theoretical Capacitance Check with Varying Capacitance	44
Table 11: Input Water Flow Rates Separated by Phase.....	46
Table 12: Outputs from TRNSYS during the Flow Pattern Test	49
Table 13: Error in Heat Transfer Rates during the Flow Pattern Test.....	49
Table 14: Error in Flow Rate during the Flow Pattern Test	50
Table 15: Sensor Uncertainties	58
Table 16: Individual Thermocouple Calibrations	67
Table 17: Creating the Reference Value.....	69
Table 18: Thermocouple Assemblies Compared to Reference Value	69
Table 19: Thermocouple Assemblies Measuring Mains Water.....	70
Table 20: Flow Meter Calibration.....	74
Table 21: Fox Thermal FT2 Calibration Chart	77
Table 22: Flow Rates and Set Temperatures used in Steady State Efficiency Test.....	81
Table 23: Uncertainty in Measurements in Steady State Efficiency Test	82
Table 24: Uncertainty in Steady State Efficiency Calculations	82
Table 25: Uncertainty from Each Measurement in Steady State Efficiency Tests.....	82
Table 26: Uncertainty in Response to Rapid Changes in Flow Rate Tests	84
Table 27: Starting Inlet Temperatures for Decreasing Inlet Water Temperature Tests	86
Table 28: Measurement Uncertainty in Gradually Decreasing Inlet Temperature Tests	86
Table 29: Overall Uncertainty in Gradually Decreasing Inlet Water Temperature Tests.....	87
Table 30: Uncertainty Caused by Each Measurement in Gradually Decreasing Inlet Water Tests	87
Table 31: Uncertainty in Minimum Flow Rate Tests	88
Table 32: Measurement Uncertainties in Validation Test	91
Table 33: Parameters in Cold Water Slug Tests	95
Table 34: Flow and Temperature Parameters in Tepid Outlet Tests.....	96
Table 35: Heater Characterization Parameters from GenOpt	132
Table 36: Heater Characterization Parameter Values and Uncertainties.....	134
Table 37: Parameters used in the Sensitivity Study	145
Table 38: Energy Consumption and Efficiency in the Two Bedroom House Simulation.....	153
Table 39: Energy Consumption and Efficiency in the Four Bedroom House Simulation.....	156
Table 40: Energy Use and Efficiency in the Low Use Draw Profile	159

List of Symbols

a = Placeholder used in solving Equation 1 in TRNSYS Type 940

A = Area of the heat exchanger

A_{Tube} = Cross – sectional area of the tube in the heat exchanger

b = Placeholder used in solving Equation 1 in TRNSYS Type 940

C_p = Specific heat of water

Cap = Thermal capacitance of the heat exchanger

h_{gas} = Energy density of natural gas

k = Thermal conductivity of the heat exchanger (copper)

L = Length of tube in the heat exchanger

m = Mass of water in one node of TRNSYS Type 4

\dot{m} = Mass flow rate of water passing from mains to a draw

\dot{m}_1 = Water mass flow rate to or from node 1 in Figure 5

\dot{m}_3 = Water mass flow rate to or from node 3 in Figure 5

\dot{m}_h = Water mass flow rate coming from an external heat source

P_{Sample} = Ambient pressure during a sampling period

$Q_{Del,now}$ = Heat delivered to the water during a sub timestep

Q_{Stored} = Thermal energy stored in the heat exchanger

\dot{Q}_{Del} = Average rate of heat transfer delivered to the water during a

\dot{Q}_{Env} = Rate at which heat is lost to the surroundings

\dot{Q}_{In} = Rate at which energy is consumed by the heater

\dot{Q}_n = The rate at which heat is added to the current node

\dot{Q}_{Pilot} = Energy consumption rate of the pilot light

\dot{Q}_{Rated} = Maximum heat consumption rate of the heater

$\dot{Q}_{Required}$ = Heat rate necessary for the heater to operate at steady state

T_{Air} = Temperature of the surrounding air

\bar{T}_{Exit} = Time averaged temperature of water exiting the heater

T_F = Average temperature of the heat exchanger at the end of a timestep

\bar{T}_{Fluid} = Temperature of the heated fluid

T_{Fluid} = Temperature of the heated fluid

\bar{T}_{HX} = Time and location averaged temperature of the heat exchanger

T_I = Temperature at the beginning of the timestep (initial temperature)

T_{In} = Inlet temperature of the heater

T_n = Temperature of the current node

\bar{T}_n = Time averaged temperature of the current node

\bar{T}_{Now} = Average temperature of the heat exchanger during a sub timestep

T_{n-1} = Temperature of the previous node

T_{n+1} = Temperature of the following node

T_{Sample} = Ambient temperature during a sampling period

T_{Set} = Set temperature of the heater

U = Heat transfer coefficient describing the heat transfer between the heat exchanger and surroundings

V_{Fox} = Voltage signal from the Fox Thermal FT2

V_{Water} = Voltage signal from the water flow meters

$x_{Experiment}$ = Data point for either heat consumption rate or temperature

$x_{Simulation}$ = Simulated value reported for either heat consumption rate or

α_n = Control constant in Type 4

β = Control constant in Type 4

Δt = Change in time

ΔT = Change in water temperature

Δt_{Now} = Time elapsed during a sub timestep

Δt_{TRN} = Time elapsed during a TRNSYS timestep

η = System efficiency of the tankless heater

η_{Conv} = Conversion efficiency of the tankless heater

η_{Pilot} = Conversion efficiency of the pilot light

$\eta_{\Delta t_{\text{TRN}}}$ = System efficiency during a single TRNSYS timestep

γ = Control constant determining the heat rate of the heater

γ_i = Tankless heater control constant in the current iteration

γ_{i+1} = Tankless heater control constant in the next iteration

γ_n = Binary constant used to describe the direction of water flow in Type 4

\dot{v}_{Fox} = Volumetric flow rate of natural gas reported by the Fox Thermal
flow meter

\dot{v}_{Res} = Volumetric flow rate of natural gas reported by the AM – 250
flow meter

ρ_{Water} = The density of water

$\sigma_{\text{Experiment}}$ = Standard deviation of measurement (either temperature or
heat consumption rate)

χ_x^2 = χ^2 term for either natural gas or temperature

$\#_{\text{Node}}$ = The number of nodes in the simulation

$\#_{pulse}$ = *The number of pulses recorded during a sampling period*

Chapter 1: Introduction and Literature Review

1.1 Introduction

Tankless water heaters behave in a fundamentally different manner from storage tank water heaters. Storage tank water heaters function by maintaining a constant temperature in a stored volume of water while tankless water heaters use a large gas burner to meet hot water demand. The high burn rate of tankless water heaters allows manufacturers to create systems that do not employ storage tanks. Removing the storage tank reduces environmental losses and increases energy factors. The trade-off is that tankless water heater required complicated sensing and control systems to be able to meet demand. A diagram depicting the sensors and controls employed in Rinnai tankless water heaters is provided in Figure 1. Tankless water heaters have several functional advantages and disadvantages which are displayed in Table 1.

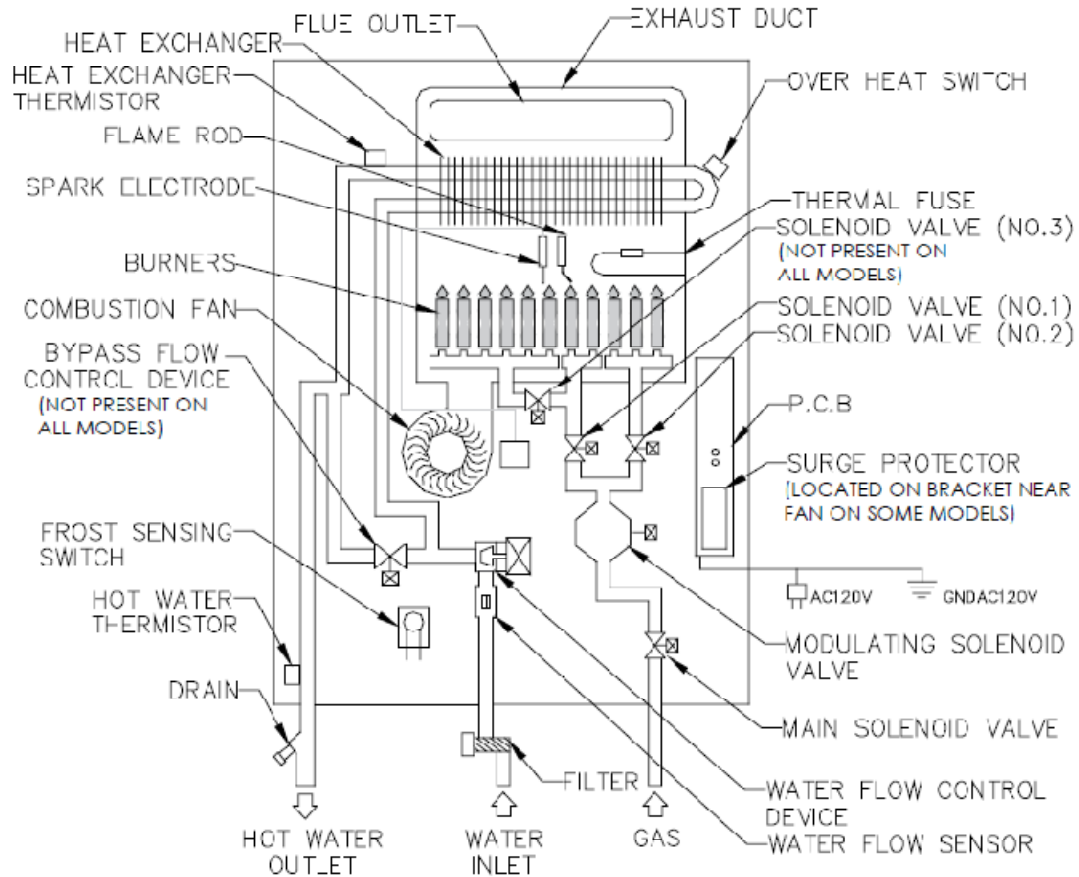


Figure 1: Schematic of Parts in Rinnai Water Heaters [13]

Table 1: Advantages and Disadvantages of Tankless Water Heaters [14]

Advantages	Disadvantages
Energy savings	Higher first cost/maintenance
Endless hot water	Increased hot water usage ¹
Compact/space savings	Imperfect temperature control
Low weight	Minimum flow rate to turn on
Builder- & DIY-friendly	Limited capacity/hi-flow limit
Calif. Title 24 Credits	Delays in hot water delivery

1. No data exists to support this theory [14]

1.2 Market Analysis

While tankless water heaters have significant market share in some parts of the world, particularly Europe, their market share has historically been low in the United States [1]. Currently tankless water heaters are sold at a rate of approximately 100,000 units per year which represents about 1% of the water heater market in the United States [1,2].

1.3 Tankless Disadvantages

The major market barrier for tankless water heaters is probably cost. The total incremental cost is expected to be around \$950 for new construction or \$1450 for a retrofit [4]. It should be noted that the cost for a retrofit installation is highly variable; several changes such as adding an electrical connection, increasing the size of the gas pipe and meter or redoing venting can dramatically add to the cost of the installation [3, 4, 5].

Another market barrier might be that tankless water heaters have been unable to adequately meet loads in the United States; however, recent developments and designs of tankless water heaters make them more suitable to serve American customers [1].

Recently there have been several improvements in tankless water heater design. First, the capacity of the heaters has been increased up to 220 MJ/hr [1]. This increase allows a single tankless unit to serve multiple showers and/or other hot water devices. At the same time the units have been designed to work with smaller loads as well; fully modulating valves have been incorporated which allow the heaters to operate with flow rates as low as 113 to 169 kg/hr depending on the unit [1, 3, 4]. Tankless manufacturers have also begun using electronic ignition thus removing the need for a pilot light and allowing for significant increases in energy

efficiency [1]. Finally, many units are set-up to allow for direct venting which allow the heaters to be installed in a wider variety of locations [1].

Analyses have shown that tankless water heaters can be used for domestic hot water, space heating and combined space and water heating [3]. They have also been shown to be effective in applications where space is limited, such as mobile homes [3]. Tankless units appear especially effective in luxury homes where access to unlimited hot water is highly desired [4]. They have very strong potential in new construction applications where the cost of the heater can be rolled into the mortgage [4]. For retrofit applications, where the cost cannot be included in a mortgage and necessary remodeling may increase costs, gas tankless heaters often have a simple payback period on the order of twenty years. Thus, retrofit is not considered to be a market for tankless water heaters [4].

Some operational and maintenance characteristics of tankless units also decrease their applicability. Tankless units require proper ventilation to start combustion and have an innate lag time associated with bringing the heat exchanger up to the desired set temperature. These delays create a time lag of five to fifteen seconds between the user turning on the hot water and the heater actually bringing water up to the set temperature [3, 4]. Another issue related to the tankless unit is associated with the minimum flow rate; tankless units require a minimum flow of 113 to 169 kg/hr before the burner will turn on [3,4]. These two downsides of tankless heaters create a large potential for wasted water; more water will be consumed before hot water gets to the tap and, in the case of a low flow application, the user may increase the flow rate specifically to engage the heater [5]. The delay period associated with turning on the burner is also known to

cause an effect called the “cold water sandwich” [3]. This occurs when the heater is turned off, leaving hot water in the lines, and turned on again shortly after. The delay period before the burner turns on can result in the heater to releasing some cold water before the heat is re-engaged. This creates a flow of cold water surrounded by hot water [3].

Tankless heaters also have some disadvantages associated with the operating conditions. Most tankless units will not operate during a power failure; electricity is required for the temperature control, flow sensor, vent fan and electronic ignition [3, 4, 5]. This is a major disadvantage relative to storage tank units which have no problem operating without electricity. Another disadvantage associated with tankless heaters is that the incoming water temperature affects the performance of the unit [3]. Cold inlet temperatures (for example, in the winter) mean that the heater cannot heat as much water to the set temperature, and fluctuations in the incoming water temperature can cause control difficulties.

Tankless heaters also require more maintenance than storage tank type heaters. Typical annual maintenance includes sensor inspections, chemical flushing to avoid scale buildup, and cleaning out the filters [3, 4, 5]. Unfortunately, it may be difficult to find qualified professionals to perform this maintenance as the infrastructure associated with tankless units is currently very immature and not many people are familiar with the technology.

Since tankless heaters are commonly used by people who care about energy efficiency and renewable energy it is important to examine how they work with solar hot water systems. Unfortunately, the minimum burner setting theoretically makes them problematic with solar

systems. Examining the specifications of one tankless heater shows that a minimum burner setting and minimum flow rate are 15825 kJ/hr and 113 kg/hr [2]. Under these conditions, with an efficiency of 85%, the water temperature would increase by 28 °C and, assuming a 52 °C set temperature, the highest inlet temperature that the heater could handle would be 24 °C [2]. Since temperatures coming out of solar hot water systems are typically above 24 °C the tankless heater will often be unable to appropriately heat the water at that flow rate [2]. In these cases the burner could turn on at the minimum capacity until the set temperature is exceeded, turn off the burner until the water is unacceptably cold and repeat the process [2]. This event will not occur with tankless heaters employing feed-forward controls. Heaters with feed-forward controls will identify the inability to meet the set temperature and not fire.

Tankless water heaters also have more difficulty with temperature control than storage tank heaters [7]. This difficulty is due to the fact that tankless water heaters must react to changing inlet conditions rapidly whereas storage water heaters merely use the stored thermal mass of the water to reduce and delay the effects of changing inlet conditions. Problems associated with changing inlet conditions include the time lag when adjusting the heat exchanger temperature, the time lag when adjusting the burner output and the fact that rapidly reacting control systems often can be unstable [7]. Another control problem is related to gradual changes in inlet temperature which is very common in applications that include solar preheated water [7].

1.4 Tankless Advantages

Many of the advantages of tankless water heaters center around having higher efficiency than

their storage tank counterparts. By removing the tank and pilot light tankless water heater manufacturers have minimized standby heat losses [3, 5]. The reduction in standby losses achieves a large percentage of energy savings; the Department of Energy (DOE) tests show tankless water heaters typically have an energy factor (EF) that is ~0.82, which is ~0.25 higher than storage tank water heaters [3, 5]. This increased efficiency correlates with lower emissions and thus better indoor air quality and lower external air pollution [5].

Another advantage of tankless heaters is their small size. Typical tankless units have a volume of approximately 0.08 m³ while storage tank type heaters occupy 0.6 m³ [3]. This smaller footprint makes tankless units more flexible to install and especially useful in applications where space is very limited [3, 5].

Other advantages of tankless water heaters are based on the functionality of the unit themselves. Because tankless units do not have a storage tank there is no maximum duration associated with water use; as long as the draw requires less heat than the maximum capacity of the heater tankless units can provide unlimited amounts of hot water [5]. In addition to this luxurious advantage preliminary data indicates that tankless units have the economic advantage of a longer life [5].

One problem comparing tankless and storage tank heaters is that they react differently to draw profiles. Due to their different operation methods the energy factor of a storage type water heater is determined by the total daily load while the energy factor of a tankless unit is determined by the detailed draw profile [4]. Because of this difference it is commonly believed that the current

DOE testing protocol is not appropriate for tankless water heaters as it does not accurately capture the effects of allowing the heat exchanger to cool down and lose heat [6]. Testing has shown that the length of delay between draws has a dramatic impact on the efficiency of the unit; long delays allow the heat exchanger to reach room temperature and dramatically decrease efficiency [6]. It should be noted that the impact on efficiency is highly dependent on the length of the draw with the delay having little effect when draws are much larger in volume than the heat exchanger volume (e.g. over 15.5 L in [6]). In order to quantify the reduction in energy efficiency associated with this cooling effect a tankless heater was tested following the Building America (BA) draw profile [6]. It was determined that the energy factor should be reduced by 8.8% to reflect this difference [6]. However, this approach is a relatively simple method of determining the energy efficiency of tankless water heaters and should be used as a basis for justifying a more rigorous investigation.

There is precedent to the concept that draw patterns affect the overall efficiency of the system. Work has been completed examining the impact of draw patterns on a storage water heater which utilized a tank full of heated water and a heat exchanger through which the domestic hot water passes [8]. Simulation analyses were completed using a modified version of one of the standard storage water heaters in TRNSYS [8,22]. The TRNSYS model was subjected to six different flow patterns with three being devised by the authors and three being commonly accepted European standard profiles [8]. All of the profiles were normalized to a total draw of 180L by increasing the volume of water in each draw proportionately [8]. The results show a minor difference in the performance of the heater; the energy consumed by the storage tank for the different profiles ranged from 7.264 kWh to 7.333 kWh [8]. The simulation results also showed

that the storage tank was unable to meet the load during some draws [8]. The authors concluded that the number and timing of draw-offs impact the performance and energy use of a storage tank heater [8].

Since the rationale for using tankless water heaters is based on energy savings it is important to examine the potential for reduced energy use associated with removing the standby loads of a storage tank water heater. An experiment analyzing the energy use associated with standby loads in storage tank water heaters has been conducted [9]. The study, conducted in 1993, examined the standby use of electric storage water heaters as well as the impact and prevalence of various energy saving measures [9]. The study considered loads for homes in the Residential Standards Demonstration Program (RSDP) and End-Use Load and Consumer Assessment Program (ELCAP) [10]. The results showed an average standby load of 1100 kWh/yr in the RSDP homes and 1200 kWh/yr in the ELCAP homes [9]. It was also found that of all the tested energy savings methods only tank wrap insulation and bottom boards saved a statistically significant amount of energy. The study reported that 41% of studied water heaters are wrapped and 9% have bottom boards [9]. While 1200 kWh/yr is a significant amount of energy to be saved it is uncertain how that estimate from 1993 compares to the current potential for energy savings; the date of this study and low occurrence of insulation on the tanks imply that the savings may be lower now.

1.5 Potential Solutions

Solutions to the tankless problems outlined above are currently being investigated. These solutions include the addition of a small damping tank in the system and a feed-forward control

system.

The use of a very small tank in the system could solve several of the problems associated with tankless water heaters. In one instance a small storage tank (approximately 1.9 L) inside the unit is kept at the desired temperature instead of controlling the temperature of the water coming out of the heat exchanger [2]. Since the tank would be very small relative to the tank used in storage tank systems the losses would also be relatively small [2]. The addition of the tank should remove the minimum flow rate by constantly having water available at the set point, reduce the delay time to hot water and dampen any oscillations associated with solar hot water system [2]. An external tank can be used; up to 10 gal max has been used [2, 14].

1.6 Rinnai Water Heater Operation

There are several control algorithms in the Rinnai units making them some of the most sophisticated tankless water heaters [13]. These algorithms are included to improve the operation of the device; some are intended to ensure that the user receives hot water at set temperature without serious fluctuations, and others govern how the heater operates in an attempt to optimize efficiency. To better understand how all these algorithms affect heater operation a description of the heaters operation is presented in this section.

Figure 1 shows a schematic diagram taken from a Rinnai technical description which displays several of the parts and sensors used in controlling their tankless water heaters [13].

The first stage in the operational process consists of identifying that there is a water flow which

is sufficient for the heater to operate [13]. This is accomplished by the water flow sensor which is located just after the water inlet. The water flow sensor is a pulse generating flow meter [13]. When a draw begins, this flow meter signals the main control board which identifies the beginning of a flow and whether or not the flow is large enough for the heater to fire [13].

Once a flow which surpasses the minimum flow rate is detected, the control board engages the combustion fan [13]. The combustion fan is a variable speed device which is controlled by varying the magnitude of DC supply voltage [13]. At the start of a draw the fan is used to pre-purge the combustion chamber before engaging the burners [13]. During a draw the combustion fan speed is monitored and adjusted to control the air/gas ratio in an attempt to ensure good combustion [13].

After the pre-purge process is complete the burners begin combusting gas. The initial gas flow rate is determined by a feed-forward calculation using the set temperature and flow rate of the water [13]. The heater then rapidly switches to a feedback control loop and identifies the correct natural gas flow rate based on how much the water temperature increased at the previous natural gas flow rate [13].

During operation the control board uses the combustion fan speed, gas flow rate and water flow rate to control the temperature of the outlet water [13]. The goals of this control process are to ensure that: (i) the heater operates at high efficiency, (ii) the outlet water temperature is very close to the set temperature and (iii) the user receives a satisfactory water flow rate [13]. However, the heater does control water flow rate and at times reduces water flow rate to ensure

that the set temperature is met when the flow rate exceeds the heaters maximum capacity [13].

If the need arises the water flow rate is reduced by means of the water flow control device which is located just upstream of the water flow sensor [13]. This device is engaged when the heater is unable to meet the set temperature at a given flow rate; in which case, the water flow rate is reduced until the heater does meet the set temperature [13].

The end of a draw is signaled by the water flow sensor [13]. Since there is no longer any water flow, the sensor ceases sending pulses to the control board resulting in the start of the shut down procedure [13]. At this point the gas modulating valve is closed and combustion ceases [13]. After a draw ends, the combustion fan is operated for a short period of time [13]. The combustion fan continues to operate as a means of increasing the speed of sending out hot water in cases of rapid on/off cycles in the hot water draw; by purging the air in the combustion chamber at the end of a draw, it is possible to avoid the pre-purge cycle at the beginning of a draw [13].

1.7 Recommended Research Needs

There are several tasks which others have recommended for future work to help increase the market penetration of tankless water heaters. First, the problem of having poor knowledge of typical draw patterns needs to be addressed [4]. Attaining a better understanding of real world draw patterns is necessary to determine the effects that draw patterns have on the operation and performance of tankless water heaters [4]. Second, there needs to be better data regarding how

tankless units react to different draw patterns [4]. It is suggested that the best approach to obtain this data is to test several different heaters against several different draw patterns [4]. Finally, the development of a computer simulation tool would be useful for evaluating how draw patterns affect the performance of tankless heaters without costly experimentation [4]. More specifically, a multiple node model which is based on experimental data identifying the behavior of specific tankless water heaters through parameter identification would greatly improve the understanding of these devices [14].

1.8 Thesis Sections

As tankless water heaters are becoming more widely used in the United States it becomes increasingly important to answer several questions about their performance. Currently there has been no research examining the standard functioning of these devices; questions still abound regarding how much variation there is in outlet temperature when there are sudden changes in flow rate, there are still questions regarding the minimum flow rate and it is unknown if steady state efficiency is impacted by any draw parameters. In addition to these most basic questions, there are also the issues of how tankless water heaters react to preheated inlet water associated with solar hot water systems, how the draw profile impacts the in-use efficiency of the devices and what can be done to overcome the disadvantages of these heaters. This thesis outlines the methods used to answer several questions and presents the results obtained from these efforts.

Chapter 2 describes previous water heater modeling and the creation of a multiple-node model which was developed to address the issues of poor tankless heater modeling capabilities. The chapter also provides information regarding a theoretical verification of the new multiple node

tankless heater model. Chapter 3 presents information on the experimental set-up including measurement uncertainties and calibrations. Chapter 4 describes how the experimental set-up was used for each test, the calculations used in each experiment and how the measurement uncertainties impact results. Chapter 5 contains results from the experiments. In Chapter 6 the model is validated against experimental data. Chapter 7 discusses a series of simulation studies using the model to determine the impact of characteristics of draw profiles on the draw profile efficiency of the tested tankless heater. Chapter 8 presents conclusions from this work as well as recommendations for future work.

Chapter 2: Multiple-Node Model for Tankless Water Heaters

The focus of this thesis is creating a multiple node tankless water heater model in TRNSYS [22]. TRNSYS is a simulation program which consists of individual components. The components can be linked together to pass variables and create an overall system.

2.1 Previous Water Heater Modeling

There are numerous models used to simulate storage tank water heaters [11, 20, 21]. However, there is only one preliminary reported effort at modeling tankless water heaters in any detail [10].

2.1.1 TRNSYS Water Heater Models

TRNSYS includes components for simulating several different water heaters. These models are of particular interest since they provide a starting point for working on a detailed tankless heater model. The most relevant models are the multiple node storage tank water heater and the single node tankless water heater models [10,11].

2.1.1.1 Type 940: Single Node Tankless Water Heater

An initial attempt of modeling tankless water heaters has been performed [14]. This modeling attempt focused on creating a single node heat transfer model utilizing feedback controls [14].

The model was compared against both theoretical calculations and experimental data; however, the validation process was weak due to the fact that the experimental data used was data from an unrelated experiment rather than data intended for validation [14]. Particularly problematic was the lack of measurement of ambient temperature. Questionable assumptions of ambient temperature were required for identification of the ambient losses. The simulation tool was then used to estimate the efficiency in realistic draw scenarios and how the heater would respond to situations with solar preheated water and with a small tank in the mix [14]. The results implied that the overall efficiency of a tankless water heater is about 8% lower than the steady state efficiency, and that the addition of a small tank could reduce the oscillations which were considered to be a potential problem of combining gas tankless heater utilizing feedback control with solar hot water systems [14].

The single node model was released as Type 940 in TRNSYS [10].

The model is based on a simple energy balance for a heat exchanger. It includes energy inputs from the burner, pilot light and entering fluid as well as energy losses to the departing fluid and surrounding air. It also incorporates the thermal mass of the heat exchanger to account for transient effects. The governing equation used in the model is displayed in Equation (1).

$$Cap \frac{dT_{Fluid}}{dt} = \eta_{Conv} \gamma \dot{Q}_{Rated} + \eta_{Pilot} \dot{Q}_{Pilot} - \dot{m} C_p (T_{Set} - T_{In}) - UA(T_{Set} - T_{Air}) \quad (1)$$

Equation (1) follows from the one node assumption. The entire heat exchanger has a constant temperature equal to the outlet water temperature.

In order to easily solve the governing equation for any timestep Equation (1) is expressed in the form displayed in Equation (2).

$$\frac{dT_{Fluid}}{dt} = a * T_{Fluid} + b \quad (2)$$

The expressions for a and b are shown in Equations (3) and (4).

$$a = \frac{-(\dot{m}C_p + UA)}{Cap} \quad (3)$$

$$b = \frac{\eta_{Conv} \dot{Q}_{Rated} + \eta_{Pilot} \dot{Q}_{Pilot} + \dot{m}C_p T_{In} + UA T_{Amb}}{Cap} \quad (4)$$

Equation (2) can easily be solved when the thermal conductivity and burner efficiency are constant and do not vary with temperature.

Type 940 features individual time-steps, subdividing the overall system time as needed to increase the precision of the model based. For example, if the water heater was to turn on at the beginning of a 15 minute time step the heater would operate at 100% capacity for the entire 15 minutes without the sub-time step method. Since this approach would produce inaccurate results the model was designed with the capability to follow the actual dynamic operation within a full time step. At the end of a full time step average values are given as outputs.

Some parameters are included to give the user more input over the controls so that the model

more accurately simulates different heaters. One parameter is the minimum flow rate for activation. If the water flow rate is below a certain level the heater will not turn on. This is an important feature to consider in the model as very few tankless water heaters will operate at all flow rates. Another is a “time delay” parameter which is designed to imitate the delay before the burner in a tankless water heater engages. The primary cause of this delay is waiting for the ventilation fans to provide sufficient ventilation to dissipate the combustion products.

The user can also specify the electrical energy consumed during standby and heating modes. These two input parameters are needed to determine the amount of electrical energy used over the course of the year.

The control logic for this model is quite complex. It first establishes whether or not the unit should fire based on previous activity of the device, fluid flow rate and current temperature. If it is determined that the unit should be on, the model proceeds to determine the appropriate control setting for the burner by examining the impact of different assumptions related to the outlet temperature. If the proper conditions for the unit to fire are not met the control logic determines whether the system should wait for the temperature to decrease or simply remain off until the next time step begins.

Three flowcharts detailing the control logic considered in the model Type 940 are shown in Figure 2, Figure 3 and Figure 4.

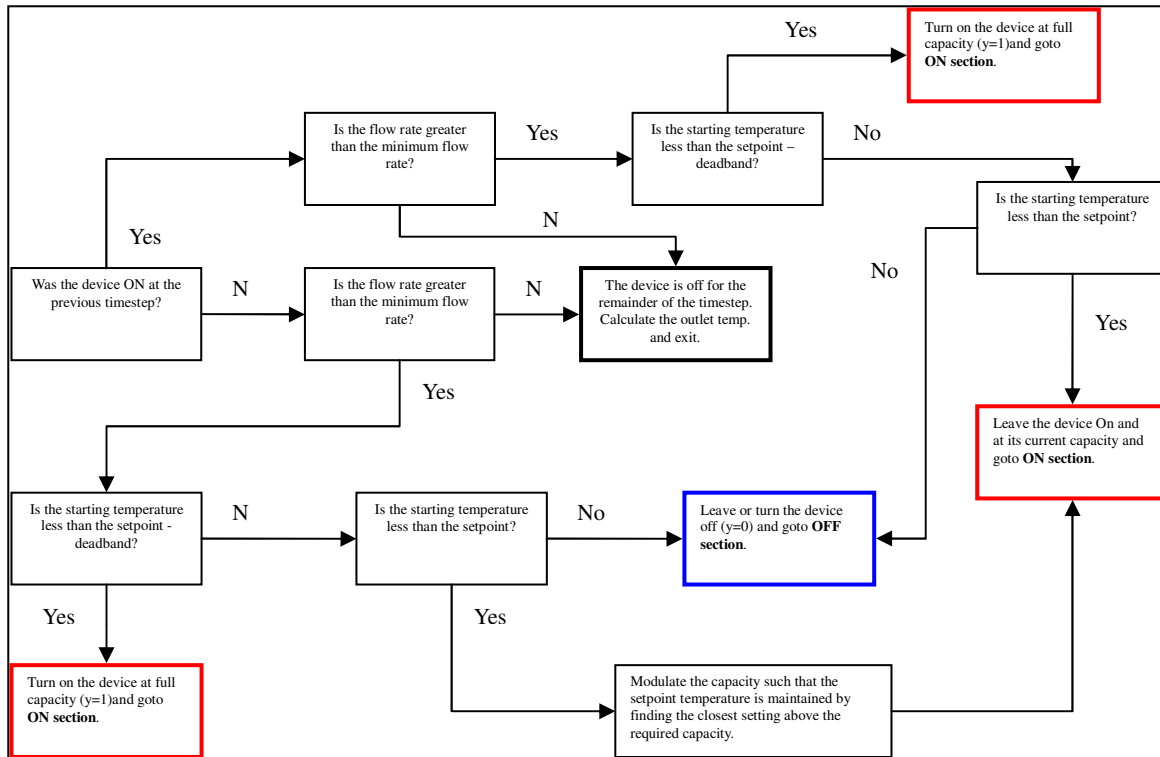


Figure 2: Flowchart of Initial Control Logic in Type 940 [10]

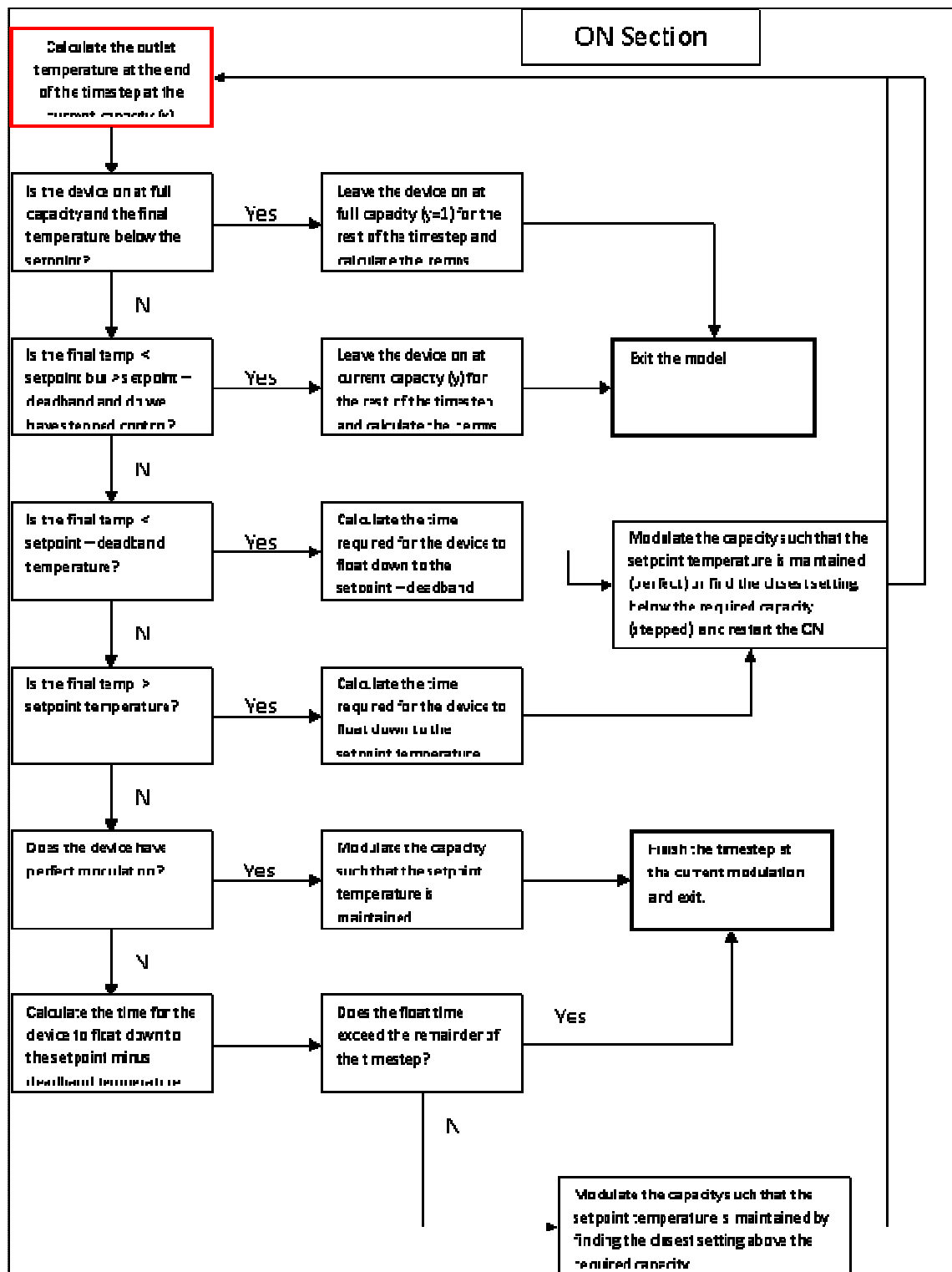


Figure 3: Flowchart of Control Logic when Heater is on in Type 940 [10]

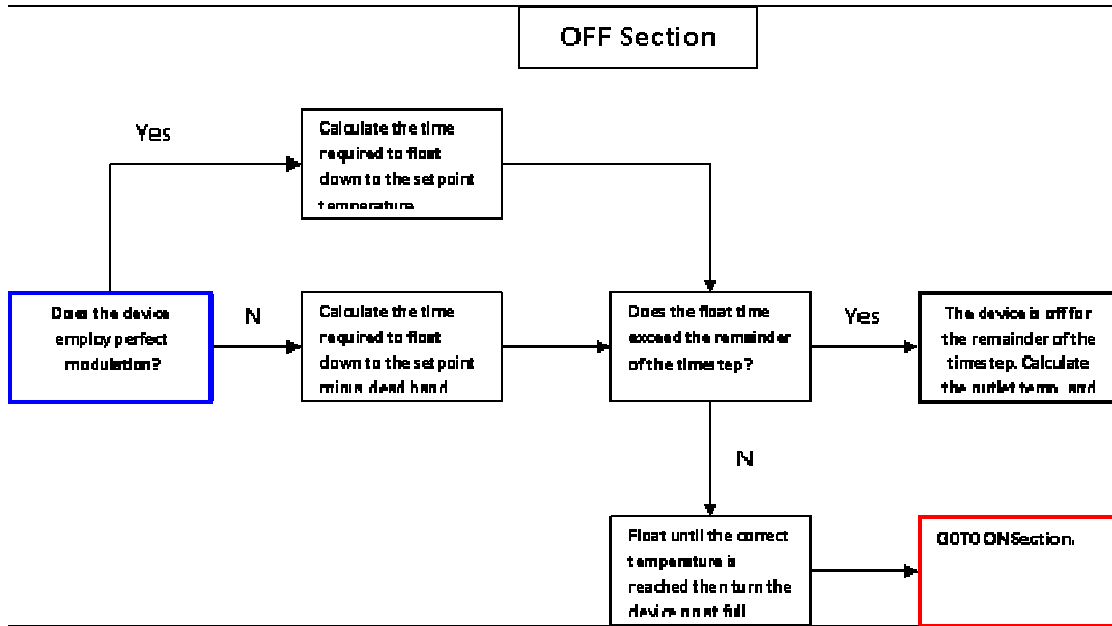


Figure 4: Flowchart of Control Logic when Heater is Off in Type 940 [10]

Once actions and calculations have been completed over one time step, the model begins to calculate the averages values of several parameters used in that time step. The outlet temperature of the fluid, which varies with each sub-time step, is averaged for the complete time step. The rate at which gas is consumed in each sub-timestep varies depending on whether or not the main burner is firing as well as whether or not the heater has a pilot light. The amount of gas used over the course of the time step is also averaged and passed to TRNSYS. Determining these values allows for easy calculation of the heat lost to the surroundings, stored in the heat exchanger and delivered via the outlet fluid. This approach allows for an energy balance check on the system.

Some factors limiting the calculation accuracy of this model have been identified. Most importantly, the assumption that the heat exchanger is operating at a constant temperature equal to the outlet water temperature is a significant modeling simplification. The heat exchanger

temperature and water temperature will both vary significantly along the length of the tube. In order to model this effect, multiple nodes would be necessary to improve the prediction accuracy of Type 940. It is not clear whether or not this improvement has an impact on the model's estimations for the average energy demands; however, it is clear that the one-node model does not accurately predict the outlet conditions or transient effects. Moreover, it is also entirely possible that the efficiency of the burner varies significantly with temperature. This behavior would drastically change the differential equation [i.e. Equation (2)] which needs to be solved. Also, there is reason to believe that tankless water heaters sometimes control fluid flow rate during transient stages to provide a more appropriate outlet temperature but the current model does not take this feature into account. Whether or not this is significant should be analyzed and potentially added to the models control logic.

As can be seen in Figure 3 Type 940 generally functions by running at full capacity for the full time step, checking to assess if the outlet temperature is at the set point then, if necessary, calculating the time of operation at full capacity to reach the set point, operating for that amount of time, then identifying the steady state heat requirement and control constant. This series of actions is explained more via the following equations.

The first step is to solve Equation (2) for a full time step at maximum capacity. This is represented by assigning a "1" to γ in Equation (4). The full time step is a user input in TRNSYS and it typically 5 minutes or less when wanting realism on draw profiles. The equation used to solve for the final temperature is presented in Equation (5).

$$T_F = T_I * e^{a*\Delta t} + \frac{b}{a} * e^{a*\Delta t} - \frac{b}{a} \quad (5)$$

After completing the calculation of the final temperature, the program determines if the final temperature is higher than the set temperature. If it is not the simulation tool progresses to the next time step. If it is, the simulation tool calculates a new sub time step based on the calculated time for the outlet water to reach set temperature. The sub time step is calculated using Equation (6).

$$\Delta t = \frac{\ln\left(\frac{T_F + b/a}{T_I + b/a}\right)}{a} \quad (6)$$

After identifying the appropriate sub time step using Equation (6), Type 940 proceeds to re-perform the calculation from Equation (5) with the shorter Δt . This calculations results in an outlet temperature which matches the set temperature at the end of the sub time step. The next step in the typical progression through the logic is to calculate the steady state heat demand and control constant. This is done by using the formulas presented by Equation (7) and Equation (8).

$$\dot{Q}_{Required} = \dot{m}C_p * (T_{Set} - T_{In}) + UA * (T_{Set} - T_{Amb}) \quad (7)$$

$$\gamma = \frac{\dot{Q}_{Required}}{\dot{Q}_{Rated} * \eta_{Conv}} \quad (8)$$

Having calculated the necessary control constant to keep the water at the set temperature Type

940 proceeds to use this control constant for the remainder of the TRNSYS time step.

An error in how the Type 940 model handles efficiency has been identified. The input value of efficiency is intended to be a very straightforward efficiency ratio based on the energy transferred to the water compared to the energy put into the heater in the form of natural gas. This efficiency is expressed mathematically using Equation (9).

$$\eta = \frac{\dot{m}C_p(T_{Set}-T_{In})}{\gamma\dot{Q}_{Rated}} \quad (9)$$

The problem is that the model does not define the heater efficiency in this manner. It uses the input system efficiency as a burner efficiency and then subtracts heat losses to the environment. This fact was discovered by solving the governing equation for efficiency. The effective efficiency as it is used in Type 940 is presented by Equation 10.

$$\eta = \frac{\dot{m}C_p(T_{Set}-T_{In})+UA(T_{Set}-T_{Amb})}{\gamma\dot{Q}_{Rated}} \quad (10)$$

This efficiency is the same as the intended efficiency with the addition of a term representing the environment losses. The problem with this definition is that the intended input efficiency already takes environment losses into account; by comparing the effective heat transfer into the fluid to the heat entering the unit losses to the environment are already accounted for. Those losses show up in the efficiency by reducing the amount of heat to the fluid. On the other hand, the efficiency implied in the governing equation of Type 940 expects that the environmental losses will not

have been removed. Type 940 ends up removing that heat later. As a result, the current simulation tool effectively double counts the environmental losses when the efficiency is input as the observed draw efficiency.

2.1.1.2 Type 4: Multiple Node Storage Tank Water Heater

TRNSYS also incorporates a model, Type 4, for use in simulating stratified fluid storage tanks [11]. The main area of interest in Type 4 is that of the use of multiple nodes. It uses a nodal design to determine the flow, heat transfer and temperature of the fluid at the node locations in the tank for each time step. Theoretically this modeling approach could be combined with the model used for Type 940 to produce a multi-node tankless water heater model. There would still be other issues to address focusing on the control and potentially the solution methods; however, it would provide a good starting point.

The Type 4 model begins by assuming that the fluid streams flowing between nodes are fully mixed before actually flowing to each other. This assumption implies that there is a constant flow rate in the tank, and the flow from one node into the next is at the instantaneous node temperature. Figure 5 provides a visual for how this assumption works.



Figure 5: Flow in TRNSYS Type 4 Stratified Storage Tank [11]

There are two flowpaths depicted in Figure 5. \dot{m}_1 and \dot{m}_2 represent hot water flow through an auxiliary heater (e.g. a solar water heater) for each node. \dot{m}_3 and \dot{m}_3 represent the flow caused by a draw for each node.

Based on the assumption mentioned above, the model adds flows 1 and 4, and adds flows 2 and 3 to analyze the overall flow rate between nodes. It also assumes that the temperature of any node is constant across the node. As a result, the temperature of all water flows exiting a node is the same. This allows for developing a simple analytical energy balance based on Equations (11) and (12).

$$mC_p \frac{dT_n}{dt} = (\dot{m}_1 - \dot{m}_3) * C_p * (T_{n-1} - T_n) \text{ if } \dot{m}_1 > \dot{m}_3 \quad (11)$$

$$mC_p \frac{dT_n}{dt} = (\dot{m}_3 - \dot{m}_1) * C_p * (T_{n+1} - T_n) \text{ if } \dot{m}_3 > \dot{m}_1 \quad (12)$$

The assumption of constant temperature in any given noden allows for the application of a simple energy balance to each node. The energy balance equation is expressed by Equation (13).

$$\begin{aligned}
mC_p \frac{dT_n}{dt} &= \alpha_n \dot{m}_h C_p (T_h - T_n) + \beta \dot{m} C_p (T_{In} - T_n) + UA(T_{Amb} - T_n) \\
&+ \gamma_n (T_{n-1} - T_n) C_p \text{ if } \gamma_n > 0 \\
&+ \gamma_n (T_n - T_{n+1}) C_p \text{ if } \gamma_n < 0 \\
&+ \dot{Q}_n \text{ for } n = 1, \#_{Node}
\end{aligned} \tag{13}$$

If $\gamma > 0$ the first term should be included in the equation and if $\gamma < 0$ the second term is correct. This is because these two terms represent the heat transfer caused by water flows and only term is needed as determined by finding the direction of water flow. The other terms represent the rate of change of temperature in the node, the energy entering into the node from the hot water inlet, the energy entering the node from the cold water inlet, the rate of energy lost to the environment through that node and the rate of energy added from a heating coil in that node.

In order to combine the multi-node analysis into Type 940 to improve the tankless water heater model some changes would be required. The terms characterizing the impacts of entering flow can be greatly simplified or removed as there is one singular inlet for a tankless heater. The portion describing the impacts of water flowing from one node to another could also be simplified; flow only progresses in one direction in a tankless water heater.

It is also necessary to make some changes to Type 940. Most importantly, the efficiency issue has to be addressed.

2.1.2 First Principles Models

In 1984, Maxwell completed a Ph.D. dissertation focusing on developing a mathematical model of tankless water heaters [12]. At the time tankless water heaters were mainly used for pool heating which required a much simpler device. Since demand for pool heating tends to be much steadier than demand for domestic hot water use the controls of the system and minimum flow rate were non-issues. Maxwell mostly focused on developing mathematical models suitable for steady state conditions.

Maxwell's model consisted of the following five components: the wall, the burner tray, the heat exchanger, the flue loss and detailed radiation from gas to surface and surface to surface. Each model started with the steady state energy balance; the energy entering a control volume equaled the exiting energy and no energy was stored. After the initial energy balance was defined the differential equations were solved by using finite difference equations.

This model delves into detailed heat transfer equations describing all of the processes occurring in the heater. Efficiency is predicted based on the calculated heat transfer. On the other hand, the modeling effort in this thesis focuses on a simpler model with experimentally derived parameters. All of the detailed nuances of the heat transfer processes are subsumed into the loss coefficient and measured efficiency. The specifics of the detailed model will be omitted.

2.2 Modifying TRNSYS Type 940

For the work here the Type 940 module is modified and extended to handle a multiple node model for tankless water heaters. In addition some redesigning of the control logic is considered necessary to handle the multiple node model.

The new model divides the heat exchanger into a user-defined number of nodes. It proceeds to track the temperature of the water as it passes through each node. Input energy from the burner is divided and applied evenly over the total number of nodes. Environmental losses and thermal mass impacts are included in the differential equation making them unique for each node. These impacts are used to determine the temperature of the water exiting the node which is then used as the temperature for water entering the next node.

The ‘a’ and ‘b’ terms in the differential equation were calculated as needed in the new component. The coefficients ‘a’ and ‘b’ are modified by adding the conduction heat transfer between nodes. The equations used to calculate ‘a’ and ‘b’ in the multiple node calculations are presented in Equation (28) and Equation (29).

$$a = \frac{-1}{Cap} * (\dot{m}C_p\#Node + UA + \frac{2kA_{Tube}\#Node(\#Node-1)}{L}) \quad (14)$$

$$b = \frac{1}{Cap} * (\eta_{Conv}\dot{Q}_{Rated} + \dot{m}C_pT_{In}\#Node + UAT_{Amb} + \frac{kA_{Tube}\#Node(\#Node - 1)}{L}) * (T_{n+1} + T_{n-1}) \quad (15)$$

Some equations which deal with the overall energy flow were changed as well. For instance, equations to estimate environmental losses are modified. The environmental losses are estimated using Equation (31).

$$\dot{Q}_{Env} = UA(\bar{T}_{HX} - T_{Amb}) \quad (16)$$

Some of the outputs from the model have also been changed. In Type 940, all of the outputs are given as heat transfer rates at the end of the time step. The main problem associated with this output method is that it did not account for transients within each time step. This fact, combined with the control logic in Type 940, means that any time a draw started the heater would run at 100% capacity until reaching the set point before settling down at the steady state operation parameters and the energy associated with the time spent at 100% capacity would be neglected. To correct this problem some of the heat transfer rates have been converted into average heat transfer rates rather than reporting the rate at the end of the timestep. To detail how this process is performed the equations used to estimate the total delivered energy are shown in Equation (32) and Equation (33).

$$Q_{Del,Now} = \dot{m}C_p(\bar{T}_{Exit} - T_{In})\Delta t_{Now} \quad (17)$$

$$\dot{Q}_{Del} = \frac{\sum Q_{Del,Now}}{\Delta t_{TRN}} \quad (18)$$

Equation (17) is used to find the energy output during any given sub-time step (Δt_{Now}). The outlet temperature is an average temperature from the final node in the heat exchanger. In Equation (17) the term Δt_{Now} represents the time period of the current sub-time step. This addition to the equation allows the simulation to convert the calculated heat transfer rate to a total energy over the sub-time step. Equation (18) then proceeds to sum the energy delivered to

the water over a full time step by combining all of the $Q_{Del,Now}$ terms from each individual sub-time step and dividing by the total timestep to create a time-based average heat transfer rate for the time step.

This method of calculating the energy consumed over a time step rather than displaying the heat transfer rate at the end of a time step was used for the energy delivered to the water, the energy combusted by the water heater and the total amount of energy entering the heater. No method for totalizing sub-time steps was needed for the energy stored in the heat exchanger; since the energy stored in the heat exchanger is simply a comparison between the initial and final temperatures a single algorithm was used. It is displayed in Equation (34).

$$Q_{Stored} = Cap(\bar{T}_F - T_I) \quad (19)$$

In Equation (19) the capacitance refers to an experimentally derived capacitance of the heat exchanger, the initial temperature refers to the temperature of the heat exchanger at the beginning of the simulation and a location average temperature of the heat exchanger at the end of the time step is used for the final temperature. This equation computes the change of energy stored in the heat exchanger from the start of the simulation.

The output describing the heat loss to the environment is calculated by means of a time and location weighted average temperature. During each sub-time step a calculation is performed to estimate the location-based weighted average temperature of the heat exchanger. Since this process is repeated for each sub-time step a time based weighted average can be estimated by

multiplying each location based weighted average by the fraction of a time step each sub-time step represents and summing them. The equations used for this calculation process are shown in Equations (35), (36) and (37).

$$\bar{T}_{Now} = \sum_0^{\#Node} \frac{\bar{T}_n}{\#Node} \quad (20)$$

$$\bar{T}_{HX} = \sum_0^{\#Node} (\bar{T}_{Now} * \frac{\Delta t_{Now}}{\Delta t_{TRN}}) \quad (21)$$

$$\dot{Q}_{Env} = UA(\bar{T}_{HX} - T_{Amb}) \quad (22)$$

In addition to modifying the calculation methods used for the preceding outputs several new outputs were reported based on these calculations. These new outputs include system efficiency for the heat exchanger in each time step, a cumulative calculation of energy delivered to the water for the entire simulation, a cumulative calculation of energy entering the tankless heater for the entire simulation and a cumulative efficiency for the entire simulation.

The equation for system efficiency in a time step is given in Equation (38).

$$\eta_{\Delta t_{TRN}} = \frac{\dot{Q}_{Del}}{\dot{Q}_{In}} \quad (23)$$

This equation compares useful energy output to total input energy. The useful energy is represented by the numerator which multiplies the average heat transfer rate by the timestep to

find a cumulative heat transfer and the total heat consumption is identified by the denominator which uses the same process.

The other three outputs added to the component are all based on summations of energy use over the course of the entire simulation. The cumulative efficiency is acquired via the same calculation as the time step efficiency with the only difference being that it uses the cumulative values for the energy delivered to the water and the total gas energy entering the heater instead of the totals for an individual time step.

The control logic from Type 940 had to be changed because multiple nodes are used. Originally the model would operate at 100% capacity until the heat exchanger, and outlet water reached the set temperature. After reaching the set temperature it would calculate the required control constant to hold steady state operating conditions. Unfortunately, the transient effects within a multiple-node model cause issues when using this simple control scheme. Not all of the nodes require the same amount of time to reach their steady state temperature which results in overheating associated with some nodes. Overheating early nodes causes the final node to be above the set point in the steady state calculation. This situation results in significant temperature fluctuations which are not real.

The control algorithm has been modified to overcome this issue. The first step in the new algorithm is to identify the steady state profile and control constant. This is done at the beginning of each TRNSYS time step. The algorithm used is very simple. It begins with the assumption that the heat exchanger is at steady state and calculates the control constant necessary

to continue that operation. This is done by solving the equation identified in Equation (1). At the same time, a linear temperature profile for the nodes in the heat exchanger is assumed. This is done by identifying the temperature difference between nodes using Equation (39) and progressively increasing the temperature of the nodes by this temperature difference as they progress through the heat exchanger.

$$\Delta T = \frac{(T_{Set} - T_{in})}{\#Node} \quad (24)$$

The correct steady state and temperature values are then found through an iterative process. The final temperatures of the nodes, assuming that the time step is nearly infinite, are calculated for a given control constant. The temperature profile is then checked for convergence using two criteria. First, the temperature of each node is checked against its' temperature during the previous iteration. The intent of this set is to check for convergence by making sure that no node is changing by more than some tolerance (e.g. 0.01 °C). Once the profile achieves convergence the outlet temperature is checked against the set temperature. If the set temperature is within 0.01 degrees Celsius it is considered correct and the program moves on. If it is not within tolerance then a new control constant is calculated. The algorithm used to identify a new control constant is shown in Equation (40).

$$\gamma_{i+1} = \gamma_i * \frac{T_{Set} - T_{Exit}}{T_{Set} - T_{In}} + \gamma_i \quad (25)$$

Should the calculated control constant be greater than one, indicating that the heater would

operate above its' maximum capacity, the control constant is set to one. Once the iterative process is completed the identified control constant is saved as the steady state control value.

After identifying the steady state solution the code moves on to analyze the transient stages of calculation. This will occur any time there is a change in operating parameters in the heater, such as when the heater is first turned on. Type 940 used a guess and check strategy. It originally operated at full capacity for the entire TRNSYS time step then examined the outlet final temperature. If the final temperature was too high it would calculate a shorter time step, and if the final temperature was either on the set temperature or below the set temperature it would move on to the next time step.

The new control algorithm was designed to be quite simple and more representative realistic operation of tankless water heaters. Since tankless water heaters do not operate at full capacity when bringing the heat exchanger up to temperature it was determined that scrapping the Type 940 control logic and starting over would be more appropriate than modifying it. The current algorithm assumes that the heater operates at the steady state control constant and accepts the fact that it will take longer to reach the set temperature than if a higher burn rate were used during the transient period.

Another change to the control logic of Type 940 focused on adding the water flow rate control of tankless water heaters. As was mentioned in the literature review, Rinnai heaters have a water flow control device which they use to reduce the water flow rate in order to avoid surpassing the capacity of the heater. Control logic to emulate this process was added to the simulation tool.

The process was simple; if a situation arose where the steady state control constant had to be greater than one, indicating that it needed more heat than could be provided, the water flow rate corresponding to the maximum heat capacity was calculated. This was done using Equation (41).

$$\dot{m} = \frac{\dot{Q}_{Rated}\eta - UA(\bar{T}_{HX} - T_{Amb})}{c_p(T_{Set} - T_{In})} \quad (26)$$

2.3 Model Verification Analysis

As part of the project the multiple node TRNSYS model was verified against analytical solutions of simple problems. This chapter includes a series of simulation results comparing several values to theoretical calculations. A series of physical tests comparing the model results to physical results are presented in Chapter 8.

Several tests allowing the TRNSYS model to be compared to the steady state calculated values based on identical inputs were performed. These tests are all intended to determine the impact of some fundamental parameters and to compare the TRNSYS model to an energy balance of the system. These tests range from extremely simple to somewhat more complex; however, the complexity of these tests was limited by the ability to compare them to hand calculations so they are all based on predictable conditions and steady state output. A description of each of the tests is presented in the following sections.

2.3.1 Steady State Efficiency and UA Values

The first test was a simple calculation to ensure that the input efficiency parameter is used correctly and that variation of the UA value has the expected impact. The test was conducted by running short simulations with a conversion efficiency of 82% and a varying UA value. In the model efficiency is defined as the rate at which heat is added to the system relative to the rate at which fossil energy enters the system while the UA value represents the heat transfer coefficient dictating the rate at which heat transfers to the environment. This definition implies that system efficiency, calculated by the ratio of heat entering the water to heat entering the system, differs from the input efficiency and varies with changes in UA values.

When performing these tests the model was considered to provide correct results if the conversion efficiency was equal to the input value, if increasing UA values showed an increase in heat lost to environment as well as a reduction in system efficiency and the outlet temperature was equal to the set temperature. All TRNSYS outputs were also checked against theoretical calculations to ensure that the model is behaving according to theory.

All of the tests were conducted with a 300 kg/hr flow rate, C_p of 4.19 kJ/kg-K, inlet temperature of 15.6 °C, environmental temperature of 20 °C, set temperature of 55 °C, a capacitance of 10 kJ/K and 82% conversion efficiency. The tests were conducted with low UA values and high UA values to determine the impact of that parameter. The number of nodes also varied to ensure that the model was converging properly with increased number of nodes. Table 2 shows the inputs (U, A, number of nodes) which were used for each test, as well as the average temperature of the heat exchanger in each test. The average temperature of the heat exchanger was taken from

TRNSYS calculations. The heat transfer rates both from TRNSYS and theoretical calculations are shown in Table 3. The resulting errors are presented in Table 4. Table 5 shows the steady state conversion efficiency to allow a comparison against the input conversion efficiency.

Table 2: Inputs and Average Heat Exchanger Temperature for Each Test

Test Number	U (kJ/(hr-m ² -K))	A (m ²)	Number of Nodes	T _{ave} (°C)
1	0.0002	9*10 ⁻⁷	5	39
2	204	13.9	5	44.8
3	0.0002	9*10 ⁻⁷	1	55
4	204	13.9	1	55

Table 3: Heat Transfers from TRNSYS and Theoretical Calculations for Each Test

Test Number	Q _{in,c} (kJ/hr)	Q _{in,T} (kJ/hr)	Q _{del,c} (kJ/hr)	Q _{del,T} (kJ/hr)	Q _{env,c} (kJ/hr)	Q _{env,T} (kJ/hr)
1	60804	60419	49859	49525	0	0
2	146919	146588	49859	49525	70614	70625
3	60804	60419	49859	49525	0	0
4	182386	182007	49859	49525	99698	99702

Table 4: Percent Error Associated with Table 2

Test Number	Q _{in} (% Error)	Q _{del} (% Error)	Q _{env} (% Error)
1	-0.63	-0.67	0.00
2	-0.23	-0.64	0.02
3	-0.63	-0.64	0.00
4	-0.21	-0.64	0.00

Table 5: Conversion Efficiencies at Steady State Conditions

Test Number	System Efficiency
1	0.82
2	0.34

3	0.82
4	0.27

The values for the average temperatures presented in Table 2 imply that the model correctly accounts for the increased number of nodes. Both tests incorporating multiple nodes showed an average temperature of the heat exchanger that is below the outlet temperature. This is only possible because there are multiple nodes each exhibiting different temperatures for the simulation to average, and so did not occur in the one node simulations which each showed an average temperature equal to the outlet temperature.

The results in Table 3 are mainly used to estimate the calculation errors reported in Table 4. One check used in each test was to calculate the percent error in the simulation for the natural gas inlet rate, the rate at which heat is delivered to the water and the rate at which heat is lost to the environment. The results shown indicate that the model is working correctly; the largest error is only -0.67%.

Table 5 summarizes the calculated system efficiencies in each test. The system efficiency was calculated by comparing the rate at which heat is delivered to the water to the rate at which energy enters the heater per equation (38). Since the conversion efficiency in the simulation was set to 0.82 a test with no environmental losses would show a conversion efficiency of 0.82 while a test with environmental losses would show a lower efficiency. This is indeed the case as is depicted in Table 5; tests 1 and 3, which incorporated exceedingly small U and A values, both reported conversion efficiencies of 0.82 while the conversion efficiencies were significantly lower for tests with high U and A values. Also, the test with only one node and high UA showed

a lower efficiency than the test with five nodes and high UA indicating that the conversion efficiency was correctly decreased in accordance with the higher average heat exchanger temperature.

2.3.2 Flow Rate Below Minimum Simulations

Tankless water heaters, having a minimum flow rate at which they can operate, may have idle time where they are not operating while water is flowing through them. Because there is potential for this condition to happen in a home it is important to ensure that the model simulates these conditions correctly. Several tests were performed to ensure that the results of simulations match expectations based on thermodynamic principles. Tests were performed with a minimum flow rate setting of 113 kg/hr and an inlet flow rate of 56 kg/hr. Tests were performed with both no pilot light and a pilot light with an efficiency of 80% and a capacity of 211 kJ/hr. The inlet temperature was always 15.6 °C, and environment temperature set at 20 °C. The simulated U value was held constant at 19 kJ/hr-m²-K. All simulations were performed with 20 nodes.

When running these simulations the outputs of interest were temperature and heat transfers. When the system did not include a pilot light the only heat transfer would take place with the environment. Specifically heat delivered to the water should be the same as heat lost to environment. Also, since the temperature entering the heater was colder than the environment temperature, the temperature entering the unit should be the coldest, followed by the outlet temperature and finally the ambient temperature. Simulations including a pilot light were also quite straightforward. The heat to the fluid should be 211 kJ/hr due to the capacity and efficiency of the pilot light. In that case it was expected that the outlet temperature would be

higher than the ambient temperature as there was an additional source of heat coming from the pilot. Table 6 describes the temperatures and the variables that were changed for each test. Table 7 depicts the heat transfer rates calculated by both TRNSYS and theoretical calculations. Table 8 depicts the percent errors for the energy flows provided in Table 7.

Table 6: Variables and Temperatures in Below Minimum Flow Rate Tests

Test Number	Q _{pilot} (kJ/hr)	A (m ²)	T _{in} (°C)	T _{out} (°C)	T _{ave} (°C)
1	0	13.9	15.6	20	19.6
2	0	13.9	20	20	20
3	211	0.09	20	20.7	20.4
4	211	0.09	15.6	16.6	16.1

Table 7: Comparing TRNSYS Component to Theoretical Calculations when Below Minimum Flow

Test Number	Q _{in,c} (kJ/hr)	Q _{in,T} (kJ/hr)	Q _{del,c} (kJ/hr)	Q _{del,T} (kJ/hr)	Q _{env,T} (kJ/hr)	Q _{env,c} (kJ/hr)
1	0	0	1056.2	1042.3	-1060	-1054
2	0	0	0	0.00	0	0
3	211	211	163.7	161	7	7.1
4	211	211	246	242.2	-74	-74

Table 8: Errors Associated with Table 4

Test Number	Q _{in} (% Error)	Q _{del} (% Error)	Q _{env} (% Error)
1	N/A	-1.34	-0.57
2	N/A	N/A	N/A
3	0	-1.56	0.84
4	0	-1.47	-0.11

The results in Table 8 show slightly higher error than desired. An error below 1% in the

environmental term is deemed acceptable for all tests. An error of 1.5% in delivered energy is considered a little high for all the tests. The model results are highly sensitive to the number of nodes as will be discussed in section 3.1.5.2.

2.3.3 Capacitance Tests

Another test focused on the temperature decay rate of the exiting water after the heater was shut off. This is a test which is theorized to be effective for determining the capacitance of the heaters as, in this situation, the rate of change of temperature leaving the heater is dominated by flow rate, inlet water temperature and capacitance. The UA value also has a role; however, it is negligible in cases where water is flowing through the heat exchanger. The flow rate and outlet temperature will be measured leaving simply the capacitance as an unknown. The model was subjected to the same condition in order to ensure that it models capacitance correctly. While running these simulations the intent was to ensure that the capacitance of the water heater calculated via the simulation data matched up with the capacitance of the water heater specified when developing the simulation model. This was done by running simulations to identify the rate at which the temperature in the heat exchanger was changing, and then calculating the effective capacitance.

The equation used to calculate capacitance is shown in Equation (42).

$$Cap = \frac{\dot{m}C_p(T_{Exit} - T_{In}) - UA(\bar{T}_{HX} - T_{Amb})}{dT_{Exit}/dt} \quad (27)$$

Most of these variables were specified in the TRNSYS input file; however, in some instances the output from TRNSYS was used in the equation. These variables include the outlet temperature and the average temperature. The dT term in the denominator was identified using the outlet temperature values reported from TRNSYS. Equation (27) was evaluated using a three point linearization method. The three points corresponded to the first and last points in time, which were used to evaluate the temperature derivative, and the second point which was halfway between the two. Once the temperature derivative was identified using points one and three the terms in the equation were evaluated at point 2.

Tests were performed varying the water flow rate and capacitance of the heat exchanger in an attempt to ensure that the model could accurately model the effects of capacitance regardless of how these variables changed. All tests were performed with a set temperature of 60 C, a U value of 0.0002 kJ/hr-m²-C, an area of 9×10^{-7} m², an inlet temperature of 15.6 C, an environmental temperature of 15.6 °C, no pilot light, 20 nodes, a TRNSYS time-step of 0.1 s, and a control update delay of 1s. The U value and area were set in attempt to remove the impact of environmental losses and leave the rate of temperature change in the heat exchanger sensitive to only water flow rate and capacitance. The TRNSYS time-step was set at the absolute minimum value (1s) due to the fact that error in this analysis increases with the time-step length.

Table 9 presents the results of the tests performed with varying flow rate and Table 10 presents the results of the tests performed with varying capacitance.

Table 9: Theoretical Capacitance Check with Varying Flow Rate

Flow Rate (kg/hr)	Capacitance (kJ/K)	dT/dt (C/hr)	Cap (kJ/K)	% Error
-------------------	--------------------	--------------	------------	---------

150	10	2783.84	10.098	0.98
175	10	3254.08	10.092	0.92
200	10	3725.90	10.068	0.68
300	10	5613.24	10.003	0.03
500	10	9387.89	9.923	-0.77

The results in Table 9 imply that the model is indeed accounting for the capacitance correctly. The calculated capacitance for all simulations is less than 1%. This low error could easily be attributed to the error inherent in the fact that the derivative of temperature is estimated numerically as a time-step average rather than evaluated instantaneously.

Table 10: Theoretical Capacitance Check with Varying Capacitance

Flow Rate (kg/hr)	Capacitance (kJ/C)	dT/dt (C/hr)	Capacitance (kJ/C)	% Error
158	10	2766	10	0.98
158	20	1373	20.3	1.45
158	30	909	30.4	1.52
158	40	677	40.6	1.56
158	50	538	50.9	1.59
158	100	260.2	101.6	1.63
158	500	37.8	508.2	1.64

The results in Table 10 also imply that the simulation is correctly modeling the effects of capacitance. The % error gradually increased with increasing capacitance value; however, with a capacitance as high as 500 kJ/K there was still only 1.6% error. Again, the small error is likely caused by the numerically calculated derivative of temperature than it is by the simulation being incorrect.

2.3.4 Subjected to a Flow Pattern

The next theoretical verification test focused on examining how the model responds to a flow

pattern which includes several different values for the flow rate. The idea was to determine how the heater responds to flow rates below the minimum, flow rates above the minimum and flow rates requiring heating above the maximum heating capacity all at once. Also of interest was the response of the model as the inlet conditions changed and whether or not the simulated control systems seemed to be operating as expected.

This test consisted of nine phases. The first phase consisted of exposing the heater to a water flow rate which was below the minimum flow rate of the heater. This was done to ensure that the heater did not fire when it should not, and to ensure that the heat transfer calculations based on heat entering from the environment were performed correctly. The second phase increased the flow rate so that the heater would be firing at 25% of its maximum capacity. In this phase the heat transfer calculations were checked to ensure that there was not significant error in the calculations, and a qualitative check that the model predicted an expected response when the flow rate changed. The desired response was a rapid increase in outlet temperature asymptotically approaching the set temperature. The third phase increased the flow rate to correspond to 75% of the heaters maximum capacity. The intent of this phase was the same as the second phase; however, the qualitative check was different. In this case it was expected that there would be a short and sharp decrease in temperature as the heater responded to the suddenly increasing demand placed on it by the higher water flow. The fourth phase increased the water flow rate to correspond to 100% of the heaters maximum capacity. This phase was used both to check the heat transfer calculations again and to set up the simulation for the fifth phase. The fifth phase increased the water flow rate to correspond to 125% of the heaters maximum capacity. The main intent of this phase of the simulation was to observe the flow rate limiting

control. With the heater already operating at full capacity it was expected that the actual flow rate would not increase with the demand flow setting increased. Phases six through nine simply reversed the process and worked back to the beginning condition. Table 11 presents the water flow rate programmed into the system for each phase of the test.

Table 11: Input Water Flow Rates Separated by Phase

Phase	Water Flow Rate (kg/hr)
1	90.2
2	203
3	654
4	857
5	1083
6	857
7	654
8	203
9	90.2

In this simulation the tankless heater had a minimum flow rate of 112.8 kg/hr, the fluid was modeled as having a specific heat 4.19 kJ/kg-K, there was no pilot light, the maximum capacity of the heater was 200,000 kJ/hr the conversion efficiency was 0.82, the U-value was modeled as 15 kJ/hr-m²-C, the area was modeled as 1 m², the capacitance was 10 kJ/K, and the control update delay was 1 s. The set temperature was 60 °C, while the inlet was 15.5 °C and the environment temperature was 20 °C. Each phase lasted 15 minutes at a 3 second time step.

Results from the test are shown in Figure 6 and Figure 7. Figure 6 displays the outlet temperature as well as the heat transfer rates while Figure 7 shows the flow rates considered in the test.

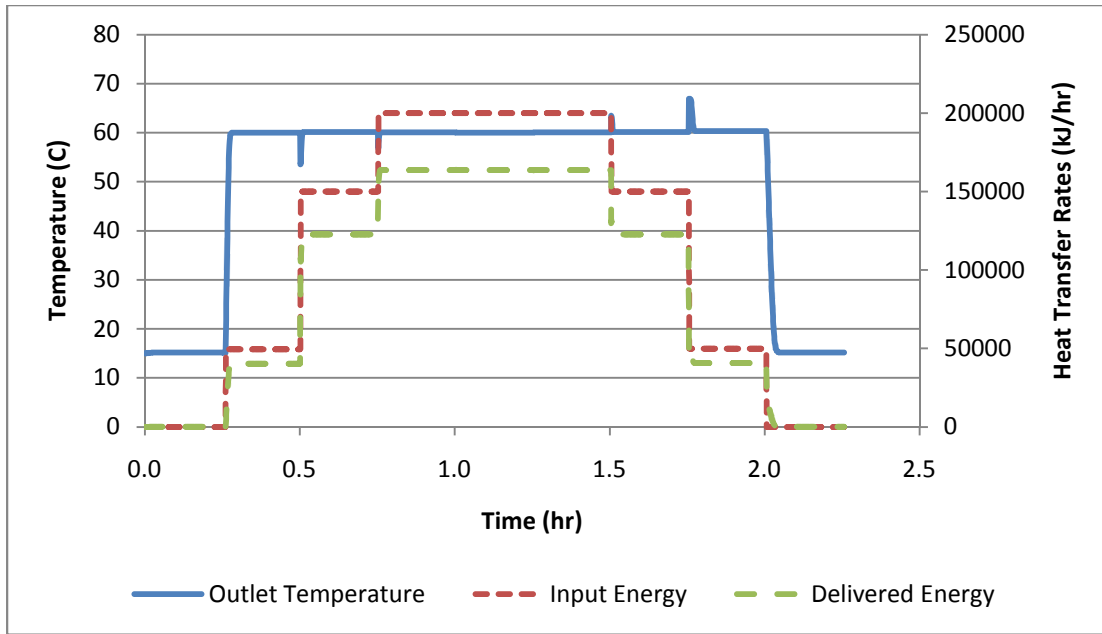


Figure 6: Temperatures and Heat Transfer Rates during the Flow Pattern

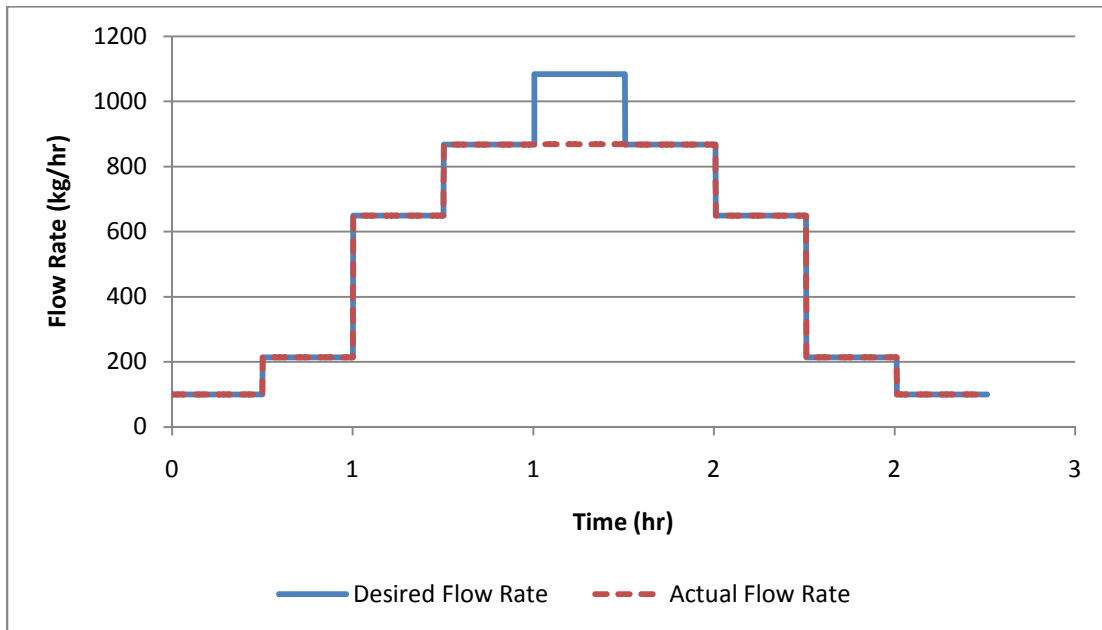


Figure 7: Water Flow Rates during the Flow Pattern

The results in Figure 6 indicate that the heater is behaving exactly as expected. In the first phase the water is approximately at the inlet temperature, and the heat transfer rates are approximately

zero. In the second phase the temperature increases to the set temperature and the heat transfer rates increase accordingly. The heater goes through a process of increasing temperature rather than an instant jump, which indicates that the capacitance of the heat exchanger is being taken into account by the model. The input energy is elevated above the delivered energy indicating that the simulation module is appropriately modeling the efficiency of the heater. As the simulation model switches to the third phase there is a sudden drop in outlet temperature, and the heat transfer rates jump to be approximately three times those obtained in phase two. This indicates that the simulation module is correctly modeling the delay before the heater updates its controls, and that the heater is correctly modulating the energy consumption in accordance with the energy demand. The switch to the fourth phase leads to similar results. The fifth phase responded as expected; there was no dramatic change in outlet temperature or heat transfer rates between the fourth, fifth and sixth phases. Phases seven through nine show the same trends as in phases one through three except in reverse; where the heat rose previously it decreases now and where the temperature dropped previously it jumps now.

The results in Figure 7 also indicate that the general logic in the heater is working correctly. The water flow rates typically pass through the heater precisely as they are programmed. The one spot where this is not the case is in phase five when the flow increases such that the heater would not be able to meet demand. In this case the heater controls the water flow rate so that the maximum heat transfer rate of which the heater is capable is used to heat as much water as is possible to the set temperature.

Results examining the error in the simulation are shown in Table 12, Table 13 and Table 14.

Table 12 presents TRNSYS model estimations while Table 13 and Table 14 examine the difference between TRNSYS calculations and theoretical calculations for heat transfer rates and flow rates.

Table 12: Outputs from TRNSYS during the Flow Pattern Test

Phase	$T_{out, TRN}$ (°C)	$Q_{in, TRN}$ (kJ/hr)	$Q_{del, TRN}$ (kJ/hr)	$Flow_{TRN}$ (kg/hr)
1	15.2	0.00	73.5	90
2	60.3	49939	40641	203
3	60.1	149962	122663	654
4	60.1	200000	163694	857
5	59.9	200000	163695	880
6	60.1	200000	163694	857
7	60.1	149962	122663	654
8	60.3	49939	40641	203
9	15.2	0.00	73.5	90

Table 13: Error in Heat Transfer Rates during the Flow Pattern Test

Phase	$Q_{del, TRN}$ (kJ/hr)	$Q_{del, calc}$ (kJ/hr)	ΔQ_{del} (kJ/hr)	Error (%)
1	74	75.4	-1.9	-2.5
2	40641	40969.3	-55.3	-0.1
3	122663	122699	-36.2	0
4	163694	163617.8	76.2	0.1
5	163695	163363.7	331	0.2
6	163694	163617.8	76.2	0.1
7	122663.1	122699.2	-36.2	0
8	40641	40696	-55.3	-0.1
9	74	75.4	-1.9	-2.5

The results in Table 13 imply that the component is working appropriately. The theoretical calculations for all situations where the heater was firing had an error of 0.2% or less. The situation when the heater was not firing showed a percent error of 2.53%. In simulations with the draw flow rate below the minimum the error is sensitive to the number of nodes used in the simulation model, as will be shown in section 2.3.5, and can be reduced by increasing the

number of nodes if deemed necessary.

Table 14: Error in Flow Rate during the Flow Pattern Test

Phase	Flow _{TRN} (kg/hr)	Flow _{calc} (kg/hr)	ΔFlow (kg/hr)	Error (%)
1	90	90	0.00	0
2	203	203	0.00	0.1
3	654	654	0.00	0.03
4	857	857	0.00	-0.04
5	880	857	-0.01	-0.2
6	857	857	0.00	-0.04
7	654	654	0.00	0.03
8	203	203	0.00	0.1
9	90	90	0.00	0

The flow rate calculations presented in Table 14 also imply that the model is working appropriately. The largest difference between the simulation results and the theoretical calculations is 0.19%.

2.3.5 Nodes Required for Convergence

The number of nodes has an impact on the temperature distribution throughout the heater. When multiple nodes are in a model an average heat exchanger temperature is used in calculating the environmental losses rather than assuming a uniform temperature equal to the set point. Because time-based average temperatures are used for the inlet and outlet temperatures of each node it may be necessary to use a large number of nodes for proper convergence. An analysis was conducted with the intent of determining the impact of number of nodes simulated on percent error compared to hand calculations which were performed using Equation (18) for the delivered energy and Equation (22) for the environmental losses. The input energy was calculated using

Equation (43). The analysis was under both conditions of water flow rate being higher than the minimum and water flow rate being below the minimum. Both tests assumed that there was no pilot light and that the system was operating under steady state conditions.

$$\dot{Q}_{In} = \frac{mC_p(T_{Set}-T_{In})+UA(\bar{T}_{HX}-T_{Amb})}{\eta_{Conv}} \quad (28)$$

Many of the variables used throughout the tests were held constant. To avoid repeating their values several times these variables are defined in this section but used in other analyses presented in this chapter. The inlet water temperature was 15.6 °C, the environment temperature was 20 °C and the set temperature was 54.4 °C. The heat loss coefficient (U-value) was 15 kJ/hr-m²-°C and the area was treated as 1 m². The minimum flow rate was 112.8 kg/hr. The burner efficiency was 0.82 percent and the maximum heating capacity of the system was 200 MJ/hr. All simulations were performed with zero for the burner input to simulate a tankless water heater without a pilot light.

The output values output obtained from the TRNSYS model were compared to hand calculations to determine how the simulated values compared to theoretical calculations. Separate calculations were performed for the energy delivered to the water, the heat transfer between the heater and the ambient environment and the total amount of fossil energy entering the heater. The equation for delivered energy, being the evident energy change in the water, was calculated using Equation (17). Since the heater was operating at steady state conditions over the TRNSYS timestep, the Δt_{Now} term can be neglected. The environmental losses were treated as $UA(T_{average} - T_{env})$. For the calculations $T_{average}$ was treated as the TRNSYS reported average temperature with

20 nodes.

2.3.5.1 Flow Rate Greater than Minimum Flow Rate

The first test performed examined this relationship with a water flow rate of 609 kg/hr. It was intended to examine how the number of nodes impacts the accuracy of the model when the burner is firing. The simulation was performed with an increment of one node with a minimum of one and a maximum of 20. The simulation results can be seen in Figure 8.

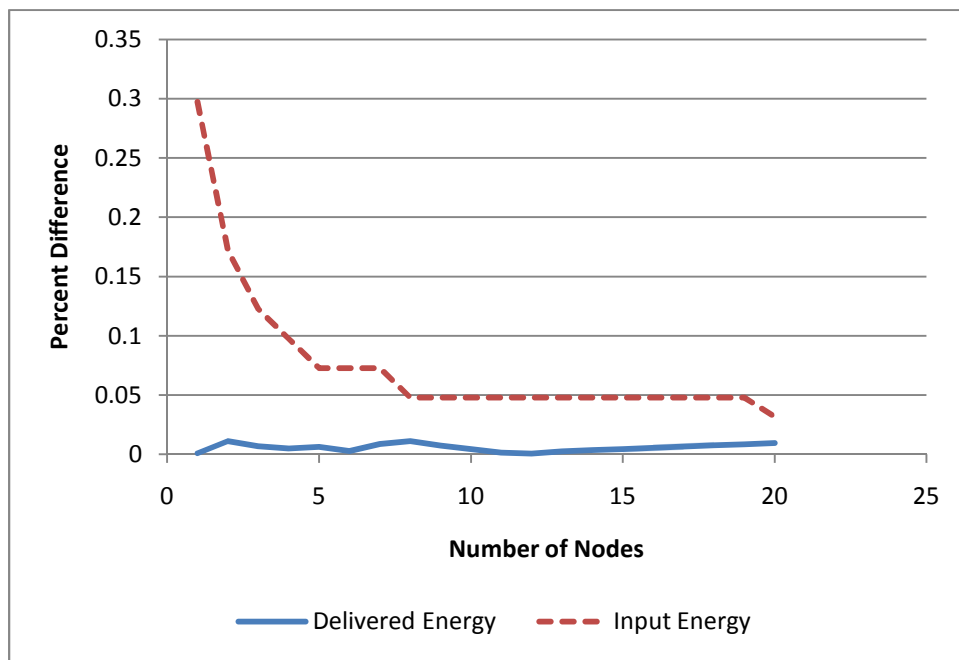


Figure 8: Percentage Differences between TRNSYS Simulation and Hand Calculations under Steady State Burning Conditions

As can be seen in Figure 8, the error in the simulation is always small. The error in delivered energy is negligible, with the highest error recorded being 0.01%. The input energy starts at

0.28% and steadily decreases as the number of nodes are increased. It eventually stabilizes, with increasing number of nodes not decreasing the error, at 0.03% error when the simulation has eight nodes.

Because of the ability to calculate an average temperature of the heat exchanger it was theorized that increasing the number of nodes would have a dramatic impact on the calculated environmental losses. This is quite intuitive from Equation (22). The rate at which heat is lost to the environment is based on the temperature difference between the heat exchanger and the environment. With only one node the heat exchanger is at a constant temperature equal to the water set temperature. Clearly this is incorrect. A multiple node model allows for the calculation of an average heat exchanger temperature which will strongly impact the heat transfer rate. Additional nodes allow for a more accurate calculation of the average heat exchanger temperature by giving a more detailed temperature profile along the heat exchanger itself. As a result of this theory simulations were performed testing the impact of increasing nodes on the estimation of environmental losses.

In order to estimate the error that is inherent in the environmental losses due to an imprecise average temperature of the heat exchanger it was necessary to make an assumption for what the average temperature really is. The assumption used for this study was that the average heat exchanger temperature is equal to the average of the inlet water temperature and set temperature. This was assumed because the heat exchanger temperature profile is modeled as linearly increasing from the inlet temperature to the set temperature implying that a simulation with an infinite number of nodes would calculate the heat exchanger temperature as such. Using this

assumption allowed for a baseline calculation against which the values reported by TRNSYS could be compared. Results are shown in Figure 9.

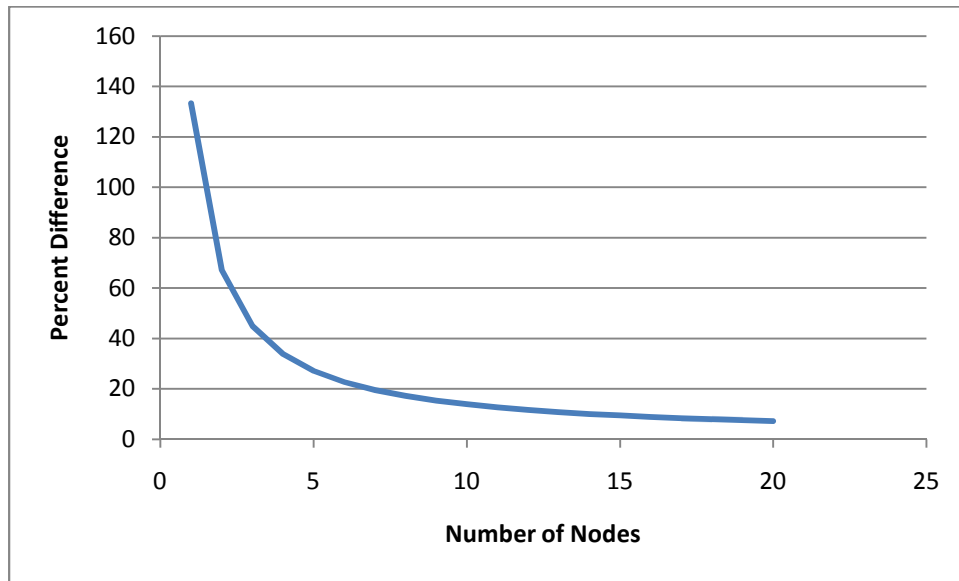


Figure 9: Error in Environmental Losses During Steady State Flow

The simulation with a single node showed a 118% error in environmental losses. This is mostly because the temperature difference associated with environmental losses was more than doubled when using the single node assumption than it actually would be in a tankless heater. Adding additional nodes causes the average temperature of the heater to be more accurate resulting in lower error. The result is an asymptotically decreasing percent error with the lowest recorded error being 7.2% at 20 nodes. This is still a large percent error; however, since the environmental losses account for approximately one percent of the energy used by the heater it may be acceptable. Also, the error is still steadily decreasing at 20 nodes so if a simulation requires high accuracy in the losses to environment term it can simply be run with a higher

number of nodes.

In order to check that the error was caused by the temperature difference from an inadequate number of nodes the error at 20 nodes was compared to the error if the average temperature in the 20 node simulation was correct. This was done by inserting the average temperature with 20 nodes into the equation instead of the perfect average. This error identified using this procedure was found to be 0% implying that the model is working correctly.

2.3.5.2 Flow Rate below Minimum Flow Rate

Since there will be times when tankless water heaters experience draws which are below the rated minimum flow rate it was important to run the same simulations for this situation as well. The heater was exposed to a flow rate of 59 kg/hr which was below the 113 kg/hr minimum rated limit. The simulations were again performed in increments of one node from one to 20 nodes. The simulation results are shown in Figure 10.

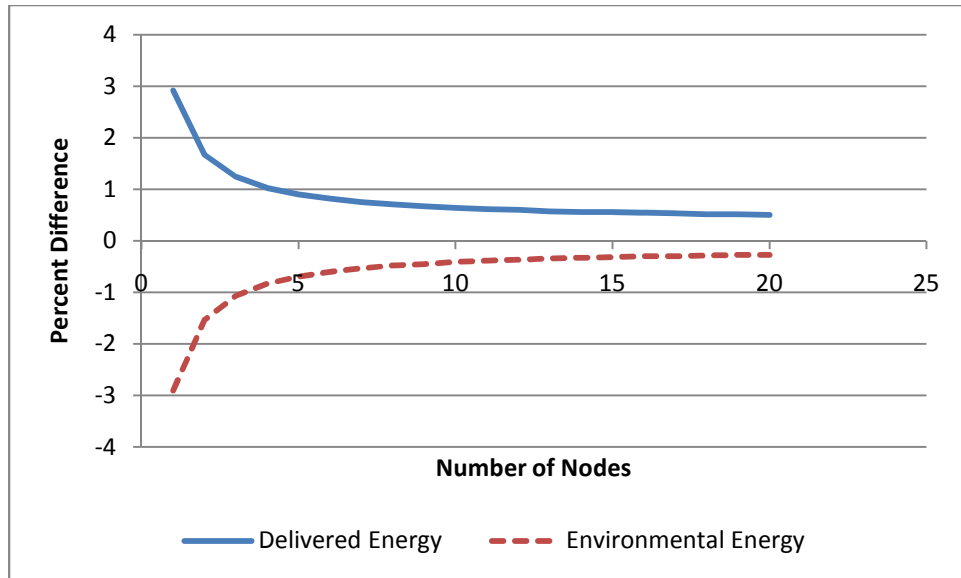


Figure 10: Percentage Difference between TRNSYS Simulation and Hand Calculations Under No Burn Conditions

The error in the simulation model is higher when the heat transfer is to the environment. This is caused by the fact that all heat transfer in the simulation is driven by the average heat exchanger temperature which is dependent on the number of nodes. As can be seen in Figure 10 the error in both terms is greatest at a single node and then exponentially decays as the number of nodes increases. In the 20 node simulation the error is reduced to 0.5% for the delivered energy, and -0.27% for the environment energy.

Chapter 3: Test Facility Description and Modes of Operation

3.1 Overall System Design

The testing set-up was designed to allow several different modes of operation and testing of several different features of the tankless unit or system configurations. A diagram of the overall system schematic is shown in Figure 11.

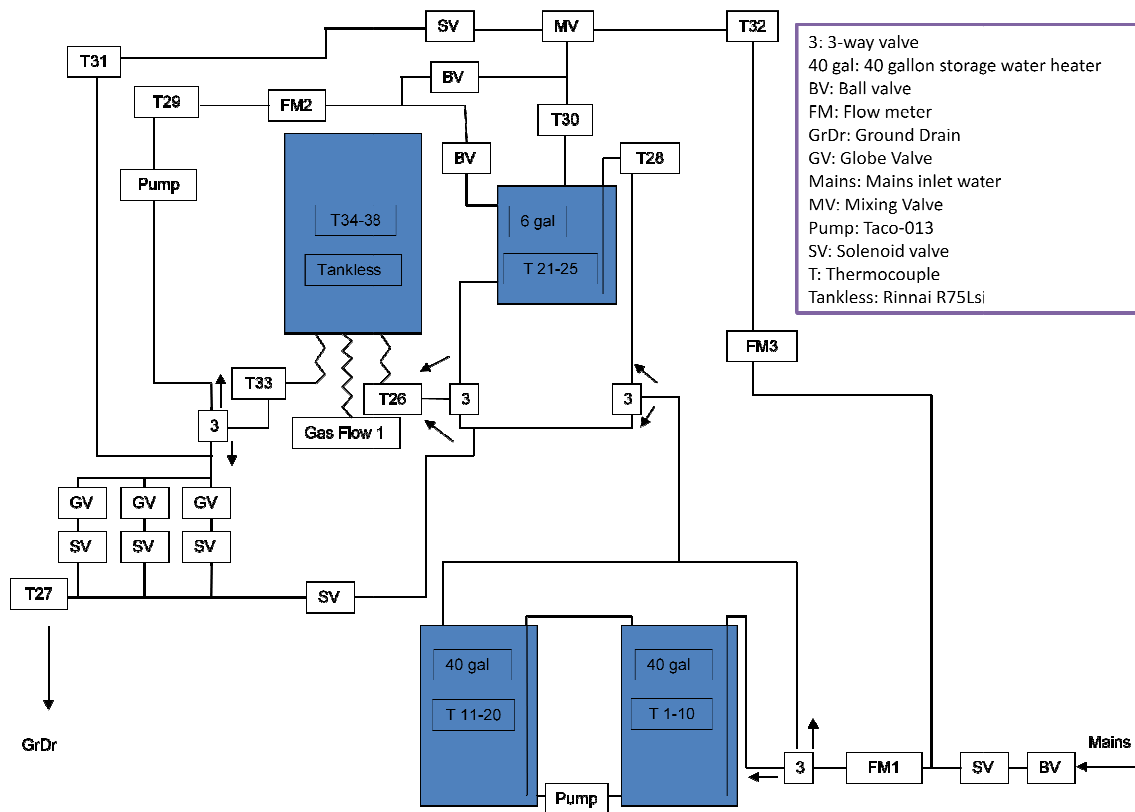


Figure 11: Schematic of Full Test System

The experimental set-up has several features and capabilities including:

- (a) It has strong abilities to record the flow rate of both water and natural gas flowing

through the system as well as important measurement points. This allows for a thermodynamic analysis of the water as it passes through several different sections of the system.

- (b) It also allows for changing flow rate which will be useful when testing how the heaters respond to rapid changes in flow rate and when comparing the TRNSYS simulation results against actual results for various standard water draw profiles.
- (c) It includes a bypass line which can be used to send water directly to drain allowing for better control of the water entering the tankless water heater and a small tank system which can be used to run experiments to assess one of the potential methods of overcoming the problems associated with tankless water heaters.

The names, measurement strategies, manufacturers and uncertainties of each sensor are shown in Table 15.

Table 15: Sensor Uncertainties

Sensor	Sensor Name	Sensor Type	Manufacturer	Uncertainty Quote	Notes
T1-33	Thermocouple	Type T	Omega Engineering	± 0.5 °C	2 sigma [20]
T34-38	Thermocouple	Type K	Omega Engineering	± 1.5 °C	2 sigma [20]
FM1-3	Model 25	Nutating Disc	Badger Meter	± 1.5 %	2 sigma [17]
Gas Flow 1	FT2	Hot Wire Anemometer	Fox Thermal	± 1 %	2 sigma [16]

The energy density of natural gas was not measured during these experiments. Per the specification by Xcel Energy the energy density of gas entering the system can vary by approximately 5% [27]. The lack of measurement of energy density of gas is treated as a 5%, 2

sigma uncertainty in this analysis.

3.2 Images of the Experimental Apparatus

Some pictures of the experimental system were taken in order to provide a better idea of the test set-up. The pictures are shown in Figure 12, Figure 13, Figure 14, Figure 15 and Figure 16.



Figure 12: Wide-Scale View of the Entire Test System

Figure 12 shows a full view of the testing set-up. The rest of the images give a more detailed view of the varying components of the experimental set-up along with more of a description of

how they will be used.



Figure 13: View of the Storage Water Heaters

Figure 13 shows the two 155 L storage water heaters. The storage water heaters will be used for controlling the temperature of water entering the storage tank. There is a copper pipe coming from the back wall running between the tanks. This pipe provides mains water to the inlet on the rightmost tank. A copper line running from the hot on the rightmost tank to the cold on the leftmost tank allows water to flow between the two tanks. This setup will allow storage of up to 310 L of water which should be more than enough to complete the desired tests. In the very center of the top of the two tanks the thermocouple assemblies which will be used to identify and

control the water temperature can be seen. When the water is conditioned to the appropriate temperature it will exit out the hot port on the left tank and head to the left towards the controls which are located above the 23.3 L tank and are depicted in Figure 14.

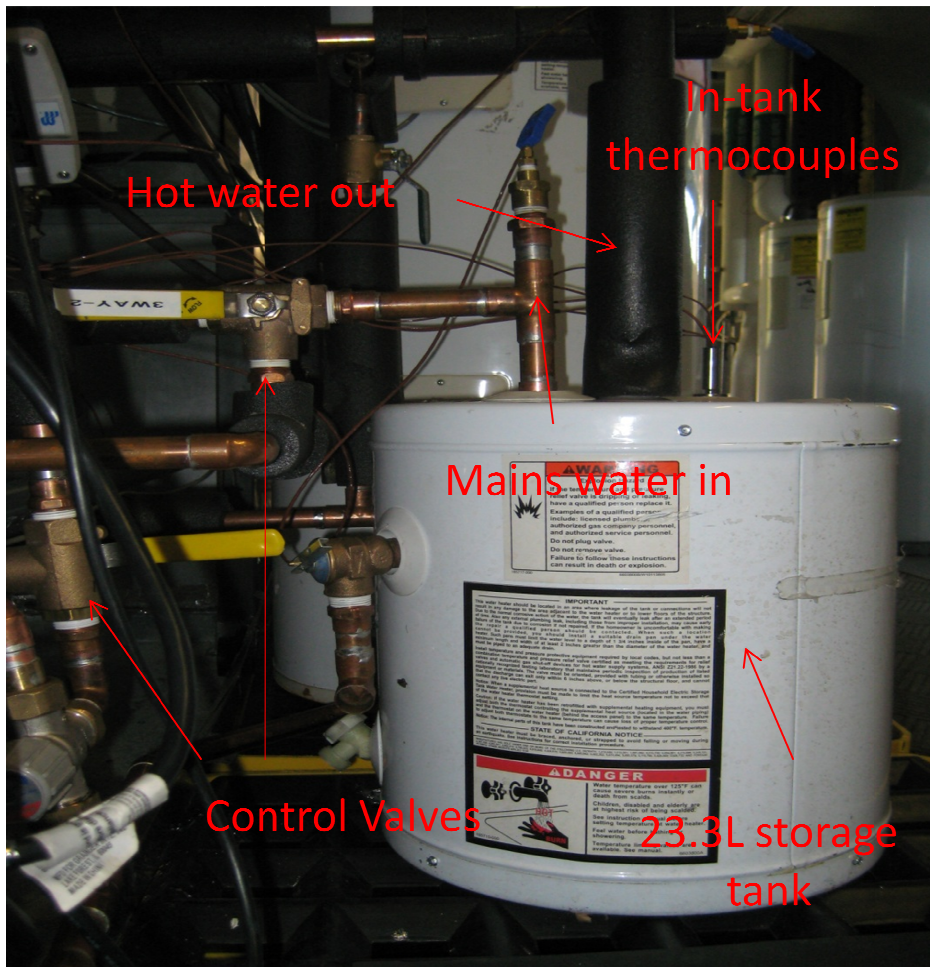


Figure 14: Close-Up View of the Controls and Thermocouples in the 23.3 L Tank

Figure 14 shows the 23.3 L storage tank which will be used with the recirculation system as well as the thermocouples used to measure the water in the tank, exiting the tank and entering the tank. Figure 14 also shows a pair of three-way valves which will be used to control the flow direction. On the right side of the tank five thermocouples are used to measure and control the

water temperature in the tank. The center of the tank has a long section of vertical pipe which directs hot water to the mixing valve and also measures the temperature of the water heading towards the mixing valve. The leftmost pipe coming out of the top of the tank is for the mains water inlet, and also measures the temperature of the water coming in.

There are two three-way valves visible to the left side of the picture. The top three way valve controls the direction of the incoming water. It directs the inlet water towards either the tankless water heater or the 23.3L storage tank. The bottom three-way valve is used to control which water stream is allowed to enter the tankless water heater. Water can enter the tankless heater from the mains line, the 155L storage tanks or the 23.3L storage tank. The pictured three way directs flow from either the 23.3L tank or one of the other sources. The valve switching between mains water and the 155L storage tanks is not shown in this picture.



Figure 15: Close-Up View of the Rinnai R75Lsi Heater

Figure 15 shows a photo of the Rinnai R75Lsi heater used in the experimental tests. It also shows the connections to the heater; the two yellow tubes carry the water in and out of the system while the blue pipe is used for delivery of natural gas. The front panel of the heater contains the controls such as an on/off button and the up and down arrows to adjust the set temperature.



Figure 16: View Depicting the Flow Rate Control Manifold

Figure 16 shows the manifold which was used to control the flow rate of the water passing through the system. The system contains three paths each with a solenoid valve and a globe valve. The globe valves were adjusted to set a specific flow rate through each path and the solenoid valves were used to control which path(s) is open. While it is not adjustable to the point of a continuously variable flow rate, the many different combinations of flow rates allowable will create some variability for the system. Also depicted in the left side of the photo is the final thermocouple which measures the temperature of the water leaving the system.

3.3 Heat Exchanger Thermocouple Placement

There were several thermocouples placed on the heat exchanger of the tankless unit in an attempt to identify the profile of temperatures as the water passed through the heater. Since the water path tube passes in and out of the heat exchanger box and the heat exchanger box is mostly closed, it was only feasible to attach the thermocouples to the tubes at points where the tube was outside the box of the heat exchanger. This set-up gave a practical method of defining a number of nodes with the distance between nodes being one pass through the heat exchanger and the measurement for nodes being taken at the point where the tube turns around and proceeds back into the heat exchanger. Since the tube passes through the heat exchanger nine times there were ten possible measurement points; one before the water enters the heat exchanger, one just after the water exits the heat exchanger and eight where the heat exchanger turns around before re-entering the heat exchanger. Since the inlet temperature is measured by other thermocouples that point was neglected and six thermocouples were placed on the remaining 9 measurement points. A schematic depicting the path of the heat exchanger and location of thermocouples is provided in Figure 17.

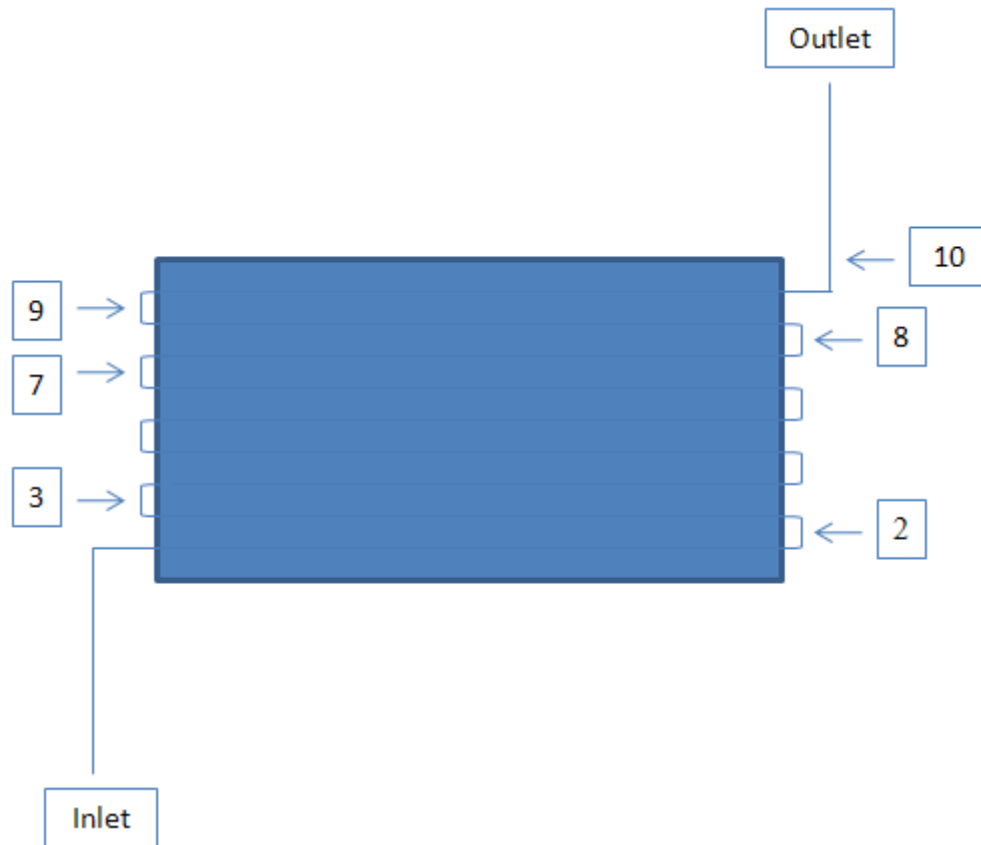


Figure 17: Location of Thermocouples on the Heat Exchanger

3.4 Water Temperature Measurement Calibration

Measuring the temperature of the water flowing through the system required a rather challenging measurements set-up. It involved a total of 38 thermocouples located throughout the system. 25 of the 38 thermocouples were used to measure the water in the storage tanks to give a clear picture of stratification. Five thermocouples were placed on the heat exchanger in the tankless heater. The remaining 7 thermocouples measuring water temperature were used to detail the temperature of the water flowing from one point of interest to another.

The majority of the thermocouples used to measure water temperature are contained in thermocouple assemblies rather than individual probes. These thermocouples can be easily identified as they are the ones located in Tank1, Tank2 and Small Tank. Tank1 and Tank2 utilize a 10 thermocouple probe assembly with the first thermocouple at the center of a node on the bottom of the tank. The rest of the thermocouples are numbered in ascending order until reaching the tenth thermocouple which measures the temperature at the center of a node on the top of the tank. The thermocouple assembly in the small tank follows the same pattern with the only difference being that it is based on a five thermocouple assembly rather than ten.

The rest of the water temperature measurements are performed using single thermocouples rather than assemblies.

The calibration of each of the individual thermocouples was checked using two conditions. The two conditions used were 0 °C and 100 °C. The check was made using a Fluke 7103 Microbath by setting the Microbath to the desired temperatures and inserting the thermocouples. Unfortunately the Microbath did not hold constant at the desired temperature so the specific temperature at the time of the reading was recorded along with the reading on the thermocouple. Since the experiment does not require extraordinarily accurate measurements it was determined that a reading within 0.5 °C of the Microbath temperature was adequate. The recorded temperatures are displayed in Table 16.

Table 16: Individual Thermocouple Calibrations

TC#	0 °C Reading	0 °C Actual	0 °C Difference	100 °C Reading	100 °C Actual	100 °C Difference

26	-0.6	-0.9	0.3	100.1	99.9	0.2
27	-0.06	0	-0.06	100.1	99.8	0.3
28	-0.3	-0.7	0.4	100.2	99.9	0.3
29	-0.1	0	-0.1	100.2	99.9	0.3
30	-0.4	-1.1	0.7	100.4	100	0.4
31	-0.1	0	-0.1	100.3	99.9	0.4
32	-0.3	-0.6	0.3	100.3	100	0.3

All of the thermocouples show an error within 0.5 °C. Since 0.5 °C is the standard margin of uncertainty for a Type T thermocouple all of the thermocouples were considered to be properly calibrated.

The thermocouple assemblies could not be checked with the same degree of rigor. Since they were entirely too large to fit into the Microbath, or any other temperature control system available, they were tested by comparison against the individual thermocouples in room air and in mains water.

The check against room air was performed by removing all three assemblies and setting them on the ground. Thermocouples 28 and 30 were used as the “correct” temperature reading. These two thermocouples were placed next to the three assemblies so that they would be measuring the same temperature as the assemblies and could be used as references. The measurements were

taken three times and averaged for each thermocouple. Then the average readings for thermocouples 28 and 30 were averaged to create a reference value. The average of each thermocouple in the assemblies was then compared to the reference value obtained from thermocouples 28 and 30 to identify an error of each probe in the assemblies. The values gathered from thermocouples 28 and 30 as well as the averages and reference temperature are displayed in Table 17. Table 18 shows the data from each of the assembly probes as well as the averages and how each probe compares to the reference value.

Table 17: Creating the Reference Value

TC#	Reading 1	Reading 2	Reading 3	Average	Difference
28	24.2	24.2	23.3	24.1	0.3
30	23.2	23.6	23.6	23.4	-0.3
Average	23.7	23.9	23.7	23.8	N/A

Table 18: Thermocouple Assemblies Compared to Reference Value

TC#	Reading	Reading	Reading	Average	Difference
1	23.4	23.4	23.6	23.4	-0.3
2	23.4	23.4	23.5	23.4	-0.4
3	23.2	23.3	23.4	23.3	-0.5
4	23.3	23.4	23.4	23.4	-0.4
5	23.4	23.4	23.4	23.4	-0.4
6	23.4	23.4	23.4	23.4	-0.4
7	23.7	23.7	23.7	23.7	-0.1
8	23.7	23.7	23.7	23.7	-0.1
9	23.4	23.4	23.5	23.5	-0.3
10	23.3	23.4	23.4	23.4	-0.4
11	23.3	23.4	23.4	23.4	-0.4
12	23.2	23.4	23.4	23.3	-0.4
13	23.6	23.4	23.4	23.5	-0.3
14	23.7	23.6	23.6	23.6	-0.2
15	24.0	24.0	24.1	24.0	0.3
16	24.1	24.2	24.2	24.2	-0.4
17	23.8	23.9	23.9	23.9	0.1
18	23.6	23.7	23.7	23.6	-0.1

19	23.3	23.4	23.3	23.3	-0.4
20	23.2	23.4	23.4	23.4	0.4
21	23.6	23.7	23.7	23.6	-0.1
22	23.6	23.7	23.7	23.7	-0.1
23	23.6	23.6	23.6	23.6	-0.2
24	23.6	23.7	23.7	23.7	-0.1
25	23.4	23.4	23.4	23.4	-0.4

All twenty five of the thermocouples located in the storage tanks read within 0.5 °C of the reference temperature indicating that none of the thermocouples need to be replaced.

The calibration of the thermocouple assemblies was also checked using mains water. This test was performed by allowing water to flow through the system and measuring the water temperature with the thermocouple assemblies as well as two individual thermocouples. Thermocouple number 32 was used to measure the inlet water temperature before the water entered the tanks and covered the thermocouple assemblies. Then the water downstream of the tanks was measured using thermocouple 26. The temperatures recorded in this test are shown in Table 19.

Table 19: Thermocouple Assemblies Measuring Mains Water

TC #	Temperature (°C)
32	12.7
1	13.2
2	13.2
3	13.2
4	13.2
5	13.2
6	13.2
7	13.2
8	13.2
9	13.2
10	13.2

11	14.2
12	14.2
13	14.2
14	14.3
15	14.3
16	14.5
17	14.7
18	14.6
19	14.8
20	18.4
26	14.8

In Table 19 the thermocouples are listed in order of location in the flowstream. The water entered the system, passed thermocouple 32 on the way to the tank, passed through the tanks and thermocouples 1-20 before exiting the tanks and passing thermocouples 26. Unfortunately the flow rate was not high enough to keep the temperature constant throughout the system without pipe insulation and some temperature variation is visible. However, the results still, for the most part, show that the thermocouples are accurately measuring the temperature of the water. The incoming mains water is the coldest temperature recorded. Thermocouples 1 through 10 report a temperature of 13.2 °C showing no stratification in the first tank. This reading is approximately 0.5 °C warmer than the inlet temperature which is reasonable considering the length of the pipe through which the water flows before entering the first tank. The water then progresses into the second tank and is measured by thermocouples 11 through 20. Immediately upon entering the second tank the temperature of the water appears to increase by 1 degree Celsius. This increase is a bit surprising considering the short length of piping present; however, since the first three thermocouples all show the exact same temperature there is no reason to believe that there is a significant error in any one of the thermocouples. Thermocouple 11 reports a temperature of 14.2 °C. There appears to be some stratification in the tank which is evidenced by the temperature slowly increasing until reaching a maximum of 14.8 °C at thermocouple 19. The

temperature at thermocouple 19 agrees with the temperature of thermocouple 26 implying that it is correct.

The only problem implied in Table 19 is shown by the 18.4 °C reported by thermocouple number 20. Since 18.3 °C is fairly close to room temperature and there is some length of assembly which is above the top of the tank it was theorized that thermocouple 20 is not actually submerged in water. This theory was tested by surrounding the portion of the assembly not contained within the tank with ice and observing what happened to the temperature reported by thermocouple 20. A picture depicting this test is shown in Figure 18.



Figure 18: Ice Used to Determine Location of Thermocouple 20

This experiment made it clear that thermocouple 20 does not provide a good reading of the temperature at the top of Tank 2. After the ice was placed around the portion of the assembly sticking out of the top of the tank the reading from thermocouple 20 began to drop rapidly. Although no final measurement was made as it was unnecessary a reading was taken showing thermocouple 20 measuring 5.9 °C despite the fact that the water was entering the system at 12.7 °C. The fact that the measurement from thermocouple 20 dropped substantially, below the incoming water temperature, indicates that it is affected by the temperature surrounding the copper pipe at the top of the tank.

3.5 Water Flow Rate

The water flow meters were not putting out a 4-20 mA signal after being installed. The low end of the signal was coming through around 3.6 mA instead of 4 mA which called the manufacturer's calibration into question. As a result of this a thorough calibration check was performed as well as a study investigating the relationship between flow rate and signal.

The calibration was checked via standard bucket tests. In these tests the flow passing through the flow meter was collected in a bucket, and the duration of the draw was timed with a stop watch. During the draw the display of the flow meter and the signal sent to the CR10X datalogger were recorded [26]. After the flow the weight of the water in the bucket was measured, and the approximate flow rate based on this weight data was calculated. The calculated flow rate and the flow rate displayed on the flow meter were used to check the calibration, and the signal sent to the datalogger was saved for future use in determining the equation converting signal to flow rate. The data recorded for checking calibration is shown in Table 20. The initial mass changes halfway through the tests because it was necessary to use a

larger bucket.

Table 20: Flow Meter Calibration

M_{initial} (kg)	M_{final} (kg)	Δm (kg)	ΔV (L)	Time (m)	Flow (L/min)	Display (L/min)
N/A	N/A	N/A	N/A	N/A	0	0
0.2	2.8	2.6	2.7	2.74	1	1.03
0.2	2.1	1.9	1.9	1.50	1.3	1.26
0.2	3.3	3.2	3.2	1.08	3	3
0.2	4.3	4.1	4.2	1.27	3.3	3.3
0.2	4.1	3.9	4	1.13	3.5	3.7
0.8	13.1	12.3	12.6	2.17	5.8	5.9
0.8	15.5	14.7	15.1	2.33	6.5	1.71
0.8	17.3	16.5	16.9	2.44	6.9	6.6
0.8	18.6	17.8	18.3	2.36	7.8	8
0.8	16.1	15.3	15.7	1.90	8.3	8.4
0.8	15.2	14.4	14.7	1.74	8.5	8.64
0.8	18.8	18.0	18.4	2.07	8.9	9.1

The bucket tests showed that the calculated flow rate and the flow rate observed by the flow meter are approximately the same. Considering that there are some clear sources of uncertainty in the bucket tests (e.g. imprecision of timing due to user error) it appears that the flow meter is measuring correctly. The values from the bucket tests are also shown graphically in Figure 19.

Once the flow meter was deemed to be measuring the water flow rate correctly several tests were conducted to identify the calibration curve comparing the flow rate of the water to the signal sent to the datalogger. This was done by simply opening the water system to an arbitrary flow rate, recording the value displayed on the flow meter as well as the signal sent to the data logger and repeating the process for a different arbitrary flow rate. These values were then entered into a spreadsheet, graphed and used to find a linear relationship between the flow rate and the signal. The chart and calibration curve are displayed in Figure 19.

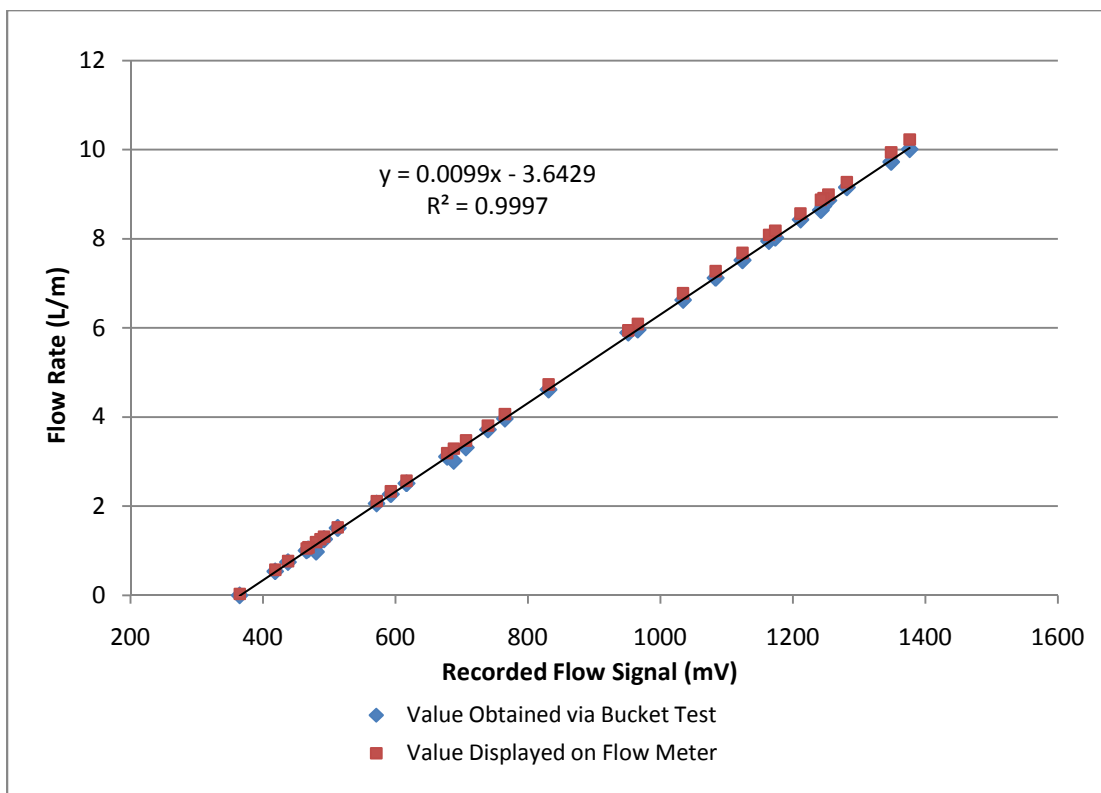


Figure 19: Comparing the Measured Water Flow Rate to the Generated Signal

The linear trendline fits well with an R^2 value of 0.9997. This implies that, while the generated signal values are not exactly what would be expected from a 4 to 20 mA sensor, the signals

generated by the flow meter can be both trusted and accurately converted from signals to flow rates. The signal was converted to a mass flow rate using Equation (29).

$$\dot{m} = (0.0099 * V_{Water} - 3.6429) * \rho_{Water} * \frac{60 \text{ Minutes}}{hr} \quad (29)$$

3.6 Natural Gas Flow Rate

The flow meter used to measure the rate at which natural gas enters the heater is a Fox Thermal Instruments Model FT2 Thermal Mass Flowmeter & Temperature Transmitter. The FT2 is a hot wire anemometer type mass flow meter designed for use with natural gas [16]. The specification sheet indicates that it is accurate to within $\pm 1\%$ of reading or $\pm 0.2\%$ of full scale [16]. This accuracy requires a length of 8 diameters upstream of the flow meter and 4 diameters downstream of the flow meter [16]. In the actual installation there are 28 diameters to the nearest valve upstream and 18 diameters before the nearest bend downstream. It has a flow response time (one time constant) of 0.9 seconds which was the fastest of the flow meter options [16]. In a 1.9 cm line it has a range of 0-3400 sL/M and a 100:1 turndown ratio [16]. Since the natural gas flow will be approximately between 6.8 L/M and 83 L/M for the Rinnai heater the available range and turndown ratio should be adequate. Since the meter is brand new it is reasonable to assume that it is still well calibrated and the calibration sheet provided by the manufacturer can be trusted. The meter was nominally calibrated to provide a 4-20 mA signal for flow rates between 0 and 142 SL/M. The data for the calibration curve are displayed in Table 21 [16].

Table 21: Fox Thermal FT2 Calibration Chart

Test Number	Input	L/min at STP
1	0.3526	0
2	0.3848	1.42
3	0.4280	3.96
4	0.4677	7.93
5	0.5014	12.46
6	0.5407	20.1
7	0.5776	29.2
8	0.6100	38.8
9	0.6413	50.7
10	0.6792	68
11	0.7014	79.6
12	0.7392	102
13	0.7663	120
14	0.7991	146
15	0.9017	255

The 4 to 20 mA signal from the Fox Thermal FT2 flow meter was converted into a volumetric flow rate using Equation (30). The output from the FT2 is in standard meters per minute, implying that corrections for pressure and temperature have already been completed. $\dot{V}_{Fox} =$

$$\frac{1420}{1600} V_{Fox} - \frac{2000}{1600} \quad (30)$$

$$\dot{V}_{Fox} = \frac{1420}{1600} V_{Fox} - \frac{2000}{1600} \quad (30)$$

The calibration of the Fox Thermal flow meter was checked using a standard residential natural gas meter. The AM-250 was fitted with a display which generated a pulse for every 0.7 L of gas which passed through the meter. The pulse signal from the AM-250 was converted to a flow rate using Equation (31). A test was run under steady state conditions. Results are shown in Figure 20.

$$\dot{V}_{Res} = \frac{\#Pulse}{3 s} * \frac{60 s}{Minute} * \frac{0.7L}{Pulse} * \frac{P_{Sample}}{101.325 kPa} * \frac{293.15 K}{T_{Sample}+273.15 K} \quad (31)$$

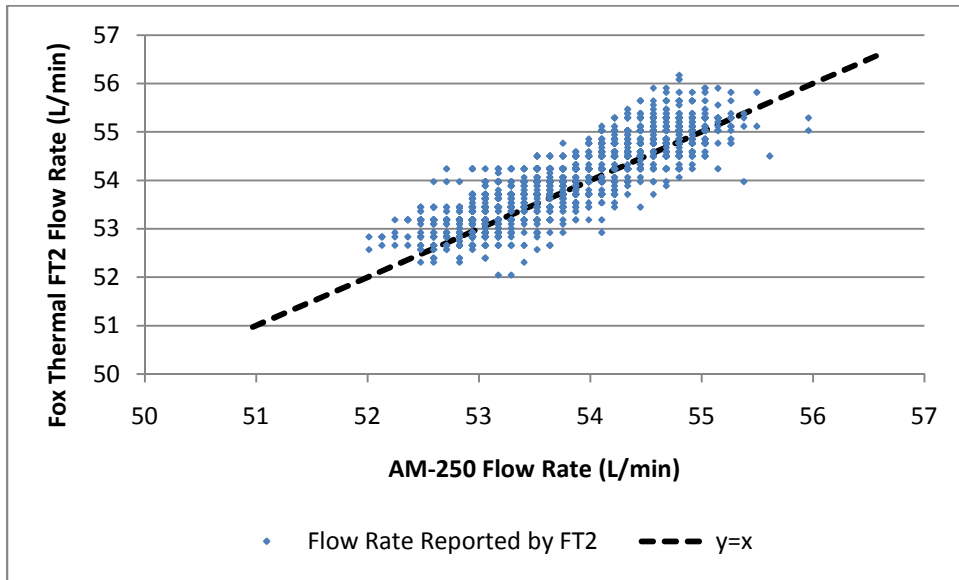


Figure 20: Comparison of Two Natural Gas Flow Meters

Figure 20 shows data recorded from both the Fox Thermal flow meter and the standard residential flow meter. The flow rate reported by the Fox Thermal FT2 is shown as dots. A reference line showing perfect agreement with the AM-250 is shown by the black dashes. Figure 20 shows only small discrepancies between the FT2 and AM-250. As a result, it is safe to conclude that the two meters are not statistically different and the Fox Thermal flow meter is

most likely reading correctly.

Chapter 4: Experimental Design

The experimental apparatus was designed to be used in many different configurations allowing for different tests. The configurations are discussed in the following sections.

4.1 Tankless Heater Performance Testing

4.1.1 Steady State Efficiency

Experiments were performed to determine the impact of various operating conditions on the steady state efficiency of the heater. These tests were run using the configuration shown in Figure 21.

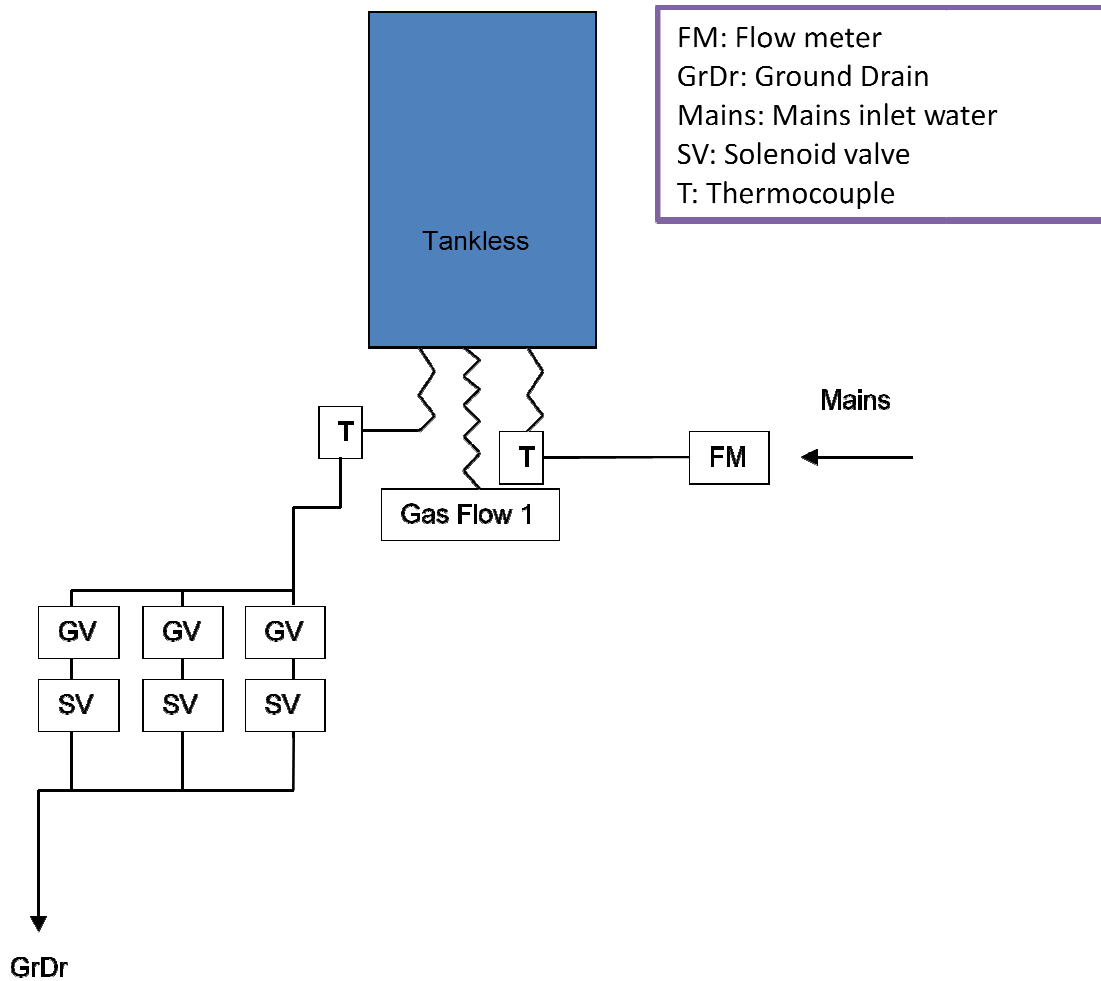


Figure 21: Steady State Efficiency Test Schematic

Mains temperature water was used in all steady state efficiency tests. Before entering the tankless heater the water flow rate and inlet temperature were measured. After passing through the heater the outlet temperature was measured. The manifold consisting of three different flow paths, each with a globe valve and solenoid valve, were used to control the water flow rate. After passing through the manifold the water exited the system by being sent to the drain. The natural gas volumetric flow rate was measured with the Fox Thermal flow meter.

In each steady state efficiency test two burns were performed. A burn was initiated by turning

the tankless heater on, and ended by turning the tankless heater off.

The steady state efficiency test was performed for several different sets of flow conditions.

Three water flow rates and five set temperatures were used, with tests performed for all combinations. The tested flow rates and temperatures are shown in Table 22.

Table 22: Flow Rates and Set Temperatures used in Steady State Efficiency Test

Water Flow Rate (kg/hr)	Set Temperature
180.5	36.7
338	43.3
Max	48.9
	54.4
	60

The water flow rate referred to as “Max” means that the test system was opened to a flow rate of approximately 23 L/min. The heat demand rate at this flow rate varied depending on set temperature, but always exceeded the capacity of the heater. The overflow caused the water flow control device to engage so that the tankless heater maintained the maximum flow rate for which it could still meet the demand.

The measurements were used to identify the steady state efficiency of the tankless water heater.

The steady state efficiency was calculated using Equation

(32).

$$\eta_{Conv} = \frac{\dot{m}C_p(T_{Exit}-T_{In})}{\dot{v}_{Fox}h_{gas}} \quad (32)$$

The uncertainties for each measurement are shown in Table 23.

Table 23: Uncertainty in Measurements in Steady State Efficiency Test

Measurement	Uncertainty
Water Flow Rate	1.50%
Outlet Temperature	0.5 C
Inlet Temperature	0.5 C
Gas Flow Rate	1%
Energy Density of Gas	5%

The uncertainty in calculated steady state efficiency ($W\eta$) for each test is shown in Table 24.

Table 24: Uncertainty in Steady State Efficiency Calculations

m _{water} (kg/min)	ΔT (°C)	Gas Flow (L/min)	$W\eta$
3	26.7	10.8	0.059
3	33.3	13.3	0.057
3	38.9	17.0	0.056
3	44.4	19.8	0.055
3	50.0	22.1	0.055
5.6	26.7	23.2	0.059
5.6	33.3	29.4	0.057
5.6	38.9	36.2	0.056
5.6	44.4	37.7	0.055
5.6	50.0	43.6	0.055
9.8	26.7	37.1	0.059
9.8	33.3	46.4	0.057
9.8	38.9	67.4	0.056
9.8	44.4	66.5	0.055
9.8	50.0	68.0	0.055

The uncertainty contributed by each measurement is shown in Table 25.

Table 25: Uncertainty from Each Measurement in Steady State Efficiency Tests

m _{water} (kg/min)	ΔT (°C)	Gas Flow (L/min)	dp/p	dv/v	dm/m	d(ΔT)/dT
-----------------------------	-----------------	------------------	------	------	------	--------------------

3	26.7	10.8	0.05	0.01	0.015	0.027
3	33.3	13.3	0.05	0.01	0.015	0.021
3	38.9	17.0	0.05	0.01	0.015	0.018
3	44.4	19.8	0.05	0.01	0.015	0.016
3	50.0	22.1	0.05	0.01	0.015	0.014
5.6	26.7	23.2	0.05	0.01	0.015	0.027
5.6	33.3	29.4	0.05	0.01	0.015	0.021
5.6	38.9	36.2	0.05	0.01	0.015	0.018
5.6	44.4	37.7	0.05	0.01	0.015	0.016
5.6	50.0	43.6	0.05	0.01	0.015	0.014
9.8	26.7	37.1	0.05	0.01	0.015	0.027
9.8	33.3	46.4	0.05	0.01	0.015	0.021
9.8	38.9	67.4	0.05	0.01	0.015	0.018
9.8	44.4	66.5	0.05	0.01	0.015	0.016
9.8	50.0	68.0	0.05	0.01	0.015	0.014

As can be seen in Table 25 the uncertainty in the natural gas energy density is larger than the uncertainty associated with the other measurements. The lack of measurement of natural gas energy density represents 5% uncertainty while the next largest error is 2.7% in the temperature difference. This indicates that the first measurement to be improved in an attempt to reduce the final uncertainty for the steady-state efficiency should be that of the natural gas energy density.

4.1.2 Response to Rapid Changes in Flow Rate System Design

The next experimental test was performed to determine how the tankless water heaters react to rapid changes in water flow rate. There is a short delay between the time the draw flow rate changes and the time the heater control logic responds. Because of this delay rapid changes in flow rate will cause periods when the outlet temperature fluctuates. For these tests the system was configured in the same manner as the steady state efficiency tests.

In these tests the flow rate was adjusted by changing which valves in the manifold were open.

The globe valves were set to 2.7, 5.8 and 9.7 L/min. Sudden changes in the flow rate were initiated by opening or closing a solenoid valve.

The parameter of interest during this test was the deviation of outlet temperature from the set temperature. The only uncertainty in measurements was from that thermocouple. It is displayed in Table 26.

Table 26: Uncertainty in Response to Rapid Changes in Flow Rate Tests

Measurement	Uncertainty
Outlet Temperature	0.5 C

4.1.3 Response to Gradually Decreasing Inlet Water Temperature System Design

The tankless water heater was also subjected to tests designed to investigate how they react to inlet conditions which require heating rates below their minimum burner rate, and to changes in required heating rates near the minimum burner rate. It has been theorized that instability and dramatic fluctuations will result if feedback control is used [14]. The schematic used to test the heaters response to varying inlet temperature is illustrated in Figure 22.

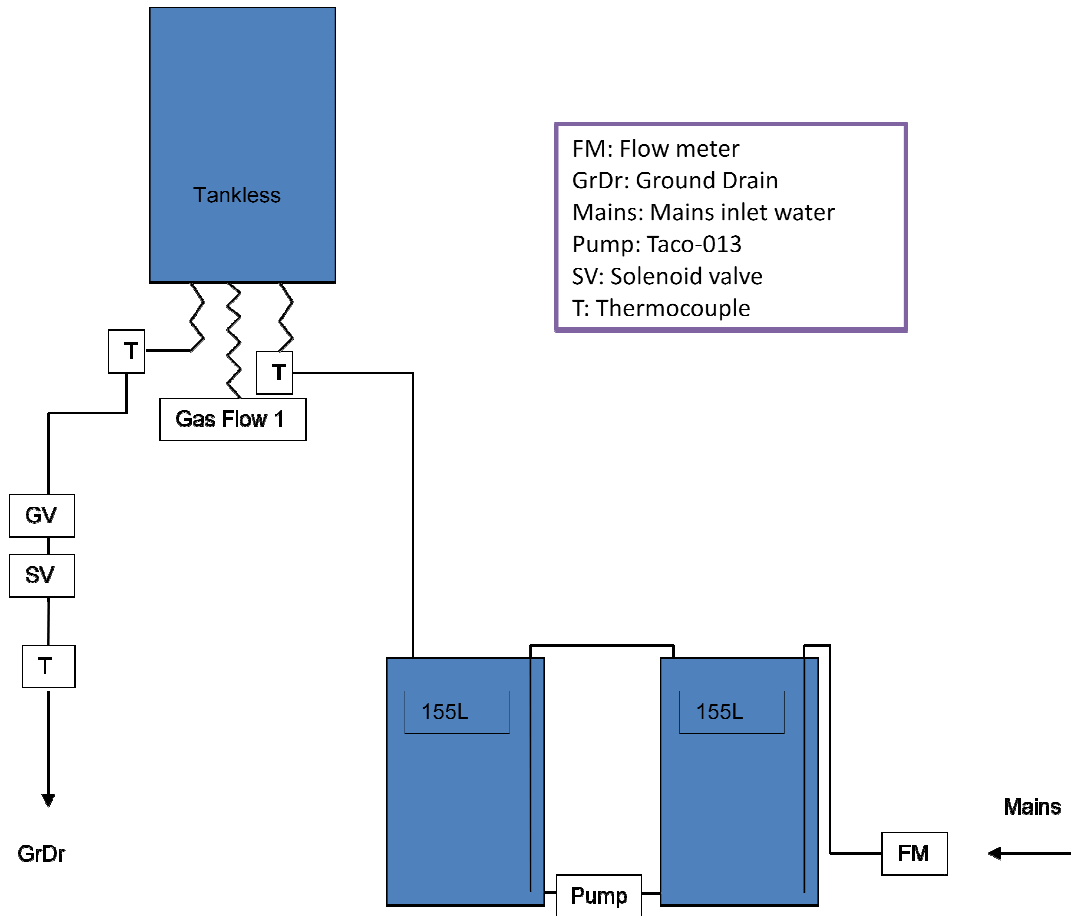


Figure 22: Response to Gradually Decreasing Inlet Temperature System Schematic

The gradually decreasing inlet temperature tests focused on how the tankless heater responds to a gradually increasing heat demand rate. The tests were designed to observe how the heaters react to these conditions when below the minimum heat rate the heater can provide. At the beginning of the test a draw was initiated such that the required heat rate was less than the minimum heat rate. As mains water replaced heated water in the 40 gallon storage tanks the water temperature decreased. A circulation pump was used to keep the water in the tanks mixed. With the draw flow rate held constant a gradually decreasing inlet water temperature resulted in a gradually increasing required heat rate. The test continued until the heater began operating in steady state.

Tests were performed for all combinations of three flow rates and three set temperatures. The test conditions and starting inlet temperatures are shown in Table 27.

Table 27: Starting Inlet Temperatures for Decreasing Inlet Water Temperature Tests

		Set Temperature (°C)		
		48.9	54.4	60
Water Flow Rate (kg/hr)	158	35.6	41.1	46.7
	338	42.7	48.2	53.8
	564	45.2	50.7	56.3

There were two desired outputs from this test. The first was a qualitative observation of how the heater behaved. Qualitative observations focused primarily on whether or not there were oscillations when the required heat rate was less than the minimum heat rate. Quantitative results identified the required heat rate at the time that the heater fired. The required heat rate was calculated using Equation (33).

$$\dot{Q}_{Required} = \dot{m}C_p(T_{Set} - T_{In}) \quad (33)$$

The measurements and associated uncertainties used in Equation

(33) are shown in Table 28. Table 29 shows the uncertainty in required heat rate for each test. Table 30 shows the uncertainty from each measurement.

Table 28: Measurement Uncertainty in Gradually Decreasing Inlet Temperature Tests

Measurement	Uncertainty
Water Flow Rate	1.50%
Inlet Temperature	0.5 C

Table 29: Overall Uncertainty in Gradually Decreasing Inlet Water Temperature Tests

m_water (kg/min)	dT (C)	W _η
3	38.89	0.024
3	44.44	0.022
3	50	0.021
5.63	38.89	0.024
5.63	44.44	0.022
5.63	50	0.021
9.78	38.89	0.024
9.78	44.44	0.022
9.78	50	0.021

Table 30: Uncertainty Caused by Each Measurement in Gradually Decreasing Inlet Water Tests

m_water (kg/min)	dT (C)	dm/m	d(dT)/dT
3	38.89	0.015	0.018183
3	44.44	0.015	0.01591
3	50	0.015	0.014142
5.63	38.89	0.015	0.018183
5.63	44.44	0.015	0.01591
5.63	50	0.015	0.014142
9.78	38.89	0.015	0.018183
9.78	44.44	0.015	0.01591
9.78	50	0.015	0.014142

As can be seen in Table 29 the overall uncertainties in required heat rate are not large. The largest uncertainty in a single test was 2.4%. Table 30 shows that neither measurement dominated the uncertainty calculation. In all tests the uncertainties in mass flow rate and in temperature change across the tankless heater were similar.

4.1.4 Minimum Flow Rate System Design

Most gas fired tankless water heaters have a minimum flow rate regardless of the minimum

burner capacity. Typically the minimum flow rate is approximately 114 to 118 kg/hr. A test was completed which focused on gradually adjusting the inlet flow rate and observing the reactions of the tankless heater. For these tests the system was used in the same configuration as in the steady state efficiency tests.

This test utilized the simplest testing procedure. The only parameter adjusted for this test was the water flow rate which was changed by manually adjusting the globe valve downstream of the heater. The test was started with a flow rate of 0 kg/hr and slowly increased until the heater began to heat the water. Efforts were made to adjust the flow rate slowly during transition periods as the heater was subject to variations in the flow rate.

There were two sources of error during these tests. The first is the adjustment of the flow rate itself. Due to the design of the system the minimum adjustment to the flow rate was 0.19 L. The second source of error comes from the water flow rate measurement. The uncertainty in this measurement is listed in Table 31.

Table 31: Uncertainty in Minimum Flow Rate Tests

Measurement	Uncertainty
Outlet Temperature	0.5 C

4.1.5 Parameter Derivation and Validation

The simulation model was checked against experimental data using a two step process. The first step focused on using experimental data to identify system parameters for the simulation model. This was accomplished using GenOpt to vary the parameters until the simulation results matched

the experimental data as closely as possible [23]. The second step focused on checking the GenOpt results by using the regressed parameters to compare simulation results to experimental data for a completely different draw pattern.

The experimental setup was used to develop a test protocol which could be used to validate the model. For this purpose a special test protocol was designed which focused on isolating the parameters of interest. The protocol was developed with the intention of including periods where the output of the system was dominated by either the environmental losses, characterizing the UA value of the heater, the steady state operation, characterizing the steady state burn efficiency, or a decay with water flowing, dominated by the capacitance of the heat exchanger.

The parameter identification test was very similar to the steady state efficiency test. The difference is that there was a period of high inlet temperature and low flow rate operation before the mains water purge. This period was intended to identify the UA value. The high inlet temperature helped to impose a large temperature difference between the heat exchanger and the ambient conditions to increase the environmental losses. The low flow rate was selected to keep the water in the heat exchanger as long as possible resulting in more total heat transfer and a higher temperature drop. The high temperature drop prevented any noise in temperature measurements from significantly impacting the measured temperature drop as the water passed through the heat exchanger and caused good and repeatable calculations of the UA value of the heat exchanger.

Once the UA of the heat exchanger was isolated the other terms were easy to identify. The

efficiency and UA value are the only two parameters which influence the heater during steady state operation, so the final few minutes of each burn were used to identify the steady state efficiency. The decay periods after each draw were governed by mainly the capacitance of the heat exchanger, with the UA value having a secondary impact. As a result the decay periods were used to identify the capacitance.

There were two different sets of measurements during the parameter identification test. The first focused on identifying the temperature change across the heat exchanger for both the UA value and capacitance calculation. The second focused on the steady state efficiency. Uncertainties in these measurements and calculations have been described in previous sections.

The parameters for the tankless heater being tested were identified by minimizing the χ^2 value over the course of a simulation. This term was calculated comparing the output from the simulation to the experimental data and normalizing to the standard deviation of the measurements Equation (34) [28].

$$\chi_x^2 = \sum_1^{\#Point} \left(\frac{x_{Experiment} - x_{Simulation}}{\sigma_{Experiment}} \right)^2 * S_x \quad (34)$$

In Equation (34) x could be any variable of interest. The two variables which were used are the outlet water temperature and the natural gas flow rate. The S term is a gating function used to identify areas of interest. The symbol could either represent a zero indicating that the data point is not appropriate for the χ^2 calculation, or a one indicating that it is.

This calculation was performed for both the outlet temperature and natural gas flow rate. The

two χ^2 values were then combined to form an aggregate χ^2 . The final χ^2 value represents χ^2 over the calculation periods for both natural gas and temperature measurements.

The second test in the validation process was intended to check the accuracy of the identified parameters when the heater simulation model is operated under different conditions. An experimental protocol was designed to test the predictions of the simulation model during the following situations: 1) when the required heat was below the heaters minimum setting, 2) the flow rate was set below the minimum flow rate, 3) the heater should operate normally, 4) the required heat was higher than the heater could supply and 5) during and following a long decay.

The validation test utilized only temperature and flow rate measurements. No calculations were completed as the point of the test was to compare the outlet temperature, water flow rate and natural gas flow rate from the simulation output to those from the experimental data. The uncertainties in measurements which impacted the validation test are shown in Table 32.

Table 32: Measurement Uncertainties in Validation Test

Measurement	Uncertainty
Water Flow Rate	1.50%
Outlet Temperature	0.5 C
Gas Flow Rate	1%
Energy Density of Gas	5%

4.2 Addition of a Small Tank Testing Design

The final tests performed focused on one proposed solution for the problems associated with a tankless water heater. These problems include such issues as minimum flow rate, minimum burner capacity, warm-up time and potential temperature oscillations. It has been proposed that these problems could be solved by adding a small (approximately 23.25 L) storage tank to the system. The tankless heater was then used to heat the water stored in the small tank. Using this approach the flow through the tankless heater can be controlled separately from the flow to the fixtures allowing the tankless heater to operate when heat is needed rather than when the flow meets the heaters' criteria. Thus it removes problems associated with the minimum flow rate and minimum burner capacity. The small tank also acts as a buffer. Storing hot water in the tank means that hot water can be sent to the fixtures even while the tankless heater is warming up. This feature removes problems associated with increased delay before hot water gets to the fixture. The small tank also reduces the impact of fluctuations in the outlet water temperature in two ways. First, any water addition which is off of the setpoint will mix with water which is at the set temperature resulting in smaller temperature fluctuations. Because of that effect any fluctuations observed by the user will not be as dramatic as without the buffer tank. Secondly, the water storage tank represents a place where the water exiting the tankless heater will remain and mix for some time before entering the house plumbing system. Depending on the size of the tank the delay may be long enough that the hot spikes in the oscillations may end up mixing with the cold portions of the oscillations. While this may not cause the outlet water to be precisely at the set temperature, it would at least provide a more constant temperature than if the user were experiencing undampened oscillations.

There are however some theoretical disadvantages to this configuration. While the addition of a

small water storage tank theoretically improves usability for the occupant it also increases the life cycle cost of the entire system which is one main drawback of tankless water heaters. Currently, installing a tankless water heater is not clearly economically attractive only in a specific set of conditions. Adding a small storage tank would increase the installation cost by adding the expense of a storage tank, a circulation pump, additional piping and additional installation labor. It would also decrease the annual energy savings by introducing standby losses to the system and increasing electricity demand because of the circulation pump. Due to the increased cost, the system with the added storage tank would only be justifiable in selected applications where the user cares more about hot water temperature than economics.

Tests performed on this system focused on replicating and understanding problems observed in a Building America home. There were four questions of interest to the Building America team. First, there were situations where the hot water going to the draw would come out at the set temperature then suddenly drop below the set temperature for a short period of time before returning to the set temperature. A better understanding of this behavior is needed. Second, there were situations where the water coming out would drop below the set temperature and never increased to the set temperature. Third, it was theorized that the poor outlet temperature might be caused by mixing in the tank and wanted a better understanding of the stratification in the tank. Fourth, the system is tested reconfigured so that the output from the tankless heater can be directed straight to the mixing valve instead of into the tank and wanted to see if this reconfiguration would help with the other problems.

A diagram illustrating the system used to test these principles can be seen in Figure 23.

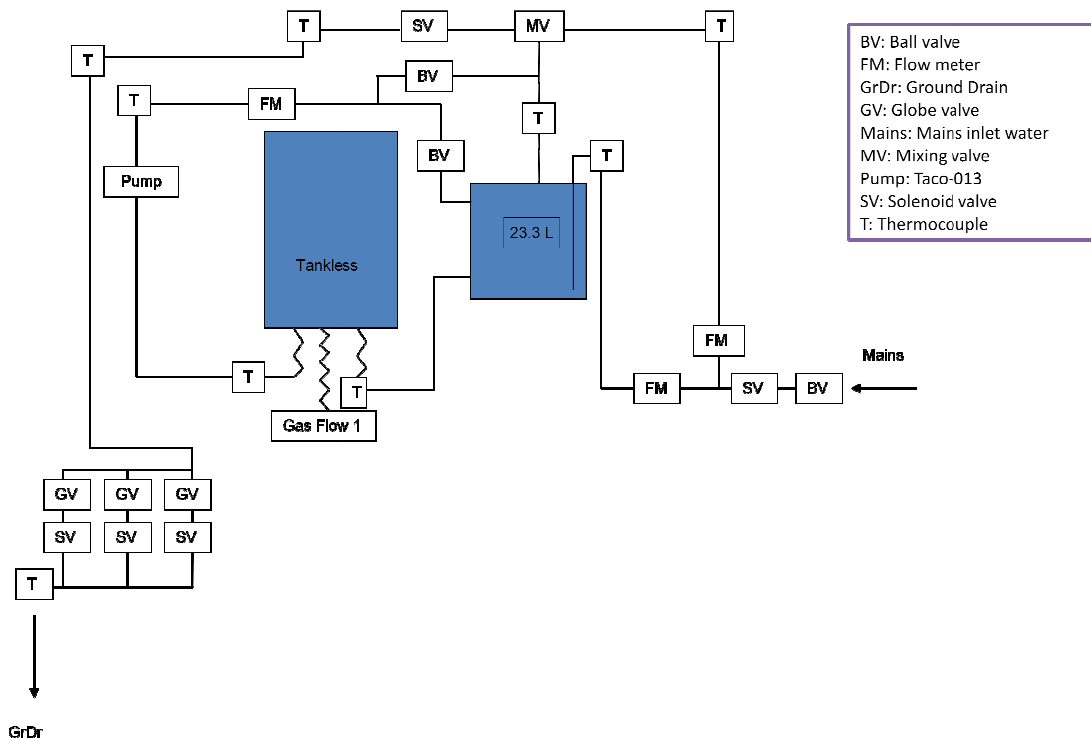


Figure 23: Small Tank System Test Schematic

4.2.1 Cold Water Slug Testing Design

The problem of having a slug of cold water pass to the draw was tested by controlling the heater and tank system with various strategies. It was assumed that the problem was caused by the tankless heater not firing soon enough resulting in water at the top of the small tank dropping below the mixing valve set temperature. Under what conditions the cold water slug problem occurs was tested by simulating draws at three flow rates with the circulation pump being controlled by differing strategies based on the height of the cold water in the tank, and the simulated deadband of the controller in the small tank. The parameters used to vary the tests are

shown in Table 33.

Table 33: Parameters in Cold Water Slug Tests

Flow Rate (kg/hr)	Cold Water Height (cm below outlet)	Deadband (°C)
156	2.5	0
338	9.5	1
451	16.5	5

The height of the cold water was described in terms of the centimeters below the hot water outlet. The deadband referred to the difference between the set temperature and the temperature measured by the control thermocouple. A test with a deadband of zero degrees was used to simulate the case of the circulation pump turning on right at the start of a draw.

All measurements in the cold water slug tests were water temperature. Because all thermocouples used were special limits of error thermocouples from the same manufacturer all measurements had 0.5 °C uncertainty. No calculations were performed.

4.2.2 Small Tank Stratification Testing Design

The question of stratification in the tank was investigated by measuring the temperature of the water at varying heights in the small tank. The amount of stratification in the tank was observed for two different settings. The first was the setting of a draw and the data was collected from the previously described cold slug tests. The second was an examination of how the temperatures in the tank would stratify during periods of heating between draws.

All measurements were temperature measurements using special limits of error thermocouples from the same manufacturer. Uncertainty on the thermocouples was 0.5 °C. No calculations were performed.

4.2.3 Tepid Outlet Testing Design

Once the theory of tank destratification had been examined the next task was to evaluate why water from the tank was colder than the set temperature of the mixing valve. This was tested by simulating draws at varying flow rates and set temperatures with the circulation pump flowing through the tankless heater. The parameter of interest was the temperature of the water flowing from the small tank to the mixing valve. The intended outcome was to assess how the draw flow rate and the tankless set temperature impacted the draw temperature. Tests were performed using all combinations of the flow and temperature parameters indicated in Table 34.

Table 34: Flow and Temperature Parameters in Tepid Outlet Tests

Flow Rate (kg/hr)	Tankless Set Temperature (°C)
158	48.9
338	54.4
451	60
564	

4.2.4 Small Tank Bypass Valve Design

The NREL team studying the small tank configuration theorized that the problems associated with installing the small tank could be overcome by reconfiguring the system. In the original

system the outlet water from the tankless heater entered the small tank. The team theorized that the tepid outlet and cold slug problems were caused by mixing in the tank; rather than the hot water going from the tankless heater to the mixing valve it appeared that the hot water was entering the tank, mixing with colder water in the tank, and resulting in cooler water to the mixing valve. As a result, the team reconfigured the system to allow the hot water to flow directly from the tankless heater to the mixing valve. The conceptual configuration would allow the hot water from the tankless to be used as the output during a draw, but the water could still flow into the small tank between draws to keep it at the desired set temperature. It would also overcome the minimum flow rate to burn problem because the flow rate passing through the tankless would be controlled by the circulation pump instead of the hot water draw.

In order to identify the impact of the bypass valve, the system with the new configuration was subjected to the same cold slug and tepid outlet tests so that they could be compared to the previous results. Instead of repeating all the previous tests, only the “worst case” tests were deemed necessary. The “worst case” tests included tests which showed a large cold slug and a tepid outlet problem.

Chapter 5: Experimental Results

As discussed in Chapter 4 several experimental tests were conducted. These experiments focused on general characterization and efficiency of the heater, the response of the heater to changing water flow rates, to pre-heated water temperatures and the overall system effects of combining a tankless heater with a small storage tank.

5.1 Performance and Behavior of Tankless Heater Results

5.1.1 Steady State Efficiency Results

As was discussed in section 4.1.1 the impact of water flow rate, set temperature and total heat demand on steady state efficiency was investigated. Tests were carried out according to the matrix specified in Table 22. The results for steady state efficiency measurements are displayed in Figure 24 and Figure 25. Figure 24 shows the impact of set temperature on steady state efficiency while Figure 25 indicates the impact of natural gas input rate.

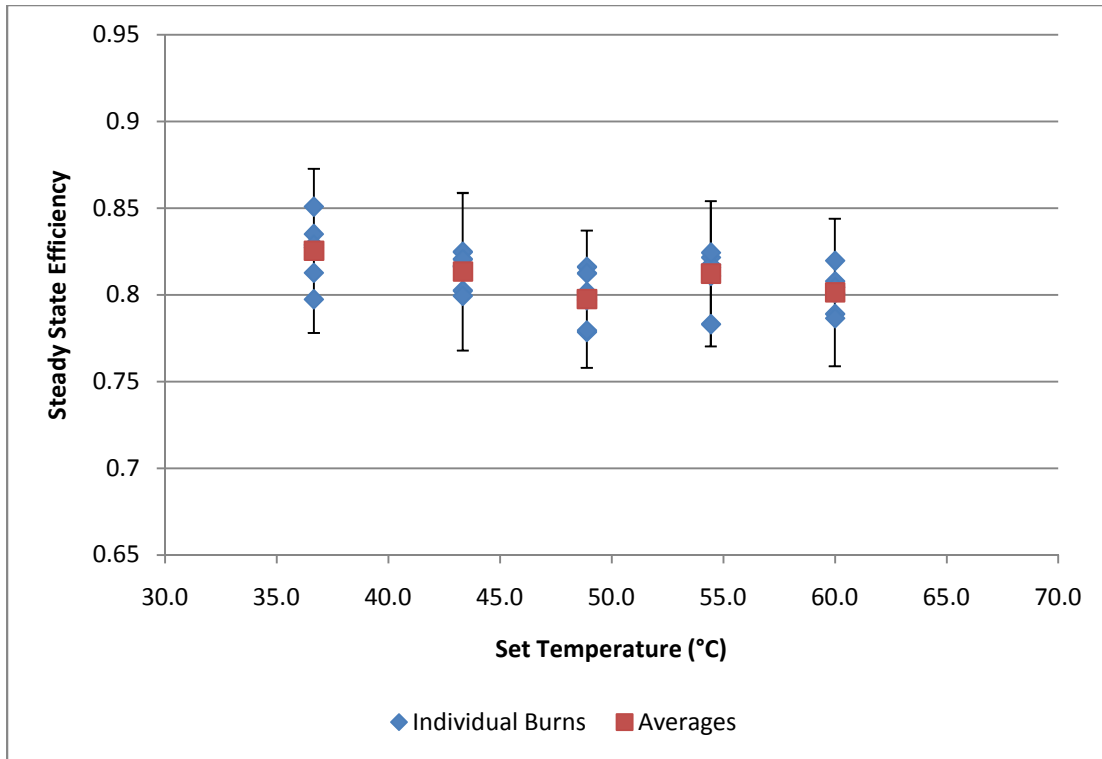


Figure 24: Steady State Efficiency as a Function of Set Temperature

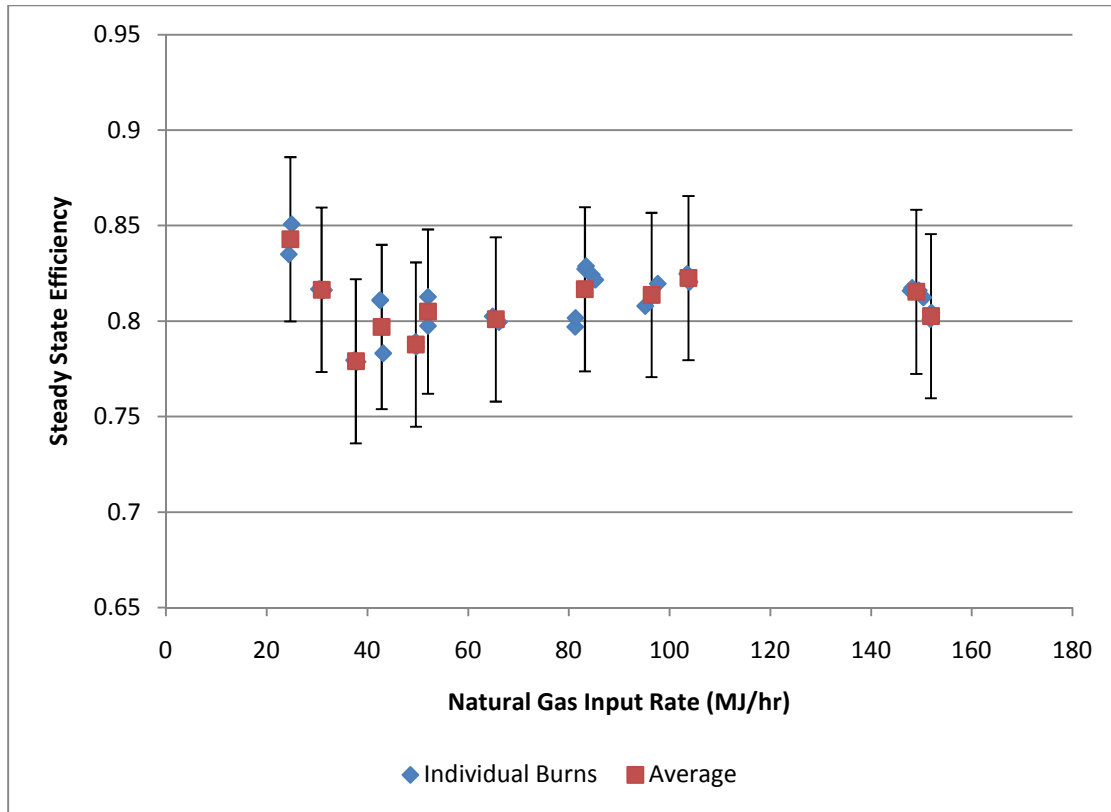


Figure 25: Steady State Efficiency as a Function of Gas Draw Rate

In both Figure 24 and Figure 25 an individual burn is represented by a diamond while averages are represented by squares. The different burns in Figure 24 are caused by differing flow rates at each set temperature. In Figure 25 the individual burns represent different flow rate and set temperature combinations plotted as a function of the natural gas input rate. Error bars in both plots represent the measurement uncertainty. Neither the results in Figure 24 or Figure 25 give any reason to believe that the steady state efficiency is changing with either variable. In both cases the variation appears to be random and does not follow an identifiable trend. Moreover the error bars representing measurement uncertainty overlap with each other implying that any variation is not statistically significant. Due to the lack of a discernable trend it was determined that steady state efficiency is a fixed value rather than a parameter which varies based on

operating conditions.

5.1.2 Response to Rapid Changes in Flow Rate

The response of the heater to rapid changes in water flow rate was examined during two tests. The first test featured bringing the system to steady state at a 564 kg/hr flow rate before fluctuating the temperature between the 564 kg/hr starting point and both 338 kg/hr and 158 kg/hr flow rates. The second test started with steady state operation at a 338 kg/hr flow rate and then reduced to 158 kg/hr. For these tests the set temperature of the heater was 60 °C. Results from these two tests are shown in Figure 26 and Figure 27. Both figures have the temperature data referenced on the left-hand axis while the water flow rate data is referenced on the right-hand axis.

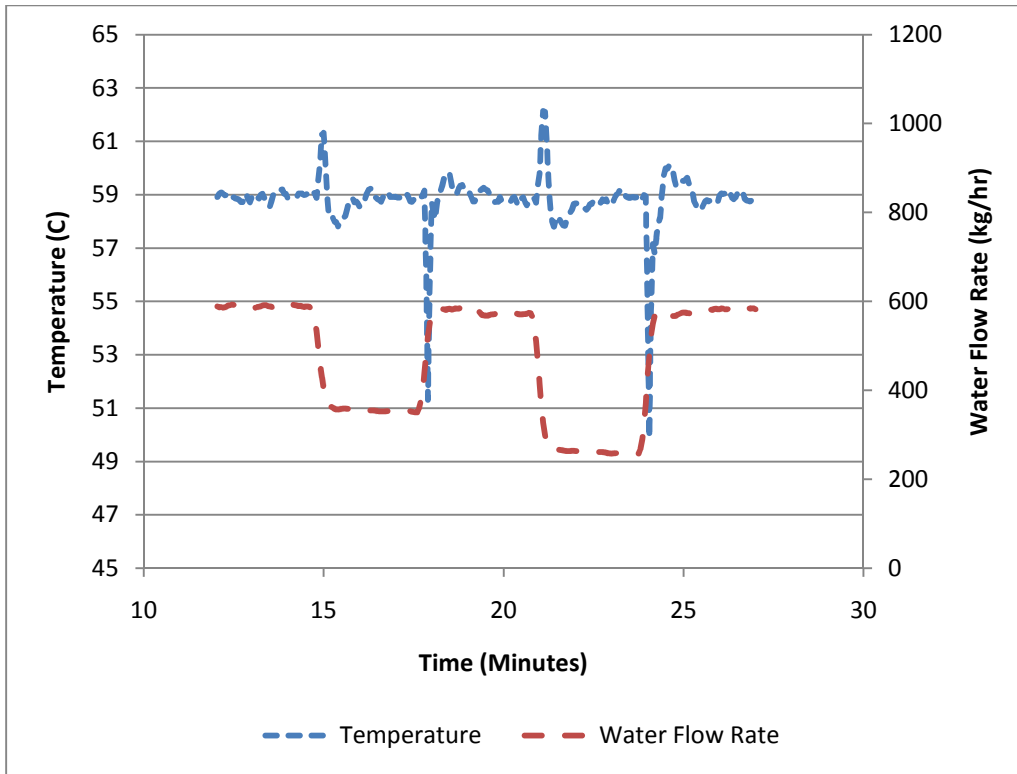


Figure 26: Temperature Fluctuations in Response to Changing Flow Rate (565 kg/hr Standard Flow)

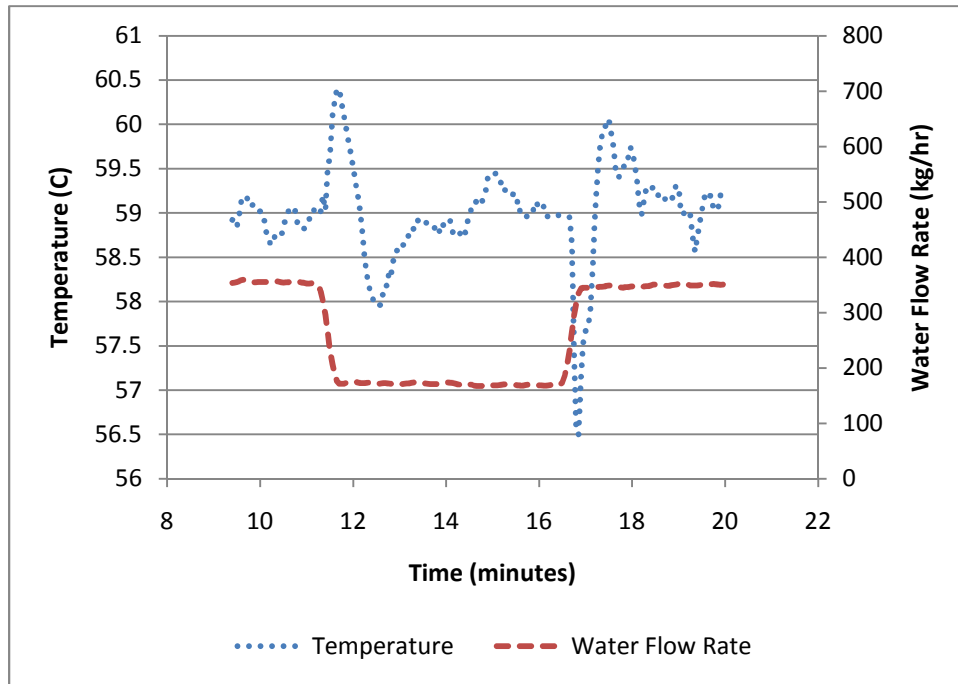


Figure 27: Temperature Fluctuations in Response to Changing Flow Rate (338 kg/hr Standard Flow)

Both sets of data show the same general trend. When the flow rate is changed the temperature fluctuates as the heater reacts. In the case of decreasing flow rate the heater response takes the form of increasing outlet temperature and in the case of increasing flow rate the outlet temperature decreases. In both cases the heater tends to over-estimate the change in control constant needed to re-achieve steady state thus inducing periodic variations of decreasing magnitude before the outlet temperature settles and returns to steady state.

As indicated in the six original temperature changes associated with the six changes in flow rate, the magnitude of the temperature fluctuations increases with the magnitude of the change in flow rate. With the steady state temperature for all changes being approximately 58.98 °C the temperature spikes caused the outlet temperature to change to 62.2 °C and 50 °C when the flow rate changed from 564 kg/hr to 158 kg/hr. The outlet temperature fluctuates from 61.7 °C to 51.1 °C when the flow rate changes from 564 kg/hr to 338 kg/hr and from 60.6 °C to 56.7 °C when the flow rate changes between 338 kg/hr and 158 kg/hr.

5.1.3 Response to Gradually Decreasing Inlet Water Temperature

Tests were performed investigating how the heater reacts to the gradual decay in water flow rate. One main focus of this series of tests was to determine how the heater reacts to inlet conditions which required heat below the minimum burner threshold. As mentioned in the literature review, based on the assumption of feed-back controls it was theorized that the outlet temperature would have large fluctuations. This series of tests was also intended as an opportunity to explore how the heater reacts to various operating conditions with the required heat rate below the minimum input heat rate.

These tests are important as they represent common occurrences in situations with solar water heaters. Solar water heaters often do not provide enough heat to meet demand instantaneously and so rely on conventional auxiliary sources to bring water up to the set temperature. The temperature of the stored water will gradually decrease as heat is removed from the tank. The storage tank water temperature in a solar preheat system will often be such that the minimum heat rate of the tankless heater exceeds the heat required by the draw water.

The behavior of the tankless heater varied with the differing conditions. There were two general behaviors; one in which the outlet temperature did not exceed the set temperature and one in which the heater did cause the outlet temperature to rise over the set temperature. Results from a test in which the temperature did not exceed the set temperature are presented in Figure 28 and Figure 29 while results from a test in which the temperature exceeded the set temperature are shown in Figure 30 and Figure 31. The test shown in Figure 28 and Figure 29 had a set temperature of 50 °C. The test in Figure 30 and Figure 31 had a set temperature of 60 °C.

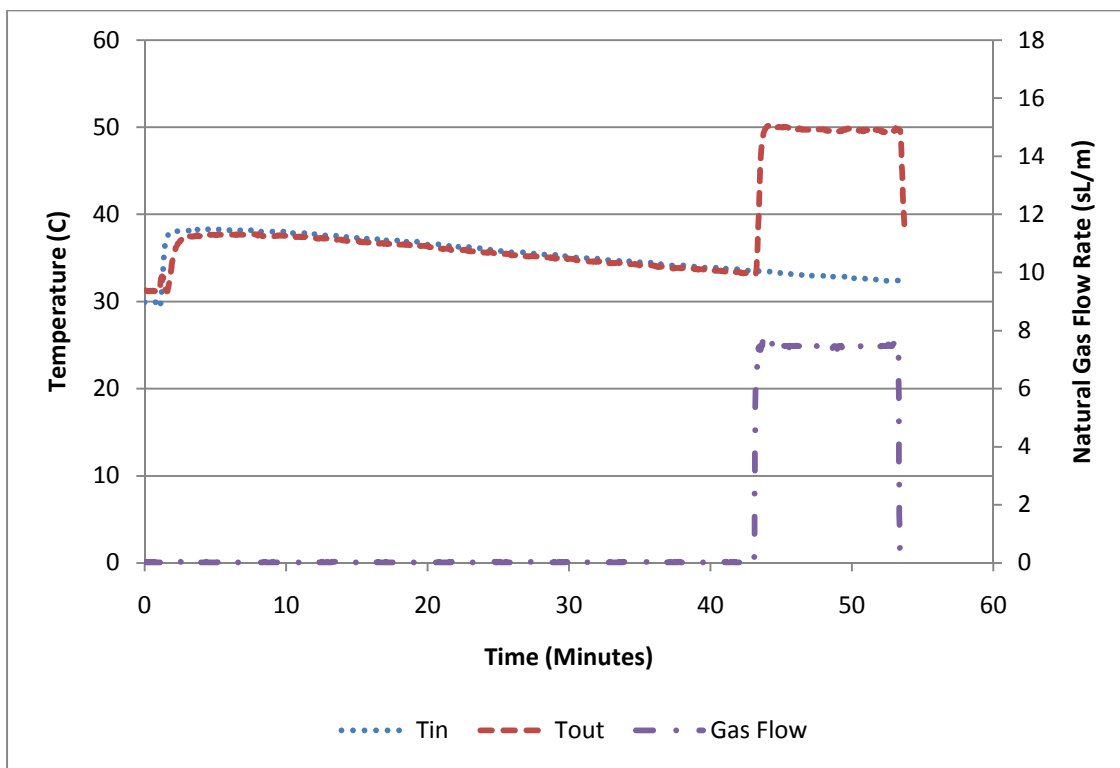


Figure 28: Temperatures and Flow Rates in a Test during Which the Outlet Temperature did not Exceed the Set Temperature

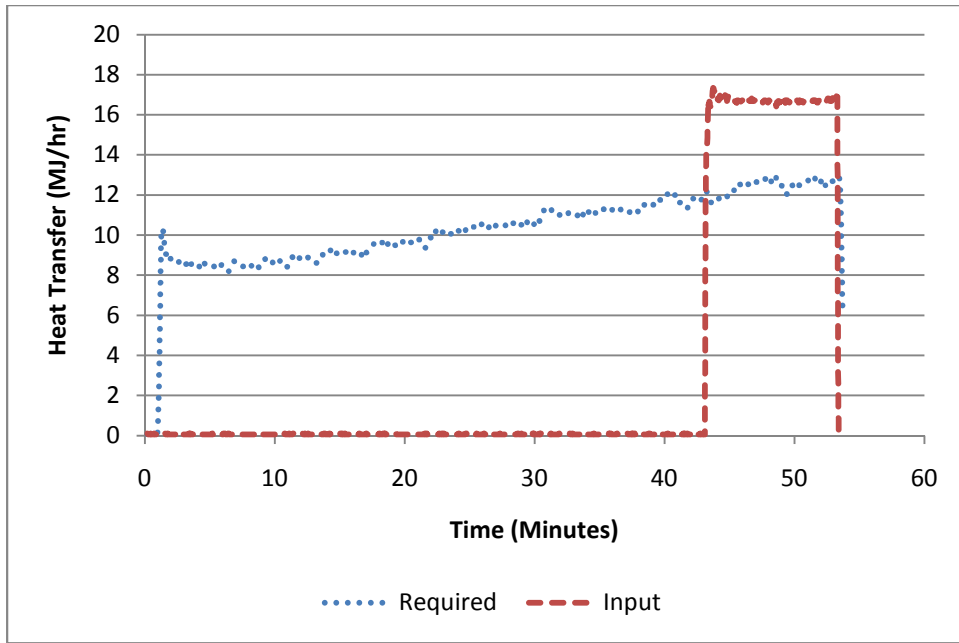


Figure 29: Calculated Heat Rates in a Test during Which the Outlet Temperature did not Exceed the Set Temperature

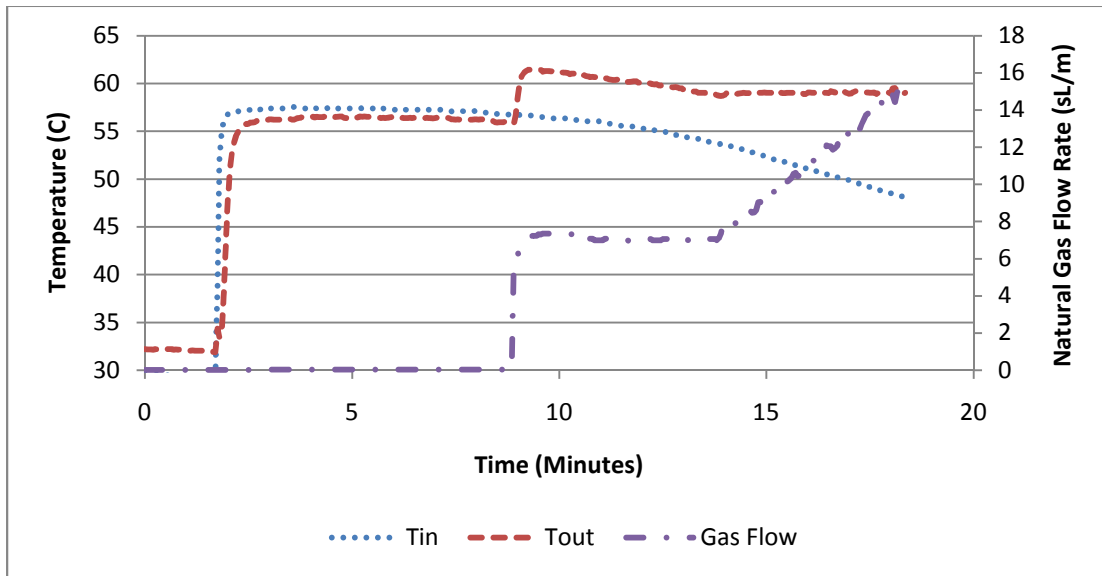


Figure 30: Temperatures and Flow Rates in a Test during Which the Outlet Temperature Exceeded the Set Temperature

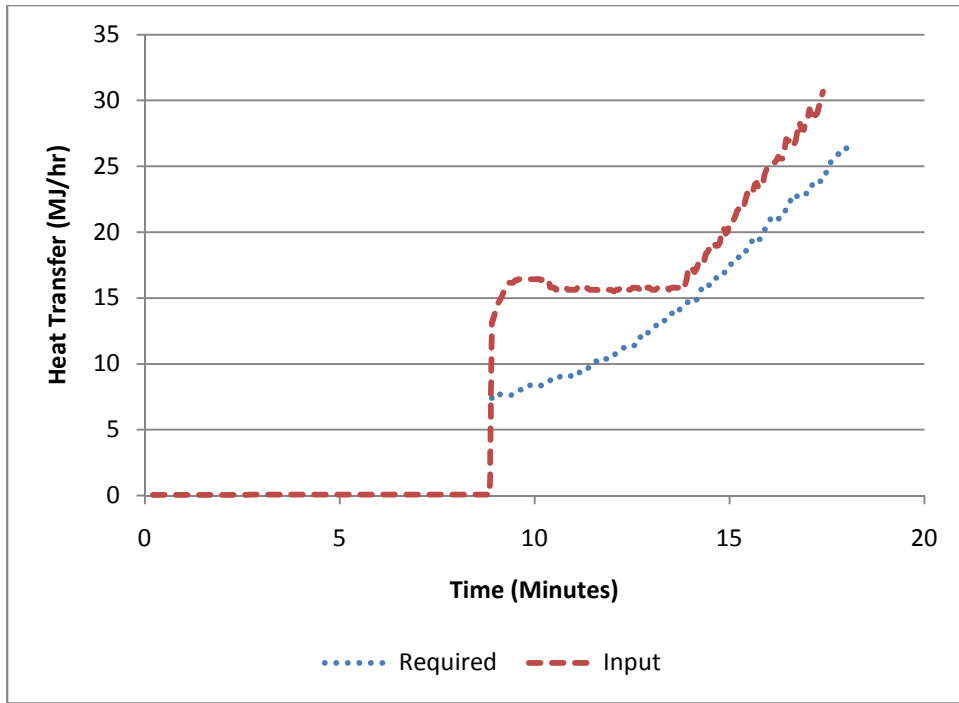


Figure 31: Calculated Heat Rates in a Test during Which the Outlet Temperature Exceeded the Set Temperature

The test results depicted in Figure 28 and Figure 29 show that the tankless water heater is behaving in a predictable manner. The inlet temperature gradually decreased until it became low enough so that the required heat rate was approximately equal to the minimum the heater can provide, at which point the heater fired and the water came out at the set temperature of 50 °C. However, the test results depicted in Figure 30 and Figure 31 indicate that the heater behaving in a different manner. The heater fired before the water required the minimum heat that the heater could provide causing the outlet temperature to exceed the set temperature. After beginning to fire, the heater continued to fire at the minimum firing rate while the required heat continued to increase (caused by decreasing inlet temperature). During this period the outlet temperature gradually ramped down to the set temperature at which point the heater burned more gas to hold the outlet temperature at the set temperature as the inlet temperature continued to decrease.

The phenomenon of the heater firing too soon was observed in many tests. An analysis was conducted to investigate what might be triggering this heater response. The required heat rate to bring inlet water up to set point when the heater began firing was plotted vs both the flow rate and set temperature of the test in an attempt to examine the sensitivity of the heaters control algorithm to those two parameters. Also plotted is the minimum heat rate of the unit. The results are shown in Figure 32 and Figure 33.

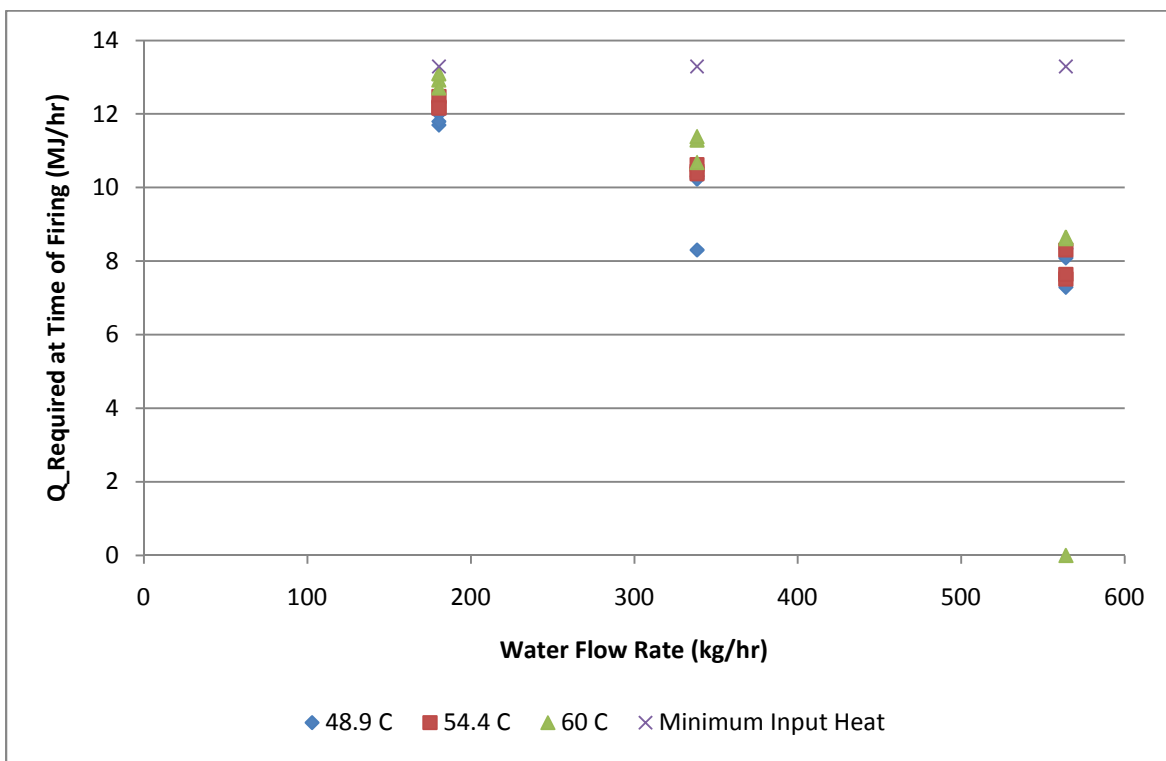


Figure 32: Sensitivity of Heater Turn-On Algorithm to Water Flow Rate

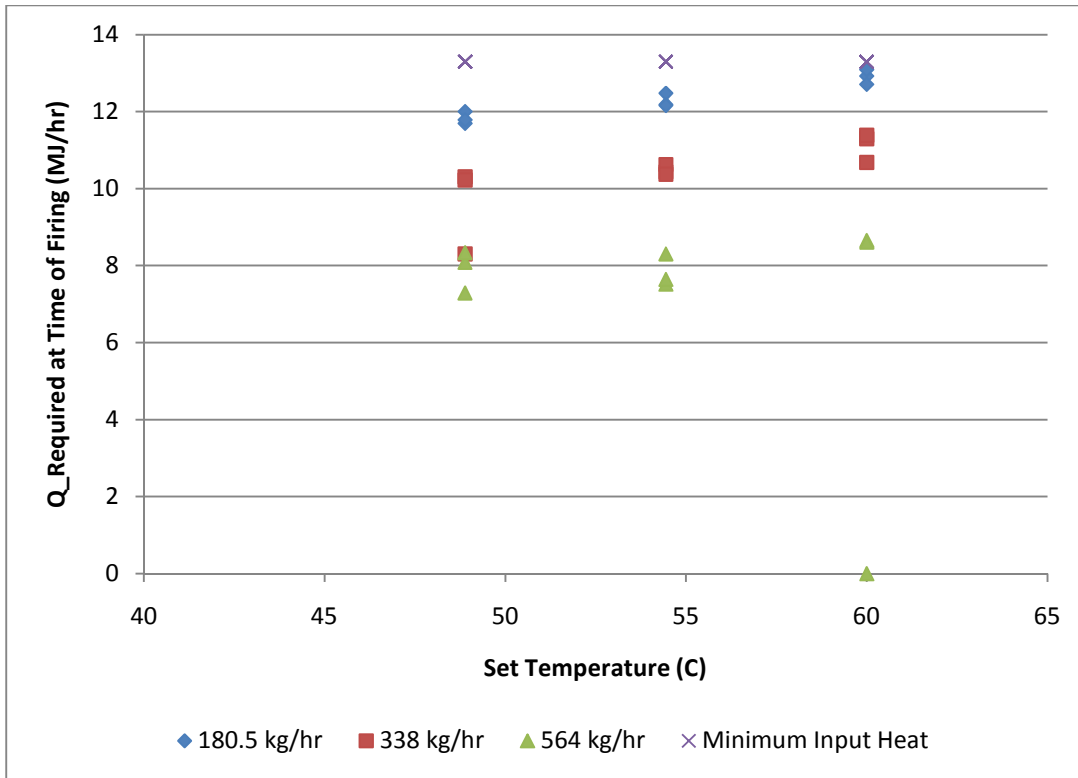


Figure 33: Sensitivity of Heater Turn-On Algorithm to Set Temperature

Figure 32 and Figure 33 display the same data presented in two different ways. In Figure 32 the required heat rate at the time of firing is plotted against the water flow rate with the set temperature being depicted via differing data series. In Figure 33 the required heat rate at the time of firing is plotted against the set temperature with the water flow rate being depicted via differing data series. In both plots the minimum heat rate, identified as 13.3 MJ/hr in Section 4.1.3, is presented as the fourth data series.

The two plots provide a clear indication that the water flow rate has a strong impact on when the heater begins firing. The higher flow rates result in more premature firing, generally causing temperature overshoot. Aside from one outlier at 338 kg/hr, the data points at each flow rate were clustered together with only minor variations with set temperature. In Figure 32 it is

particularly evident that there was a gap between the lowest recorded heat rate of firing at one flow rate and the highest recorded heat rate of firing at the next flow rate, with the exception of one point at 338 kg/hr.

Figure 33 indicates that there is a weaker relationship between heat rate of firing and set temperature. The data implies, via an upward slope, that increasing the set temperature will cause the heater to begin firing at a higher set temperature; however, the impact of set temperature appears to be much smaller than the impact of flow rate.

5.1.4 Minimum Flow Rate Results

The minimum flow rate test was performed several times at different set points. The three set temperatures used were 48.9 °C, 54.4 °C and 60 °C. Each test was performed ten times; however, it was only after the first two series of tests that the need to test the flow rate at which the heater shuts off was realized resulting in eight tests for each set temperature with decreasing flow rates. Results from these tests are shown in Figure 34.

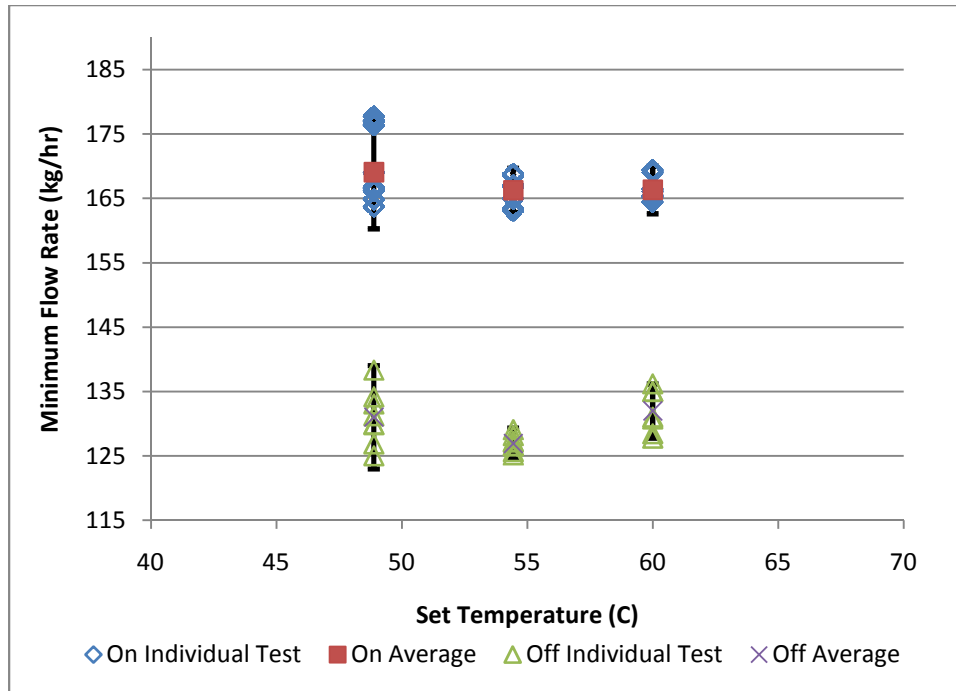


Figure 34: Compiled Minimum Flow Rate Results

In Figure 34 the diamond data points represent flow rates at which the heater turned on with squares indicating the average at each set temperature. The same is true of the data for the point at which the heater turned off; the triangle data points show the flow rate for an individual test while the xs show the averages for a given flow rate. Each average temperature has error bars showing the uncertainty in the tests. In all cases the uncertainty bars are using a t statistic with 99.9% confidence, except for the 60 °C off flow case which used a t statistic with 99% confidence.

As can be seen in Figure 34 there is a fair amount of scatter in the collected data. This scatter is a function of the test protocol. Since the flow rate was adjusted by changing the position of a globe valve the results were highly sensitive to how precisely the globe valve was turned. Speaking more practically, a minimal rotation of the globe valve resulted in a flow rate change

on the order of 11.3 kg/hr which caused scatter in the results.

The most interesting result of the tests is the difference between the minimum flow rate to make the heater turn on, and the minimum flow rate to make the heater turn off. The tests indicated a minimum flow rate to make the heater turn on to be on the order of 169 kg/hr while the flow rate at which point the heater turns off is approximately 129 kg/hr.

The minimum flow rate does not appear to vary with set temperature. This is partly because there is scatter in the averages; for example, increasing the set temperature from 49 °C to 54 °C appears to cause a decrease in the minimum flow rate for the heater to turn off, but increasing from 54 °C to 60 °C appears to cause an increase implying that this effect is likely random. Secondly, the error bars of every set temperature for each data series overlap with those of the other set temperatures. This implies that any change in minimum flow rate with set temperature would be statistically meaningless.

5.1.5 Parameter Characterization and Validation Results

The experimental data used for the parameter characterization consisted of two tests following the previously detailed test protocol. The data from the two tests were combined to obtain one long experimental data file. The intent of this combination was to capture the variations from one test to the next by using multiple tests. It also created a large data set which could be used for the parameter regression. A graphical representation of the data is presented in Figure 35 and Figure 36.

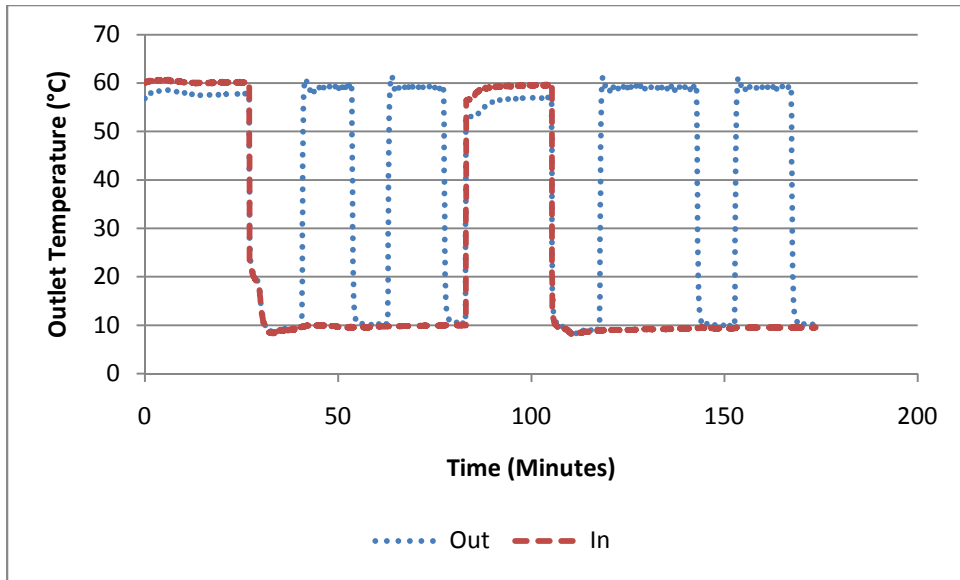


Figure 35: Temperatures during Parameter Characterization Data

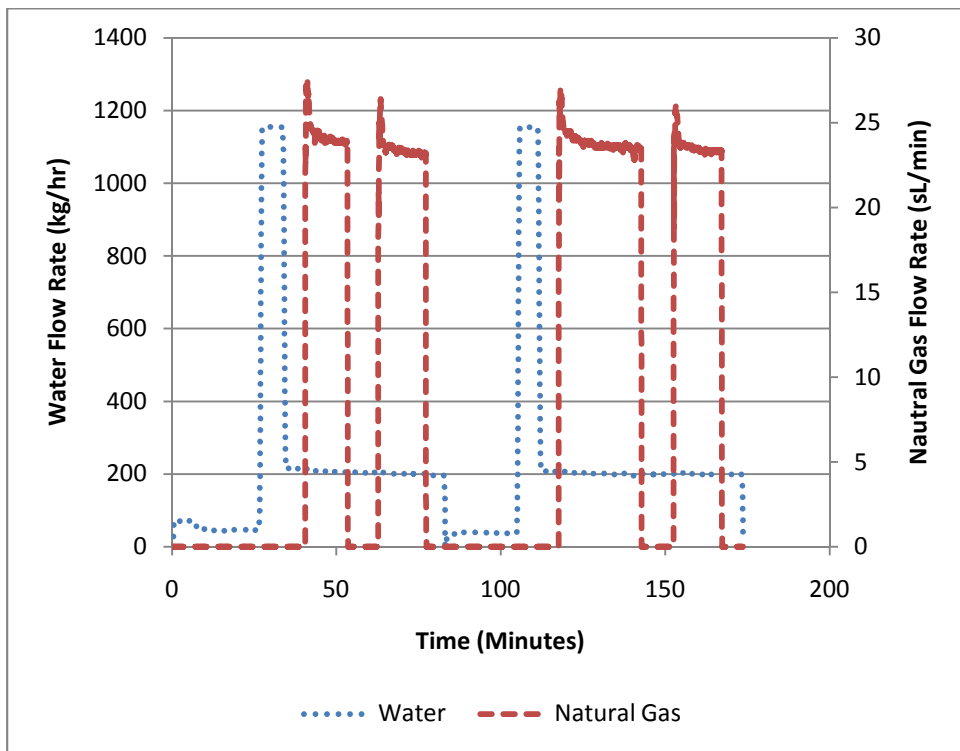


Figure 36: Water and Gas Flow Rates during Parameter Characterization Data

From the data set two periods were used to find the UA value, four periods were used to find the

efficiency and four periods were considered to find the capacitance.

The experimentally collected temperature data is shown in Figure 37 and the water flow rate data set is shown in Figure 38.

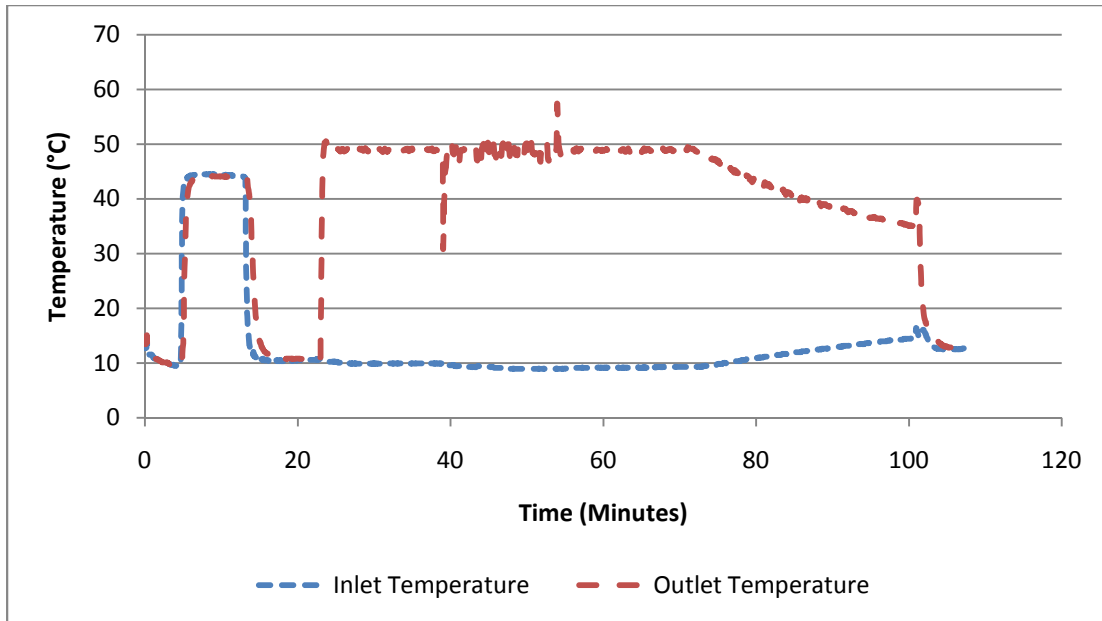


Figure 37: Temperatures during Model Validation Test

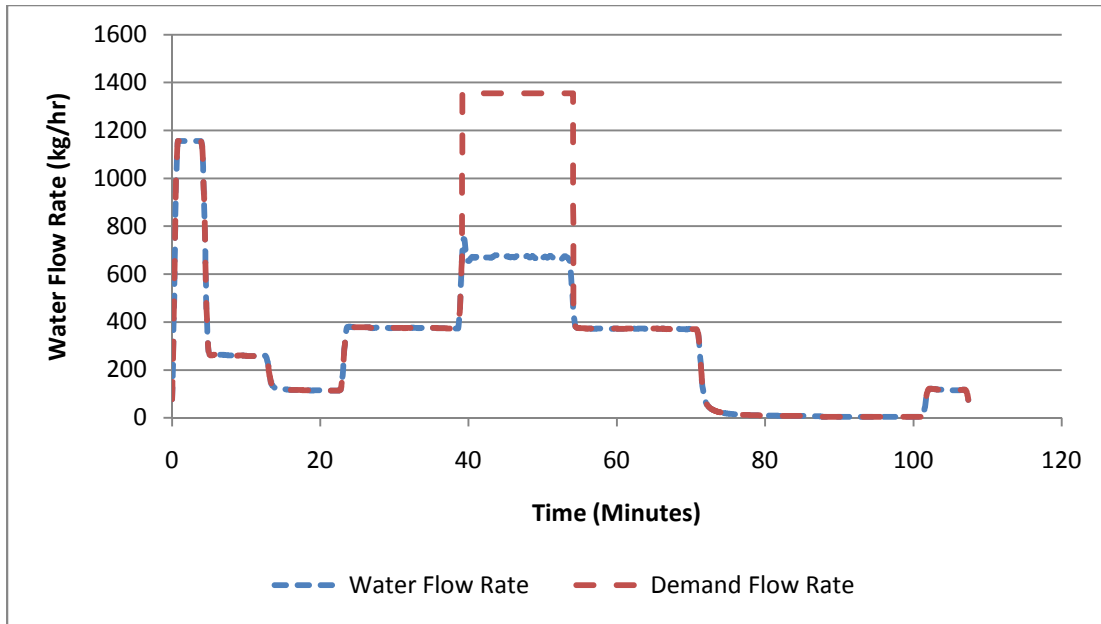


Figure 38: Flow Rates during Model Validation Test

The experimental results show almost exactly what was expected based on the protocol design. During the first three phases the heater did not fire. In the first phase the heater was turned off while purging the lines. In the second phase the heat required to bring the water temperature to the set temperature was lower than the minimum the heater could provide. In the third phase the flow rate was below the minimum. In the fourth phase the heater fired increasing the outlet water temperature. During the fifth phase the required heat surpassed the heaters maximum capacity. The heater limited the water flow rate to approximately 700 kg/hr and nearly maintained the set temperature. However, during this section there were fluctuations in the outlet temperature as well as variation in the water flow rate. It appears that the heater struggled to identify and maintain the conditions which would allow it to meet the set temperature.

The sixth phase, as a repeat of the fourth phase, was based on a decrease in the flow rate to 380 kg/hr. During this phase the outlet temperature became more stable and matched the set

temperature.

The seventh phase shows a slow decrease in outlet water temperature as the heat exchanger leaks heat to the environment, followed by a short spike when the water flow resumes. This spike occurred because the water temperature within the heat exchanger was higher than the temperature at the outlet from the heater and, when water flow was resumed, this small quantity of higher temperature water exited the heat exchanger.

5.2 Addition of a Small Tank Results

5.2.1 Cold Water Slug Results

Several tests were conducted to determine the aspects of the system that are most responsible for the cold water slug problem. As stated in section 4.2.1 the variations included the draw flow rate, the depth of the cold water before the heater circulation pump was engaged, and the simulated deadband of the heater control logic in the small tank.

There were two main types of results obtained from these tests. The measured data were grouped into tests which did and did not exhibit a cold water slug. The information taken as the output of each test was the difference between the set temperature of the mixing valve and the coldest point of the cold water slug.

Figure 39 shows an example of a test in which no cold water slug was observed.

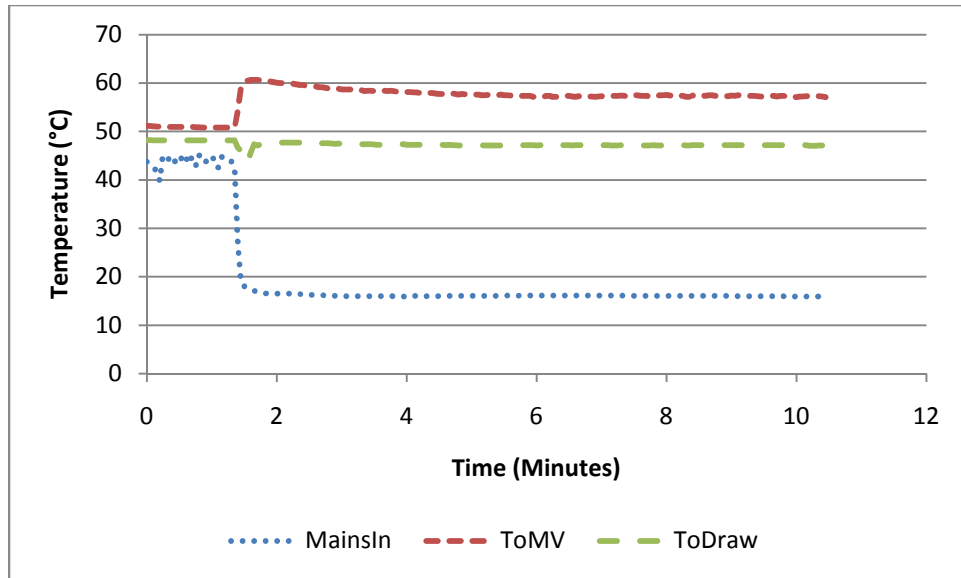


Figure 39: Temperatures Recorded During a Cold Slug Test with no Cold Water Slug

Figure 39 shows measurements taken from a test which was based on a 158 kg/hr hot water draw and operation of the circulation pump beginning at the same time as the draw. The sudden drop in the “MainsIn” temperature indicates that the draw began at approximately the 1.5 minute mark. At this point there was a short fluctuation in the temperature leaving the mixing valve. As this behavior happens in every test it was determined to be a result of the mixing valve reacting to the change in flow rate and not a parameter of interest in this test. After that short waver the temperature of the water heading to the draw remained quite steady for the rest of the test. As a result this test was classified as a test with no cold water slug problem.

Figure 40 shows an example of a test in which a cold water slug was observed.

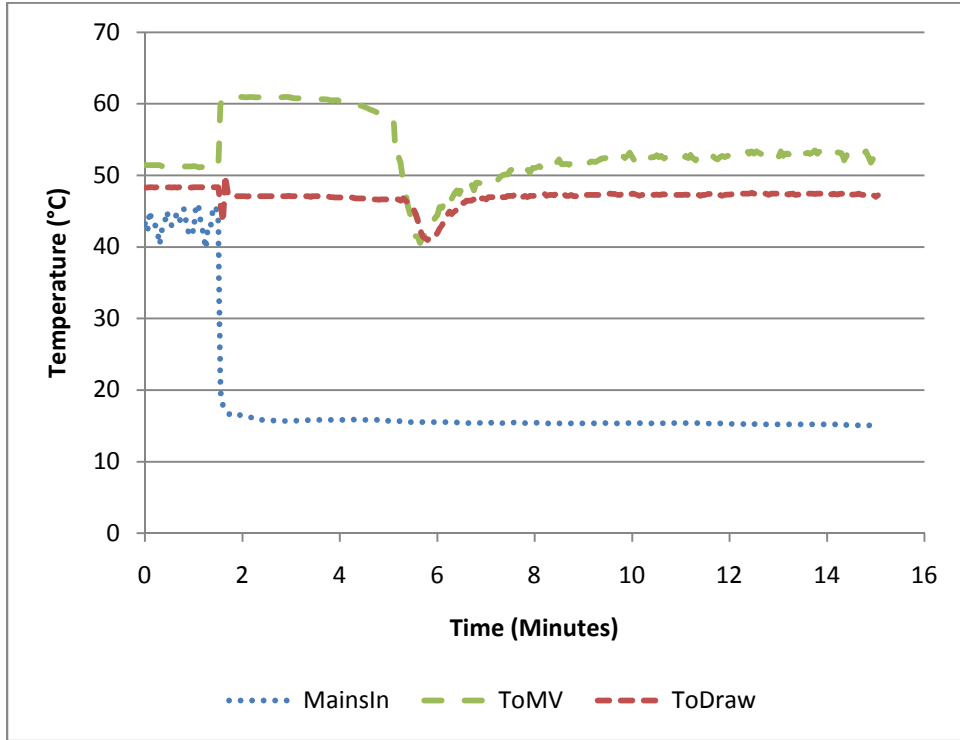


Figure 40: Temperatures Recorded During a Cold Slug Test with a Cold Slug

Figure 40 shows a test with a 338 kg/hr flow rate in which the circulation pump was turned on after the top thermocouple in the small tank fell to 5 °C below the set temperature of 60 °C. As can be seen by the sudden drop in the “MainsIn” temperature the draw started approximately two minutes into the test. Beginning at 5 minutes, a sharp drop in the “ToDraw” line to approximately 41 °C indicates that there was a period when the water coming out of the small tank was not high enough to meet the set temperature of the mixing valve. This test was classified as a test which did exhibit a cold water slug.

Two graphs were composed to present the data collected from all of the cold water slug tests. These graphs compare the magnitude of the cold water slug to the draw flow rate and depth of

the cold water front used to control the circulation pump. The magnitude of the slug was taken as the difference between the minimum temperature of the draw and the average temperature at the end of the draw. The result is that any unsteadiness in the mixing valve shows up as a small change in temperature even though the test was classified as having no cold water slug. Two graphs are presented; one using a control deadband of 1 °C and the other using a control deadband of 5 °C. They are presented in Figure 41 and Figure 42.

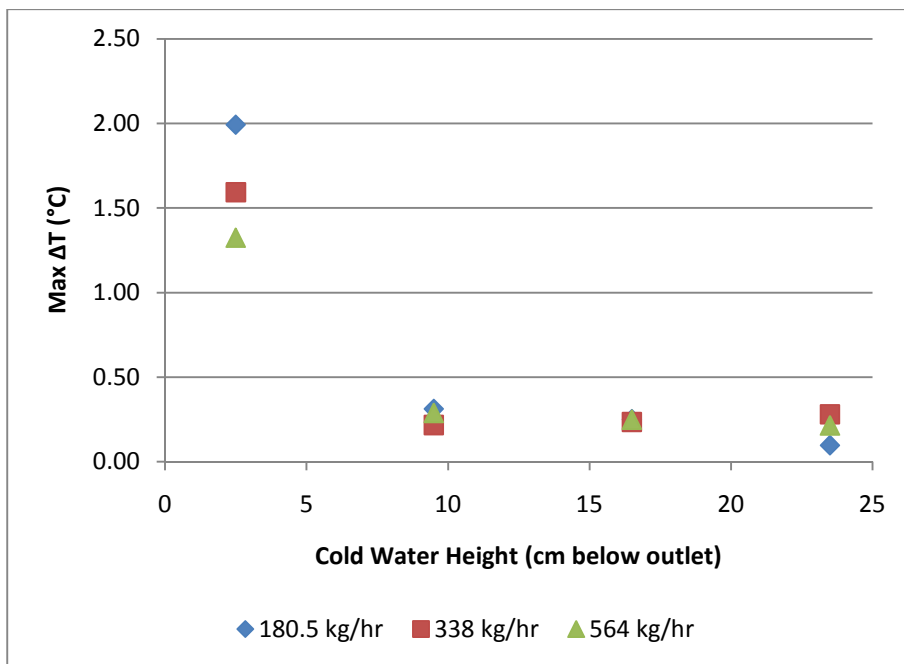


Figure 41: Summary of Cold Water Slug Results with 1 °C Deadband

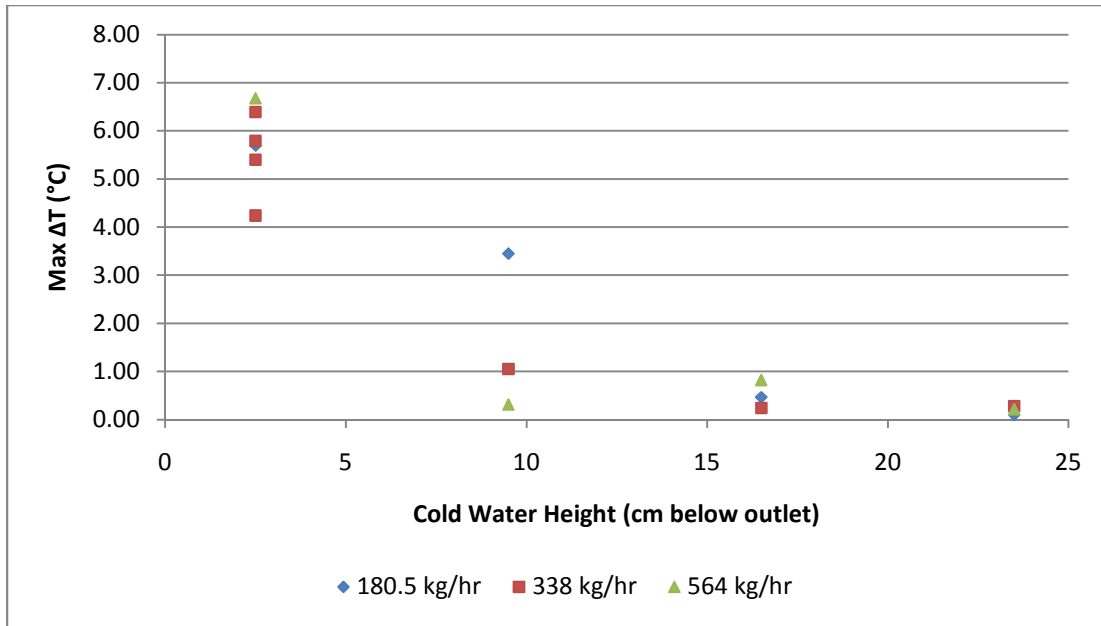


Figure 42: Summary of Cold Water Slug Results with 5 °C Deadband

Figure 41 shows a summary of all tests conducted with a 1 °C control deadband on the small tank. The magnitude of the cold water slug remained small (less than 0.5 °C) when the circulation pump was engaged before the cold water rose to within 5 cm of the outlet. However, when the temp at 2.5 cm below the outlet was used the magnitude of the cold slug rose to 1.4 – 1.9 °C. This result implies that the cold water slug problem is sensitive to the height of the cold water front in the small tank when the circulation pump is engaged. There is no clear connection between draw flow rate and magnitude of the cold water slug implying that the cold water slug effect is not sensitive to draw flow rate.

Figure 42 depicts a similar graph with the assumed control deadband of the small tank being 5 °C. The results of Figure 42 indicate a similar trend as that noted for Figure 41. In particular, Figure 42 shows that the magnitude of the cold water slug is highly sensitive to the height of the cold water front at the time the circulation pump is engaged but not very sensitive to flow rate.

However, there are two major differences between the results obtained for 1 °C and 5 °C deadband. In the 5 °C deadband case the cold water slug starts being observable at 9 cm below the outlet whereas at 1 °C it was negligible until the height of the water was 2.5 cm below the outlet. This likely occurs because the height of the cold water front continued to rise in the time it takes for the thermocouple in question to notice a temperature 4 °C lower than in the 1 °C control case. The second major difference is that, at 2.5 cm cold water depth, the magnitude of the cold water slug is much higher in the 5 °C deadband case than in the 1 °C deadband case. Again, this is likely caused by the fact that requiring the temperature to get lower at the reference thermocouple allowed more time for the cold water front to rise resulting in colder water at the outlet.

These results show that the control of the circulation pump is far more important in terms of avoiding the cold water slug than the flow rate of the draw. One of the potential solutions put forth by the Building America team was to control the circulation pump so that it would automatically turn on when the draw was initiated; the fact that both graphs show a negligible cold slug when the circulation pump is run continuously implies that this solution can indeed be effective.

5.2.2 Small Tank Stratification Results

The data investigating small tank stratification came in two forms. The first is a measure of the temperature at different heights during a cold water slug test and the second is a measure of the temperature at different heights during a full day simulation intended to emulate situations of keeping the small tank at temperature with no draws.

Figure 43 and Figure 44 depict the information regarding stratification from a cold water slug test. Figure 43 shows the temperatures recorded by thermocouples in the small tank while Figure 44 shows the water flow rates during the same test. In Figure 43 the names of the data sets represent the depth of the thermocouple in the tank.

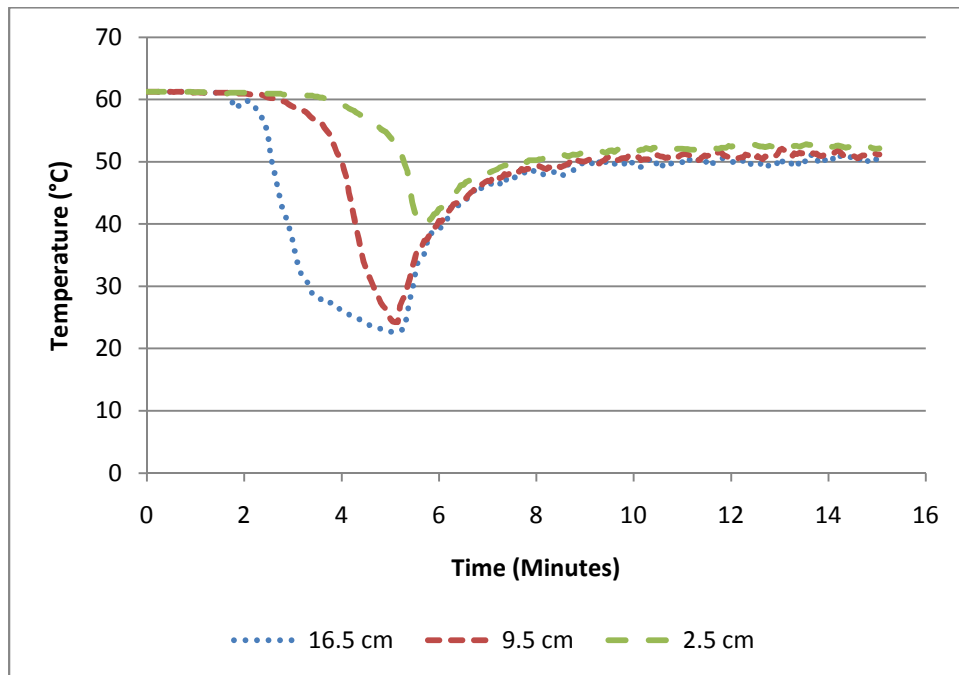


Figure 43: Temperatures Recorded in the Small Tank during a Cold Water Slug Test

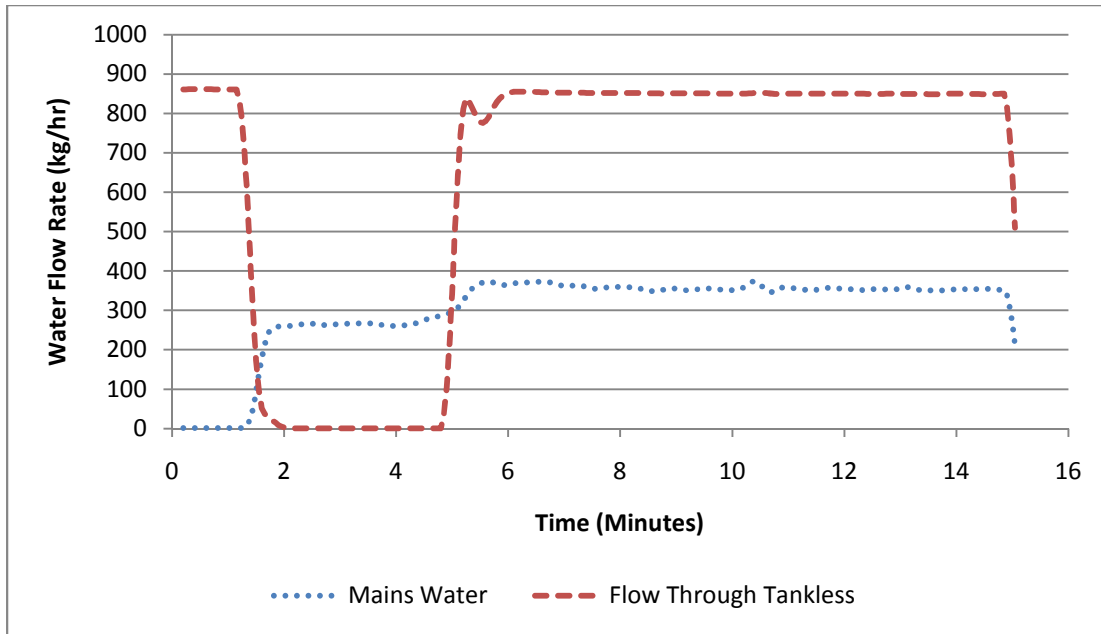


Figure 44: Water Flow Rates Recorded During the same Cold Water Slug Test

Figure 43 and Figure 44 indicate that the stratification in the tank is a function of whether or not the circulation pump is operating. At the very beginning of the test, just after the circulation has been shut off from heating the small tank, the thermocouples are showing no stratification. Then, around one minute into the test, the draw was initiated. Shortly thereafter the thermocouples begin to sequentially record lower temperatures; first the lowest thermocouple temperature drops, then the second lowest, followed by the highest. This indicates that the draw flow rate is not inducing significant amounts of turbulent mixing and the small tank does exhibit some stratification during a draw. Right around the five minute marker the circulation pump is turned on, as is indicated by the increase to 850 kg/hr. At this point the stratification in the tank is rapidly eliminated. For the remainder of the test, with the circulation pump running, there is very little stratification in the tank implying that the circulation pump brings enough turbulence into the system that it ends up well mixed. Limitations on thermocouple placement imply that

the stratification in the bottom of the tank is not observed.

Figure 45 depicts the temperature profile recorded in the small tank during a test emulating the behavior of the system as it keeps the tank at the set point without a draw. The names of the data sets indicate the depth of the thermocouples in the tank.

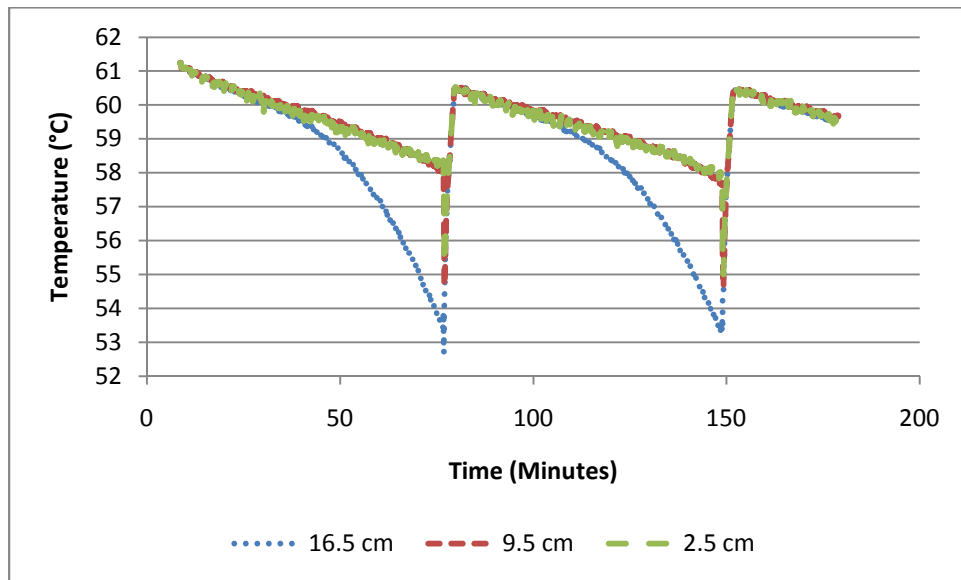


Figure 45: Temperatures in Small Tank When Maintaining Set Point

The results shown in Figure 45 also indicate that the small tank will not ever be stratified. The test was simulating a situation in which a temperature sensor located halfway up the tank would signal to the circulation pump to engage when the observed temperature fell more than 5 °C below the set temperature. As can be seen in Figure 45 this behavior keeps the small tank from achieving a fully stratified profile; the stratification profile is still being established when the circulation pump engages and returns the tank to a mixed condition.

5.2.3 Tepid Outlet Results

The focus of the tepid outlet in the small tank test was a study of how draw flow rate and tankless heater set temperature impacted the temperature coming out of the small tank. Based on the results from the stratification tests it was determined that the tank would be mostly mixed. As a result, it appears that the tepid outlet problem was from mixing in cold inlet water with the outlet from the tankless. The study of the tepidness problem focused on identifying the steady state outlet temperature under different draw flow and tankless set temperature conditions. Results are depicted in Figure 46.

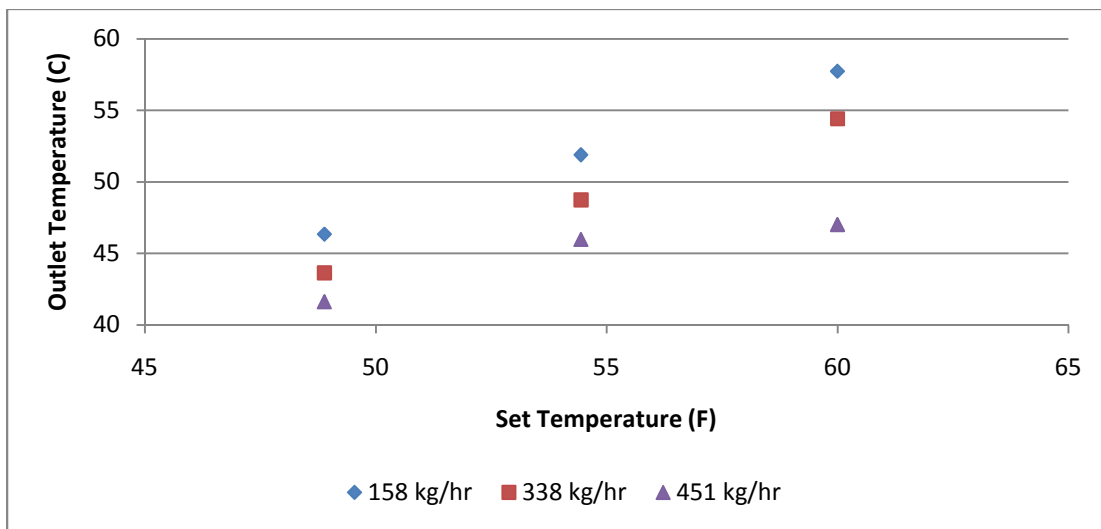


Figure 46: Steady State Outlet Temperature from the Small Tank under Varying Set and Flow Conditions

The main result is the clear change in outlet temperature with both set temperature and with flow rate. In each case, increasing the set temperature caused the outlet temperature to increase and increasing the draw flow rate caused the outlet temperature to decrease. This result was exactly as expected, and agrees with the mixed energy balance theory. Because the water in the tank is

well mixed the outlet temperature is dictated by a standard energy balance.

5.2.4 Small Tank Bypass Valve Results

The impact of the bypass valve was determined by repeating both cold water slug and tepid outlet tests. The repeated cold water slug tests were chosen because they exhibited a cold water slug and thus had a problem which could potentially be solved by the modification of the system. The repeated tepid outlet test had a set temperature of 60 °C as this would allow the most potential to view the difference between the water temperature heading to the mixing valve and the water temperature leaving the mixing valve.

Results from the repeated cold water slug test with the bypass valve are depicted in Figure 47 and the results from a similar test without the bypass valve are presented in Figure 48.

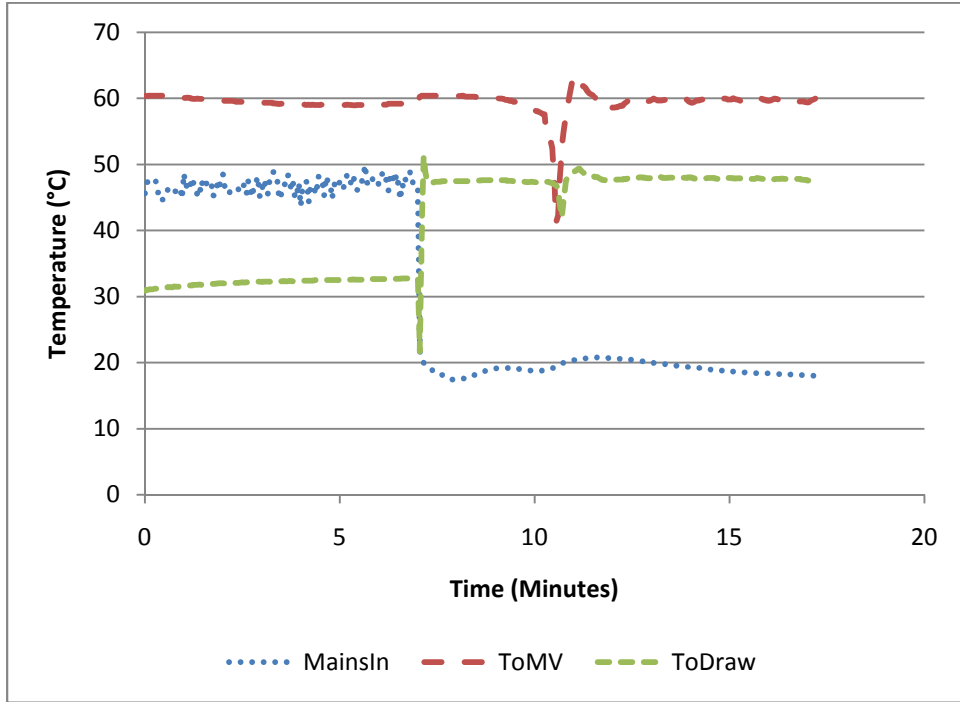


Figure 47: Temperatures Recorded During a Cold Water Slug Test with the Bypass Valve

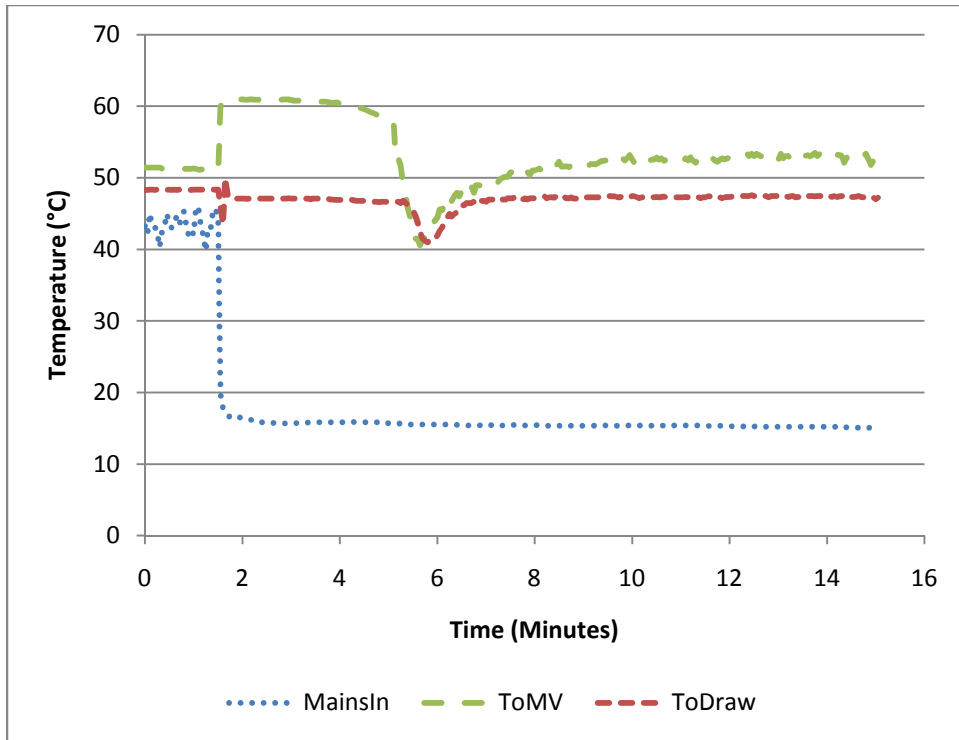


Figure 48: Temperatures Recoded During a Similar Cold Water Slug Test without the Bypass Valve

The test depicted in Figure 47 was based on a flow rate of 338 kg/hr, a set temperature of 60 °C and the circulation pump engaging when the top thermocouple reported a temperature below a 5 °C deadband. This test was chosen because the test performed before the bypass valve was installed, as illustrated in Figure 48 for reference, showed a cold water slug of 6.4 °C and did not return to the set temperature for 1.8 minutes.

The results after the installation of the bypass valve show a very different trend. There is still a cold water slug as a result of the circulation pump simply not being turned on soon enough; however, with the bypass valve open the magnitude is reduced to 5.8 °C and the duration is reduced to 0.4 minutes. There is a different problem with the bypass valve in the system; as was

shown during the section on gradually decreasing inlet temperature there are situations where the outlet of the tankless heater temporarily rises above set temperature. This is evident in Figure 47 as the water to the mixing valve rises to 63 °C before settling down to 60 °C. This situation is mimicked in the water heading to the draw as the mixing valve could not react quickly enough to accommodate the rapidly changing temperature entering the hot water side with the result being water hotter than the desired temperature heading towards the draw. This resulted in a hot water slug with a magnitude of 5.8 °C and a duration of 0.45 minutes.

The question of tepid water going to the draw was addressed by repeating a tepid outlet test with a tankless set temperature of 60 °C and a flow rate of 338 kg/hr. Results from the test with a bypass valve are shown in Figure 49 and the results from the same test without the bypass valve are shown in Figure 50.

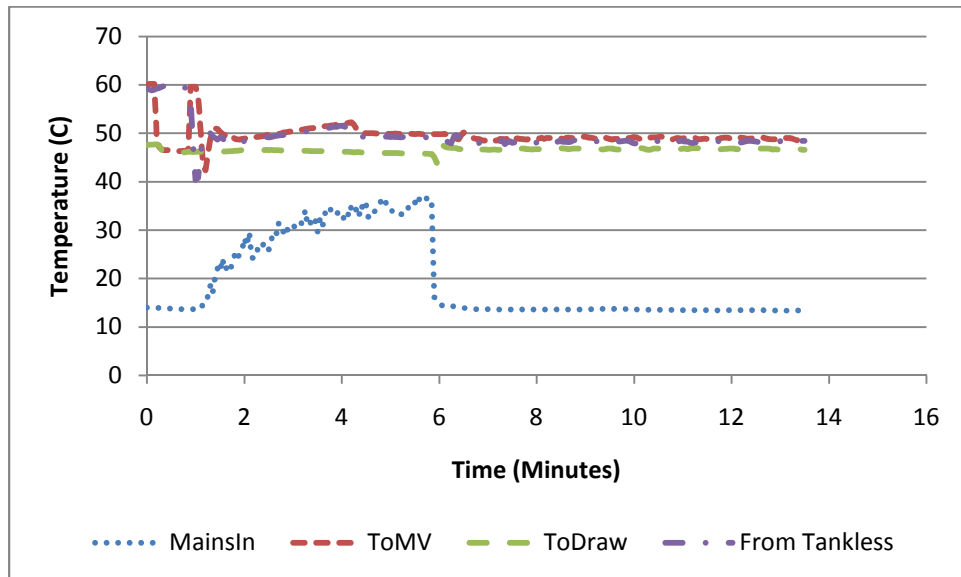


Figure 49: Temperatures Recorded During a Tepid Outlet Test with Bypass Valve

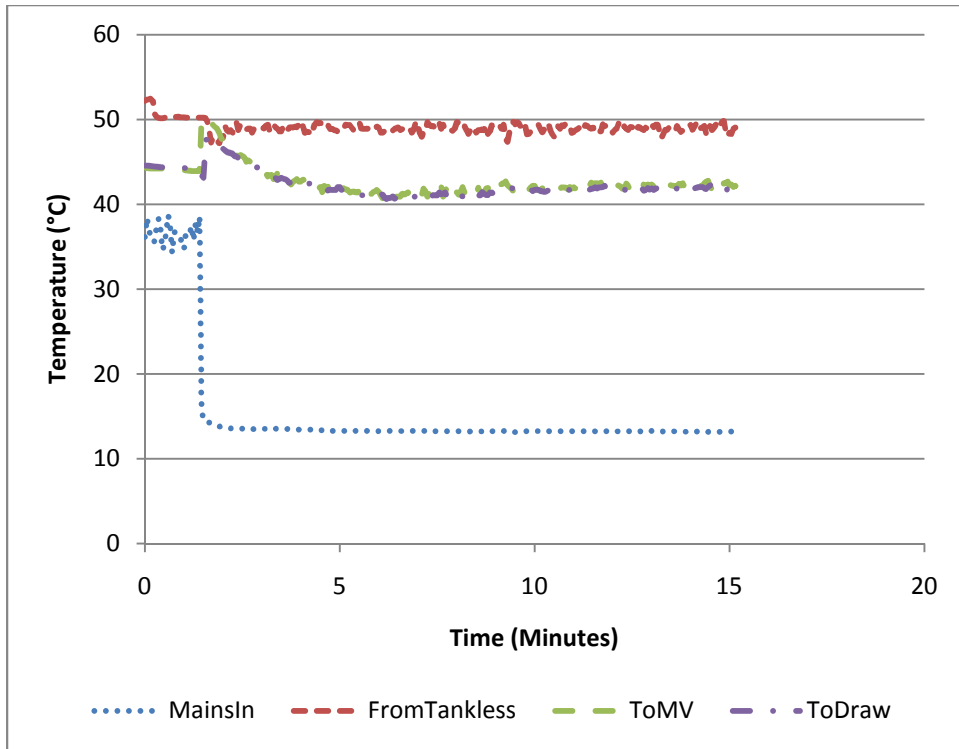


Figure 50: Temperatures Recoded During a Tepid Outlet Test without the Bypass Valve

In Figure 49 the draw started at about the six minute mark as can be identified by the sudden drop in MainsIn temperature. After this point the temperature exiting the tankless heater stabilizes right at 60 °C. The temperature entering the mixing valve stays right at the temperature exiting the tankless heater. This is because the hot water passes directly to the mixing valve with the excess flow heading back towards the small tank.

The steady state temperature heading to the mixing valve is lower without the bypass valve, as shown in Figure 50. In the test without the bypass valve the temperature of water heading to the mixing valve steadily drops below the temperature of water leaving the tankless heater. This is caused by mixing with colder water as the hot water from the heater enters the tank. The end

result is that, in Figure 50, the water heading to the mixing valve gradually decreases to 54 °C whereas the temperature with the bypass valve installed stays right at 60 °C. During the test with the bypass valve there was no decrease in draw temperature.

These tests show that reconfiguring the system so that the hot water from the tankless heater heads straight toward the mixing valve reduces some problems but creates new ones. The addition of a bypass valve made the cold water slug far less drastic; however, it has shown the potential to add a hot water slug instead. The bypass valve has better results with the tepid outlet problem. By redirecting the hot water flow, the bypass valve avoids the problem of water mixing in the tank. As a result, the water temperature to the mixing valve is the same as the water temperature leaving the tankless heater. This finding means that there are situations where the water heading to the draw would be tepid without the bypass valve, but would be satisfactory with the bypass valve.

Chapter 6: Model Validation Analysis

6.1 GenOpt Results

A TRNSYS simulation file was developed to emulate the experimental protocol shown in section 5.1.5. The simulation file used experimental data for input variables as much as possible. The input variables which were directly taken from experimental data were the inlet water temperature and ambient temperature. TRNSYS would not allow the water flow rate data file to be used as an input variable, a water draw profile which matched the experimental data was created using Type 14b [21]. The simulation water flow profile was matched to the experimental profile by plotting the two profiles and ensuring that at all times the flow rate was the same. Since no data was collected regarding when the heater was turned on or off this was matched to the data as well as possible using a Type 14h [21]. The times at which the heater was turned on and off were matched by plotting the natural gas flow rate, both experimental data and simulation results, and matching the times at which the gas flow increased or decreased in both.

The goal of pairing the GenOpt optimization engine with the TRNSYS simulations was to have GenOpt minimize the χ^2 value indicating that the heater parameters were estimated as accurately as could be obtained from the simulation. The results from the GenOpt simulation are displayed in Table 35.

Table 35: Heater Characterization Parameters from GenOpt

Capacitance (kJ/K)	8.36
--------------------	------

Efficiency	0.802
UA (kJ/hr-K)	12.99

It is estimated that there are approximately 8 kg of copper and 0.78 kg of water in the heat exchanger. These estimates result in an approximate capacitance of 6.5 kJ/K which is reasonably close to the 8.36 kJ/K reported by GenOpt. The UA value is significantly harder to estimate due to thermal shorts, and no physical approximation was completed. The 12.99 kJ/hr-K value is on the same order of magnitude as values reported in previous research [14].

The χ^2 value corresponding to these parameters was 2770 with 2661 degrees of freedom, corresponding to the 2664 data points minus the three conditions imposed, used in the calculation. For a test with 2661 degrees of freedom there is a 7% chance that the reported χ^2 will be lower than 2770 for a correct model.

These identified parameters were used in multiple simulations to check the accuracy of the simulation model. This was done by comparing the output from the TRNSYS simulation to the experimental data with particular attention paid to the difference between the total natural gas consumption during a test.

The uncertainty of the parameters was analyzed by observing the plotting the change in χ^2 with the change in parameters. The uncertainty range was specified as the range bounded by the $\chi^2 = \text{sqrt}(2) * \chi^2$. Results are shown in Figure 51.

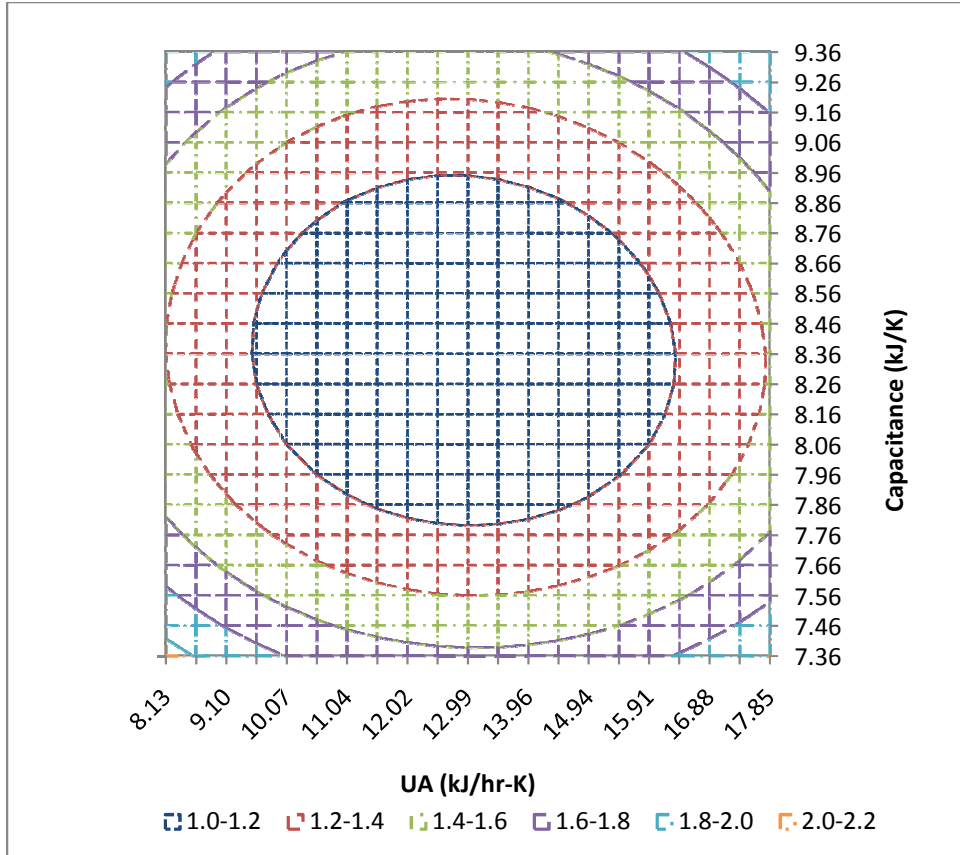


Figure 51: Normalized χ^2 Values with Changing UA and Capacitance

Figure 51 shows the range of χ^2 with varying UA and capacitance parameters in simulations. The values shown are normalized to the minimum χ^2 value. Figure 51 was used to find the uncertainty in the UA and capacitance terms, while the uncertainty in efficiency was the experimental uncertainty.

Table 36: Heater Characterization Parameter Values and Uncertainties

Capacitance (kJ/K)	8.36 ± 0.6
Efficiency	$0.802 \pm .06$
UA (kJ/hr-K)	12.99 ± 4.0

6.2 Validation via Characterization Test

The first test which was used to examine the validity of the parameters obtained from GenOpt was the same test used in the GenOpt simulation. Results comparing the cumulative natural gas consumption are shown in Figure 52 and the natural gas flow rates are shown in Figure 53.

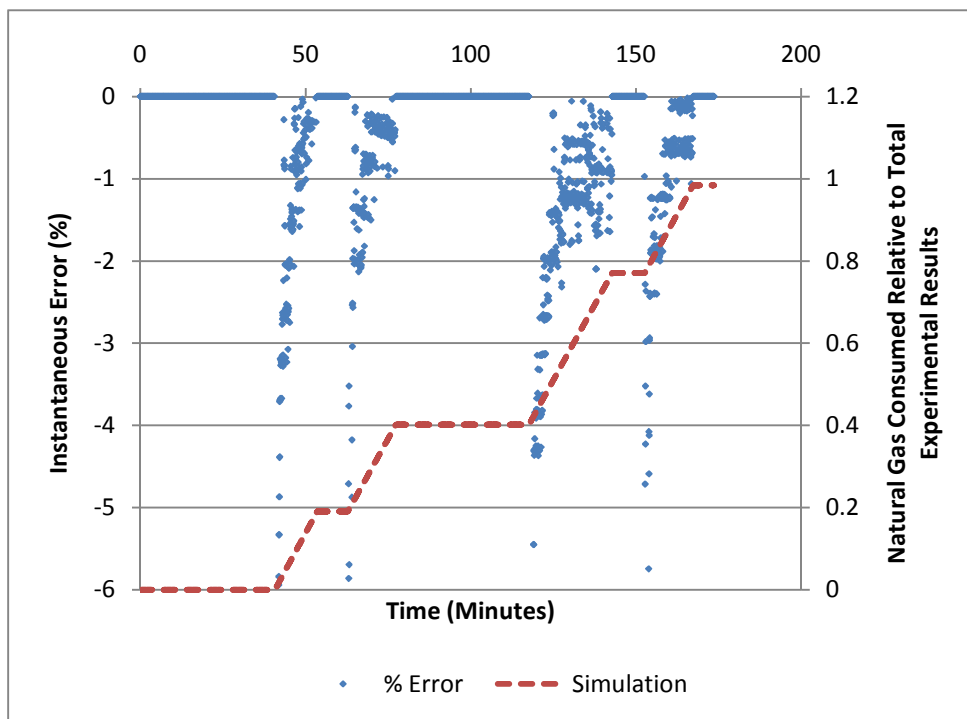


Figure 52: Error in Cumulative Natural Gas Consumption during Characterization Test

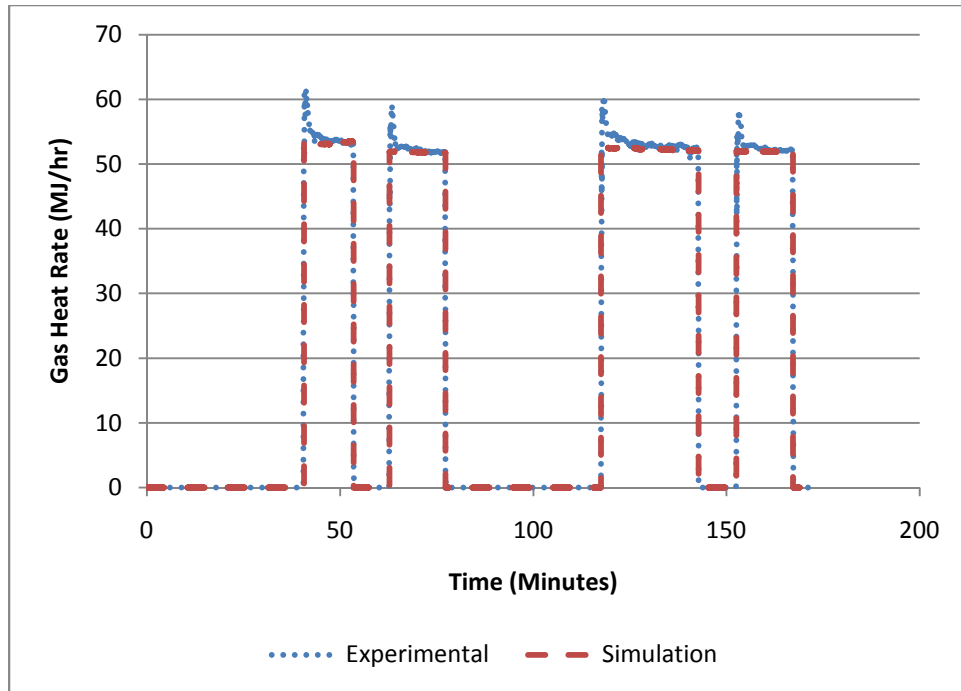


Figure 53: Natural Gas Flow Rates during Characterization Test

Figure 52 shows a comparison between cumulative simulation gas consumption and total experimental gas consumption. The left axis shows the calculated percent error in the instantaneous flow rates as a function of time. Figure 53 shows the natural gas flow rate from both the experimental data and the simulation over time during the test, and can be used to explain the errors noted in Figure 52.

Based on the trends in Figure 52 it is apparent that the largest contributor of error in natural gas flow occurs at the start of a draw. The reason for this is evident in Figure 53 as well as most other figures showing experimental natural gas flow measurements. At the start of a draw the heater consumes extra gas until coming to steady state. This is presumed to be caused by the controls of the heater; this implies that the heater opts to burn additional gas at the start of a draw to bring the heat exchanger to temperature and begin supplying adequately hot water as soon as

possible. While this explanation makes sense, it is uncertain that this is truly the case. However, due to this being the most likely explanation it was decided to be out of the scope of the project; precisely modeling the control logic of one heater would be pointless as it would mean that the model is incorrect as soon as a different heater was considered. There are also small jumps at the beginning and ending of every draw. This is because both the simulation water draw profile could not be made to exactly match the experimental water draw profile and because the simulation heater model reacts instantly to changes in flow rate while the actual heater requires a few seconds to adjust.

At the end of the simulation the total error in cumulative energy consumption was -1.6% implying that the simulation model predicted 1.6% lower energy use than the heater actually drew. This error compares well to the 3.6% to 5% uncertainty in the efficiency measurements and implies that the simulation model is adequately predicting the performance of the heater.

6.3 Validation via Changing Flow Pattern

The model, with GenOpt regressed parameters, was also used to compare to a separate test protocol. The second protocol was described in sections 4.2.5 and 7.1.5. The main purpose of this comparison is to examine both the behavioral aspects of the heater and the accuracy of the simulated energy consumption. Outlet temperatures are shown in Figure 54, natural gas flow rates are shown in Figure 55 and water flow rates are shown in Figure 56.

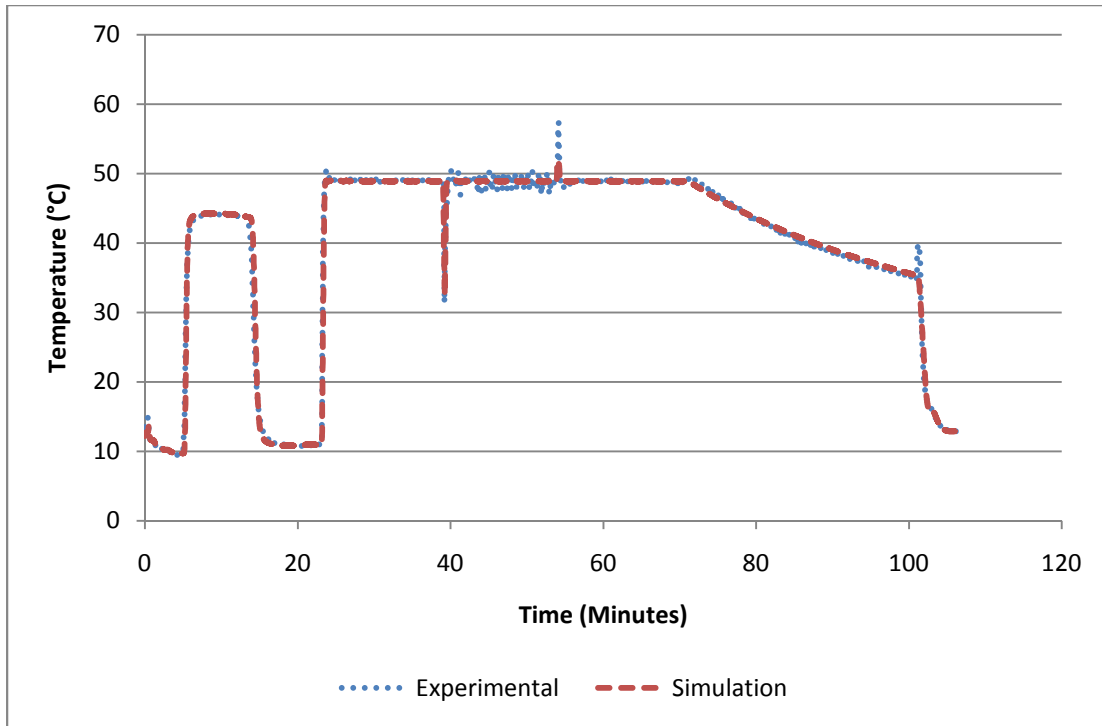


Figure 54: Outlet Temperatures during the Changing Flow Pattern Test

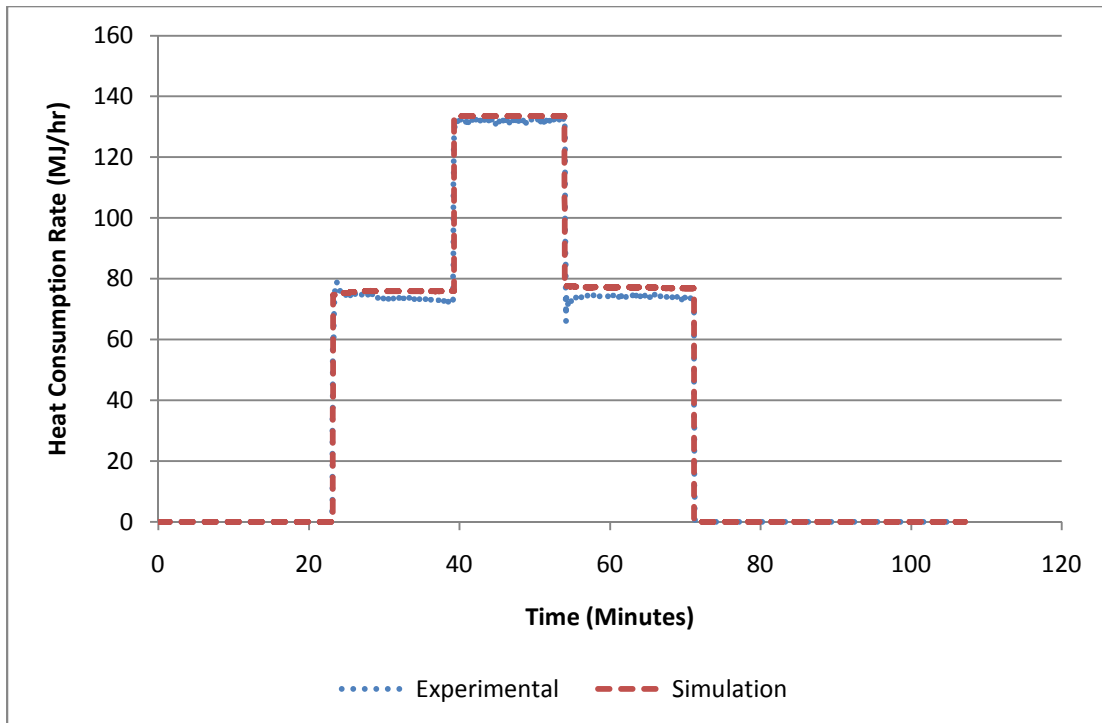


Figure 55: Natural Gas Flow Rates during the Changing Flow Pattern Test

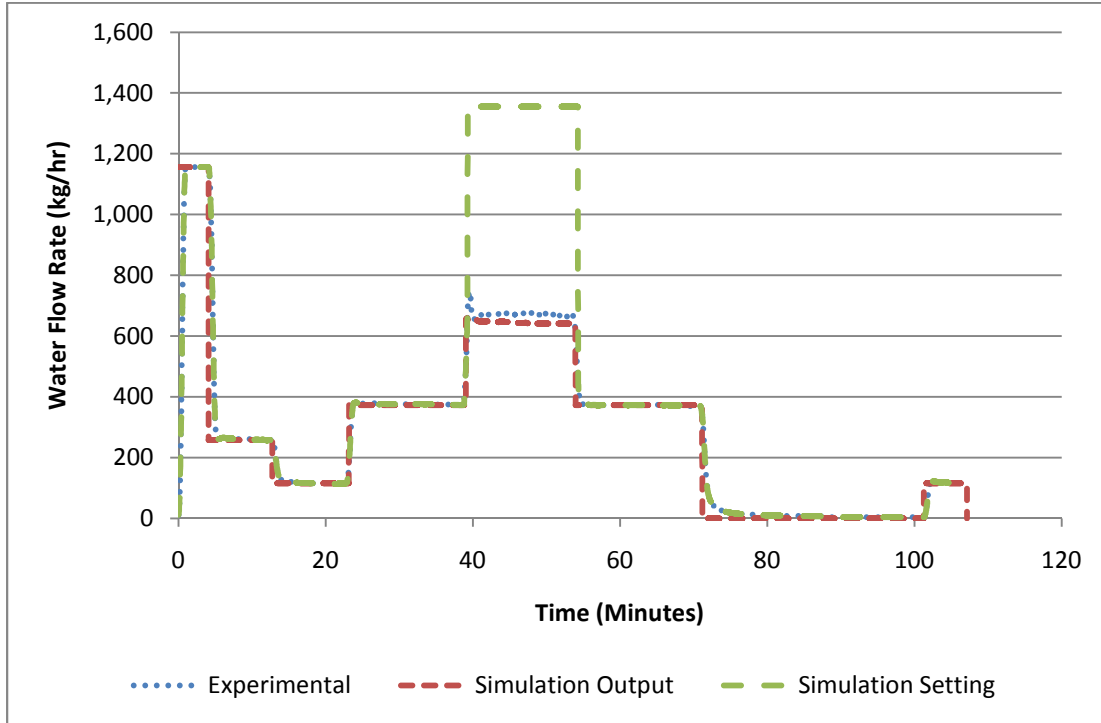


Figure 56: Water Flow Rates during Changing Flow Pattern Test

The results shown in Figure 54 and Figure 55 indicate that the simulation model is correctly predicting the outlet temperature and natural gas flow rate. During the purge phase and at the very beginning of the test the simulated outlet temperature drops in the same manner as the experimental measurements. After five minutes of purging the inlet water was switched to the heated inlet water. The preheated inlet water caused outlet temperature results of 44 °C from both the simulation and experiment. The heat consumption rate for both the experiment and simulation, depicted in Figure 55, remained at 0 MJ/hr indicating that the heater did not fire, as predicted by the simulation model. At 13 minutes into the test the water flow rate was reduced to 115 kg/hr and the inlet water was switched back to mains. For the next 10 minutes (until the 23rd minute of the test) the reported outlet temperature in both experimental results and simulation

predictions was just over 10 C, and there was no natural gas consumption. This result indicates that the model correctly responds to water flow rates below the minimum flow rate.

At 23 minutes into the test the water flow rate was increased to 380 kg/hr. This resulted in the outlet temperature obtained from both the experimental test and simulation model rising to 49 °C and the natural gas flow rate increased. The heat consumption rate in the simulation increased to 76 MJ/hr while the heat consumption rate in the experimental results increased to 73 MJ/hr. This discrepancy is assumed to be caused by the variation in natural gas energy density. The heater was modeled with a steady state efficiency of 80.2% but an apparent efficiency of 83% was recorded during the test. This could be caused by the energy density of the natural gas changing during the time between the validation test and the test used to identify the parameters in GenOpt. This apparent over-estimation of gas consumption, presumably caused by changes in the natural gas energy density, continued for the rest of the burn phases. 40 minutes into the test the water flow rate was increased to 1353 kg/hr resulting in a required heat rate which surpassed the capacity of the heater. At this point the heat consumption rate increased to a maximum rate of 133 MJ/hr. During this phase the experimentally recorded outlet temperature data showed significant fluctuation with a maximum temperature of 50.4 °C and a minimum temperature of 46.8 °C. The simulation results did not report the same fluctuation and reported a steady outlet temperature of 49 °C. The final burn phase consisted of decreasing the water flow rate back to 380 kg/hr and repeating the first burn phase. During the final burn the simulation model predicted a heat consumption rate of 77 MJ/hr while the experimental results indicated a heat consumption rate of 74 MJ/hr.

The final draw phase ended 70 minutes into the test and was followed by a 30 minute decay period. The decay period was used to check the capacitance and UA values obtained from GenOpt by examining the heat stored in the heat exchanger predicted by the simulation model compared to the heat stored in the experimental heat exchanger. The heat stored in the heat exchanger was identified by setting the flow rate to 116 kg/hr (below the minimum) and measuring the outlet temperature as water passed through the heat exchanger. The flow rate and temperature were then used to identify the heat extracted from the heat exchanger during each time step and summed over time to identify the total heat removed from the heat exchanger. The calculated stored energy in the heat exchanger was 167.4 kJ. As can be seen in Figure 54 the water in the heat exchanger was hotter than predicted by the simulation model causing an under-prediction of stored heat was expected. The simulation tool predicted 136.9 kJ remained in the heat exchanger.

The flow reduction portion of the experimental data and simulation results took place during the 40th to 55th minutes of the test. The experimental apparatus was configured for a 1355 kg/hr flow rate and the simulation model setting was also 1355 kg/hr. During this phase of the test the heater reduced the flow rate to 678 kg/hr and the simulation tool predicted a flow rate of 641 kg/hr. This discrepancy is also presumed to be caused by a change in the natural gas energy density. With the heater operating at an apparent 83% efficiency and the simulation tool using the GenOpt 80.2% efficiency the simulation tool would not be able to supply as much heat as the experimental heater. This would result in the simulation tool not being able to reach the set temperature at as high of a flow rate as the experimental heater.

Figure 57 shows the percent error in natural gas consumption during the model validation test.

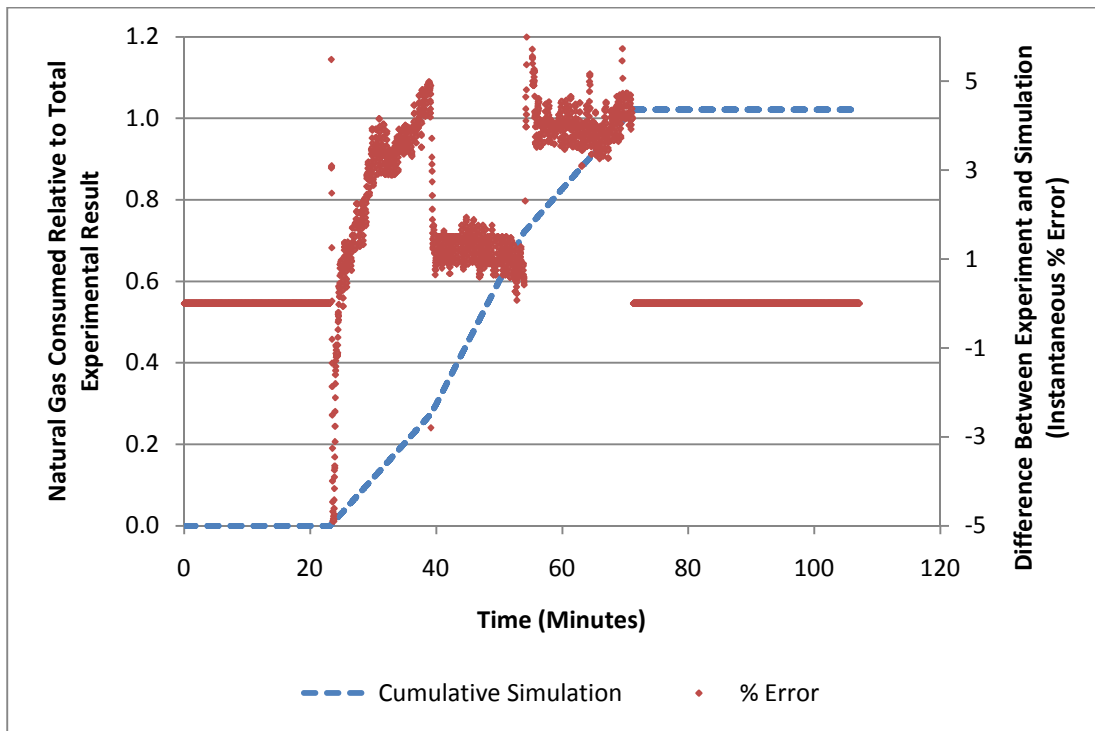


Figure 57: Error in Cumulative Natural Gas Consumption during the Changing Flow Pattern Test

In Figure 57 the “Cumulative Simulation” line is used to show the cumulative gas consumption predicted by the simulation tool relative to the total gas consumption in the experiment. The final value represents the error in total natural gas consumption. The “% Error” data shows the difference between simulation results and experimental values at any point in time.

The results depicted in Figure 57 are opposite to those obtained from the GenOpt parameter characterization test. In the previous comparison the simulation model predicted lower energy consumption than the experimental data showed. In Figure 57 the simulation model is predicting

higher energy use. As previously mentioned this result is believed to be due to the uncertainty in the efficiency calculation; the apparent efficiency of the heater during the changing flow pattern test was higher than the value reported by GenOpt and the simulation consumed more natural gas during each burn as a result.

The total value for error in energy consumption during the changing flow pattern test was 2.1%. The 3.6-5% uncertainty band around the efficiency measurement during any draw is greater than the error in the validation test and implies that the simulation model is in agreement with measurements.

The 2.1% error in the validation test was an over-estimate, as opposed to the under-estimate in the GenOpt parameter test. As was previously mentioned, this is likely caused by a change in the natural gas energy density resulting in an apparent change in efficiency value and the model over-predicting. In the GenOpt regression test the simulation under-predicted the energy use due to the transient portions which are not modeled in the simulation model.

Chapter 7: Efficiency Simulations

In this chapter a simulation analysis was performed using the validated TRNSYS tankless water heater model described in Chapter 2. The main objective of this simulation analysis is to investigate the efficiency of the tankless water heater under realistic draw patterns. The simulation analysis focused on adjusting the draw duration, duration of delays between draws, flow rate and ambient temperature. The realistic draw patterns were taken from the Standard Benchmark Hot Water Profiles created by the Building America organization.

7.1 Efficiency Sensitivity Analysis

The sensitivity analysis was designed to identify the impact of draw duration, delay between draws, total energy per draw and ambient temperature on the overall efficiency of the heater. The draw duration was considered in the analysis because it has an impact on the time period that the heater takes to reach and remain at steady state conditions. The time between draws impacts the amount of energy lost from the heat exchanger to the environment which must be replaced at the start of each draw. The flow rate was also included in the analysis as a means of adjusting the total heat input rate during each draw. Higher flow rates mean higher heat transfer rates. The ambient temperature was also included in the analysis as it impacts the heat transfer rate to the surrounding environment. When located outdoors, the water heater can experience a wide range of ambient temperatures. Table 37 provides a summary of the parameters considered in the sensitivity analysis.

Table 37: Parameters used in the Sensitivity Study

Draw Duration (min)	Delay Duration (min)	Flow Rate (kg/hr)	Ambient Temperature (°C)
0.5	0.5	180	50
1	1	338	68
2	2	415	86
4	4	N/A	
8	8	N/A	
16	16	N/A	
	32	N/A	
	64	N/A	
	128	N/A	

The parameters used to describe the heater were as presented in Section 8.1. The set temperature considered in all simulations was 60 °C.

The sensitivity analysis focused first on the impacts of draw duration and delay duration. Simulations were performed at 415 kg/hr flow rate and 20 °C ambient temperature for all combinations of the draw and decay durations. Sample results from a single simulation which featured a 4 min draw and 16 min delay are shown in Figure 58.

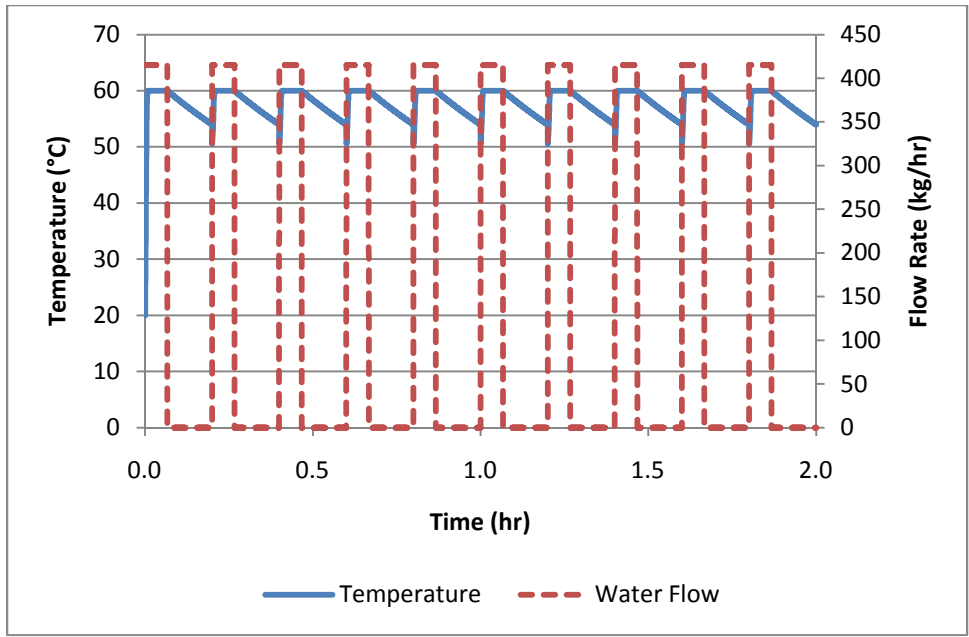


Figure 58: Sample Results from a Simulation

Results from the sensitivity analysis are displayed in Figure 59. Results are the draw efficiency, not the instantaneous system efficiency.

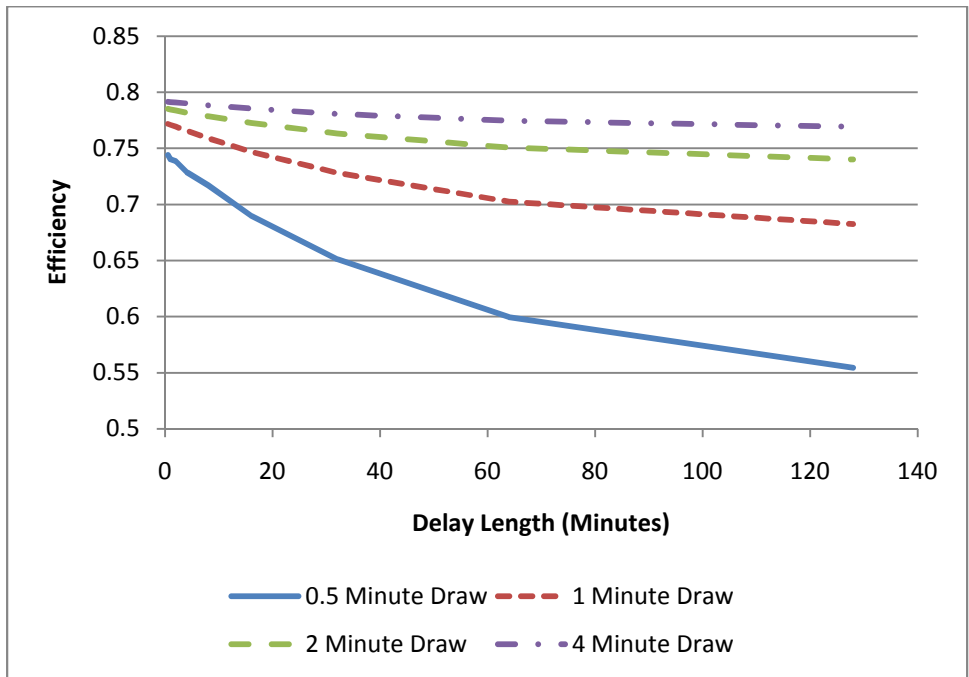


Figure 59: Effect of Draw Duration and Delay Length on Cumulative Efficiency

The results in Figure 59 show that the heaters sensitivity to draw length and delay length depends on each other. When the delay between draws is only 30 seconds the heat exchanger does not cool much which results in a lower portion of the heat in the next draw going to the heat exchanger. As a result, reducing the draw duration from 4 minutes to 30s results in a decrease in efficiency from 79% to 74%. This is a small effect when compared to the same reduction in draw duration combined with a delay of 2.13 hr. In this case the heat exchanger loses much more heat to the environment and the thermal mass of the heat exchanger represents a more significant portion of the consumed energy. In this case (i.e. for a delay of 2.13 hr), a reduction from a 4 min draw to a 30s draw results in an efficiency decrease from 77% efficiency to 55% efficiency for the draw.

The second set of simulations in the sensitivity analysis focused on the heat demand of draws. The total heat demand was varied by changing both the flow rate and the draw duration. Simulations were again performed with varying delay durations. Simulation results are shown in Figure 60.

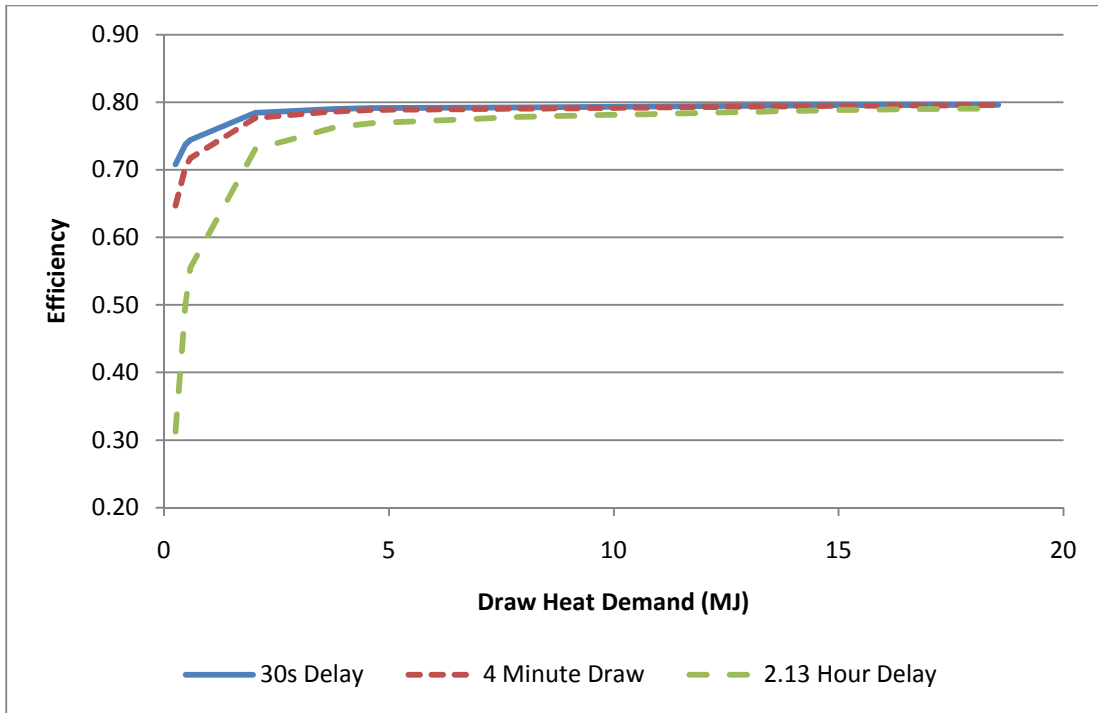


Figure 60: Impact of Draw Heat Demand and Delay Duration on Cumulative Efficiency

Figure 60 shows the same behavior as is displayed in Figure 59; when the heat demand of each draw is low the cumulative efficiency of the heater is highly sensitive to delay duration. This is shown by the minimum points on each line; the minimum draws, each at 253 kJ, have a wide range of efficiencies from 31% to 70% when the delay duration varies from 2.13 hr to 30s. When the total heat demand is high then the heat lost between draws is negligible and delay duration has little impact on the cumulative efficiency of the heater. This is clearly shown when the heat demand is larger than 8.4 MJ; at 8.4 MJ in a draw the cumulative efficiencies only range between 78% and 79% efficiency.

The results shown in Figure 59 and Figure 60 indicate that the cumulative efficiency of tankless water heaters is sensitive to the draw profile. A draw profile which consists of draws requiring

little heat (caused by low flow rates, low draw durations, or both) combined with long delays will exhibit a low cumulative efficiency. On the other hand, profiles with short delays between long draws will be significantly less impacted by draw duration or draw flow rate. When the draws are small the heater efficiency is highly sensitive to delay duration, but when the draws are large it is not. When delays are small the heater efficiency is not particularly sensitive to draw heat required, but when the delays are large the heater efficiency is significantly affected by the draw heat demand.

The next set of simulations in the sensitivity analysis focused on the impact of the ambient temperature. Since several tankless water heaters are designed so that they can be installed either inside or outside of a building it is important to evaluate the impact of the weather on the efficiency of heaters installed outdoors [18, 24, 25]. This effect was investigated by considering three different ambient temperatures with three different draw durations. The simulation results are presented in Figure 61 and Figure 62. Figure 61 shows the results with a 30s delay between draws and Figure 62 shows the results with a 2.13 hr delay between draws.

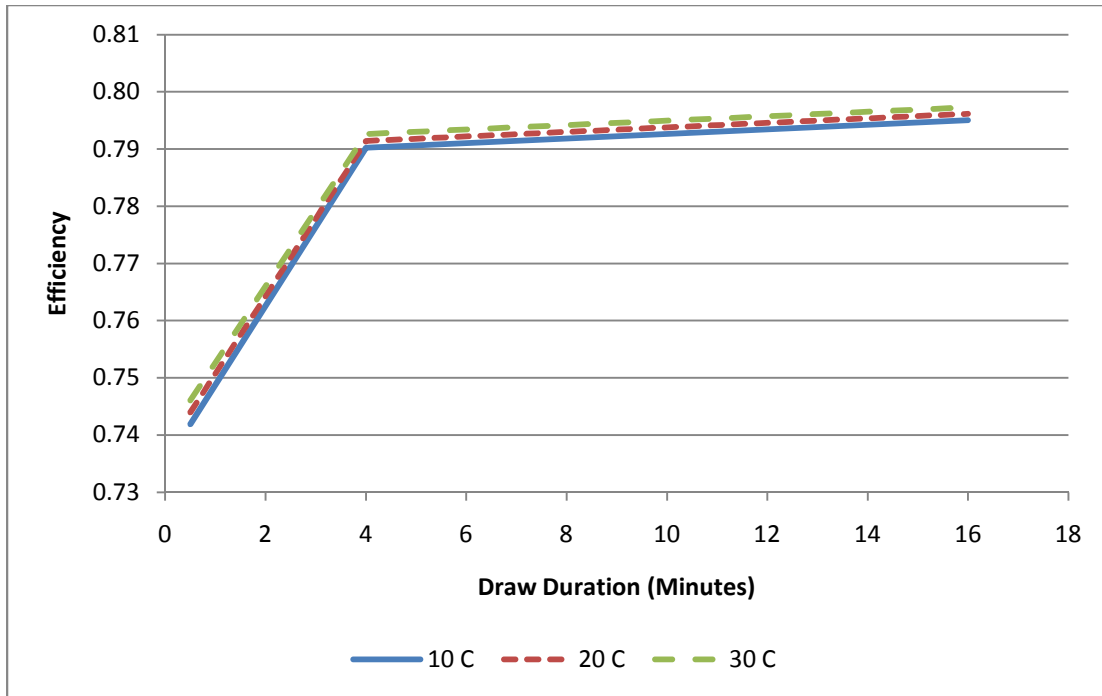


Figure 61: Impact of Draw Duration and Ambient Temperature on Cumulative Efficiency with 30s Delays

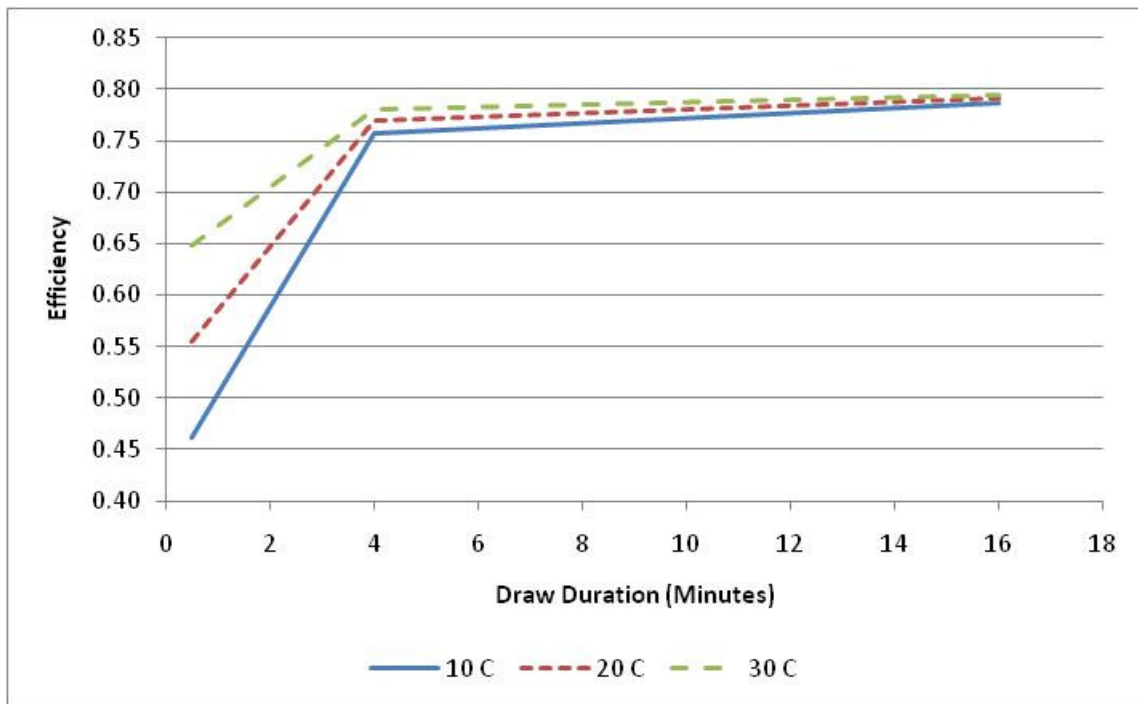


Figure 62: Impact of Draw Duration and Ambient Temperature on Cumulative Efficiency with 2.13 hr Delays

The results shown in Figure 61 and Figure 62 indicate a very similar trend. When the delay durations between draws were short there was little variation in efficiency. The highest efficiency was 79.5% at 16 minute draws, and the lowest was 74.5% at 30s draws. The efficiency depends mostly on the draw duration. There is a slight variation with ambient temperature for short delay durations. The results with 2.13 hr delay durations show a significantly more dramatic variation of the heater efficiency. At 16 minute draw durations the heater efficiency is almost the same at 79% for all ambient temperatures considered in this analysis. However, reducing the draw length to 30s causes a wider variation in the heater efficiency ranging from 46% to 65%. This result indicates that the cumulative efficiency of the heater is sensitive to ambient temperature only when the delay durations are long relative to the draw durations and the environmental losses become significant.

7.2 Building America Standard Benchmark Draw Profiles

In order to assess how these effects impact the efficiency of an in-use system, a series of simulations was performed using two of the Building America Standard Benchmark Draw Profiles [15]. The draw profiles used were for two bedroom and four bedroom houses located in Boulder, CO. The simulations consist of one day draw patterns, with the selected day being the first of January. The settings used to describe the tankless heater were representative of the tested unit, and are as discussed in Section 8.1. The heater was simulated as having a minimum flow rate of 169 kg/hr.

7.2.1 Two Bedroom House

The draw pattern used for the two bedroom house is shown in Figure 63.

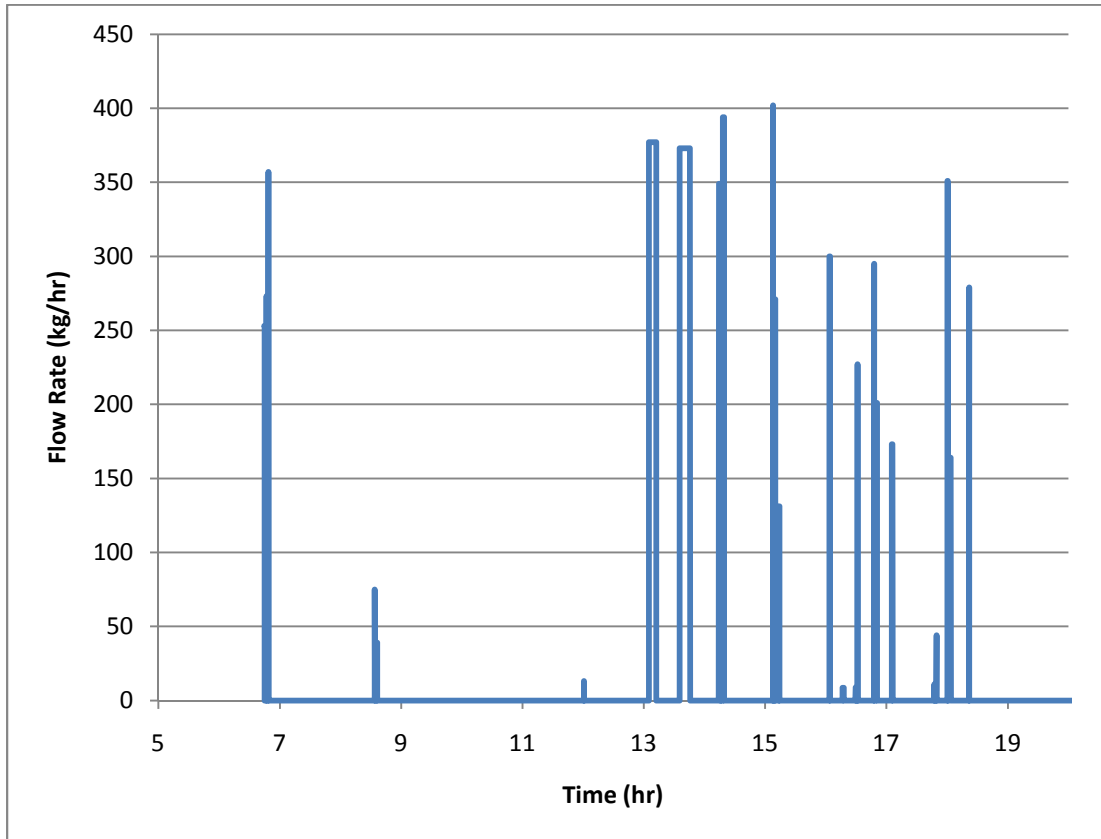


Figure 63: The Two Bedroom House Draw Profile

As can be seen in Figure 63 ten of the thirty total draws have a flow rate below the minimum required by the heater. These draws were included in the simulation despite the fact that the heater did not fire as they had the effect of removing energy from the heat exchanger, thus representing a loss of energy which occurs in actual homes.

The simulation results are depicted in Figure 64 and Table 38. Figure 64 shows the flow rates

and outlet temperature at each point in the simulation to show the behavior of the simulation.

Table 38 depicts the total amount of inlet and consumed energy predicted by the model as well as the efficiency over the draw profile.

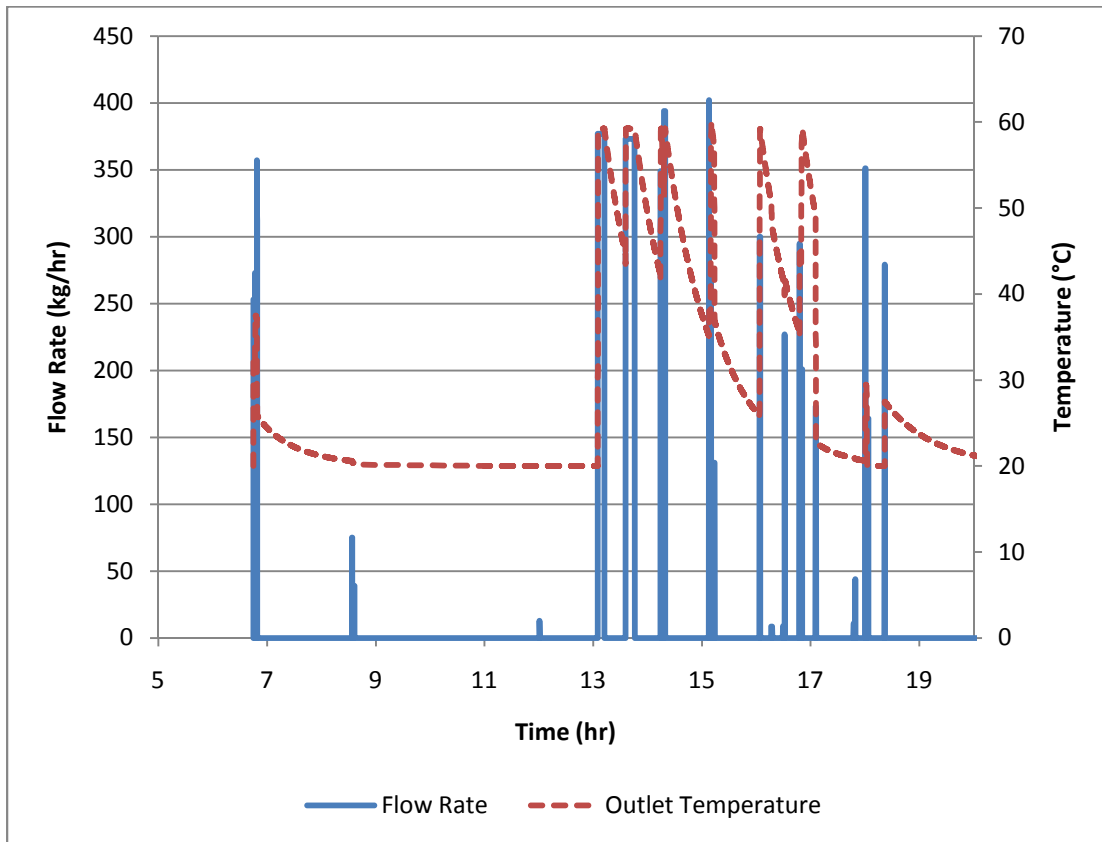


Figure 64: Flow Rates and Temperatures during the Two Bedroom House Draw Profile

Table 38: Energy Consumption and Efficiency in the Two Bedroom House Simulation

Delivered Energy (kJ)	22464
Consumed Energy (kJ)	29110
Efficiency	0.77

The results in Table 38 indicate that the parameters which were shown to reduce efficiency in Section 9.1 do not play a major role in the performance of a tankless water heater operating using

the draw profile of Figure 63. With a combustion efficiency of 80% the simulation reported a cumulative efficiency of 77% over one day for the two bedroom house draw profile. The efficiency of the heater over the 2 bedroom draw profile is 3% less than the test derived 80% steady state efficiency. The simulation for the two bedroom house consisted of 30 draws at an average duration of 1.12 minutes. The average delay between draws was 30 minutes. Referencing Figure 59 this should result in an overall efficiency of 73%. However, there was a very long delay between the initial draws (before 7 AM) and the rest of the draws which exceeded the minimum flow rate (after 1 PM). The morning draws, which lasted 0.6 minutes out of the 33.6 minutes in the simulation, represented a minor 1.7% of the total draw duration. Repeating the same estimates for the afternoon draws resulted in an average draw of 1.33 minutes and an average delay of 19.3 minutes. According to Figure 59, 1 minute draws with 20 minute delays result in ~75% efficiency. The efficiency in the two-bedroom house simulation should be slightly higher since the draws are longer and delays shorter.

7.2.2 Four Bedroom House

The draw pattern used for the four bedroom house is shown in Figure 65.

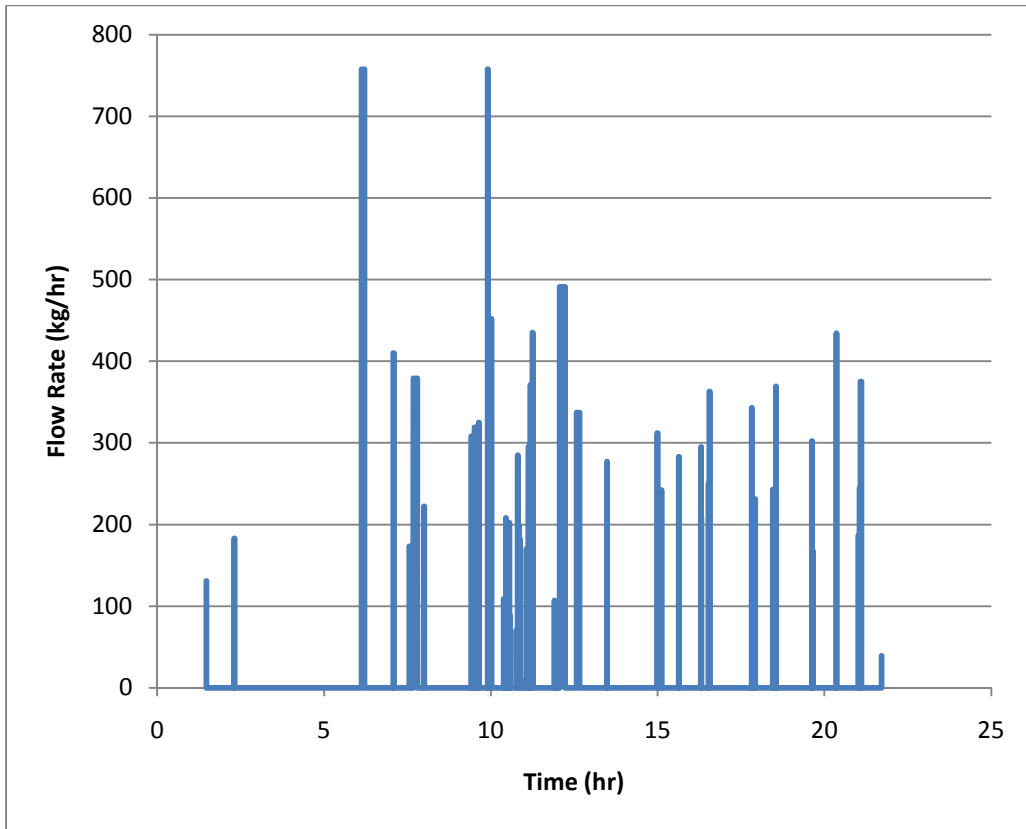


Figure 65: Draw Pattern for the Four Bedroom House

Similar to the profile shown in Figure 63 the water draw profile for the four bedroom house includes several draws which are below the minimum flow rate for the tankless heater. These draws were again included due to the fact that they will remove energy from the heat exchanger and potentially increase the amount of energy required to bring the heat exchanger up to temperature at the start of the next draw.

The simulation results are depicted in Figure 66 and Table 39. Figure 66 shows the water flow rate and outlet temperature during the simulation to show the predicted behavior of the heater. Table 39 depicts the predicted total energy delivered to the water, the predicted total energy consumed by the heater and the predicted efficiency over the course of the draw profile.

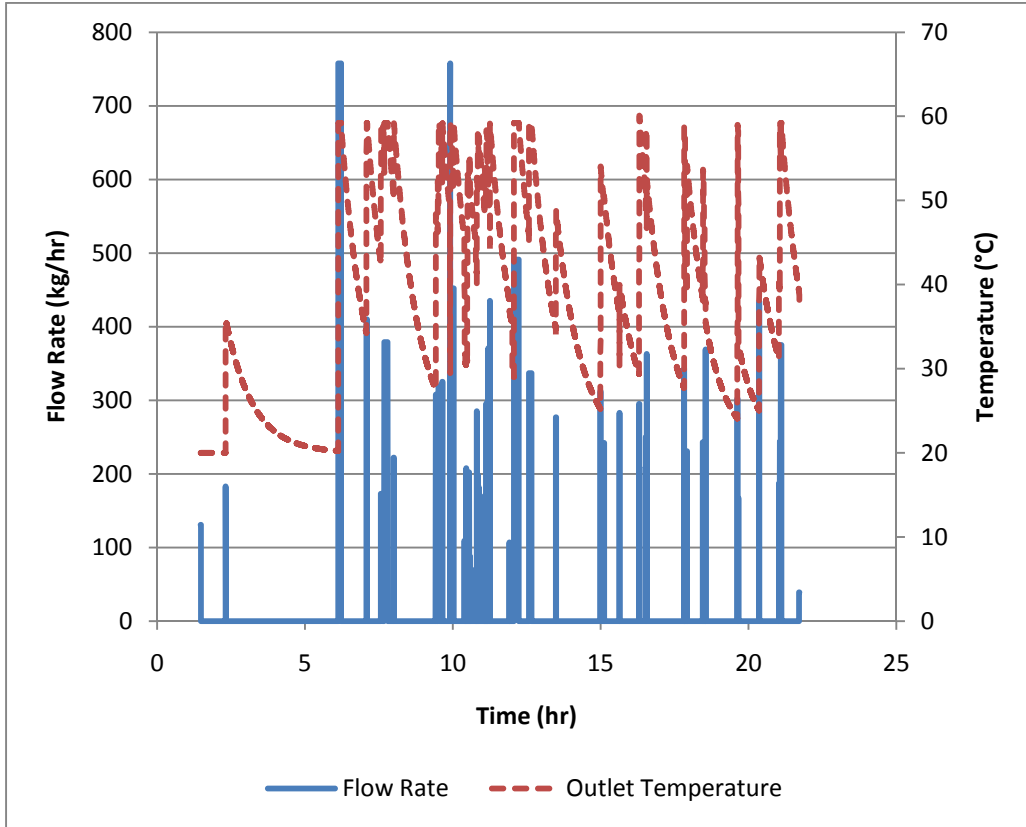


Figure 66: Flow Rates and Temperatures during the Four Bedroom House Draw Profile

Table 39: Energy Consumption and Efficiency in the Four Bedroom House Simulation

Delivered Energy (kJ)	51809
Consumed Energy (kJ)	67801
Efficiency	0.76

The results in Table 39 indicate a heater performance that is similar to that reported in Table 38 for the two bedroom house draw profile. Once again the draw profile was such that the efficiency of the heater was not dramatically decreased by the short draws and delay periods. This result is not surprising considering the results of Section 9.1. There were 58 draws with a total duration of 57.5 minutes over the 1215 minute (20.2 hr) draw profile. This results in an

average draw of 0.99 minutes and an average delay of 19.95 minutes. Referencing Figure 59, this value is just before the impact of delay duration causes dramatic decreases in efficiency. With an average draw duration of 0.99 minutes an efficiency of approximately 75% would be expected. In the simulation analysis for the four bedroom house the model predicted an efficiency of 76% over the course of the day, which is only 4% lower than the 80% conversion rated heater efficiency which was an input to the model.

7.2.3 101 Liter/Day Household

A variation of the Building America Standard Draw Profile was considered to imitate the hot water use in a low use household. The water usage in this draw profile totaled 101 liters and represented an average house in the bottom 25% of houses, implying that 12.5% of houses use less hot water than in the created profile. The draw profile is presented in Figure 67.

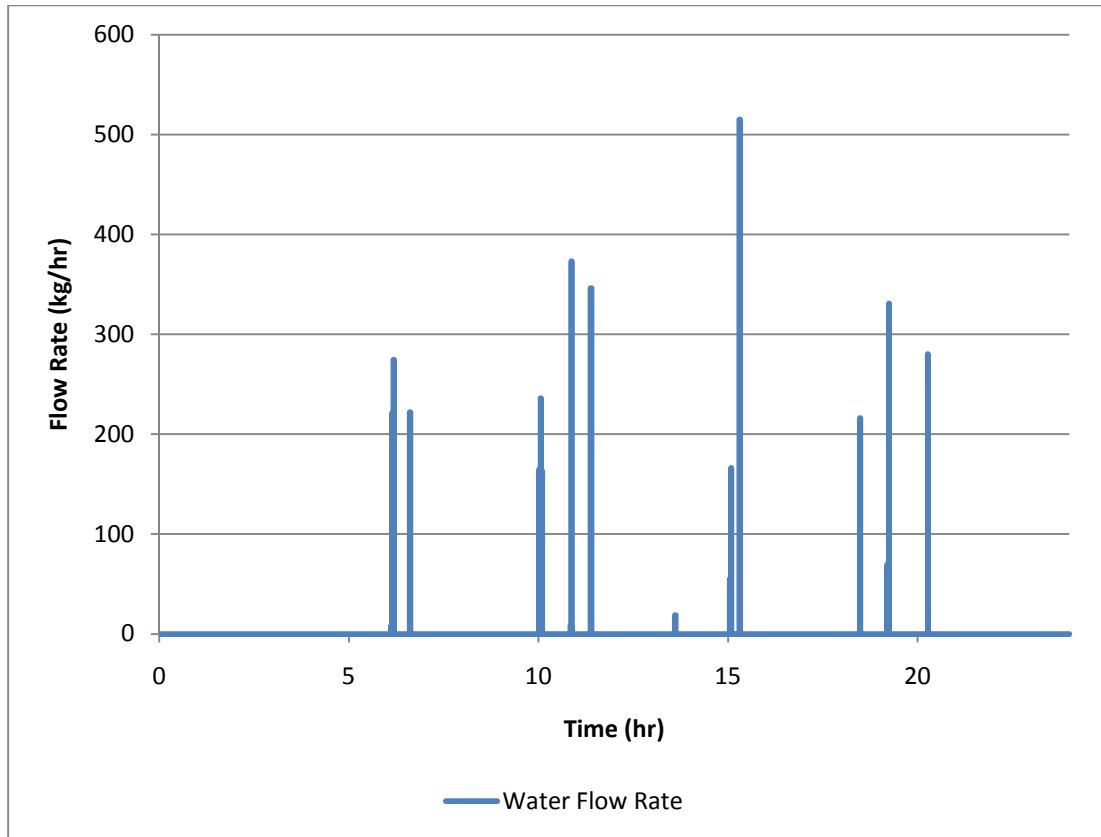


Figure 67: Low Use Household Draw Profile

This profile included nine out of 18 total draws which were below the minimum flow rate. There was no shower in the draw profile thus removing one of the main sources of longer hot water draws. In this profile the most substantial draw was the clothes washer which drew water at 515 kg/hr for 66s.

The simulated response to this profile is shown in Figure 68.

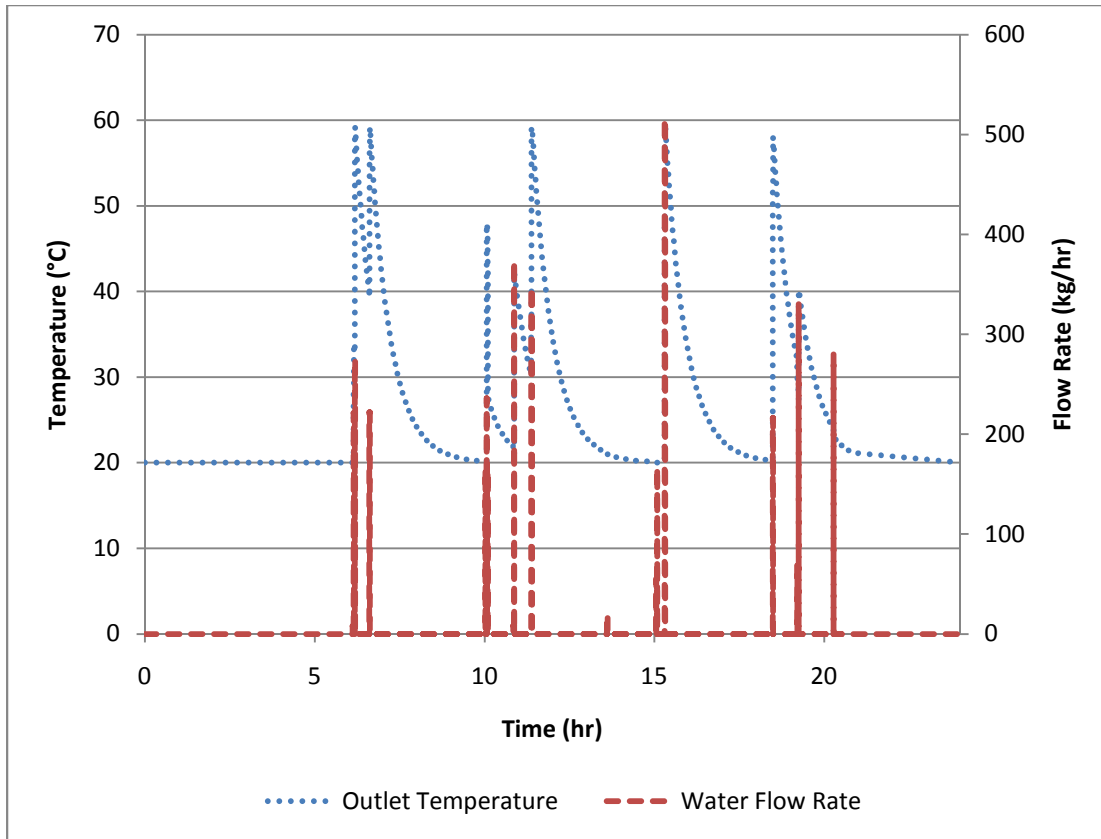


Figure 68: Simulated Results to the Low Use Draw Profile

The energy use and efficiency predictions from the model are shown in Table 40.

Table 40: Energy Use and Efficiency in the Low Use Draw Profile

Delivered Energy (kJ)	4202
Consumed Energy (kJ)	6441
Efficiency	0.65

This profile showed a more dramatic decrease in efficiency. This was caused by the fact that removing the shower pushed a larger portion of the energy use to small draws such as hand washing. In this case the in-use profile efficiency decreased from the 80% steady state value to 65%, representing a 15% reduction. The draw profile consisted of 18 draws averaging 38 seconds per draw. The simulation spanned 14.16 hr with an average delay of 47 minutes

between draws. Figure 59 reports an overall efficiency of 63% for a draw profile with 30 second draws and 47 minute delays. Due to the 38 second draws the efficiency reported in the low-use household simulation model should be slightly higher than the 63% predicted in Figure 59.

Chapter 8: Conclusions and Recommended Continued Research

The main objective of this research work is to develop a multiple node model to predict the performance of tankless water heaters. The model, validated using results from experimental testing, allows for a stronger understanding of how tankless water heaters operate, a more accurate concept of how tankless water heaters work in conjunction with solar hot water systems and predictions of how in-use energy efficiency compares to the steady state efficiency. However, there are still some areas that need further analysis and additional research.

8.1 The Model

The multiple-node tankless water heater model described in this thesis has been validated. When compared to two different draw profiles it predicted energy use with errors of -1.6% and 2.1%. These errors are both within the uncertainty of the experimental measurements, and can be explained by changes in the natural gas energy density which could not be measured due to a lack of accurate measurement equipment.

There are still some areas in which the model and experimental testing can be improved. Foremost, the calibration and validation process should be repeated with an accurate measurement of the natural gas energy density. This measurement will allow for a better validation process and more confidence that the model is predicting energy use accurately. Secondly, the model uses a very simple control algorithm which could be improved. The control algorithm is appropriate when the heater functions at steady state. In contrast the tested Rinnai

heater draws additional gas during the transient conditions at the start of a draw. Modeling this control logic was deemed to be unnecessary due to the fact that other water heaters might not employ the same control logic; however, if more tankless heaters are tested and all exhibit similar behavior a control algorithm could be developed to accurately predict energy use.

8.2 Steady State Efficiency

According to the tests performed no operating conditions impact the steady state efficiency. This finding may be attributed to the fact that the effects are insignificant relative to the uncertainty in the measurements. The steady state efficiency experiments should be repeated with measurement of the natural gas energy density to possibly capture a detectable impact with a smaller measurement uncertainty.

8.3 Use in Conjunction with Solar Hot Water

The tested heater, when exposed to a gradually reducing inlet water temperature as is the case when operated in conjunction with solar hot water, did not fire until the required heat input rate was able to increase the water to approximately the set temperature. There is some instability in the control algorithm as the heater occasionally overshoot the set temperature by a few degrees Celsius; however, the theorized oscillations which would result from feedback control did not occur. This implies that people using solar hot water systems with a tankless water heater for backup will sometimes receive water which is colder than the set temperature, but will not have to accept rapidly changing water temperature.

This is only known for the tested heater. Additional testing using additional tankless water heater models should be performed to determine if the other heaters respond to preheated water in the same manner.

8.4 Efficiency Sensitivity and Draw Profile Efficiency

Results from the sensitivity analysis showed that the draw profile efficiency of tankless water heaters is sensitive to the characteristics of the draw profile. Results indicated that a draw profile featuring draws of high energy use will have draw profile efficiencies similar to the steady state conversion efficiency because the delivered energy during a draw far exceeds the energy lost from the heat exchanger between draws. However, draw profiles with short draws become sensitive to the delay length and ambient temperature. During draw profiles with short draws the energy delivered to the fluid no longer dominates the total energy use and the energy lost from the heat exchanger between each draw becomes more important. Therefore any factor that affects the energy lost to the environment between draws, such as the delay length or the ambient temperature, will now have an effect on the draw profile efficiency.

To investigate how these effects impact the draw profile efficiency of tankless water heaters in realistic draw profiles simulations were performed using draw profiles from the Building America Standard Benchmark Draw Profiles. The simulation models the energy consumption and efficiency of the heater over one day of draws. Simulations were performed for both two-bedroom and four-bedroom house profiles as well as a profile focusing on a very low use house. The simulations showed a draw profile efficiency of 77% for the two bedroom house draw profile, 76% for the four bedroom house draw profile and 65% for the low use household. The

results for the standard two and four bedroom house are 3% and 4% lower than the 80% steady state efficiency indicating that the draw profiles common in higher use houses do not have a dramatic effect on the heater. The draw profile for the low use household, without large draws such as showers, showed a profile efficiency of 65% indicating that there are situations where the characteristics of the draw profile dramatically reduces the in-use efficiency of tankless water heaters.

Since a single derate factor for tankless heaters which can be applied to all draw profiles would be the most applicable means of describing this decrease in efficiency future work should focus on performing an extensive simulation analysis using several different draw profiles. The results from these draw profiles could then be used to identify a derate factor which would approximate the decrease in efficiency across the entire spectrum of draw profiles.

Works Cited

- [1] David Hewitt, J. P. (2005). *Tankless Gas Water Heaters: Oregon Market Status*. Energy Trust of Oregon.
- [2] Armin Rudd, H. F. (2007). Introducing the Market to High Performance Green Building on Hilton Head Island. *Whole House Research Performance Results* .
- [3] Kalensky, D. (2006, October). ACEEE Summit Presentation. Gas Technology Institute.
- [4] Davis Energy Group. (2007). *Residential Feasibility Assessment of Gas Tankless Water Heaters in PG&E Service Territory*. Pacific Gas and Electric Company.
- [5] Gas Technology Institute. (2007). *Literature Review of Tankless Water Heaters*. California Energy Commission.
- [6] Davis Energy Group, Inc. (2008). Measure Information Template: Tankless Gas Water Heaters. *California Building Energy Efficiency Standards* .
- [7] Yuill, D. G. (2005). Development of an Accurate Feed Forward Temperature Control Tankless Water Heater. U.S. Department of Energy Building Technologies Program.
- [8] Roman Spur, D. F. (2006). Influence of the domestic hot-water daily draw-off profile on the performance of a hot-water store. *Applied Energy* , 749-773.
- [9] R. G. Pratt, B. A. (1993). Analysis of water heater standby energy consumption from ELCAP homes. *Energy and Buildings* , 221-234.
- [10] TESS. (2008). *Type 940: Tankless Water Heater*. Madison, WI: Thermal Energy System Specialists.
- [11] TESS. Type 4: Stratified Fluid Storage Tank. In *TRNSYS 16 - Mathematical Reference* (pp. 365 - 369). Madison, WI: Thermal Energy System Specialists.
- [12] Maxwell, G. M. (1985). *Mathematical modeling of an instantaneous gas-fired water heater*. Lafayette: Purdue University.
- [13] Rinnai. (2008, May). Water Heater Technical Description.
- [14] Buch, J., Thornton, J., Hoeschle, M., Springer, D., & Rudd, A. (2008). Preliminary Modeling, Testing and Analysis of a Gas Tankless Water Heater. *SOLAR 2008*. San Diego.

- [15] Hendron, R., Burch, J., & Barker, G. (2010). Draft: Tool for Generating Realistic Residential Hot Water Event Schedules. *Submitted to: Simbuild.*
- [16] Fox Thermal Instruments, Inc. (2009). *Model FT2 Thermal Mass Flow Meter & Temperature Transmitter.* Marina, CA.
- [17] BadgerMeter, Inc. (2007). *Recordall Cold Water Bronze Disc Meter Technical Brief.* Milwaukee, WI: BadgerMeter, Inc.
- [18] Rinnai America Corporation. (2008). *Rinnai Direct Vent Tankless Water Heater Operation and Installation Manual.* Peachtree City, GA: Rinnai American Corporation.
- [19] Omega Engineering, Inc. (2010). *FMA-900 Series Air Velocity Transducers.* Stamford, CT: Omega Engineering, Inc.
- [20] Omega Engineering Services, Inc. (2009). *Thermocouples - An Introduction.* Retrieved February 25, 2010, from Omega Engineering Technical Reference: <http://www.omega.com/thermocouples.html>
- [21] TESS. Type 14: Time Dependent Forcing Function. In *TRNSYS 16 - A Mathematical Reference* (pp. 397-398). Madison, WI: Thermal Energy System Specialists.
- [22] TESS. What is TRNSYS. In *TRNSYS 16 - A Mathematical Reference* (p. 7). Madison, WI: Thermal Energy System Specialists.
- [23] Bushnell, D. (1990). GENOPT - a program that writes user-friendly optimization code. *International Journal of Solids and Structures* , 1173-1210.
- [24] Takagi. (2008). *Instantaneous Water Heater Installation Manual and Owner's Guide.* Irvine, CA: Takagi Industrial Co. USA Inc.
- [25] Bosch Thermotechnology Corporation. (2009). *Outdoor Kit Installation Manual.* Londonderry, NH: Bosch Thermotechnology Corp.
- [26] Campbell Scientific, Inc. (1997). *CR10X Measurement and Control Module Owners Manual.* Campbell Scientific, Inc.
- [27] Public Service Company of Colorado. (1998). *Rules and Regulations Natural Gas Service Standards.* Denver: Public Service Company of Colorado.
- [28] Press, W. H., Flannery, B. P., Teukolsky, S. A., & Vetterling, W. T. (New York). *Numerical Recipes: The Art of Scientific Computing.* 1992: Cambridge University Press.

Appendix A: Derivation of Multiple Node 'a' and 'b' Terms

$$\frac{Cap}{\#_{Node}} \frac{dT_n}{dt} = \frac{\eta\lambda\dot{Q}_{Rated}}{\#_{Node}} - \dot{m}_{Fluid}C_p(T_n - T_{n-1}) - \frac{UA(T_n - T_{Amb})}{\#_{Node}} + \frac{kA(T_{n+1} - T_n)}{L/\#_{Node} - 1} - \frac{kA(T_n - T_{n-1})}{L/\#_{Node} - 1}$$

$$\frac{Cap}{\#_{Node}} \frac{dT_n}{dt} = \frac{\eta\lambda\dot{Q}_{Rated}}{\#_{Node}} - \dot{m}_{Fluid}C_p(T_n - T_{n-1}) - \frac{UA(T_n - T_{Amb})}{\#_{Node}} + \frac{kA(\#_{Node} - 1)(T_{n+1} - T_n)}{L} - \frac{kA(\#_{Node} - 1)(T_n - T_{n-1})}{L}$$

$$Cap \frac{dT_n}{dt} = \eta\lambda\dot{Q}_{Rated} - \dot{m}_{Fluid}C_p\#_{Node}(T_n - T_{n-1}) - UA(T_n - T_{Amb}) + \frac{kA\#_n(n - 1)(T_{n+1} - T_n)}{L} - \frac{kA\#_{Node}(\#_{Node} - 1)(T_n - T_{n-1})}{L}$$

$$\frac{dT_n}{dt} = \frac{\eta\lambda\dot{Q}_{Rated}}{Cap} - \frac{\dot{m}_{Fluid}C_p\#_{Node}(T_n - T_{n-1})}{Cap} - \frac{UA(T_n - T_{Amb})}{Cap} + \frac{kA\#_{Node}(\#_{Node} - 1)(T_{n+1} - T_n)}{Cap * Length} - \frac{kA\#_{Node}(\#_{Node} - 1)(T_n - T_{n-1})}{Cap * L}$$

$$\begin{aligned} \frac{dT_n}{dt} = & \frac{-\dot{m}_{Fluid}C_p\#_{Node}T_n}{Cap} - \frac{UAT_n}{Cap} - \frac{kA\#_{Node}(\#_{Node} - 1)T_n}{Cap * L} - \frac{kA\#_{Node}(\#_{Node} - 1)T_n}{Cap * L} \\ & + \frac{\eta\lambda\dot{Q}_{Rated}}{Cap} + \frac{\dot{m}_{Fluid}C_p\#_{Node}T_{Node-1}}{Cap} + \frac{UAT_{Amb}}{Cap} + \frac{kA\#_{Node}(\#_{Node} - 1)T_{n+1}}{Cap * L} \\ & + \frac{kA\#_{Node}(\#_{Node} - 1)T_{n-1}}{Cap * L} \end{aligned}$$

$$\begin{aligned}
\frac{dT_n}{dt} = & \frac{-1}{Cap} * \left(\dot{m}_{Fluid} C_p \#_{Node} + UA + \frac{2kA\#_{Node}(\#_{Node} - 1)}{L} \right) T_n + \frac{1}{Cap} * (\eta\lambda\dot{Q}_{Rated} \\
& + \dot{m}_{Fluid} C_p \#_{Node} T_{n-1} + UAT_{Amb} + \frac{kA\#_{Node}(\#_{Node} - 1)T_{n+1}}{L} \\
& + \frac{kA\#_{Node}(\#_{Node} - 1)T_{n-1}}{L})
\end{aligned}$$

Appendix B: Solution of Differential Equation for Final Temperature

$$\frac{dT_n}{dt} = a * T_n + b$$

$$\frac{1}{a * T_n + b} dT = dt$$

$$\frac{1}{a} \ln(a * T_n + b) = t$$

$$\frac{1}{a} \ln(a * T_{n,F} + b) - \frac{1}{a} \ln(a * T_{n,I} + b) = t_F - t_I$$

$$\ln(a * T_{n,F} + b) - \ln(a * T_{n,I} + b) = a * (t_F - t_I)$$

$$\ln\left(\frac{a * T_{n,F} + b}{a * T_{n,I} + b}\right) = a * (t_F - t_I)$$

$$\frac{a * T_{n,F} + b}{a * T_{n,I} + b} = e^{a*(t_F-t_I)}$$

$$a * T_{n,F} + b = (a * T_{n,I} + b) * e^{a*(t_F-t_I)}$$

$$T_{n,F} = \left(T_{n,I} + \frac{b}{a}\right) * e^{a*(t_F-t_I)} - \frac{b}{a}$$

Appendix C: Derivation of Δt From the Solution for $T_{\text{Node,Final}}$

See Appendix B for solution to $T_{\text{Node,Final}}$

$$T_{n,F} = \left(T_{n,I} + \frac{b}{a} \right) * e^{a*(t_F - t_I)} - \frac{b}{a}$$

Let $\Delta t = t_F - t_I$

$$T_{n,F} + \frac{b}{a} = \left(T_{n,I} + \frac{b}{a} \right) * e^{a*(\Delta t)}$$

$$\frac{T_{n,F} + b/a}{T_{n,I} + b/a} = e^{a*(\Delta t)}$$

$$\ln \left(\frac{T_{n,F} + b/a}{T_{n,I} + b/a} \right) = a * \Delta t$$

$$\Delta t = \frac{1}{a} * \ln \left(\frac{T_{n,F} + b/a}{T_{n,I} + b/a} \right)$$

Appendix D: Building America Draw Profiles

Two Bedroom Draw Profile

Start Time	Duration (sec)	Flow Rate (kg/hr)
1/1 6:44:42 AM	12	247.0
1/1 6:46:42 AM	6	266.6
1/1 6:48:36 AM	18	351.2
1/1 8:33:42 AM	18	73.3
1/1 8:35:42 AM	36	38.6
1/1 12:44:00 PM	6	12.7
1/1 1:05:00 PM	438	367.7
1/1 1:35:30 PM	612	363.5
1/1 2:14:12 PM	84	340.8
1/1 2:16:06 PM	18	197.3
1/1 2:18:06 PM	78	384.2
1/1 3:07:42 PM	6	392.4
1/1 3:09:36 PM	36	264.5
1/1 3:13:36 PM	30	127.7
1/1 4:03:30 PM	48	293.0
1/1 4:16:24 PM	78	8.3
1/1 4:29:18 PM	30	8.5
1/1 4:31:18 PM	6	221.1
1/1 4:47:42 PM	12	288.2
1/1 4:49:36 PM	72	196.5
1/1 5:05:24 PM	42	168.8
1/1 5:47:24 PM	6	10.9
1/1 5:49:24 PM	6	42.9
1/1 6:00:24 PM	6	343.1
1/1 6:01:30 PM	132	160.3
1/1 6:21:42 PM	6	272.5
1/1 8:21:48 PM	42	180.0
1/1 8:23:48 PM	6	11.5
1/1 8:59:00 PM	48	155.5
1/1 10:17:18 PM	78	124.4

Four Bedroom House Draw Profile

Start Time	Duration (sec)	Flow Rate (kg/hr)
1:58:18 AM	18	131.1
2:18:42 AM	18	183.3
6:07:18 AM	336	866.2
7:04:24 AM	90	410.3
7:33:24 AM	252	173.2
7:40:30 AM	426	378.8
7:59:30 AM	54	222.5
9:25:00 AM	18	308.1
9:28:54 AM	12	223.7
9:30:48 AM	84	319.1
9:38:00 AM	42	324.8
9:54:06 AM	42	298.6
10:00:36 AM	48	452.3
10:23:12 AM	36	109.1
10:25:06 AM	6	53.8
10:27:00 AM	6	207.7
10:29:00 AM	30	201.7
10:30:54 AM	18	8.9
10:32:48 AM	24	202.2
10:34:48 AM	6	87.5
10:46:12 AM	12	71.0
10:48:12 AM	24	284.9
10:50:06 AM	36	198.9
10:52:00 AM	36	181.9
11:01:54 AM	30	9.0
11:03:48 AM	30	170.0
11:05:48 AM	6	18.2
11:07:42 AM	30	296.0
11:09:36 AM	6	87.2
11:11:30 AM	6	371.4
11:14:48 AM	30	435.4
11:54:42 AM	6	106.8
12:00:06 PM	48	53.8
12:03:36 PM	600	490.7
12:34:06 PM	318	337.5
1:28:54 PM	18	277.2

2:59:18 PM	24	311.8
3:06:36 PM	6	242.1
3:37:48 PM	30	283.0
4:17:48 PM	60	208.1
4:17:54 PM	24	86.8
4:31:18 PM	36	250.5
4:33:18 PM	18	362.9
5:49:00 PM	30	343.1
5:50:54 PM	36	82.7
5:52:48 PM	12	223.2
5:54:48 PM	24	231.4
6:27:06 PM	24	242.5
6:29:06 PM	12	118.5
6:31:00 PM	42	146.6
6:32:54 PM	6	369.3
7:37:12 PM	36	302.1
7:39:12 PM	30	167.1
8:21:24 PM	12	434.1
9:01:12 PM	12	187.1
9:03:06 PM	60	244.4
9:05:00 PM	90	375.4
9:42:36 PM	24	38.7

Low Use House Draw Profile

Start Time	Duration (sec)	Flow Rate (kg/hr)
6:06:36 AM	42	7.7
6:08:36 AM	12	221.3
6:10:30 AM	48	274.3
6:36:24 AM	60	222.0
10:01:30 AM	6	164.9
10:03:24 AM	24	236.0
10:05:24 AM	36	162.7
10:50:18 AM	102	8.3
10:52:12 AM	12	372.9
11:22:24 AM	90	346.1
1:36:12 PM	60	18.7
3:02:54 PM	6	55.0
3:04:48 PM	18	166.0
3:18:00 PM	66	514.8
6:28:48 PM	42	216.1
7:12:00 PM	30	69.5
7:14:48 PM	12	330.7
8:16:12 PM	12	281.1

Appendix E: Campbell Scientific Datalogger Program

;
{CR10X}

;
NOTE: for CR10X with AM16/32 and SDM-CD16AC

;
Program Name: PeterGrant_v**

;
Revision History:

;
12/31/08 (GMB) (v01) - Program written

;

;
Channel Connections:

;

;
CR10X Sensor

;
1H AM16/32#1 : COM H (ODD) (switch set to "2 X 32")

;
1L AM16/32#1 : COM L (ODD) (switch set to "2 X 32")

;
2H AM16/32#2 : COM L (ODD) (switch set to "2 X 32")

;
2L AM16/32#2 : COM H (ODD) (switch set to "2 X 32")

;
3H,3L Flow Meter #1

;4H,4L Flow Meter #2
;5H,5L Flow Meter #3
;6H TC Reference Thermistor #2
;6L TC Reference Thermistor #1

;P1 Gas Flow 2 (Residential Meter)
;P2

;C1 SDM-CD16D
;C2 SDM-CD16D
;C3 SDM-CD16D
;C4 AM16/32#1 Clk
;C5 AM16/32#1 Reset
;C6 AM16/32#2 Reset
;C7 AM16/32#2 Clk
;C8

;E1 TC Reference Thermistor #1
;E2 TC Reference Thermistor #2
;E3

;AG TC Reference Thermistor #1
;AG TC Reference Thermistor #2

;12V

;-----

;AM16/32 (switch set to "2 X 32")

; 1H, 1L TC, TC01 (Type T)

; 2H, 2L TC, TC02 (Type T) Tank1-2

; 3H, 3L TC, TC03 (Type T) Tank1-3

; 4H, 4L TC, TC04 (Type T) Tank1-4

; 5H, 5L TC, TC05 (Type T)

; 6H, 6L TC, TC06 (Type T)

; 7H, 7L TC, TC07 (Type T)

; 8H, 8L TC, TC08 (Type T) Tank1-8

; 9H, 9L TC, TC09 (Type T) Tank1-9

;10H,10L TC, TC10 (Type T)

;11H,11L TC, TC11 (Type T) Tank2-1

;12H,12L TC, TC12 (Type T) Tank2-2

;13H,13L TC, TC13 (Type T) Tank2-3

;14H,14L TC, TC14 (Type T) Tank2-4

;15H,15L TC, TC15 (Type T) Tank2-5

;16H,16L TC, TC16 (Type T) Tank2-6

;17H,17L TC, TC17 (Type T) Tank2-7
;18H,18L TC, TC18 (Type T) Tank2-8
;19H,19L TC, TC19 (Type T) Tank2-9
;20H,20L TC, TC20 (Type T) Tank2-10
;21H,21L TC, TC21 (Type T) SmallTank-1
;22H,22L TC, TC22 (Type T) SmallTank-2
;23H,23L TC, TC23 (Type T) SmallTank-3
;24H,24L TC, TC24 (Type T) SmallTank-4
;25H,25L TC, TC25 (Type T) SmallTank-5
;26H,26L TC, TC26 (Type T) EnteringTankless
;27H,27L TC, TC27 (Type T) FinalExit
;28H,28L TC, TC28 (Type T) SmallTankInlet
;29H,29L TC, TC29 (Type T) Htr->SmallTank
;30H,30L TC, TC30 (Type T) SmallTank->MixingValve
;31H,31L TC, TC31 (Type T) MixingValve->Drain
;32H,32L TC, TC32 (Type T) MainsInlet

;-----

;AM16/32 (switch set to "2 X 32")

; 1H, 1L Gas, F_Gas_lpm <Fox Thermal>
; 2H, 2L TC, TC33 (Type K) HX pt2
; 3H, 3L TC, TC34 (Type K) HX pt3

; 4H, 4L TC, TC35 (Type K) HX pt7
; 5H, 5L TC, TC36 (Type K) HX pt8
; 6H, 6L TC, TC37 (Type K) HX pt9
; 7H, 7L TC, TC38 (Type K) HX pt10
; 8H, 8L TC, TC41 (Type T) Ambient Temp1
; 9H, 9L TC, TC42 (Type T) Ambient Temp2
;10H,10L TC, TC43 (Type T) Exiting Heater
;11H,11L TC, TC42 (Type T) Exhaust Air
;12H,12L TC, TC43 (Type T)
;13H,13L TC, TC44 (Type T)
;14H,14L TC, TC45 (Type T)
;15H,15L TC, TC46 (Type T) Heater Exit (submersed)
;16H,16L TC, TC47 (Type T)
;17H,17L TC, TC48 (Type T)
;18H,18L TC, TC49 (Type T)
;19H,19L TC, TC50 (Type T)
;20H,20L TC, TC51 (Type T)
;21H,21L TC, TC52 (Type T)
;22H,22L TC, TC53 (Type T)
;23H,23L TC, TC54 (Type T)
;24H,24L TC, TC55 (Type T)
;25H,25L TC, TC56 (Type T)
;26H,26L TC, TC57 (Type T)

;27H,27L TC, TC58 (Type T)
;28H,28L TC, TC59 (Type T)
;29H,29L TC, TC60 (Type T)
;30H,30L TC, TC61 (Type T)
;31H,31L TC, TC62 (Type T)
;32H,32L TC, TC63 (Type T)

;-----

;SDM-CD16D

; 1 SS Relay: FromMixingValve
; 2 SS Relay: Manifold1
; 3 SS Relay: Manifold2
; 4 SS Relay: Manifold3
; 5 SS Relay: Post-TankPurge
; 6 SS Relay: CirculationPump
; 7 SS Relay: MixingPump
; 8 SS Relay: Tank1Bottom
; 9 SS Relay: Tank2Bottom
;10 SS Relay: Tank1Top
;11 SS Relay: Tank2Top
;12 SS Relay: Cntl12
;13 SS Relay: Cntl13

;14 SS Relay: Cntl14

;15 SS Relay: Cntl15

;16 SS Relay: Cntl16

;

*Table 1 Program

01: 3 Execution Interval (seconds)

1: If (X<=>F) (P89)

1: 56 X Loc [FirstPass]

2: 4 <

3: 0.5 F

4: 30 Then Do

2: Z=F x 10^n (P30)

1: 1 F

2: 0 n, Exponent of 10

3: 56 Z Loc [FirstPass]

3: End (P95)

;------

4: Batt Voltage (P10)

1: 59 Loc [V_loggr_V]

;

5: Internal Temperature (P17)

1: 58 Loc [T_loggr_C]

;

; TC Reference:

6: Temp (107) (P11)

1: 1 Reps

2: 12 SE Channel

3: 1 Excite all reps w/E1

4: 75 Loc [T_ref_1]

5: 1.0 Multiplier

6: 0.0 Offset ;

7: Temp (107) (P11)

1: 1 Reps

2: 11 SE Channel

3: 2 Excite all reps w/E2

4: 76 Loc [T_ref_2]

5: 1.0 Multiplier

6: 0.0 Offset ;

8: Pulse (P3)

1: 1 Reps

2: 1 Pulse Channel 1

3: 2 Switch Closure, All Counts

4: 50 Loc [F_Gas_2]

5: 1.0 Mult

6: 0.0 Offset ;

9: Pulse (P3)

1: 1 Reps

2: 2 Pulse Channel 2

3: 2 Switch Closure, All Counts

4: 53 Loc [F_02_lpm]

5: 1.0 Mult

6: 0.0 Offset

;------

;Activate MUX1:

10: Do (P86)

1: 45 Set Port 5 High

;-----

;Type T thermocouples on AM16/32 channels 1-32:

11: Beginning of Loop (P87)

1: 0 Delay

2: 32 Loop Count

12: Do (P86)

1: 74 Pulse Port 4

13: Excitation with Delay (P22)

1: 2 Ex Channel

2: 0 Delay W/Ex (0.01 sec units)

3: 1 Delay After Ex (0.01 sec units)

4: 0 mV Excitation

14: Thermocouple Temp (DIFF) (P14)

1: 1 Reps

2: 23 25 mV 60 Hz Rejection Range

3: 1 DIFF Channel
4: 1 Type T (Copper-Constantan)
5: 75 Ref Temp (Deg. C) Loc [T_ref_1]
6: 1 -- Loc [T_TC01_C]
7: 1.0 Multiplier
8: 0.0 Offset

15: End (P95) ;loop through channels 1-32

;

;Disable MUX1:

16: Do (P86)

1: 55 Set Port 5 Low

;

;Activate MUX2:

17: Do (P86)

1: 46 Set Port 6 High ;

;

;Read gas meter:

18: Do (P86)

1: 77 Pulse Port 7

19: Excitation with Delay (P22)

1: 2 Ex Channel

2: 0 Delay W/Ex (0.01 sec units)

3: 1 Delay After Ex (0.01 sec units)

4: 0 mV Excitation

20: Volt (Diff) (P2)

1: 1 Reps

2: 25 2500 mV 60 Hz Rejection Range

3: 2 DIFF Channel

4: 51 Loc [F_Gas_lpm]

5: 1.0 Multiplier

6: 0.0 Offset

;-----

;Type K thermocouples on AM16/32 channels 2-7:

21: Beginning of Loop (P87)

1: 0 Delay

2: 6 Loop Count

22: Do (P86)

1: 77 Pulse Port 7

23: Excitation with Delay (P22)

1: 2 Ex Channel

2: 0 Delay W/Ex (0.01 sec units)

3: 1 Delay After Ex (0.01 sec units)

4: 0 mV Excitation

24: Thermocouple Temp (DIFF) (P14)

1: 1 Reps

2: 23 25 mV 60 Hz Rejection Range

3: 2 DIFF Channel

4: 3 Type K (Chromel-Alumel)

5: 76 Ref Temp (Deg. C) Loc [T_ref_2]

6: 77 -- Loc [T_TC33_C]

7: 1.0 Multiplier

8: 0.0 Offset

25: End (P95) ;loop through channels 2-9

;-----

;Type T thermocouples on AM16/32 channels 7-12:

26: Beginning of Loop (P87)

1: 0 Delay

2: 6 Loop Count

27: Do (P86)

1: 77 Pulse Port 7

28: Excitation with Delay (P22)

1: 2 Ex Channel

2: 0 Delay W/Ex (0.01 sec units)

3: 1 Delay After Ex (0.01 sec units)

4: 0 mV Excitation

29: Thermocouple Temp (DIFF) (P14)

1: 1 Reps

2: 23 25 mV 60 Hz Rejection Range

3: 2 DIFF Channel

4: 1 Type T (Copper-Constantan)

5: 76 Ref Temp (Deg. C) Loc [T_ref_2]

6: 85 -- Loc [T_TC41_C]

7: 1.0 Multiplier

8: 0.0 Offset

30: End (P95) ;loop through channels 7-11

;------

;Read gas meter:

31: Do (P86)

1: 77 Pulse Port 7

32: Excitation with Delay (P22)

1: 2 Ex Channel

2: 0 Delay W/Ex (0.01 sec units)

3: 1 Delay After Ex (0.01 sec units)

4: 0 mV Excitation

33: Volt (Diff) (P2)

1: 1 Repts

2: 25 2500 mV 60 Hz Rejection Range

3: 2 DIFF Channel

4: 61 Loc [FAir_SFPM]

5: 1.0 Multiplier

6: 0.0 Offset

;-----

;-----

;Disable MUX2:

34: Do (P86)

1: 56 Set Port 6 Low

;-----

;Read water flow meter #1:

35: Volt (Diff) (P2)

1: 1 Reps

2: 25 2500 mV 60 Hz Rejection Range

3: 3 DIFF Channel

4: 52 Loc [F_01_lpm]

5: 1.0 Multiplier

6: 0.0 Offset

;-----

;Read water flow meter #3:

36: Volt (Diff) (P2)

- 1: 1 Reps
- 2: 25 2500 mV 60 Hz Rejection Range
- 3: 5 DIFF Channel
- 4: 54 Loc [F_03_lpm]
- 5: 1.0 Multiplier ;
- 6: 0.0 Offset

;

;Write stati to SDM-CD16D:

37: SDM-CD16 / SDM-CD16AC (P104)

- 1: 1 Reps
- 2: 00 SDM Address
- 3: 34 Loc [Stat_01]

;

=====
;

;Output

=====
;

;-----

;9-second:

38: If time is (P92)

- 1: 0 -- Minutes (Seconds --) into a
- 2: 1 Interval (same units as above)
- 3: 10 Set Output Flag High (Flag 0)

39: Set Active Storage Area (P80)^11943

- 1: 1 Final Storage Area 1
- 2: 1 Array ID

40: Real Time (P77)^20007

- 1: 1221 Year,Day,Hour/Minute,Seconds (midnight = 2400)

41: Sample (P70)

- 1: 2 Reps
- 2: 26 Loc [T_TC26_C]

42: Sample (P70)

- 1: 6 Reps
- 2: 77 Loc [T_TC33_C]

43: Sample (P70)

1: 4 Reps

2: 85 Loc [T_TC41_C]

44: Sample (P70)

1: 1 Reps

2: 90 Loc [T_TC46_C]

45: Sample (P70)

1: 5 Reps

2: 50 Loc [F_Gas_2]

46: Sample (P70)

1: 4 Reps

2: 34 Loc [Stat_01]

47: Sample (P70)

1: 2 Reps

2: 58 Loc [T_loggr_C]

48: Sample (P70)

1: 1 Reps

2: 61 Loc [FAir_SFPM]

;=====

=====

*Table 2 Program

01: 0.0000 Execution Interval (seconds)

*Table 3 Subroutines

End Program

Appendix F: TRNSYS Component Code

SUBROUTINE TYPE201(TIME,XIN,OUT,T,DTDT,PAR,INFO,ICNTRL,*)

C-----

C DESCRIPTION:

C THIS SUBROUTINE MODELS A GAS/ELECTRIC TANKLESS WATER HEATER.

C

C MODIFIED:

C FEBRUARY 2008 - JWT - RE-WORKED THE CONTROL ALGORITHMS TO MORE
ACCURATELY REFLECT THE WAY THE DEVICES ARE BEING CONTROLLED

(TYPE940)

C FEBRUARY 2008 - JWT - ADDED A MODE WHERE THE INPUT ENERGY IS USED
TO HEAT THE FLUID (TYPE940)

C DECEMBER 2008 - PWG - MODIFIED TYPE 940 TO INCLUDE MULTIPLE NODES
(THIS MODEL)

C JUNE 2009 - PWG - CHANGED SKIN LOSS, STORED, AND DELIVERED OUTPUT
TO BE TOTALLED ENERGY USE OVER TIMESTEP RATHER THAN INSTANT RATE AT
THE END OF THE TIMESTEP

C-----

! Copyright © 2008 Thermal Energy System Specialists, LLC. All rights reserved.

C-----

!Export this subroutine for its use in external DLLs.

!DEC\$ATTRIBUTES DLLEXPORT :: TYPE201

C-----

C-----

C ACCESS TRNSYS FUNCTIONS

USE TrnsysConstants

USE TrnsysFunctions

C-----

C-----

C TRNSYS DECLARATIONS

IMPLICIT NONE

DOUBLE PRECISION XIN,OUT,TIME,PAR,T,DTDT,STORED,TIME0,TFINAL,DELT

INTEGER*4 INFO(15),NPMAX,NI,NOUT,ND,IUNIT,ITYPE,ICNTRL,NSTOREDMAX,

1 NP,NSTORED,NDMAX

CHARACTER*3 OCHECK,YCHECK

C-----

C-----

C USER DECLARATIONS

PARAMETER (NPMAX=100,NOUT=100,NI=6,NDMAX=10,NSTOREDMAX=100)

C-----

C-----

C REQUIRED TRNSYS DIMENSIONS

DIMENSION XIN(INFO(3)),OUT(INFO(6)),PAR(INFO(4)),YCHECK(NI),

1 OCHECK(NOUT),STORED(NSTOREDMAX)

C-----

C-----

C DECLARATIONS AND DEFINITIONS FOR THE USER-VARIABLES

```

DOUBLE PRECISION AA, CAPACITANCE,T_FLUID_IN,FLOW_FLUID,
      1 FLOW_MIN,EFF_GAS,Q_RATED,AREA,DEADBAND,CONTROL_MIN,
1 EFF_PILOT,Q_PILOT,T_ENV,T_SET,U_VALUE,CONTROL_LAST,
      1
CONTROL_NOW,T_FLUID_OUT,Q_COMBUSTED_TOT,Q_GAS_TOT,DELT_NOW,
      1 TAVE_TOT,Q_STORED,DELT_TOT,EFFICIENCY,Q_COMBUSTED,
      1 Q_COMBUSTED_NEEDED,TIME_DELAY,TIME_ON,Q_DEL_TOT,SMALL,
1 CONTROL_AVE,P_ELEC_TOT,P_ELEC_STANDBY,P_ELEC_HEATING,
1 CONTROL_NEXT,Q_INPUT,Q_SKIN_TOT,TAVE_I,CP_FLUID,T_INIT,TI,BB,TF
1 ,TAVE,TI_NOW,LENGTH_TUBE,TAVE_NOW,TAVE_IN,TAVE_INIT,
1 EFFICIENCY_STEP, CUMUL_Q_DEL,CUMUL_Q_GAS,EFFICIENCY_CUMUL,
      1 I_CONVERGED,DELTA_TEMP_EST,TOL,ITER,ITER_MAX,TSS,TSS_OLD,
      1 Q_NEEDED_SS,CONTROL_SS,Q_SS,R_FLUID,K_FLUID,R_PIPE,K_PIPE,
      1 CONDUCTION_KA,PI,TI_SS,TF_OLD,ITER_TIME,TOL_TIME,DELTA_TFN,
      1
DERIV_TFN,B_SINGLE,A_SINGLE,TAVE_SS,DELT_SS,TIME_REMAINING,TEST,
      1 CONTROL_OLD,FLOW_OLD,UPDATE_DELAY,DELT_STEADY
      INTEGER I,J,N_STEPS,A,NUMBER_NODE,Q_DEL_NOW,ARB,TAVE_OLD
      LOGICAL FOUND_END
      DATA SMALL/1.D-08/

```

C DECLARING ARRAYS

```

DIMENSION T_INIT(INFO(4)-20),TI(INFO(4)-20),BB(INFO(4)-20),

```

```
1 TF(INFO(4)-20),TI_NOW(INFO(4)-20),TAVE(INFO(4)-19),
1 TAVE_IN(INFO(4)-20),TSS(INFO(4)-20),TSS_OLD(INFO(4)-20),
  1 TI_SS(INFO(4)-20),TF_OLD(INFO(4)-20),TAVE_SS(INFO(4)-19)
```

```
C-----
```

```
----
```

```
C-----
```

```
----
```

```
C GET GLOBAL TRNSYS SIMULATION VARIABLES
```

```
  TIME0=getSimulationStartTime()
```

```
  TFINAL=getSimulationStopTime()
```

```
  DELT=getSimulationTimeStep()
```

```
C-----
```

```
----
```

```
C-----
```

```
----
```

```
C SET THE VERSION INFORMATION FOR TRNSYS
```

```
  IF(INFO(7).EQ.-2) THEN
```

```
    INFO(12)=16
```

```
    RETURN 1
```

```
  ENDIF
```

C-----

C-----

C DO ALL THE VERY LAST CALL OF THE SIMULATION MANIPULATIONS HERE

IF (INFO(8).EQ.-1) THEN

RETURN 1

ENDIF

C-----

C-----

C PERFORM ANY "AFTER-ITERATION" MANIPULATIONS THAT ARE REQUIRED

IF(INFO(13).GT.0) THEN

CALL getStorageVars(STORED,NSTORED,INFO)

STORED(NUMBER_NODE+7)=TAVE_I

STORED(NUMBER_NODE+9)=TAVE_INIT

STORED(NUMBER_NODE+2)=STORED(NUMBER_NODE+3)

STORED(NUMBER_NODE+4)=STORED(NUMBER_NODE+5)

CALL SetStorageVars(STORED,NSTORED,INFO)

RETURN 1

ENDIF

C-----

C-----

C DO ALL THE VERY FIRST CALL OF THE SIMULATION MANIPULATIONS HERE

IF (INFO(7).EQ.-1) THEN

C RETRIEVE THE UNIT NUMBER AND TYPE NUMBER FOR THIS COMPONENT
FROM THE INFO ARRAY

IUNIT=INFO(1)

ITYPE=INFO(2)

C SET THE NUMBER OF PARAMETERS (NP) AND DERIVATIVES (ND) BASED ON
INFORMATION PASSED FROM THE TYPE

NP = INFO(4)

ND = INFO(5)

C SET SOME INFO ARRAY VARIABLES TO TELL THE TRNSYS ENGINE HOW THIS
TYPE IS TO WORK

INFO(6)=NOUT

INFO(9)=1

INFO(10)=0

C CALL THE TYPE CHECK SUBROUTINE TO COMPARE WHAT THIS COMPONENT
REQUIRES TO WHAT IS SUPPLIED IN THE TRNSYS INPUT FILE

IF ((ND.LT.0).OR.(ND.GT.10)) CALL TYPECK(5,INFO,0,0,0)

IF ((NP.LE.1).OR.(NP.GT.100)) CALL TYPECK(4,INFO,0,0,0)

C SET THE YCHECK AND OCHECK ARRAYS TO CONTAIN THE CORRECT
VARIABLE TYPES FOR THE INPUTS AND OUTPUTS

DATA YCHECK/'TE1','MF1','TE1','TE1','HT1','PW1'/

DATA OCHECK/'TE1','MF1','PW1','PW1','PW1','PW1','PW1','DM1',

1 'PW1','TE1','TE1','TE1','TE1','TE1','TE1','TE1',
1 'TE1','TE1','TE1','TE1','TE1','TE1','TE1','TE1',
1 'TE1','TE1','TE1','TE1','TE1','TE1','TE1','TE1',
1 'TE1','TE1','TE1','TE1','TE1','TE1','TE1','TE1',
1 'TE1','TE1','TE1','TE1','TE1','TE1','TE1','TE1',
1 'TE1','TE1','TE1','TE1','TE1','TE1','TE1','TE1',
1 'TE1','TE1','TE1','TE1','TE1','TE1','TE1','TE1',
1 'TE1','TE1','TE1','TE1','TE1','TE1','TE1','TE1',

```
1          'TE1','TE1','TE1','TE1','TE1','TE1','TE1','TE1',
1          'TE1','TE1','TE1','TE1','TE1','TE1','TE1','TE1',
1          'TE1','TE1','TE1','TE1'/
```

C CALL THE RCHECK SUBROUTINE TO SET THE CORRECT INPUT AND OUTPUT
TYPES FOR THIS COMPONENT

```
CALL RCHECK(INFO,YCHECK,OCHECK)
```

C SET THE NUMBER OF STORAGE SPOTS NEEDED FOR THIS COMPONENT

```
CALL SetStorageSize(NSTOREDMAX,INFO)
```

C RETURN TO THE CALLING PROGRAM

```
RETURN 1
```

```
ENDIF
```

C-----

C-----

C DO ALL OF THE INITIAL TIMESTEP MANIPULATIONS HERE - THERE ARE NO
ITERATIONS AT THE INTIAL TIME

```
IF (TIME.LT.(TIME0+DELT/2.D0)) THEN
```

C SET THE UNIT NUMBER FOR FUTURE CALLS

IUNIT=INFO(1)

C CREATE A NEW VARIABLE DECLARING THE NUMBER OF NODES IN THE
SIMULATION

C THE NUMBER 14 REPRESENTS THE NUMBER OF PARAMETERS WHICH
EXIST REGARDLESS OF THE NUMBER OF NODES

NUMBER_NODE = INFO(4)-20

C READ IN THE VALUES OF THE PARAMETERS IN SEQUENTIAL ORDER

CAPACITANCE=PAR(1)

DO I=1,NUMBER_NODE

T_INIT(I)=PAR(I+1)

ENDDO

FLOW_MIN=PAR(NUMBER_NODE+2)

EFF_GAS=PAR(NUMBER_NODE+3)

Q_RATED=PAR(NUMBER_NODE+4)

AREA=PAR(NUMBER_NODE+5)

IF(PAR(NUMBER_NODE+6).LT.0) THEN

```
N_STEPS=-1  
ELSE  
N_STEPS=JFIX(PAR(NUMBER_NODE+6)+0.5)  
ENDIF
```

```
DEADBAND=PAR(NUMBER_NODE+7)  
CONTROL_MIN=PAR(NUMBER_NODE+8)  
EFF_PILOT=PAR(NUMBER_NODE+9)  
Q_PILOT=PAR(NUMBER_NODE+10)  
CP_FLUID=PAR(NUMBER_NODE+11)  
TIME_DELAY=PAR(NUMBER_NODE+12)  
P_ELEC_STANDBY=PAR(NUMBER_NODE+13)  
P_ELEC_HEATING=PAR(NUMBER_NODE+14)  
LENGTH_TUBE = PAR(NUMBER_NODE+15)  
R_PIPE = PAR(NUMBER_NODE+16)  
R_FLUID = PAR(NUMBER_NODE+17)  
K_FLUID = PAR(NUMBER_NODE+18)  
K_PIPE = PAR(NUMBER_NODE+19)  
UPDATE_DELAY=PAR(NUMBER_NODE+20)
```

```
C    CHECK THE PARAMETERS FOR PROBLEMS AND RETURN FROM THE  
SUBROUTINE IF AN ERROR IS FOUND
```

```
IF(CAPACITANCE.LE.0.) CALL TYPECK(-4,INFO,0,1,0)
```

```

IF(FLOW_MIN.LT.0.) CALL TYPECK(-4,INFO,0,3,0)
IF(EFF_GAS.LE.0.) CALL TYPECK(-4,INFO,0,4,0)
IF(EFF_GAS.GT.1.) CALL TYPECK(-4,INFO,0,4,0)
IF(Q_RATED.LE.0.) CALL TYPECK(-4,INFO,0,5,0)
IF(AREA.LT.0.) CALL TYPECK(-4,INFO,0,6,0)
IF(DEADBAND.LE.0.) CALL TYPECK(-4,INFO,0,8,0)
IF(CONTROL_MIN.LT.0.) CALL TYPECK(-4,INFO,0,9,0)
IF(CONTROL_MIN.GT.1.) CALL TYPECK(-4,INFO,0,9,0)
IF(EFF_PILOT.LE.0.) CALL TYPECK(-4,INFO,0,10,0)
IF(EFF_PILOT.GT.1.) CALL TYPECK(-4,INFO,0,10,0)
IF(Q_PILOT.LT.0.) CALL TYPECK(-4,INFO,0,11,0)
IF(CP_FLUID.LE.0.) CALL TYPECK(-4,INFO,0,12,0)
IF(TIME_DELAY.LT.0.) CALL TYPECK(-4,INFO,0,13,0)
IF(P_ELEC_STANDBY.LT.0.) CALL TYPECK(-4,INFO,0,14,0)
IF(P_ELEC_HEATING.LT.0.) CALL TYPECK(-4,INFO,0,15,0)

```

C CALCULATIONS AND DECLARATIONS IMPACTING INITIAL STORED VALUES

```

DO I=1,NUMBER_NODE
  TI_NOW(I)=T_INIT(I)
  STORED(I+1)=T_INIT(I)
  TAVE_I = TAVE_I + T_INIT(I)/NUMBER_NODE
  TAVE_INIT = TAVE_INIT+T_INIT(I)/NUMBER_NODE
  TF(I)=TI_NOW(I)

```

TAVE(I)=TI_NOW(I)

ENDDO

CUMUL_Q_DEL=0

CUMUL_Q_GAS=0

PI=3.1415926

CONDUCTION_KA = PI*R_FLUID*R_FLUID*K_FLUID+(PI*R_PIPE*R_PIPE-PI
1 *R_FLUID*R_FLUID)*K_PIPE

C PERFORM ANY REQUIRED CALCULATIONS TO SET THE INITIAL VALUES OF
THE OUTPUTS HERE

C OUT(1)=T_INIT(NUMBER_NODE)

OUT(2)=0.

OUT(3:9)=0.

C PERFORM ANY REQUIRED CALCULATIONS TO SET THE INITIAL STORAGE
VARIABLES HERE

STORED(NUMBER_NODE+7)=TAVE_I

STORED(NUMBER_NODE+9)=TAVE_INIT

STORED(NUMBER_NODE+10)=CUMUL_Q_DEL

STORED(NUMBER_NODE+11)=CUMUL_Q_GAS

C PUT THE STORED ARRAY IN THE GLOBAL STORED ARRAY

```
CALL SetStorageVars(STORED,NSTORED,INFO)
```

```
C RETURN TO THE CALLING PROGRAM
```

```
RETURN 1
```

```
ENDIF
```

```
C-----
```

```
----
```

```
C-----
```

```
----
```

```
C *** ITS AN ITERATIVE CALL TO THIS COMPONENT ***
```

```
C-----
```

```
----
```

```
C-----
```

```
----
```

```
C RE-READ THE PARAMETERS IF ANOTHER UNIT OF THIS TYPE HAS BEEN  
CALLED
```

```
IF(INFO(1).NE.IUNIT) THEN
```

```
C RESET THE UNIT NUMBER
```

```
IUNIT=INFO(1)
```

ITYPE=INFO(2)

C READ IN THE VALUES OF THE PARAMETERS IN SEQUENTIAL ORDER

CAPACITANCE=PAR(1)

DO I=1,NUMBER_NODE

T_INIT(I)=PAR(I+1)

TAVE_INIT = TAVE_INIT+T_INIT(I)/NUMBER_NODE

ENDDO

FLOW_MIN=PAR(NUMBER_NODE+2)

EFF_GAS=PAR(NUMBER_NODE+3)

Q_RATED=PAR(NUMBER_NODE+4)

AREA=PAR(NUMBER_NODE+5)

IF(PAR(7).LT.0) THEN

N_STEPS=-1

ELSE

N_STEPS=JFIX(PAR(NUMBER_NODE+6)+0.5)

ENDIF

DEADBAND=PAR(NUMBER_NODE+7)

CONTROL_MIN=PAR(NUMBER_NODE+8)

```
EFF_PILOT=PAR(NUMBER_NODE+9)
Q_PILOT=PAR(NUMBER_NODE+10)
CP_FLUID=PAR(NUMBER_NODE+11)
TIME_DELAY=PAR(NUMBER_NODE+12)
P_ELEC_STANDBY=PAR(NUMBER_NODE+13)
P_ELEC_HEATING=PAR(NUMBER_NODE+14)
```

```
ENDIF
```

```
C-----
----
```

```
C-----
----
```

```
C  RETRIEVE THE CURRENT VALUES OF THE INPUTS TO THIS MODEL FROM THE
XIN ARRAY IN SEQUENTIAL ORDER
```

```
T_FLUID_IN=XIN(1)
```

```
FLOW_FLUID=XIN(2)
```

```
T_ENV=XIN(3)
```

```
T_SET=XIN(4)
```

```
U_VALUE=XIN(5)
```

```
Q_INPUT=XIN(6)
```

```
IF(FLOW_FLUID.LT.0.) CALL TYPECK(-3,INFO,2,0,0)
```

IF (ERRORFOUND()) RETURN 1

C-----

C-----

C RETRIEVE THE VALUES IN THE STORAGE ARRAY FOR THIS ITERATION

CALL GetStorageVars(STORED,NSTORED,INFO)

DO I=1,NUMBER_NODE

TI(I)=STORED(I+1)

TAVE(I)=STORED(NUMBER_NODE+I+13)

ENDDO

CONTROL_LAST=STORED(NUMBER_NODE+3)

TIME_ON=STORED(NUMBER_NODE+5)

TAVE_I=STORED(NUMBER_NODE+7)

TAVE_INIT=STORED(NUMBER_NODE+9)

CUMUL_Q_DEL=STORED(NUMBER_NODE+10)

CUMUL_Q_GAS=STORED(NUMBER_NODE+11)

CONTROL_OLD=STORED(NUMBER_NODE+12)

FLOW_OLD=STORED(NUMBER_NODE+13)

TAVE_OLD=STORED(NUMBER_NODE+15)

C-----

C-----

C PERFORM ALL THE CALCULATION HERE FOR THIS MODEL.

C SET CONSTANTS USED FOR ITERATION

TOL=0.000001

TOL_TIME=0.000001

ITER_MAX=1000

C RESET THE TOTALS

Q_COMBUSTED_TOT=0.

Q_GAS_TOT=0.

P_ELEC_TOT=0.

Q_DEL_TOT=0

TAVE_NOW=0

TAVE_TOT=0

ITER_TIME=0

C TEMPORARY FOR THE SAKE OF TESTING

```

IF(DELT_STEADY.GE.UPDATE_DELAY) THEN
    P_ELEC_TOT=0
ENDIF

IF (T_SET.GT.T_FLUID_IN) THEN
    FLOW_FLUID=DMIN1(FLOW_FLUID,(Q_RATED*EFF_GAS-
U_VALUE*AREA*(TAVE
1 _OLD-T_ENV))/(CP_FLUID*(T_SET-T_FLUID_IN)))
ENDIF

IF (DABS(FLOW_FLUID-FLOW_OLD).GT.0.1) THEN
    DELT_STEADY=0
ENDIF

C    SET INITIAL VALUES OF SOME CONSTANTS
    TIME_REMAINING=DELT
    TAVE_SS(NUMBER_NODE+1)=T_SET
    TAVE(NUMBER_NODE+1)=T_SET

    DO I=1, NUMBER_NODE
        TI_NOW(I)=TI(I)
    ENDDO

```

C SEE IF THE DEVICE SHOULD BE OPERATING THIS TIMESTEP

IF(N_STEPS.LT.0) THEN

C SET UP THE GOVERNING DIFFERENTIAL EQUATION IN THE FORM

DT/DT=AT+B

DELT_NOW=DELT

EFFICIENCY=EFF_GAS

Q_COMBUSTED_TOT=DMIN1(Q_RATED,Q_INPUT)*EFFICIENCY

CONTROL_AVE=Q_COMBUSTED_TOT/(Q_RATED*EFFICIENCY)

DO I=1,NUMBER_NODE

IF(I.EQ.1.)THEN

TAVE_IN(I) = T_FLUID_IN

ELSE

TAVE_IN(I) = TAVE(I-1)

ENDIF

AA=-((FLOW_FLUID*CP_FLUID*NUMBER_NODE+U_VALUE*AREA)/

1 CAPACITANCE

BB(I)=(Q_COMBUSTED+FLOW_FLUID*CP_FLUID*NUMBER_NODE*TAVE_IN(I)+

1 U_VALUE*AREA*T_ENV)/CAPACITANCE

```

C      SOLVE THE DIFFEQ ANALYTICALLY

      IF(AA.EQ.0.) THEN

          TF(I) = TI_NOW(I) + BB(I) * DELT_NOW

          TAVE(I) = TI_NOW(I) + BB(I) * DELT_NOW / 2

      ELSE

          TF(I)=TI_NOW(I)*(DEXP(AA*DELT_NOW))+BB(I)/AA*
1      (DEXP(AA*DELT_NOW))-BB(I)/AA

          TAVE(I)=1./AA/DELT_NOW*(TI_NOW(I)+BB(I)/AA)*((DEXP(AA *
1      DELT_NOW))-1.) - BB(I) / AA

      ENDIF

C      CALCULATE THE ELECTRICAL CONSUMPTION

      IF(CONTROL_NOW.LE.0.) THEN

          P_ELEC_TOT=P_ELEC_STANDBY

      ELSE

          P_ELEC_TOT=P_ELEC_HEATING

      ENDIF

C      CALCULATE THE AVERAGE TEMPERATURE OF THE HX AT THE END OF THE
TIMESTEP

          TAVE_NOW=TAVE_NOW + TAVE(I) / NUMBER_NODE

      ENDDO

```

```

C      CALCULATE THE ENERGY FLOWS

      Q_SKIN_TOT=U_VALUE*AREA*(TAVE_NOW-T_ENV)

      Q_DEL_TOT=FLOW_FLUID*CP_FLUID*(TF(NUMBER_NODE)-
T_FLUID_IN)*DELT

      Q_STORED=CAPACITANCE*(TAVE_NOW-TAVE_INIT)

      TAVE_TOT=TAVE_TOT+TAVE_NOW*DELT_NOW/DELT

ELSE IF(FLOW_FLUID.LE.FLOW_MIN) THEN

      CONTROL_NOW=-1.

      Q_COMBUSTED=Q_PILOT*EFF_PILOT

      Q_GAS_TOT=Q_PILOT

      P_ELEC_TOT=P_ELEC_STANDBY

15     CONTINUE

      I_CONVERGED=1

      TAVE_NOW=0

      DO I = 1,NUMBER_NODE

      IF(I.EQ.1.)THEN

          TAVE_IN(I) = T_FLUID_IN

```

```

ELSE
    TAVE_IN(I) = TAVE(I-1)
ENDIF

C    RUN FOR THE FULL TIMESTEP

DELT_NOW=DELT

C    SET UP THE GOVERNING DIFFERENTIAL EQUATION IN THE FORM
DT/DT=AT+B

BB(I)=(Q_COMBUSTED+FLOW_FLUID*CP_FLUID*NUMBER_NODE*TAV
1    E_IN(I)+U_VALUE*AREA*T_ENV+CONDUCTION_KA*NUMBER_NOD
1        E*(NUMBER_NODE-1)/LENGTH_TUBE*(TAVE(I+1)+TAVE_IN(I)
1        ))/CAPACITANCE

AA=-((1/CAPACITANCE)*(FLOW_FLUID*CP_FLUID*NUMBER_NODE+U
1
_VALUE*AREA+2*CONDUCTION_KA*NUMBER_NODE*(NUMBER_NOD
1    E-1)/LENGTH_TUBE)

C    ENTER TF_OLD VALUES FOR CONVERGENCE CHECK

TF_OLD(I)=TF(I)

C    SOLVE THE DIFFEQ ANALYTICALLY

IF(AA.EQ.0.) THEN

```

TF(I) = TI_NOW(I)+BB(I) * DELT_NOW

TAVE(I) = TI_NOW(I)+BB(I) * DELT_NOW/2.

ELSE

TF(I)=TI_NOW(I)*(DEXP(AA*DELT_NOW))+BB(I)/AA*(DEXP(AA

1 * DELT_NOW)) - BB(I) / AA

TAVE(I)=1./AA/DELT_NOW*(TI_NOW(I)+BB(I)/AA)*

1 ((DEXP(AA*DELT_NOW))-1.)-BB(I)/AA

ENDIF

TAVE(NUMBER_NODE+1)=TAVE(NUMBER_NODE)

C CALCULATE THE AVERAGE TEMPERATURE OF THE HX AT THE END OF THE
TIMESTEP

TAVE_NOW=TAVE_NOW+TF(I)/NUMBER_NODE

IF(DABS(TF(I)-TF_OLD(I)).GT.TOL) THEN

I_CONVERGED=0

ENDIF

ENDDO

IF (I_CONVERGED.EQ.0) THEN

GOTO 15

ENDIF

C CALCULATE THE ENERGY FLOWS

Q_SKIN_TOT=U_VALUE*AREA*(TAVE_NOW-T_ENV)

Q_DEL_TOT=FLOW_FLUID*CP_FLUID*(TF(NUMBER_NODE)-T_FLUID_IN)

Q_STORED=CAPACITANCE*(TAVE_NOW-TAVE_INIT)

TAVE_TOT=TAVE_TOT+TAVE_NOW*DELT_NOW/DELT

C UPDATE THE COUNTER OF HOW LONG THE DEVICE HAS BEEN RUNNING

TIME_ON=0.

CONTROL_AVE=0.

ELSE IF(N_STEPS.GT.0) THEN

C SEE HOW THE DEVICE SHOULD BE CONTROLLED AT THE BEGINNING OF THE
TIMESTEP

IF(CONTROL_LAST.GE.0.) THEN

IF(TI(NUMBER_NODE).LT.(T_SET-DEADBAND-SMALL)) THEN

CONTROL_NOW=1.

ELSE IF(TI(NUMBER_NODE).LE.T_SET) THEN

CONTROL_NOW=CONTROL_LAST

ELSE

CONTROL_NOW=0.

ENDIF

ELSE

IF(TI(NUMBER_NODE).LE.(T_SET-DEADBAND-SMALL)) THEN

CONTROL_NOW=1.

ELSE IF(TI(NUMBER_NODE).LE.T_SET) THEN

C CALCULATE THE NEW CONTROL SIGNAL BASED ON A STEADY STATE
APPROACH

Q_COMBUSTED_NEEDED=FLOW_FLUID*CP_FLUID*(T_SET-T_FLUID_IN)

1 +U_VALUE*AREA*(TAVE_NOW-T_ENV)

CONTROL_NOW=Q_COMBUSTED_NEEDED/(Q_RATED*EFFICIENCY)

I=0

DO J=1,N_STEPS

IF(DBLE(J)/DBLE(N_STEPS).LE.CONTROL_NOW) I=J

ENDDO

CONTROL_NOW=DBLE(I+1)/DBLE(N_STEPS)

CONTROL_NOW=DMIN1(1.,CONTROL_NOW)

CONTROL_NOW=DMAX1(CONTROL_MIN,CONTROL_NOW)

ELSE

CONTROL_NOW=0.

ENDIF

ENDIF

C INITIALIZE A FEW VARIABLES

DELT_NOW=DELT

FOUND_END=.FALSE.

DELT_TOT=0.

CONTROL_AVE=0

C RETURN HERE EACH TIME

30 CONTINUE

C THE WATER HEATER IS ON

IF((CONTROL_NOW.GT.0.).AND.(TIME_ON.LT.TIME_DELAY)) THEN

C SEE IF THE MANDATORY DELAY TIME PUSHES US OUT OF THE TIMESTEP

IF((TIME_DELAY-TIME_ON).GE.DELT_NOW) THEN

FOUND_END=.TRUE.

ELSE

DELT_NOW=DMIN1(DELT_NOW,(TIME_DELAY-TIME_ON))

FOUND_END=.FALSE.

ENDIF

```
EFFICIENCY=EFF_PILOT
Q_COMBUSTED=Q_PILOT*EFF_PILOT
```

```
DO I = 1,NUMBER_NODE
```

```
IF(I.EQ.1.)THEN
    TAVE_IN = T_FLUID_IN
ELSE
    TAVE_IN = TAVE(I-1)
ENDIF
```

```
C    SET UP THE GOVERNING DIFFERENTIAL EQUATION IN THE FORM
```

```
DT/DT=AT+B
```

```
AA=-(FLOW_FLUID*CP_FLUID*NUMBER_NODE+U_VALUE*AREA)/
```

```
1    CAPACITANCE
```

```
BB(I)=(Q_COMBUSTED+FLOW_FLUID*CP_FLUID*NUMBER_NODE*TAVE_IN(I)
```

```
1    +U_VALUE*AREA*T_ENV)/CAPACITANCE
```

```
C    SOLVE THE DIFFEQ ANALYTICALLY
```

```
IF(AA.EQ.0.) THEN
```

```
    TF(I)=TI_NOW(I)+BB(I)*DELT_NOW
```

```
    TAVE(I)=TI_NOW(I)+BB(I)*DELT_NOW/2.
```

ELSE

```
TF(I)=TI_NOW(I)*(DEXP(AA*DELT_NOW))+BB(I)/AA*(DEXP(
1 AA*DELT_NOW))-BB(I)/AA
TAVE(I)=1./AA/DELT_NOW*(TI_NOW(I)+BB(I)/AA)*((DEXP(AA
1 *DELT_NOW))-1.))-BB(I)/AA
ENDIF
```

C UPDATE THE TIME_ON COUNTER

```
TIME_ON=TIME_ON+DELT_NOW
```

C SET THE CONTROL AT THE NEXT TIME

```
CONTROL_NEXT=CONTROL_NOW
```

ENDDO

```
Q_DEL_NOW=FLOW_FLUID*CP_FLUID*(TAVE(NUMBER_NODE)-T_FLUID_IN)
```

C THE WATER HEATER IS ON

```
ELSE IF(CONTROL_NOW.GT.0.) THEN
```

C RUN FOR THE FULL TIMESTEP AT THE CURRENT SETTINGS AND SEE WHAT
HAPPENS

C GET THE EFFICIENCY OF THE DEVICE (MAY BE EXPANDED LATER TO BE A
FILE LOOK-UP ETC)

EFFICIENCY=EFF_GAS

C GET THE HEAT INPUT TO THE FLUID

Q_COMBUSTED=EFFICIENCY*CONTROL_NOW*Q_RATED

DO A = 1, NUMBER_NODE

IF (A.EQ.1.) THEN

TAVE_IN(A) = T_FLUID_IN

ELSE

TAVE_IN(A) = TAVE(A-1)

ENDIF

C SET UP THE GOVERNING DIFFERENTIAL EQUATION IN THE FORM

DT/DT=AT+B

BB(A)=(Q_COMBUSTED+FLOW_FLUID*CP_FLUID*NUMBER_NODE*TAVE_IN(A)

1 +U_VALUE*AREA*T_ENV)/CAPACITANCE

AA=-((FLOW_FLUID*CP_FLUID*NUMBER_NODE+U_VALUE*AREA)/

1 CAPACITANCE

C SOLVE THE DIFFEQ ANALYTICALLY

IF(AA.EQ.0.) THEN

TF(A) = TI_NOW(A) + BB(A) * DELT_NOW

TAVE(A) = TI_NOW(A) + BB(A) * DELT_NOW/2.

ELSE

TF(A)=TI_NOW(A)*(DEXP(AA*DELT_NOW))+BB(A)/AA*

1 (DEXP(AA * DELT_NOW)) - BB(A) / AA

TAVE(A) = 1./AA/DELT_NOW*(TI_NOW(A)+BB(A)/AA)*

1 ((DEXP(AA*DELT_NOW))-1.)-BB(A)/AA

ENDIF

C CHECK THE RESULTANT TEMPERATURE

IF((TF(NUMBER_NODE).LE.T_SET).AND.(CONTROL_NOW.GE.1.))THEN

DELT_NOW=DELT_NOW

CONTROL_NEXT=CONTROL_NOW

FOUND_END=.TRUE.

Q_DEL_NOW=FLOW_FLUID*CP_FLUID*(TAVE(NUMBER_NODE)-

1 T_FLUID_IN)

ELSE IF((TF(NUMBER_NODE).LE.T_SET).AND.(TF(NUMBER_NODE).GE.(

1 T_SET-DEADBAND))) THEN

```

DELT_NOW=DELT_NOW

CONTROL_NEXT=CONTROL_NOW

FOUND_END=.TRUE.

Q_DEL_NOW=FLOW_FLUID*CP_FLUID*(TAVE(NUMBER_NODE)-
1          T_FLUID_IN)

ELSE IF(TF(NUMBER_NODE).LE.(T_SET-DEADBAND)) THEN

    FOUND_END=.FALSE.

C    CALCULATE THE TIME TO GET DOWN TO THE SETPOINT-DEADBAND
TF(NUMBER_NODE)=T_SET-DEADBAND
IF(AA.EQ.0.) THEN
    DELT_NOW=DMIN1(DELT_NOW,((TF(NUMBER_NODE)-TF(A-1))/
1          BB(A)))
IF(DELT_NOW.LE.0.) THEN
    DELT_NOW=0.
    TF(A)=TF(A-1)
    TAVE(A)=TF(A-1)
ELSE
    TF(A)=TI_NOW(A)+BB(A)*DELT_NOW
    TAVE(A)=TI_NOW(A)+BB(A)*DELT_NOW/2.
ENDIF
ELSE

```

```

DELT_NOW=DMIN1(DELT_NOW,(DLOG((TF(A)+BB(A)/AA)/(
1      TI_NOW(A) + BB(A)/AA))/AA))
IF(DELT_NOW.LE.0.) THEN
    DELT_NOW=0.
    TF(A)=TF(A-1)
    TAVE(A)=TF(A-1)
ELSE
    TF(A)=TI_NOW(A)*(DEXP(AA*DELT_NOW))+BB(A)/AA*
1      (DEXP(AA*DELT_NOW))-BB(A)/AA
    TAVE(A)=1./AA/DELT_NOW*(TI_NOW(A)+BB(A)/AA)*
1      (DEXP(AA*DELT_NOW))-1.)-BB(A)/AA
ENDIF
ENDIF

```

$Q_DEL_NOW=FLOW_FLUID*CP_FLUID*(TAVE(NUMBER_NODE)-T_FLUID_IN)$

C CALCULATE THE NEW CONTROL SIGNAL BASED ON A STEADY STATE
APPROACH

$Q_COMBUSTED_NEEDED=FLOW_FLUID*CP_FLUID*(T_SET-T_FLUID_IN)$

1 $+U_VALUE*AREA*(TAVE_NOW-T_ENV)$

$CONTROL_NEXT=Q_COMBUSTED_NEEDED/(Q_RATED*EFFICIENCY)$

```

I=0
DO J=1,N_STEPS
  IF(DBLE(J)/DBLE(N_STEPS).LE.CONTROL_NEXT) I=J
ENDDO

CONTROL_NEXT=DBLE(I+1)/DBLE(N_STEPS)
CONTROL_NEXT=DMIN1(1.,CONTROL_NEXT)
CONTROL_NEXT=DMAX1(CONTROL_MIN,CONTROL_NEXT)

```

```

ELSE IF(TF(NUMBER_NODE).GT.(T_SET+SMALL)) THEN

```

```

C   CALCULATE THE TIME TO GET TO THE SETPOINT

```

```

TF(NUMBER_NODE)=T_SET

```

```

IF(AA.EQ.0.) THEN

```

```

  DELT_NOW=DMIN1(DELT_NOW,((TF(NUMBER_NODE)-
TI_NOW(NUMBER_NODE))/

```

```

1      BB(NUMBER_NODE)))

```

```

IF(DELT_NOW.LE.0.) THEN

```

```

  DELT_NOW=0.

```

```

  DO I = 1, NUMBER_NODE

```

```

    TF(I)=TI_NOW(I)

```

```

    TAVE(I)=TI_NOW(I)

```

```

  ENDDO

```

```

ELSE
    DO I = 1, NUMBER_NODE
        TF(I)=TI_NOW(I)+BB(I)*DELT_NOW
        TAVE(I)=TI_NOW(I)+BB(I)*DELT_NOW/2.
    ENDDO
ENDIF
ELSE
    DELT_NOW=DMIN1(DELT_NOW,(DLOG((TF(NUMBER_NODE)+BB(
1    NUMBER_NODE)/AA)/(TF(NUMBER_NODE-
1)+BB(NUMBER_NODE)/AA
1    ))/AA))
    IF(DELT_NOW.LE.0.) THEN
        DELT_NOW=0.
        DO I = 1, NUMBER_NODE
            TF(I)=TI_NOW(I)
            TAVE(I)=TI_NOW(I)
        ENDDO
    ELSE
        DO I = 1, NUMBER_NODE
            TF(I)=TI_NOW(I)*(DEXP(AA*DELT_NOW))+BB(I)/AA*(DEXP(
1    AA*DELT_NOW))-BB(I)/AA
            TAVE(I)=1./AA/DELT_NOW*(TI_NOW(I)+BB(I)/AA)*((DEXP(
1    AA*DELT_NOW))-1.)-BB(I)/AA

```

```

                ENDDO

            ENDIF

        ENDIF

        Q_DEL_NOW=FLOW_FLUID*CP_FLUID*(TAVE(NUMBER_NODE)-T_FLUID_IN)

C      CALCULATE THE NEW CONTROL SIGNAL BASED ON A STEADY STATE
APPROACH

        Q_COMBUSTED_NEEDED=FLOW_FLUID*CP_FLUID*(T_SET-T_FLUID_IN)
1      +U_VALUE*AREA*(TAVE_NOW-T_ENV)

        CONTROL_NEXT=Q_COMBUSTED_NEEDED/(Q_RATED*EFFICIENCY)

        I=0

        DO J=1,N_STEPS

            IF(DBLE(J)/DBLE(N_STEPS).LE.CONTROL_NEXT) I=J

        ENDDO

        CONTROL_NEXT=DBLE(I)/DBLE(N_STEPS)

        CONTROL_NEXT=DMIN1(1.,CONTROL_NEXT)

        IF(CONTROL_NEXT.LT.CONTROL_MIN) CONTROL_NEXT=0.

        ELSE

        CALL TYPECK(-1,INFO,0,0,0)

        ENDIF

```

```

        ENDDO

C      UPDATE THE TIME_ON COUNTER
      TIME_ON=TIME_ON+DELT_NOW

      ELSE

C      SET UP THE GOVERNING DIFFERENTIAL EQUATION IN THE FORM
DT/DT=AT+B

      EFFICIENCY=EFF_PILOT

      Q_COMBUSTED=Q_PILOT*EFF_PILOT

      DO I = 1, NUMBER_NODE
        IF (I.EQ.1) THEN
          TAVE_IN(I) = T_FLUID_IN
        ELSE
          TAVE_IN(I) = TAVE(I-1)
        ENDIF

      BB(I)=(Q_COMBUSTED+FLOW_FLUID*CP_FLUID*NUMBER_NODE*TAVE_IN(I)
1      +U_VALUE*AREA*T_ENV)/CAPACITANCE

      AA=-((FLOW_FLUID*CP_FLUID*NUMBER_NODE+U_VALUE*AREA)/
1      CAPACITANCE

C      SOLVE THE DIFFEQ ANALYTICALLY

```

IF(AA.EQ.0.) THEN

TF(I)=TI_NOW(I)+BB(I)*DELT_NOW

TAVE(I)=TI_NOW(I)+BB(I)*DELT_NOW/2.

ELSE

TF(I)=TI_NOW(I)*(DEXP(AA*DELT_NOW))+BB(I)/AA*(DEXP(AA
1 *DELT_NOW))-BB(I)/AA

TAVE(I)=1./AA/DELT_NOW*(TI_NOW(I)+BB(I)/AA)*((DEXP(AA
1 *DELT_NOW))-1.))-BB(I)/AA

ENDIF

ENDDO

C CHECK THE RESULTANT TEMPERATURE

IF(TF(NUMBER_NODE).GE.T_SET) THEN

DELT_NOW=DELT_NOW

CONTROL_NEXT=0.

FOUND_END=.TRUE.

Q_DEL_NOW=FLOW_FLUID*CP_FLUID*(TAVE(NUMBER_NODE)-
1 T_FLUID_IN)

ELSE

C CALCULATE THE TIME TO GET DOWN TO THE SETPOINT

TF(NUMBER_NODE)=T_SET-DEADBAND

IF(AA.EQ.0.) THEN

DELT_NOW=(TF(NUMBER_NODE)-TF(NUMBER_NODE-1))/BB(

1 NUMBER_NODE)

IF(DELT_NOW.LE.0.) THEN

DELT_NOW=DELT-DELT_TOT

CONTROL_NEXT=0.

FOUND_END=.TRUE.

ELSE IF(DELT_NOW.GE.(DELT-DELT_TOT)) THEN

DELT_NOW=DELT-DELT_TOT

CONTROL_NEXT=0.

FOUND_END=.TRUE.

ELSE

C CALCULATE THE NEW CONTROL SIGNAL BASED ON A STEADY STATE
APPROACH

Q_COMBUSTED_NEEDED=FLOW_FLUID*CP_FLUID*

1 (T_SET-T_FLUID_IN)+U_VALUE*AREA*(TAVE_NOW-T_ENV)

CONTROL_NEXT=Q_COMBUSTED_NEEDED/(Q_RATED*EFFICIENCY)

I=0

DO J=1,N_STEPS

IF(DBLE(J)/DBLE(N_STEPS).LE.CONTROL_NEXT) I=J

```

        ENDDO

CONTROL_NEXT=DBLE(I+1)/DBLE(N_STEPS)

CONTROL_NEXT=DMIN1(1.,CONTROL_NEXT)

CONTROL_NEXT=DMAX1(CONTROL_MIN,CONTROL_NEXT)

        ENDIF

DO I = 1, NUMBER_NODE

        TF(I)=TI_NOW(I)+BB(I)*DELT_NOW

        TAVE(I)=TI_NOW(I)+BB(I)*DELT_NOW/2.

ENDDO

ELSE

DELT_NOW=DLOG((TF(NUMBER_NODE)+BB(NUMBER_NODE)/AA)/(
1      TI_NOW(NUMBER_NODE)+BB(NUMBER_NODE)/AA))/AA

IF(DELT_NOW.LE.0.) THEN

        DELT_NOW=DELT-DELT_TOT

CONTROL_NEXT=0.

FOUND_END=.TRUE.

ELSE IF(DELT_NOW.GE.(DELT-DELT_TOT)) THEN

        DELT_NOW=DELT-DELT_TOT

```

```

CONTROL_NEXT=0.
FOUND_END=.TRUE.
ELSE
C      CALCULATE THE NEW CONTROL SIGNAL BASED ON A STEADY STATE
APPROACH
Q_COMBUSTED_NEEDED=FLOW_FLUID*CP_FLUID*(T_SET-
1      T_FLUID_IN)+U_VALUE*AREA*(TAVE_NOW-T_ENV)

CONTROL_NEXT=Q_COMBUSTED_NEEDED/(Q_RATED*EFFICIENCY)
I=0
DO J=1,N_STEPS
    IF(DBLE(J)/DBLE(N_STEPS).LE.CONTROL_NEXT) I=J
ENDDO
CONTROL_NEXT=DBLE(I+1)/DBLE(N_STEPS)
CONTROL_NEXT=DMIN1(1.,CONTROL_NEXT)
CONTROL_NEXT=DMAX1(CONTROL_MIN,CONTROL_NEXT)
ENDIF

DO I = 1, NUMBER_NODE

TF(I)=TI_NOW(I)*(DEXP(AA*DELT_NOW))+BB(I)/AA*(
1      DEXP(AA*DELT_NOW))-BB(I)/AA
TAVE(I)=1./AA/DELT_NOW*(TI_NOW(I)+BB(I)/AA)*(

```

```
1      (DEXP(AA*DELT_NOW))-1.)-BB(I)/AA
```

```
ENDDO
```

```
ENDIF
```

```
ENDIF
```

```
Q_DEL_NOW=FLOW_FLUID*CP_FLUID*(TAVE(NUMBER_NODE)-T_FLUID_IN)
```

```
ENDIF
```

```
C  UPDATE THE TEMPERATURES
```

```
DO I = 1, NUMBER_NODE
```

```
  TI_NOW(I)=TF(I)
```

```
    TAVE_NOW = TAVE_NOW+TF(I)/NUMBER_NODE
```

```
  ENDDO
```

```
  TAVE_TOT=TAVE_TOT+TAVE_NOW*DELT_NOW/DELT
```

```
  CONTROL_AVE=CONTROL_AVE+CONTROL_NOW*DELT_NOW/DELT
```

```
C  UPDATE THE TOTAL GAS CONSUMPTION
```

```
  Q_COMBUSTED_TOT=Q_COMBUSTED_TOT+Q_COMBUSTED*DELT_NOW/DELT
```

```
  Q_GAS_TOT=Q_GAS_TOT+Q_COMBUSTED/EFFICIENCY*DELT_NOW/DELT
```

```
C  CALCULATE THE ELECTRICAL CONSUMPTION
```

IF(CONTROL_NOW.LE.0.) THEN

P_ELEC_TOT=P_ELEC_TOT+P_ELEC_STANDBY*DELT_NOW/DELT

ELSE

P_ELEC_TOT=P_ELEC_TOT+P_ELEC_HEATING*DELT_NOW/DELT

ENDIF

C SET THE REMAINING TIME

DELT_TOT=DELT_TOT+DELT_NOW

DELT_NOW=DELT-DELT_TOT

CONTROL_NOW=CONTROL_NEXT

C CHECK TO SEE IF WE SHOULD RUN AGAIN

IF(.NOT.FOUND_END) GOTO 30

C CALCULATE THE ENERGY FLOWS

Q_SKIN_TOT=U_VALUE*AREA*(TAVE_NOW-T_ENV)

Q_STORED=CAPACITANCE*(TAVE_NOW-TAVE_INIT)

Q_DEL_TOT=Q_DEL_TOT+Q_DEL_NOW*DELT_NOW/DELT

ELSE

C DO I = 1, NUMBER_NODE

C TAVE_NOW=TAVE_NOW+TI(I)/NUMBER_NODE

C ENDDO

C IDENTIFY THE ORIGINAL GUESS OF STEADY STATE CONTROL AND
TEMPERATURE PROFILE

TAVE_NOW = 0

DELTA_TEMP_EST=(T_SET-T_FLUID_IN)/NUMBER_NODE

DELT_SS=1000*DELT_NOW

DO I=1,NUMBER_NODE

IF (I.EQ.1) THEN

TI_SS(I)=T_FLUID_IN+DELTA_TEMP_EST

TSS_OLD(I)=TI_SS(I)

TAVE(I) = TI_SS(I)

ELSE

TI_SS(I)=TI_SS(I-1)+DELTA_TEMP_EST

TSS_OLD(I)=TI_SS(I)

TAVE(I)=TI_SS(I)

ENDIF

TAVE_NOW=TAVE_NOW+TI_SS(I)/NUMBER_NODE

ENDDO

EFFICIENCY=EFF_GAS

$Q_NEEDED_SS = FLOW_FLUID * CP_FLUID * (T_SET - T_FLUID_IN) +$

1 $U_VALUE * AREA * (TAVE_NOW - T_ENV)$

IF $(Q_NEEDED_SS > Q_RATED * EFFICIENCY)$ THEN

$FLOW_FLUID = (Q_RATED * EFFICIENCY - U_VALUE * AREA * (TAVE_NOW -$

1 $T_ENV)) / (CP_FLUID * (T_SET - T_FLUID_IN))$

$Q_NEEDED_SS = Q_RATED * EFFICIENCY$

$TAVE_OLD = TAVE_NOW$

ENDIF

$CONTROL_SS = Q_NEEDED_SS / (Q_RATED * EFFICIENCY)$

45 CONTINUE

C RUN FOR THE FULL TIMESTEP AT THE CURRENT SETTINGS AND SEE WHAT HAPPENS

C GET THE EFFICIENCY OF THE DEVICE (MAY BE EXPANDED LATER TO BE A FILE LOOK-UP ETC)

$TAVE_NOW = 0$

C GET THE HEAT INPUT TO THE FLUID

Q_SS=EFFICIENCY*CONTROL_SS*Q_RATED

DO I = 1, NUMBER_NODE

IF (I.EQ.1) THEN

TAVE_IN(I) = T_FLUID_IN

ELSE

TAVE_IN(I) = TAVE_SS(I-1)

ENDIF

C SET UP THE GOVERNING DIFFERENTIAL EQUATION IN THE FORM

DT/DT=AT+B

BB(I)=(Q_SS+FLOW_FLUID*CP_FLUID*NUMBER_NODE*TAVE_IN

1 (I)+U_VALUE*AREA*T_ENV+CONDUCTION_KA*NUMBER_NODE*

1 (NUMBER_NODE-1)*(TAVE_IN(I)+TAVE_SS(I+1))/LENGTH_TUBE)/

1 CAPACITANCE

AA=-(FLOW_FLUID*CP_FLUID*NUMBER_NODE+U_VALUE*AREA+2*

1 CONDUCTION_KA*NUMBER_NODE*(NUMBER_NODE-
1)/LENGTH_TUBE)/

1 CAPACITANCE

IF(AA.EQ.0.) THEN

TSS(I)=TI_SS(I)+BB(I)*DELT_SS

```

        TAVE_SS(I)=TI_NOW(I)+BB(I)*DELT_SS/2
ELSE
    TSS(I)=-BB(I)/AA
    TAVE_SS(I)=-BB(I)/AA
ENDIF

TAVE_NOW=TAVE_NOW+TSS(I)/NUMBER_NODE

ENDDO

TAVE_SS(NUMBER_NODE+1)=TAVE_SS(NUMBER_NODE)

C    SEE IF THE TEMPERATURES HAVE CONVERGED

    I_CONVERGED=1

DO I=1,NUMBER_NODE
    IF (DABS(TSS(I)-TSS_OLD(I)).GT.TOL) THEN
        I_CONVERGED=0
    ENDIF
    TSS_OLD(I)=TSS(I)
ENDDO

IF ((I_CONVERGED.EQ.0).AND.(ITER.LT.ITER_MAX))THEN
    GOTO 45

```

ENDIF

IF (DABS(TSS(NUMBER_NODE)-T_SET).GT.TOL) THEN

DO I=1,NUMBER_NODE

TSS_OLD(I)=TSS(I)

ENDDO

I_CONVERGED=0

ENDIF

IF ((I_CONVERGED.EQ.0).AND.(ITER.LT.ITER_MAX)) THEN

ITER=ITER+1

CONTROL_SS=DMIN1(1.,DMAX1(0.,(CONTROL_SS*(T_SET - TSS(NUMBER
1 _NODE)))/(T_SET-T_FLUID_IN))+CONTROL_SS))

GOTO 45

ENDIF

IF (CONTROL_SS.GT.1) THEN

CONTROL_SS = 1

ENDIF

C THIS SECTION OF CODE HAS BEEN REMOVED AS IT IS UNNECESSARY WITH
THE CURRENT CONTROL LOGIC. SHOULD THE CONTROL LOGIC EVER BE

CHANGED TO INCLUDE CHANGING GAMMA FOR TRANSIENTS IT WILL BE USEFUL
SO IT HAS NOT BEEN REMOVED

C SEE HOW THE DEVICE SHOULD BE CONTROLLED AT THE BEGINNING OF THE
TIMESTEP

C IF(CONTROL_LAST.GT.0.) THEN

C IF(CONTROL_LAST.GE.1.) THEN

C THIS SECTION WAS PREVIOUSLY USED TO KEEP THE CONTROL
CONSTANT AT 1 SHOULD IT HAVE BEEN 1 IN THE PREVIOUS TIMESTEP

C CONTROL_NOW=CONTROL_SS

C ELSE IF(TI_NOW(NUMBER_NODE).LT.(T_SET-DEADBAND-SMALL)) THEN

C THIS SECTION WAS PREVIOUSLY USED TO SET THE CONTROL
CONSTANT TO 1 IF THE OUTLET TEMPERATURE WAS NOTED TO BE LESS THAN
THE SET TEMPERATURE

C CONTROL_NOW=1

C ELSE

IF (DELT_STEADY.LT.UPDATE_DELAY) THEN

CONTROL_NOW=CONTROL_OLD

ELSE

CONTROL_NOW=DMIN1(1.,CONTROL_SS)

ENDIF

```

        IF(CONTROL_NOW.LT.CONTROL_MIN) THEN
            CONTROL_NOW=0.
        ENDIF
C        ENDIF
C    ELSE
C        IF(TI(NUMBER_NODE).LE.(T_SET-DEADBAND-SMALL)) THEN
C            CONTROL_NOW=1
C        ELSE
C            CONTROL_NOW=0.
C        ENDIF
c    ENDIF

C    INITIALIZE A FEW VARIABLES
        DELT_NOW=DELT
        TI_NOW=TI
        FOUND_END=.FALSE.
        DELT_TOT=0.
        CONTROL_AVE=0.

C    RETURN HERE EACH TIME
60    CONTINUE

```

```
IF (DABS(DELT_STEADY-UPDATE_DELAY).LE.(-SMALL)) THEN
    DELT_NOW=DMIN1(UPDATE_DELAY-DELT_STEADY,TIME_REMAINING)
ENDIF
```

C THE WATER HEATER WANTS TO BE ON

```
IF((CONTROL_NOW.GT.0.).AND.(TIME_ON.LT.TIME_DELAY)) THEN
```

```
    CONTROL_NOW=0
```

C SEE IF THE MANDATORY DELAY TIME PUSHES US OUT OF THE TIMESTEP

```
IF((TIME_DELAY-TIME_ON).GE.DELT_NOW) THEN
```

```
    FOUND_END=.TRUE.
```

```
ELSE
```

```
    DELT_NOW=DMIN1(DELT_NOW,(TIME_DELAY-TIME_ON))
```

```
    FOUND_END=.FALSE.
```

```
ENDIF
```

65 CONTINUE

```
I_CONVERGED = 1
```

```
TAVE_NOW=0
```

```
EFFICIENCY=EFF_PILOT
```

Q_COMBUSTED=Q_PILOT*EFF_PILOT

DO I = 1, NUMBER_NODE

IF (I.EQ.1) THEN

TAVE_IN(I) = T_FLUID_IN

ELSE

TAVE_IN(I) = TAVE(I-1)

ENDIF

C SET UP THE GOVERNING DIFFERENTIAL EQUATION IN THE FORM

DT/DT=AT+B

BB(I)=(Q_COMBUSTED+FLOW_FLUID*CP_FLUID*NUMBER_NODE*TAV

1 E_IN(I)+U_VALUE*AREA*T_ENV+CONDUCTION_KA*NUMBER_NOD

1 E*(NUMBER_NODE-1)/LENGTH_TUBE*(TAVE(I+1)+TAVE_IN(I)

1))/CAPACITANCE

AA=-(1/CAPACITANCE)*(FLOW_FLUID*CP_FLUID*NUMBER_NODE+U

1

_VALUE*AREA+2*CONDUCTION_KA*NUMBER_NODE*(NUMBER_NOD

1 E-1)/LENGTH_TUBE)

C ENTER TF_OLD VALUES FOR CONVERGENCE CHECK

TF_OLD(I)=TF(I)

```

C      SOLVE THE DIFFEQ ANALYTICALLY
      IF(AA.EQ.0.) THEN
          TF(I)=TI_NOW(I)+BB(I)*DELT_NOW
          TAVE(I)=TI_NOW(I)+BB(I)*DELT_NOW/2.
      ELSE
          TF(I)=TI_NOW(I)*(DEXP(AA*DELT_NOW))+BB(I)/AA*(DEXP(AA
1          *DELT_NOW))-BB(I)/AA
          TAVE(I)=1./AA/DELT_NOW*(TI_NOW(I)+BB(I)/AA)*((DEXP(AA
1          *DELT_NOW))-1.)-BB(I)/AA
      ENDIF

      TAVE(NUMBER_NODE+1)=TAVE(NUMBER_NODE)

      IF(DABS(TF(I)-TF_OLD(I)).GT.TOL) THEN
          I_CONVERGED=0
      ENDIF

      TAVE_NOW=TAVE_NOW+TF(I)/NUMBER_NODE

      ENDDO

      IF (I_CONVERGED.EQ.0) THEN
          GOTO 65

```

```

ENDIF

      Q_DEL_NOW=FLOW_FLUID*CP_FLUID*(TAVE(NUMBER_NODE)-
T_FLUID_IN)

      CONTROL_NEXT=CONTROL_SS

C      UPDATE THE TIME_ON COUNTER

      TIME_ON=TIME_ON+DELT_NOW

C      THE WATER HEATER IS ON

      ELSE IF(CONTROL_NOW.GT.0)THEN

C      GET THE EFFICIENCY OF THE DEVICE (MAY BE EXPANDED LATER TO BE A
FILE LOOK-UP ETC)

      EFFICIENCY=EFF_GAS

C      GET THE HEAT INPUT TO THE FLUID

      Q_COMBUSTED=EFFICIENCY*CONTROL_NOW*Q_RATED

C      THIS SECTION OF CODE HAS BEEN COMMENTED OUT BECAUSE IT IS
NOT NECESSARY WITH THE CURRENT CONTROL LOGIC ASSUMPTION. KEEPING IT
IN COMMENTED FORM AS IT MAY BE VERY USEFUL SHOULD THE CONTROL
LOGIC ASSUMPTIONS BE CHANGED

```

```

C          IF (CONTROL_NOW.EQ.1) THEN

C          CREATE AN INTIAL GUESS FOR DELT_NOW BASED ON A SINGLE NODE
ASSUMPTION

C          B_SINGLE = (Q_COMBUSTED+U_VALUE*AREA*T_ENV+FLOW_FLUID*CP_
C 1          FLUID*T_FLUID_IN)/CAPACITANCE

C          A_SINGLE = (-U_VALUE*AREA-FLOW_FLUID*CP_FLUID)/CAPACITANC
C 1          E

C          DELT_NOW=DMIN1(TIME_REMAINING,(1/A_SINGLE)*DLOG((T_SET+B_
C 1          SINGLE/A_SINGLE)/(T_FLUID_IN+B_SINGLE/A_SINGLE)))

C75        CONTINUE

C          I_CONVERGED=1

C          DO I = 1, NUMBER_NODE

C              IF (I.EQ.1) THEN

C                  TAVE_IN(I) = T_FLUID_IN

C              ELSE

C                  TAVE_IN(I) = TAVE(I-1)

C              ENDIF

C          SET UP THE GOVERNING DIFFERENTIAL EQUATION IN THE FORM

```

DT/DT=AT+B

C BB(I)=(Q_COMBUSTED+FLOW_FLUID*CP_FLUID*NUMBER_NODE*TAV

C 1 E_IN(I)+U_VALUE*AREA*T_ENV+CONDUCTION_KA*NUMBER_NOD

C 1 E*(NUMBER_NODE-

1)/LENGTH_TUBE*(TAVE(I+1)+TAVE_IN(I)

C 1))/CAPACITANCE

C AA=-(1/CAPACITANCE)*(FLOW_FLUID*CP_FLUID*NUMBER_NODE+U

C 1

_VALUE*AREA+2*CONDUCTION_KA*NUMBER_NODE*(NUMBER_NOD

C 1 E-1)/LENGTH_TUBE)

C ENTER TF_OLD VALUES FOR CONVERGENCE CHECK

C TF_OLD(I)=TF(I)

C SOLVE THE DIFFEQ ANALYTICALLY

C IF(AA.EQ.0.) THEN

C TF(I)=TI_NOW(I)+BB(I)*DELT_NOW

C TAVE(I)=TI_NOW(I)+BB(I)*DELT_NOW/2.

C ELSE

C TF(I)=TI_NOW(I)*(DEXP(AA*DELT_NOW))+BB(I)/AA*(

C 1 DEXP(AA*DELT_NOW))-BB(I)/AA

C TAVE(I)=1./AA/DELT_NOW*(TI_NOW(I)+BB(I)/AA)*((

C 1 DEXP(AA*DELT_NOW))-1.))-BB(I)/AA

```

C      ENDIF
C      TAVE_NOW=TAVE_NOW+TF(I)/NUMBER_NODE
C      IF(DABS(TF(I)-TF_OLD(I)).GT.TOL_TIME) THEN
C          I_CONVERGED=0
C      ENDIF

C      ENDDO

C          IF (I_CONVERGED.EQ.0) THEN
C      GOTO 75
C      ENDIF

C      IF ((DABS(TF(NUMBER_NODE)-T_SET).GT.TOL_TIME).AND.
C 1      (DELT_NOW.LT.TIME_REMAINING)) THEN
C          DELTA_TFN=T_SET-TF(NUMBER_NODE)
C          DERIV_TFN=(TF(NUMBER_NODE)-TI_NOW(NUMBER_NODE))/DEL
C 1      T_NOW
C          DELT_NOW=DELT_NOW+DELTA_TFN/DERIV_TFN

C          IF (DELT_NOW.GT.TIME_REMAINING) THEN
C              DELT_NOW=TIME_REMAINING
C          ENDIF

```

```

C          GOTO 75
C          ENDIF
C          ENDIF

C          IF(CONTROL_NOW.LT.1)THEN

90          CONTINUE

              I_CONVERGED=1
              TAVE_NOW=0

              DO I = 1, NUMBER_NODE
                  IF (I.EQ.1) THEN
                      TAVE_IN(I) = T_FLUID_IN
                  ELSE
                      TAVE_IN(I) = TAVE(I-1)
                  ENDIF
              ENDIF

C          SET UP THE GOVERNING DIFFERENTIAL EQUATION IN THE FORM
DT/DT=AT+B

              BB(I)=(Q_COMBUSTED+FLOW_FLUID*CP_FLUID*NUMBER_NODE*TAV
1          E_IN(I)+U_VALUE*AREA*T_ENV+CONDUCTION_KA*NUMBER_NOD
              1          E*(NUMBER_NODE-
1)/LENGTH_TUBE*(TAVE(I+1)+TAVE_IN(I)

```

```

1          ))/CAPACITANCE
          AA=-((1/CAPACITANCE)*(FLOW_FLUID*CP_FLUID*NUMBER_NODE+U
1
VALUE*AREA+2*CONDUCTION_KA*NUMBER_NODE*(NUMBER_NOD
1          E-1)/LENGTH_TUBE)
C          ENTER TF_OLD VALUES FOR CONVERGENCE CHECK
          TF_OLD(I)=TF(I)
C          SOLVE THE DIFFEQ ANALYTICALLY
IF(AA.EQ.0.) THEN
          TF(I)=TI_NOW(I)+BB(I)*DELT_NOW
          TAVE(I)=TI_NOW(I)+BB(I)*DELT_NOW/2.
ELSE
          TF(I)=TI_NOW(I)*(DEXP(AA*DELT_NOW))+BB(I)/AA*(
1          DEXP(AA*DELT_NOW))-BB(I)/AA
          TAVE(I)=1./AA/DELT_NOW*(TI_NOW(I)+BB(I)/AA)*((
1          DEXP(AA*DELT_NOW))-1.))-BB(I)/AA
ENDIF
          TAVE(NUMBER_NODE+1)=TAVE(NUMBER_NODE)
          TAVE_NOW=TAVE_NOW+TF(I)/NUMBER_NODE

```

```
IF(DABS(TF(I)-TF_OLD(I)).GT.TOL) THEN
```

```
  I_CONVERGED=0
```

```
ENDIF
```

```
ENDDO
```

```
  IF (I_CONVERGED.EQ.0) THEN
```

```
    GOTO 90
```

```
  ENDIF
```

C THIS 'ENDIF' CORRESPONDS TO THE "IF GAMMA < 1" STATEMENT

WHICH HAS BEEN REMOVED FOR CONTROL LOGIC REASONS

C ENDIF

```
  Q_DEL_NOW = FLOW_FLUID*CP_FLUID*(TAVE(NUMBER_NODE)-T_FLUI
```

```
1            D_IN)
```

C CHECK THE RESULTANT TEMPERATURE

```
  IF((TF(NUMBER_NODE)+TOL.LT.T_SET).AND.(CONTROL_
```

```
1            NOW.GE.1.)) THEN
```

```
    DELT_NOW=DELT_NOW
```

```
    CONTROL_NEXT=1.
```

```
    FOUND_END=.TRUE.
```

```

ELSEIF((DABS(TF(NUMBER_NODE)-T_SET).LT.TOL).AND.
1   (DELT_TOT.LT.DELT))THEN
    FOUND_END=.FALSE.
    CONTROL_NEXT=CONTROL_SS

ELSE
    DELT_NOW=DELT_NOW
    CONTROL_NEXT=CONTROL_SS
    FOUND_END=.TRUE.

ENDIF

C   UPDATE THE TIME_ON COUNTER
TIME_ON=TIME_ON+DELT_NOW

ELSE

    TAVE_NOW=0

    DO I = 1, NUMBER_NODE
    IF (I.EQ.1) THEN
        TAVE_IN(I) = T_FLUID_IN

```

```

ELSE
TAVE_IN(I) = TAVE(I-1)

ENDIF

C      SET UP THE GOVERNING DIFFERENTIAL EQUATION IN THE FORM
DT/DT=AT+B

EFFICIENCY=EFF_PILOT

Q_COMBUSTED=Q_PILOT*EFF_PILOT

BB(I)=(Q_COMBUSTED+FLOW_FLUID*CP_FLUID*NUMBER_NODE*TAVE_IN
1      (I)+U_VALUE*AREA*T_ENV)/CAPACITANCE

AA=-((FLOW_FLUID*CP_FLUID*NUMBER_NODE+U_VALUE*AREA)/
1      CAPACITANCE

C      SOLVE THE DIFFEQ ANALYTICALLY

IF(AA.EQ.0.) THEN

    TF(I)=TI_NOW(I)+BB(I)*DELT_NOW

    TAVE(I)=TI_NOW(I)+BB(I)*DELT_NOW/2.

ELSE

    TF(I)=TI_NOW(I)*(DEXP(AA*DELT_NOW))+BB(I)/AA*
1      (DEXP(AA*DELT_NOW))-BB(I)/AA

    TAVE(I)=1./AA/DELT_NOW*(TI_NOW(I)+BB(I)/AA)*((
1      DEXP(AA*DELT_NOW))-1.)-BB(I)/AA

ENDIF

```

TAVE(NUMBER_NODE+1)=TAVE(NUMBER_NODE)

TAVE_NOW=TAVE_NOW+TF(I)/NUMBER_NODE

ENDDO

Q_DEL_NOW=FLOW_FLUID*CP_FLUID*(TAVE(NUMBER_NODE)-
T_FLUID_IN)

1 *DELT_NOW

C CHECK THE RESULTANT TEMPERATURE

IF(TF(NUMBER_NODE).GE.T_SET) THEN

DELT_NOW=DELT_NOW

CONTROL_NEXT=0.

FOUND_END=.TRUE.

ELSE

C CALCULATE THE TIME TO GET DOWN TO THE SETPOINT

TF(NUMBER_NODE)=T_SET-DEADBAND

IF(AA.EQ.0.) THEN

```

DELT_NOW=(TF(NUMBER_NODE)-TI_NOW(NUMBER_NODE))/
1  BB(I)
    IF(DELT_NOW.LE.0.) THEN
        DELT_NOW=DELT-DELT_TOT
        CONTROL_NEXT=0.
        FOUND_END=.TRUE.
    ELSE IF(DELT_NOW.GE.(DELT-DELT_TOT)) THEN
        DELT_NOW=DELT-DELT_TOT
        CONTROL_NEXT=0.
        FOUND_END=.TRUE.
    ELSE
CONTROL_NEXT=1.
        ENDIF

        DO I = 1, NUMBER_NODE
            TF(I)=TI_NOW(I)+BB(I)*DELT_NOW
            TAVE(I)=TI_NOW(I)+BB(I)*DELT_NOW/2.
        ENDDO

    ELSE

DELT_NOW=DLOG((TF(NUMBER_NODE)+BB(NUMBER_NODE)/AA)/
1  (TI_NOW(NUMBER_NODE)+BB(NUMBER_NODE)/AA))/AA

```

```

IF(DELT_NOW.LE.0.) THEN
    DELT_NOW=DELT-DELT_TOT
    CONTROL_NEXT=0.
    FOUND_END=.TRUE.
ELSE IF(DELT_NOW.GE.(DELT-DELT_TOT)) THEN
    DELT_NOW=DELT-DELT_TOT
    CONTROL_NEXT=0.
    FOUND_END=.TRUE.
ELSE
    CONTROL_NEXT=1.
ENDIF

```

```

DO I = 1, NUMBER_NODE
TF(I)=TI_NOW(I)*(DEXP(AA*DELT_NOW))+BB(I)/
1      AA*(DEXP(AA*DELT_NOW))-BB(I)/AA
TAVE(I)=1./AA/DELT_NOW*(TI_NOW(I)+BB(I)/AA
1      )*((DEXP(AA*DELT_NOW))-1.)-BB(I)/AA

```

```

ENDDO

```

```

ENDIF

```

```

ENDIF

```

```

ENDIF

```

```

C    UPDATE THE TEMPERATURES

```

TAVE_TOT=TAVE_TOT+TAVE_NOW*DELT_NOW/DELT

CONTROL_AVE=CONTROL_AVE+CONTROL_NOW*DELT_NOW/DELT

DO I = 1, NUMBER_NODE

TI_NOW(I) = TF(I)

ENDDO

C UPDATE THE TOTAL GAS CONSUMPTION

Q_COMBUSTED_TOT=Q_COMBUSTED_TOT+Q_COMBUSTED*DELT_NOW/DELT

Q_GAS_TOT=Q_GAS_TOT+Q_COMBUSTED/EFFICIENCY*DELT_NOW/DELT

Q_DEL_TOT=Q_DEL_TOT+Q_DEL_NOW

C CALCULATE THE ELECTRICAL CONSUMPTION

IF(CONTROL_NOW.LE.0.) THEN

P_ELEC_TOT=P_ELEC_TOT+P_ELEC_STANDBY*DELT_NOW/DELT

ELSE

P_ELEC_TOT=P_ELEC_TOT+P_ELEC_HEATING*DELT_NOW/DELT

ENDIF

C SET THE REMAINING TIME

DELT_TOT=DELT_TOT+DELT_NOW

DELT_NOW=DELT-DELT_TOT

TIME_REMAINING=DELT-DELT_TOT

CONTROL_NOW=CONTROL_NEXT

IF (DELT_TOT.EQ.DELT) THEN

FOUND_END=.TRUE.

ENDIF

C CHECK TO SEE IF WE SHOULD RUN AGAIN

IF(.NOT.FOUND_END) GOTO 60

ENDIF

C CALCULATE THE ENERGY FLOWS

Q_SKIN_TOT=U_VALUE*AREA*(TAVE_TOT-T_ENV)

Q_STORED=CAPACITANCE*(TAVE_NOW-TAVE_INIT)

CUMUL_Q_DEL = CUMUL_Q_DEL + (Q_DEL_TOT*DELT)

CUMUL_Q_GAS = CUMUL_Q_GAS + (Q_GAS_TOT*DELT)

IF (Q_GAS_TOT.LE.0) THEN

EFFICIENCY_STEP = -99

```

ELSE
EFFICIENCY_STEP = Q_DEL_TOT / Q_GAS_TOT
ENDIF

IF (CUMUL_Q_GAS.LE.0) THEN
    EFFICIENCY_CUMUL = -99
ELSE
    EFFICIENCY_CUMUL = CUMUL_Q_DEL / CUMUL_Q_GAS
ENDIF

DELT_STEADY=DELT_STEADY+DELT

```

C PUT THE STORED ARRAY IN THE GLOBAL STORED ARRAY

```

DO I=1,NUMBER_NODE
    STORED(I+1)=TF(I)
    STORED(NUMBER_NODE+I+13)=TAVE(I)
ENDDO

STORED(NUMBER_NODE+3)=CONTROL_NOW
STORED(NUMBER_NODE+5)=TIME_ON
STORED(NUMBER_NODE+10)=CUMUL_Q_DEL
STORED(NUMBER_NODE+11)=CUMUL_Q_GAS

```

```
    STORED(NUMBER_NODE+13)=FLOW_FLUID
STORED(NUMBER_NODE+15)=TAVE_OLD
```

```
IF (DELT_STEADY-DELT.GE.UPDATE_DELAY) THEN
    STORED(NUMBER_NODE+12)=CONTROL_NOW
ENDIF
```

```
CALL setStorageVars(STORED,NSTORED,INFO)
```

```
IF(ErrorFound()) RETURN 1
```

```
C-----
```

```
----
```

```
C-----
```

```
----
```

```
C  SET THE OUTPUTS FROM THIS MODEL IN SEQUENTIAL ORDER AND GET OUT
```

```
OUT(1)=TF(NUMBER_NODE)
```

```
    OUT(2)=FLOW_FLUID
```

```
    OUT(3)=Q_COMBUSTED_TOT
```

```
    OUT(4)=Q_GAS_TOT
```

```
OUT(5)=Q_SKIN_TOT
```

```
OUT(6)=Q_DEL_TOT
```

```
OUT(7)=Q_STORED
      OUT(8)=CONTROL_AVE
      OUT(9)=P_ELEC_TOT
      OUT(10)=CUMUL_Q_GAS
      OUT(11)=CUMUL_Q_DEL
      OUT(12)=EFFICIENCY_STEP
      OUT(13)=EFFICIENCY_CUMUL
```

```
DO I = 1, NUMBER_NODE
```

```
      OUT(13+I)=TF(I)
```

```
ENDDO
```

```
C-----
```

```
----
```

```
C-----
```

```
----
```

```
C  EVERYTHING IS DONE - RETURN FROM THIS SUBROUTINE AND MOVE ON
```

```
      RETURN 1
```

```
      end
```

```
C-----
```

```
----
```